A Framework for Considering Resource Availability, Experimental Performance, and Environmental Impacts to Advance Alternative Mineral Admixtures

By

PATRICK R. CUNNINGHAM
DISSERTATION

Submitted in partial satisfaction of the requirements for the degree of

DOCTOR OF PHILOSOPHY

in

Civil and Environmental Engineering

in the

OFFICE OF GRADUATE STUDIES

of the

UNIVERSITY OF CALIFORNIA

DAVIS

Approved:

Sabbie A. Miller, Chair

John E. Bolander

John T. Harvey

Committee in Charge

2024

Abstract

Concrete is the most used building material. Due to the scale of use, Portland cement and concrete production drive a large portion of the global greenhouse (GHG) emissions. High-GHG-emitting industries are under increased pressure to decrease their GHG impacts to minimize the impacts of climate change and avoid the worst-case climate scenarios. As Portland cement production is the primary driver for the GHG emissions of cement-based materials, partially replacing Portland cement with supplementary cementitious materials (SCMs) and/or mineral fillers is one of the primary strategies for reducing the clinker content of binder materials. However, the supply of common SCMs is already regionally restricted with constrained supplies of coal fly ash (fly ash) and ground blast furnace slag (GBFS) available for cement-based material production. Notably, as the high-GHG emitting electricity and metal industries work to decrease their own GHG impacts, the generation of fly ash and GBFS will decrease and further restrict the availability of SCMs that decrease the GHG emissions of Portland cement-based binders. Alternative mineral admixtures are needed to meet the continued demand. In this work, alternative mineral admixtures are investigated. Specifically, regionally available flows from agricultural rice hull and rice straw residues and post-consumer flows from waste carpet in Northern California are evaluated using experimental characterization coupled with material flow analysis and environmental impact assessment. Insights from these efforts are then used to present a national-level analysis of material availability and identify promising alternatives.

Post-consumer carpet calcium carbonate (PC4), from waste carpeting, was investigated as a filler material (like limestone). Material flow analysis is used to evaluate the potential annual flow of PC4 materials from post-consumer carpeting, the performance of PC4 in cement-based materials is characterized, and the environmental impacts of Portland cement-PC4 mixtures was quantified. Results showed a loss of performance when PC4 is used, but the potential to decrease GHG impacts in Portland cement-based materials. To address performance loss, PC4 materials was treated to improve mechanical performance, leading to strengths similar to mixtures made with limestone and Portland cement.

Rice hull ash (RHA) and rice straw ash (RSA) were investigated as reactive SCMs. Rice hull and rice straw are lower-value residues from rice cultivation. Rice hulls are already a well investigated bioderived SCM. A material flow analysis was used to model the generation of rice hull and rice straw from rice cultivation and the potential ash generation. One challenge with rice straw combustion is the higher levels of alkali-metals (K, Na) and Cl which can cause slagging and fouling in biomass combustion reactors. Leaching that reduces slagging was performed and the effect on compressive strength of Portland cement-ash mortars and the environmental impacts of these ashes was investigated. Results indicate that the use of ashes from leached biomass may be best coupled with energy production systems. Importantly, ash production in these systems is optimized for energy generation, not material properties. Thus, additional investigations were performed into post-combustion processing of RHA and RSA.

These insights from material flow analysis, material performance, and environmental impacts were coupled together to evaluate alternative mineral flows in comparison to conventional mineral admixtures (i.e., fly ash, GBFS, limestone, metakaolin, and silica fumes). Recent trends in material generation are compared to the potential production of alternatives. Projections are made for the future generation of fly ash, GBFS, total coal combustion products (CCPs) and electric arc furnace (EAF) slags under shifting production technologies. By coupling performance needs, environmental impact assessment, and modeled material supply, the potential masses of binary Portland cement-RSA, -RHA, or -PC4 blends are shown to be smaller even compared to decreasing generation of fly ash and GBFS. Notably, EAF slag and CCPs remain larger flows compared to fly ash and GBFS. Demonstrating a coupled assessment of environmental impacts, supply, and performance can be used to identify alternative flows to meet the growing demand for Portland cement-replacing mineral admixtures.

Acknowledgements

As I write this acknowledgement, I feel exceptionally fortunate for the many people who have supported, guided, and advised me while I pursued my degrees.

Firstly, I own an immense amount of gratitude to Professor Sabbie Miller, my advisor and dissertation committee chair. I never thought that my undergraduate research in 2017/2018 would lead to a Ph.D. I cannot concisely express how fortunate I feel to have this opportunity, but I will try my best. I have benefited from your encouragement, knowledge, and trust. Thank you for sharing your network with me, being generous with your time (and patience), for challenging me to do the best work I could, and for encouraging me to seek out opportunities I didn't, at the time, have the confidence to pursue on my own. I am excited for what the future holds and remain excited about research in our field. Thank you so very much for taking a chance on me!

To the members of my dissertation committee, Professor John Harvey and Professor John Bolander: You both supported my academic and research development (even before my Ph.D.) and—no doubt—your feedback and guidance have improved my research and made this dissertation better. Thank you for sharing laboratory resources, your thoughtful insights, and your kind encouragement .

Important thanks are owed to Dr. Peter Green and Professor Bryan Jenkins, who both went beyond just being co-PI's on research projects, by also providing important interdisciplinary context to my work and helping me understand pathways through academics. I have learned so much. The guidance and encouragement from you both has helped me developed as an interdisciplinary researcher. Thank you for being generous: with your time, with your research connections, and in supporting my professional development. I hope I can, one day, be as academically exceptional as you both have modeled for me.

A thanks is owed to others who supported my research and were always willing to provide their thoughts, time, and expertise. In particular, I owe thanks to Daret Kehlet, Jessica Hazard, Dr. Peter Thy, and Jeffrey Buscheck. I am appreciative for the four of you helping me progress, helping me find equipment and space, and teaching me more about experimental work. Similarly, I owe Lauren Worrell an acknowledgement for helping me navigate the administrative ins-and-outs of grad studies at UC Davis.

Many other faculty members have helped me shape my own views points and interests as an academic and assisted me as I explored this field: Dr. Colleen Bronner, Dr. Jeanie Darby, Dr. Sashi Kunnath, and Dr. Mark Rashid, you all provided counseling during key decisions points in my academic career. I am very grateful for the guidance and advice provided.

In a similar vein, but different mentorship world, Mark Huising should be recognized for supporting my professional endeavors and demonstrating how informed science can play a role in advocating for change and environmental progress in our system. I am not as bold as you, but [maybe?] one day.

To my German Friends at BAM: Meine Zeit an der BAM war eine außergewöhnliche Zeit der beruflichen Entwicklung. Ein großes dankeschön an Dr. Wolfram Schmidt, der mich wie seiner eigenen Doktoranden aufgenommen hat. Sie haben meine verrücktesten Forschungsideen (auch die dummen) unterstützt und mich bei der Erforschung neuer Bereiche unseres Fachgebiets begleitet. Vielen Dank auch an Professor Dr. Sabine Kruschwitz, die mein Projekt unterstützt hat und mich bei meiner Forschungsarbeit so freundlich aufgenommen hat. Vielen Dank auch an alle meine Freunde in Deutschland. Noah und der Vorspielen wasserball-team danken ihnen auch dass sie mir Berlin gezeigt haben. [Thanks, Herr Brunn, for proofing].

Additionally, I have been blessed with wonderful colleagues: successful Ph.D.'s: Dr. Kanotha Kamaudevers (the original!), Dr. Yaming Pan, and Dr. Sonoko Ichimaru; and soon-to-be Ph.D.'s: Josephine Olsson, Kelli Knight, Li Wang, Leah Brinkman, Elisabeth van Roijen, Camille King, and Alyson Kim. In all, I am thankful for such a wonderful, supportive, and collaborative lab group. I hope to be as lucky with coworkers in my future endeavors! I must also acknowledge research students who put up with my flawed guidance: Audrey Florman, Angani Vigneswaran, Hung Yu, Justin Caverly, Cameron Schultz, and Asahi Amitani.

A big thank you is owed specifically to Lizzie and Aly. You two were great officemates and always willing to listen. Thank you for being open to discussing our research challenges. Our friendships have genuinely helped me better understand my research questions. Having two people next to me, in the trenches, and who understood the challenges of a Ph.D., but also told me I could make it, was key to my success at the end (and you were right, we made it!).

I could not be successful if not for the support and encouragement of my family. Till min familj, tusen tack (☺) för allt. Ni uppmuntrade mig att gå framåt. Mom och Dad, tack för er kärlek och stöd. Ni lyssnade på mig prata om mattor eller ris och betong så många gånger, och fortsätter gärna att göra det. Jag kommer aldrig att förstå varför, men jag är tacksam. Annie, Brit, och Jessie: Ni lyssnade också, om än något mer motvilligt. Tack för att ni läste mina artiklar och forskningsanslag, jag är säker på att de var tråkiga som betong. Moster Boel and 'morbror' Lars, jag tackar er också för er generositet, för att jag fick besöka er i skogen (och gömma mig från jobbet). [Tack, Freddie, for proofing].

Niels, ik wou dat ik beter Nederlands sprak. Ik ben zo blij dat we elkaar ontmoet hebben. Zonder meer heb je het doen van deze Ph.D. zoveel leuker gemaakt. Op moeilijke dagen weet jij hoe je me kunt laten lachen. Ik hoop dat ik ooit net zo'n goede wetenschapper kan worden als jij. Maar, tot die tijd ben ik beter in wetenschap, zul je het moeten doen met mijn betere kookkunsten. Ik kijk uit naar meer tijd met jou. Helaas zal/gaat dat ook betekenen dat je naar meer klachten over beton moet luisteren. Helaas pindakaas. [Dank je, Jacques, for proofing]. Gaan met die banaan.

Funding Acknowledgement

The author gratefully acknowledges dissertation funding and support from the National Center for Sustainable Transportation (NCST) which has been integral to this work, especially the final chapter.

The author acknowledges support from the UC Davis Department of Civil and Environmental Engineering endowed graduate awards (including the Takashi and Holly Newcomb Asano Fellowship); the Concrete Masonry Association of California and Nevada; matching funds from UC Davis Graduate Studies; the Deutsch-Amerikanishe Fulbright Kommission; and the Fulbright U.S. Student Program (a program of the US Department of State).

This research and works included in this dissertation have been supported by grants from the California Rice Research Board, the Carpet America Recovery Effort (CARE), the National Science Foundation (NSF), and the NCST at UC Davis.

The views in this work are those of the author. The contents of this work are solely the responsibility of the author and do not reflect the views of the Deutsch-Amerikanishe Fulbright Kommission, the Fulbright program, the German Government, the Government of the United States, or any other organizations.

Contents

List of figures

List of tables

CHAPTER 1

Introduction

1.1.Concrete, Portland cement and the climate crisis

Concrete is an ubiquitous construction material composed of aggregates held together by a binder composed of Portland cement and water. Concrete is the most consumed human-produced material, with over 4 billion metric tons of Portland cement consumed annually [1], [2] and the estimated mass of concrete production is even greater. With relatively low greenhouse gas (GHG) emissions associated with the production of other constituents, Portland cement is the main driver of GHG emissions from concrete production [3], [4]. The large amount of Portland cement and concrete production contributes approximately 6% of all anthropogenetic GHG emissions [5] or 7-10% of anthropogenic CO_2 emissions [5], [6] globally. Because GHG emissions are the driving force behind global climate change and the growing climate crisis [3], there has been notable urgency placed on decarbonizing the cement industry. To mitigate the impacts of climate change, all aspects of the global economy, including concrete and cement production [7], must reach net-zero GHG emissions by 2050 [8], [9].

Concrete is an integral and pervasive part of the built environment. It comprises an important component of transportation and mobility networks, buildings and structures, and water and energy systems. The wide-ranging use of concrete is in part due to its high compressive strength, durability, and relative ease of construction along with its commonly available constituents and low costs of production. Thus—while there is an urgent need to decrease the environmental impacts of concrete and Portland cement production—concrete consumption continues to grow. Historically, regional economic development has coincided with expanded consumption of cement and concrete as construction of physical infrastructure increased. From 1960 to 2019 the cement production in the United States nearly doubled, which was paired

with significant economic growth (**Figure 1.1a**). Similarly, reported Chinese Portland cement production has increased rapidly, which also coincided with an increase in economic output (**Figure 1.1b**).

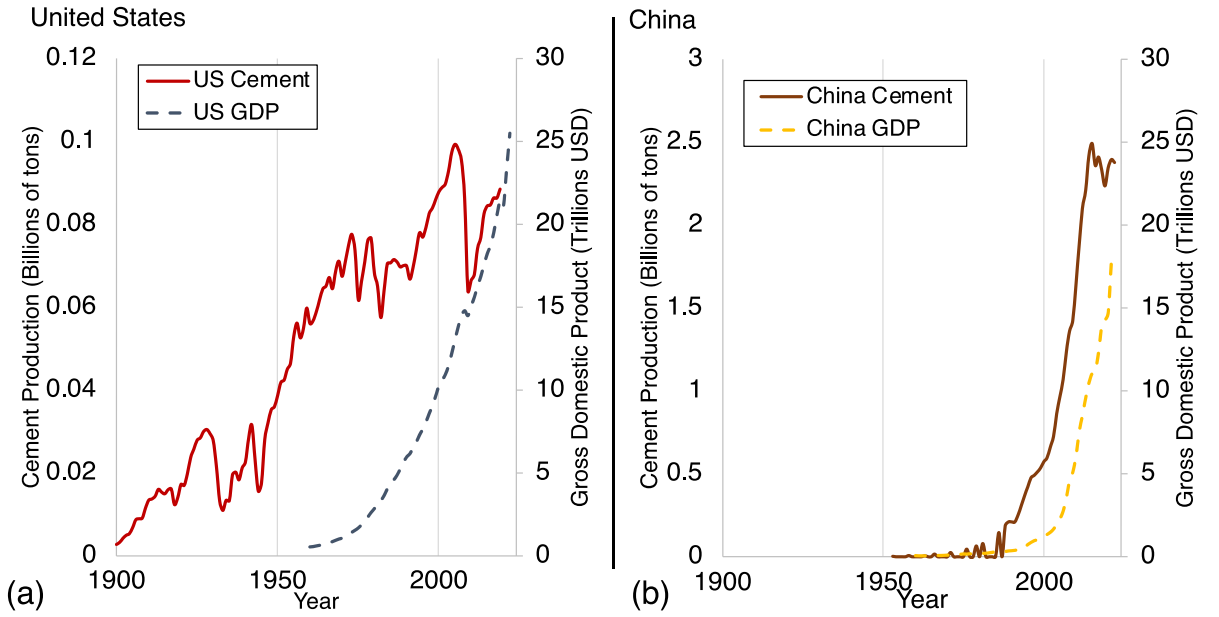

Figure 1.1. Annual cement production and gross domestic product of (a) the United States and (b) China. With cement production in billions of metric tons on the left-hand axis and gross domestic product shown in trillions of US dollars, present day value (2022), on the right-hand axis of each plot. Note: the scale changes for cement production between the two plots. Data from United States Geologic Survey cement reports [10], the National Bureau of Statistics of China [11] and the World Bank [12].

Notably, production of Cement in China is projected to decrease in coming year (**Figure 1.2**). This follows existing trends in US and European cement production [3], [13]. However, cement production in other regions (India, Africa, and Parts of Asia) is projected to increase and led to a ~20% increase by 2050 in global cement production (compared to 2020) under high consumption scenarios [14]. As other economies and populations expand across Asia, South America, and sub-Saharan Africa, demand for new infrastructure and housing is expected to increase and, with it, the environmental impacts associated with materials production will also increase [15], [16], [17].

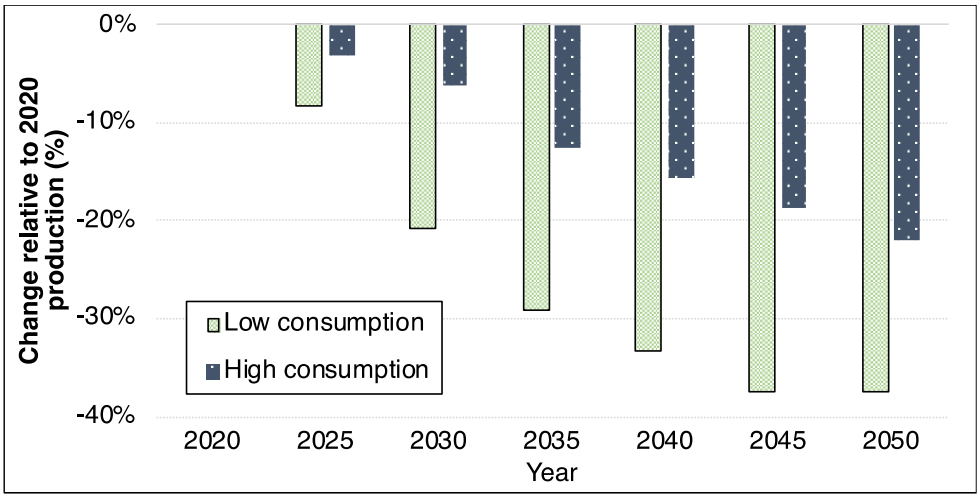

Figure 1.2. Projected change in Portland cement consumption in China (relative to 2020 production) based on IEA project high [14] and low [3] cement consumption scenarios for China.

This increasing materials demand, coupled with the need to avoid GHG emissions, has led to growing interest in alternative building materials with potentially lower environmental impacts. Apart from novel alternative binder chemistries, wood construction has increased across Europe and North America [18], [19], [20]. Notably, the majority of the tallest wood buildings require other material resources, and they remain hybrid concrete-timber, steel-timber, or concrete-steel-timber structures [21]. While some have argued that planted forests could be increased to meet the demands for soft and hardwoods on a global scale [22], recent studies suggest that a regional scale analysis is required to balance loss of carbon storage with using biomass materials as carbon sinks [23]. The applications of timber may be further restricted by ecological considerations [23] and the limited ability to scale if global demands are to dramatically shift to increased wood construction [22]. The current trend in timber construction is likely supported by the location of fellable forest mass being concentrated in North America and Europe (regions with plateauing populations and less-sharply increasing demands for construction materials) [19]. As such, timber-only construction is not expected to be feasible for most countries, and concrete will be needed across many regions.

Similarly, interest in "vernacular" materials (i.e., locally sourced, often lower performance materials such as adobe bricks or wattles) has reemerged in architectural and some engineering fields [24], [25], [26], which has been paired with increased efforts to standardize their implementation in parts of Europe (especially in France) [27]. While vernacular materials tend to be limited to lower-performance applications, these materials can curb some demand for concrete in specific applications. However, they are regionally specific, require specialized training, and are typically very manual construction practices [25], [28], [29]. For many applications, especially higher-performance applications, it is anticipated that concrete will remain an important building material. In some regions with growing infrastructure demands, concrete is also the only material with suitable performance and with suitable resource availability to meet engineering needs and supply demands of the future [15], [30]. Thus, reaching net-zero emissions in building materials requires reducing the GHG emissions from concrete production.

1.2. Cement as a concrete binder and GHG emission driver

Portland cement is a hydraulic cement that, when mixed with water, hydrates to form a binder that can hold together the aggregates and other additives used to produce concrete and other cement-based materials. Portland cement is comprised predominately of Ca and Si oxides, with smaller concentrations of metal (i.e., Al, Mg, Fe) oxides. These oxides are produced by calcining and pyro-processing (kilning) limestone (as the Ca source) and other Al, Si, and Fe minerals (e.g., clays, shales, and ores) at ~1400°C [31, p. 19], [32]. This process forms a product called "clinker", which is then milled with gypsum to produce Portland cement [31]. This kilning process create specific Ca-, Si-, Al-, and Fe-bearing oxides in the Portland cement (namely: alite, belite, aluminate, and ferrite). These oxides react hydraulicly in the presence of water and assemble into calcium-silicate-hydrates (C-S-H), calcium-aluminate-silicate hydrates (C-A-S-H), calcium hydroxide (CH), and ettringite hydration products [33]. Of which, C-S-H, C-A-S-H, and ettringite contribute to the densification and structural development of the hydrated binder [33]. A summary of the cement chemistry notation used here is provided in **Table 1.1**.

Table 1.1. Summary of key abbreviations from cement chemistry notation and the indicated compound

Notation	Compound
C	CaO
S	SiO_2
A	Al_2O_3
H	H_2O
C-S-H	calcium-silicate hydrate
C-A-S-H	calcium-aluminate-silicate hydrate
CH	calcium hydroxide

* based on the notation and reactions described in [33], [34], [35]

As noted, Portland cement accounts for the majority of the GHG emissions in concrete production [4], [36]. The calcining of limestone during Portland cement production ($CaCO_3$) is a chemical conversion that results in the release of CO_2 and contributes over 60% of the GHG emissions from Portland cement production. The second highest driver of the GHG emissions is energy resources that are commonly fossil fuels required for the high-temperature kilning [5]. The contribution to GHG emissions from the production

of aggregate (despite making up the largest volume of the concrete), constituent transportation, and batching processes are small relative to the Portland cement produced. As a result, strategies to reduce the GHG emissions from concrete target reduction in the Portland cement demand [3], [37]. This demand reduction is often achieved via partially replacing the Portland cement with other materials [38] or fully replacing Portland cement with alternative binder chemistries [2], [38], [39].

Since the 1970's, significant progress has been made to improve the fuel and energy efficiency of Portland cement production (production illustrated in **Figure 1.3**) [40]. These efforts have included increasing thermal efficiency by implementing pre-heating and pre-calcining processes before kilning. Additionally, switching to dry conveyance of feedstocks instead of wet slurry methods reduces the need to first drive off water in the kiln and further improves the energy efficiency [31]. Together, these improvements in dry rotary kilns can increase energy efficiency and significantly reduce GHG emissions by reducing the energy resources required for production [41]. While these energy savings can result in cost savings due to the long-lived functionality of cement kilns, the operating savings do not always outweigh the capital investment costs. As a result, some regions, especially those with established kilns, have not implemented all of these methods [40]. These lower-efficiency kilns lead to some countries producing Portland cement that is much higher in embodied energy and production GHG emissions.

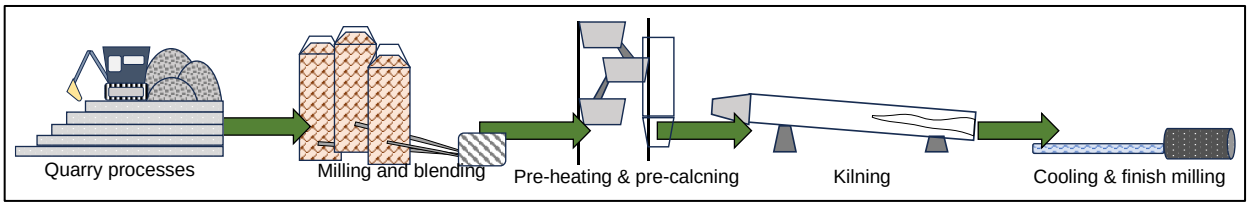

Figure 1.3. Pictorial illustration of Portland cement production process.

Alternative clinkers and binder chemistries, such as ye'elimite-based (calcium sulfoaluminate), periclase-based (MgO), and various alkali-activated binders, have been investigated as potential, lower-impact alternatives [5], [39]. Currently, ye'elimite- and periclase-based binders are still produced from

carbonate feedstocks. While these materials can have lower chemical CO_2 emissions compare to Portland cement clinker, they still release CO_2 during the clinkering stage [5] and have similar embodied energies to Portland cements [2]. Notably, production of periclase-based binders derived from $MgCO_3$ can lead to larger GHG emissions than Portland cement [2] and, thus, be dependent on post-curing carbonation to achieve GHG emission parity. If these binders are carbonated after hydration, both ye'elimite and periclase-based binders could further reduce CO_2 emissions [5], especially if alternative (non-carbonate) feedstocks are used [2], [5].

Alkali-activated materials (AAMs) are an alternative binder system comprised of alumnio-silicate precursor that are activated by a Na- or K-based alkali-activators [42]. Typically, these activators are NaOH, KOH, and $NaSiO_3$ solutions that are then combined with precursors. Common precursors are also materials used as SCMs (i.e., coal fly ash, ground blast furnace slags, or metakaolin clays [43], [44]). Importantly, multiple studies have shown that AAMs have 57-60% lower GHG emissions compared to Portland cement [36], [45]. Notably, these reductions in GHG emissions coincided with increased volatile organic compounds (VOC) and particulate matter smaller than 10μm (PM_{10}) impacts, largely driven by the alkali-activator and precursor production systems [39]. In either mineral admixture use case (i.e., as a partial cement replacement or as a precursor in AAM), the supplies of these mineral admixtures will need to scale in order to meet the demand for greater Portland cement replacement.

While GHG emissions are the primary environmental impact examined in this work, it is important to note the high levels of cement and concrete use drive additional environmental burdens [46]. For example, cement and concrete production accounts for 9% of industrial water withdrawals [47], 9% of mercury emissions [48], and 5% of particulate matter smaller than 10μm (PM_{10}) [4]. In some cases, these burdens have greater impact at local or regional scales [49], [50], which in tandem can disproportionally affect marginalized, less-resourced, and/or historically disadvantaged communities [51]. Notably, reducing Portland cement clinker content does not necessarily drive down other environmental impacts [39].

1.3. Supplementary cementitious materials can reduce GHG impacts

This work investigates SCMs to reduce the clinker content of Portland cement binders. Partially replacing Portland cement with SCMs is a common method to reduce the GHG emissions associated with concrete mixtures. Some SCMs, such as coal fly ash (fly ash) and ground blast furnace slags (GBFS), are industrial byproducts and, without diversion, can be a hazardous waste flow from industrial processes. For example, using coal fly ashes and slags in concrete can sequester harmful compounds and may help to avoid other negative environmental impacts that could otherwise occur (such as preventing the leaching of heavy metals) [52], [53]. SCMs, considered a subset of mineral admixtures, contribute to hydration products through pozzolanic or cementitious reactions or as a filler material, allowing for the reduction of clinker in the binder powder.

Common industrial byproduct SCMs include fly ash (from coal combustion), GBFS, (from pig iron production), and silica fume (from the ferrosilicon and silicon alloy industry). Though the annual generation of silica fume is relatively small [54], it is a highly reactive SCM comprised primarily of silica [34]. Pozzolanic SCMs containing reactive silica (e.g., Class F fly ash), can react with the Portland cement during hydration products to yield C-S-H and, in the presence of Al, C-A-S-H [34], [55]. These hydration products contribute to the densification and strength development in the hydrated binder. Materials with higher CaO contents, like GBFS, can also contribute Ca oxides, which react with silica and water to create C-S-H and C-A-S-H [34].

With growing demand for mineral admixtures, mined and processed materials are becoming more common. Notable among these are limestone (as a “filler” – used here to refer to a less or non-reactive mineral admixture) and calcined clays (e.g., metakaolin). Portland-limestone cement (PLC) has garnered much regional acceptance in standards and, as of April 2024, is accepted in all 50 United States (US) states [56]. The limestone particles improve the performance of the binder materials via more efficient particle packing, which enables better mechanical load transfer in the material matrix and, via better cement

dispersion, improves the hydration and microstructural development of the Portland cement [57]. Typically PLCs contain ~15% limestone by mass with reduced clinker content [58], and such PLCs can achieve compressive strengths comparable to traditional Portland cement-only mixtures [59], [60], [61]. Calcined clays are produced by calcining certain mined clays. Kaolinite clays, when calcined, dehydroxylate into reactive alumina- and silicate- rich material [62], [63]. This conversion can require notable energy inputs and increases the associated GHG emissions. However, the calcining temperature for clays (~700-800°C, [63]) is below that of Portland cement production, and the GHG emissions from calcined clays are usually lower than those of Portland cement clinker. Like other reactive SCMs, calcined clay reacts with CH to form C-A-S-H and other hydration products [64].

Binary cement mixes containing Portland cement and a mineral admixture (i.e., SCM or filler) are commonplace, tertiary blends—for example "LC3" cements (limestone calcined clay cements) with limestone, calcined clays, and Portland cement clinker—are garnering increase interest and are gaining acceptance in blended cement standards (e.g., [65]). These ternary blends of mineral fillers and reactive SCMs could be a viable means of extending limited supplies of SCMs if there are localized scarcities. Ternary blends also allow for larger reductions in Portland clinker content than PLCs, and can lead to even lower GHG emissions compared to binary Portland cement-SCM mixtures [66].

1.4. Common supplemental cementitious materials are regionally scarce.

SCMs and mineral fillers remain popular and effective at reducing the GHG emissions from cement and concrete production. Namely, partially replacing Portland clinker with SCMs is a key strategy in industry [37], national [38], and global [3] emissions mitigation roadmaps. Increased urgency to decarbonize cement production has led to a growing demand for mineral admixtures. At the same time, production of industrial byproduct SCMs (e.g., coal fly ash) is decreasing in some regions, such as the US, as energy grids transition towards more renewable energy resources [67]. Changing steel production processes (namely, coupled direct reduce iron and electric arc furnace production systems with increased recycled steel and scrap feedstocks) will reduce the generation of GBFS [68]. As such, it is expected that the availability of these products, especially in North America, will become more restricted [54]. At the same time, regional alternatives to conventional SCMs are being identified [69], [70]. However, the types, availability, and quality of these alternative mineral resources varies [69].

Identifying the most effective and promising mineral admixtures to decrease GHG emissions is imperative to continue driving down Portland cement-caused GHG emissions. Transitioning to alternative materials may require shifting the paradigm of the traditional SCMs supply chain, wherein byproduct materials are collected from the factory gate and diverted into Portland cement production systems. Valorizing alternative materials flows may require different supply chains, additional processing (or beneficiation) steps, and tailored mixture design to achieve desired performance. Notably, these shifting systems also opens opportunities to find new synergies between industries where there is potential to divert mineral flows from waste systems into beneficial resources. This work aims to create a framework for considering resource diversion for recovery and reuse to advance further material circularity with the primary focusing being to decrease the GHG emissions from Portland cement and concrete production.

1.5. Outline of dissertation

This dissertation advances the evaluation of alternative mineral admixtures produced from residue and byproduct materials. Herein, alternative mineral fillers and SCMs are evaluated based on performance, material availability, and GHG emissions. In Chapters 2-3, candidate material flows (from agricultural residue and post-consumer waste) are considered using experimental investigations, material flow analysis, and environmental impact assessment. This perspective is then expanded in Chapter 4, where a framework is developed to evaluated the system-level availability of different mineral resources in context of material production, GHG emissions, and mechanical performance. Finally, Chapter 5 provides concluding remarks on this work with a focus on future applications and future research opportunities.

Chapter 2 investigates post-consumer carpet calcium carbonate (PC4), a mineral resource that is diverted from landfills, as a mineral filler. A material flow analysis is used to quantify the annual generation of PC4 and current end-of-life outcomes for waste carpet. Results from experimental characterization of as-received PC4 is concrete mixtures is shown and used in tandem with an environmental impact assessment to understand the changes in properties of concrete mixtures made with PC4 and its potential to reduce the GHG emissions from concrete production. In the last section, PC4 is processed and engineered to identify strategies that can improve the performance as a filler material and changes in the PC4-Portland cement mortars are investigated and compared to specimens made with virgin limestone filler.

In Chapter 3, residue rice hull ash (RHA) and rice straw ash (RSA) from combusting biomass for energy generation are evaluated as SCMs. A material flow analysis is performed to quantify the flow and potential mass of rice-biomass ashes in the US. As rice is produced only in some regions in the country, a spatiotemporal analysis is applied to understand the cement replacement potential in a regional context. Noting there are potential added benefits if rice residues are used for both energy generation and ash production, the influence of different leaching pre-treatment conditions (necessary to reduce slagging in energy generation) and different oxidation temperatures are evaluated. In this work, the chemical

composition of the ash is characterized, the mechanical performance of mortars with ash is investigated, and an environmental impact assessment is conducted to understand the potential for GHG emissions savings. Based on the findings of the environmental impact assessment, additional experimental testing is performed with industrial produced RHAs and a lab-produced RSA to evaluated different post-combustion treatment strategies that could improve the performance of ashes from biomass energy generation.

In Chapter 4, findings are harmonized to formulate a systematic approach to investigate alternative mineral admixtures (including PC4, RHA, and RSA) and develop an assessment framework. Namely, the potential generation of alternative mineral flows is compared to the recent supply of traditional SCMs. As coal fly ash and GBFS are expected to decrease in the future, projections are made for future fly ash and GBFS generation up to 2050. To compare the GHG emissions, two strategies are demonstrated. First, a comparison index approach is used to integrate shifts in the compressive strength of the SCM mixtures evaluated in Chapter 2 and Chapter 3. Then, the assessment framework is developed with, a second comparison strategy, to provide supply-informed comparisons. By combining performance considerations to evaluate multiple binder proportions, this framework allows for the GHG emissions from SCM-Portland cement paste blends to be compared in context of the potential production masses of the pastes and a fixed compressive strength. This supply-based comparison is then used with SCM generation projections to provides insights into potential material flows and the need to identify alternative mineral admixtures.

In Chapter 5, key findings from earlier chapters are highlighted and used as a foundation to identify and discuss future applications of this work. Specific focus is given to residue- and waste-flow diversion and techniques that can advance future work in identifying and evaluating alternative mineral admixtures.

1.6. List of supporting publications

Much of the work is from parts of peer-reviewed academic journal articles. These works include:

i. **P.R. Cunningham**, L. Wang, P. Thy, B.M. Jenkins, S.A. Miller. *Effects of Leaching Method and Ashing Temperature of Rice Residues for Energy Production and Construction Materials*. ACS Sustain Chem ENG. (2021).

ii. **P.R. Cunningham**, P.G. Green, S.A. Miller. *Utilization of Post-consumer Carpet Calcium Carbonate (PC4) from Carpet Recycling as a Mineral Resource in Concrete*. Resour Conserv Recy. 169, 105496. (2021).

iii. **P.R. Cunningham**, S.A. Miller. *A Material Flow Analysis of Carpet in the United States: Where Should the Carpet Go?*. J Clean Prod. 368, 13324. (2022).

iv. **P.R. Cunningham**, P.G. Green, S.J. Parikh, J.T. Harvey, S.A. Miller. *Engineering the Performance of Post-consumer Calcium Carbonate from Carpet in Cement-Based Materials through Pre-treatment Methods*. Constr Build Mater. 368, 130451. (2023).

v. **P.R. Cunningham**, L. Wang, S. Nassiri, P. Thy, J.T. Harvey, B.M. Jenkins, and S.A. Miller. *Evaluation of performance and supply of rice straw and rice hull ashes as regional supplementary cementitious materials*. (Under review, anticipated 2024).

For harmonized environmental impact quantifications, this work builds on the LCI data and processing concepts used in the following publication co-authored by the writer (however, no figures or text from this work is used in this dissertation):

vi. A. Kim, **P.R. Cunningham**, K. Kamau-Devers, S.A. Miller. *OpenConcrete: a tool for estimating the environmental impacts from concrete production*. Env Resour Infrastruct Sustain. 2 (4), 041001. (2022)

CHAPTER 2

Post-consumer Calcium Carbonate from Carpet (PC4)

Author Note

This chapter is comprised of portions from the following peer-review journal articles. The author is grateful for the expertise and advice provided by co-authors: P.G. Green, S.J. Parikh, J.T. Harvey, and S.A. Miller.

i. **P.R. Cunningham**, S.A. Miller. *A Material Flow Analysis of Carpet in the United States: Where Should the Carpet Go?*. J Clean Prod. 368, 13324. (2022). https://doi.org/10.1016/j.jclepro.2022.133243.

ii. **P.R. Cunningham**, P.G. Green, S.A. Miller. *Utilization of Post-consumer Carpet Calcium Carbonate (PC4) from Carpet Recycling as a Mineral Resource in Concrete*. Resour Conserv Recy. 169, 105496. (2021). https://doi.org/10.1016/j.resconrec.2021.105496.

iii. **P.R. Cunningham**, P.G. Green, S.J. Parikh, J.T. Harvey, S.A. Miller. *Engineering the Performance of Post-consumer Calcium Carbonate from Carpet in Cement-Based Materials through Pre-treatment Methods*. Constr Build Mater. 368, 130451. (2023). https://doi.org/10.1016/j.conbuildmat.2023.130451.

2.1. Introduction

Carpet is an ubiquitous flooring material used across commercial and residential applications. Carpet is a relatively short-lived component of buildings, with typical lifespans below 25 y [71]. A carpet may be replaced many times over the lifespan of a structure [72]. Initial estimates suggest carpet post-consumer carpet (PCC) flows of 2-3.5 Mt to landfills in the United States (US) annually [73]. Wang [74] estimates that the US is responsible for ~50% of global carpet disposals. PCC was estimated to be 3.2% of California landfill volume [75] and to be 2% of landfill mass in the United Kingdom [76]. This unused material had an estimated $750M value in 2004 [77]. PCC represents a large, but underutilized, resource

[77], [78], [79]. Understanding these material flows is imperative to moving towards a more circular economy [80].

With such a large mass of PCC, the carpet industry has garnered legislative and regulatory scrutiny around the end-of-life (EOL) processing in the US. A key example is the expanded producer responsibility (EPR) legislation to increase carpet diversion from landfills and recycling adopted in California. In California, the Carpet America Recovery Effort (CARE) is the organization tasked with developing and administering plans to meet requisite carpet diversion and recycling rates [75], [81]. Actions to meet these regulatory requirements has led to 103 carpet collection locations in California, which is twice the number of collection sites as in the remaining 47 contiguous states combined [82], [83]. Similar carpet recycling regulations are now under consideration in four other state legislatures [84], [85], [86], [87]. These bills propose a consumer-paid fee on carpet, with funds used to incentivize carpet collection, recycling, and re-use [75]. California Assembly Bill 1158 required a 24% diversion rate in California by 2020 [88]. If passed, proposed legislation would require a 14% diversion rate in Minnesota by 2024 [84], a 25% diversion rate in Illinois by 2023 [86], and a 25% diversion rate in New York by 2027 [85]. Drafted legislation in Oregon would set a phased transition to a 75% recycling rate with a required 40% being “close-loop” recycled (dates for the transition have not been set) [87]. With increased interest in supporting a circular economy and the use of policy mechanisms to drive such action, the availability of resources from carpet at its EOL is expected to grow. Quantifying these material flows by constituent is needed to demonstrate the secondary resource availability and to identify industries that could utilize these flows.

2.2. A material flow analysis of US carpets

The composite nature of carpets can make end of life (EOL) processing challenging. While natural fiber carpets can be diverted from landfills by leveraging their unique composition (e.g., applying the waste fibers as fertilizer [89]), natural fiber carpets constitute less than 1% of carpets in the United States [90]. Ubiquitous synthetic-polymer carpets do not readily biodegrade in a landfill environment [91]. Some manufacturers have attempted short-lived carpet leasing schemes to shift the responsibility for EOL processing to manufacturers, thus encouraging carpet design to re-utilize waste flows [92]. These systems rely on specific waste-carpet compositions and material availability can be limited [93]. As is the case in all EOL resource utilization, PCC decision making needs to consider the environmental impacts associated with EOL processes [76].

Beyond landfilling, common EOL pathways for carpet include carpet reuse, material recycling, or thermal energy recovery. Using life-cycle assessment (LCA) methodologies, Morris [94] and the US EPA [95] examined landfilling, energy recovery, and recycling EOL processes for polymer carpets to show recycling offsets more CO_2-eq than it produces. Specific studies on certain carpeting types have shown that nylon recycling contributes less than 1% of the CO_2-eq emissions over its life cycle with the raw material acquisition accounting for ~70% of CO_2-eq emissions [96].While different polymer types in carpets can lead to a range of environmental impacts, they typically perform the same function [97]. Such findings demonstrate how the production of carpet is ripe for redesign under a circular-economy perspective [96], [97].

Energy recovery as an EOL pathway involves using PCC as a feedstock for heat or electricity waste-to-energy (WTE) generation or as a high-temperature fuel for industrial processes. WTE conversion of carpet could produce 13 trillion BTUs of energy while reducing landfill volume [90]; however, the environmental impacts may be greater than other energy feedstocks [98]. While post-consumer carpeting (PCC) led to lower emissions than coal power [94], the impacts are greater than energy from natural gas

combustion and the 2003 average US electricity mix emissions [94], [95]. As an industrial process fuel, Lemieux, et al. [99] measured no increased CO emissions, but a 3-8% increase in NO emissions when co-firing shredded carpet with natural gas. These findings suggest that energy recovery may not be the most desirable utilization of PCC [95].

Reuse of PCC as an EOL pathway has been most successful with carpet tiles, largely used in commercial applications. The modularity of tiles facilitates cleaning and refurbishment [92]. Successful reuse of PCC as equestrian flooring has also been noted in the UK [98], with appropriate blending and treatment to remove hazardous materials [100]. Typically, carpet recycling can be broken into three categories: (1) physical separation and recovery; (2) chemical depolymerization; and (3) processing PCC for extrusion in to heterogenous composites [101]. Physical separation and recovery of carpet components, which has been considered for decades [102], involves the separation of polymers and textiles from the granulated backing (called post-consumer calcium carbonate or PC4, a CARE marketing term). The recovered portions are then process according to the material type. For example, polymers recovered through mechanical separation have been explored as reinforcement in concrete [103] or as reinforcement for laminate composites [74] and can substitute for virgin polymers in some applications. The PC4 contains $CaCO_3$ as well as residual impurities, including some polymer fibers and styrene-butane latex. These residual impurities have complicated the diversion of PC4 into value added production [72]. However, initial research has suggested PC4, with treatment, could find a second life as a concrete additive [72]. In depolymerization, the polymer components are broken down into the base monomers that can then be processed back into polymers that performs like virgin materials [73], [101]. Chemical recycling can support reuse of the resources without limitations associated with loss of performance during prior use [74], [104], [105]. The final recycling category involved the processing of carpets into polymer composites, but without separating constituents. This method has been used to produce molded plastic composites [92], such as for auto parts [95], and resin-treated structural materials [106]. While this strategy diverts carpet from landfills, the drastic performance variations of carpet-composites in literature restrict the potential

structural applications [98].

Literature on carpet recovery has focused on the logistical challenges of EOL collection, sorting, and processing with a primary focus on nylon recovery, potentially due to economic value [74]. Yet the large fraction of other material types is neglected. Realff et al. [77], [79] has published on optimizing carpet recycling systems, including models to optimize facility capacities and locations for nylon carpet collection, sorting and depolymerization recycling. Biehl et al. [107] considers the nylon carpet recycling and find that the PPC flow would not meet demand for recycled nylon without additional incentive to increase PCC diversion. Sas et al. [108] models carpet collection site coverage in the US and shows optimizing geolocation would allow reducing sites by over 50% while maintaining comparable coverage. Thoney et al. [105] incorporates the locations of PCC material consumers to optimize the geolocation and sizing of a nylon carpet recycling systems. Lu et al. [93] uses environmental consideration to inform pathway selection for new carpets made in part with recovered PCC and highlight the need for design to accept recycled materials as a key limitation. Data on non-nylon constituent flows is needed to better design recycling and reuse by considering the other material flows in carpets. In this analysis, we quantify the material flows which could facilitate future modeling of logistical systems to process a larger fraction of the PCC flows.

To quantify PCC flows, this work focuses on tufted carpets, which have made up the majority of the carpet market since 1957 [109] and remains the predominant carpet consumed in the US [110]. Tufted carpet is a composite material of front-fibers (i.e., tufts) that protrude from a textile backing material and are held in place by a styrene-butadiene latex adhesive mixed with calcium-carbonate ($CaCO_3$), which provides weight to the backing [74]. A schematic of this system is depicted in **Figure 1.1**. Since the 1970's, the predominate fiber and textile components of carpets have been synthetic polymers, such as nylon, polypropylene (PP), and polyethylene terephthalate (PET) [111].

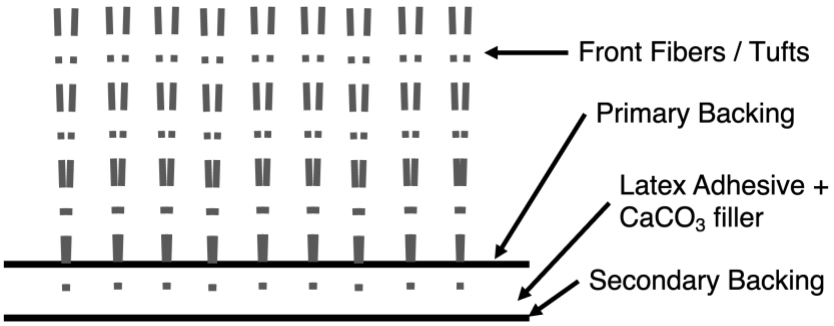

Figure 2.1. An illustration depicting the simplified construction of typical tufted carpet

Here in, we quantify PCC flow by material constituents to systematically quantify for the first time resources available from PCC disposal stream. We model in-use stock and PCC flows in the US. Using annual production data and a lifespan distribution for carpet we quantify the annual waste flows by material constituent (e.g., polymer fibers, backing materials, etc.). To demonstrate the potential for these flows to advance a more circular economy, we compare the annual disposed carpet polymers to production statistics of virgin polymers in the US and disposed PC4 to limestone in cement production. Further, we illustrate the ability for this materials substitution to contribute to sustainability by quantifying the potential avoided environmental impacts from virgin material production.

2.2.1.Methods

This work uses a material flow analysis (MFA) to evaluate carpeting and the flows of the material constituents in carpeting in the US. MFA relies on the conservation of mass as flows move through processes. Using a mass balance, we quantify the amount of PCC not diverted to reutilization or recovery pathways and is released to the environmental or landfilled. From this, we quantify the unrecovered material flows and compare them to virgin production of similar materials. This is used to highlight potential materials markets that could increase sustainability through resource reuse.

2.2.1.1. Goal, system, and scope

The goal of this MFA is to quantify the EOL fiber, textile, and mineral flows in carpet removed

from stock, where findings can be used to advance PCC diversion from landfills and to inform the design of systems for material recovery and reuse. The mass conservation implicit in MFA allows us to identify the current EOL outcomes for all carpet produced, a new understanding that is needed to establish pathways to mitigate environmental damages, to understand the ability to meet current regulatory goals, and to understand resource valorization markets. A system diagram for the MFA is shown in **Figure 2.2**.

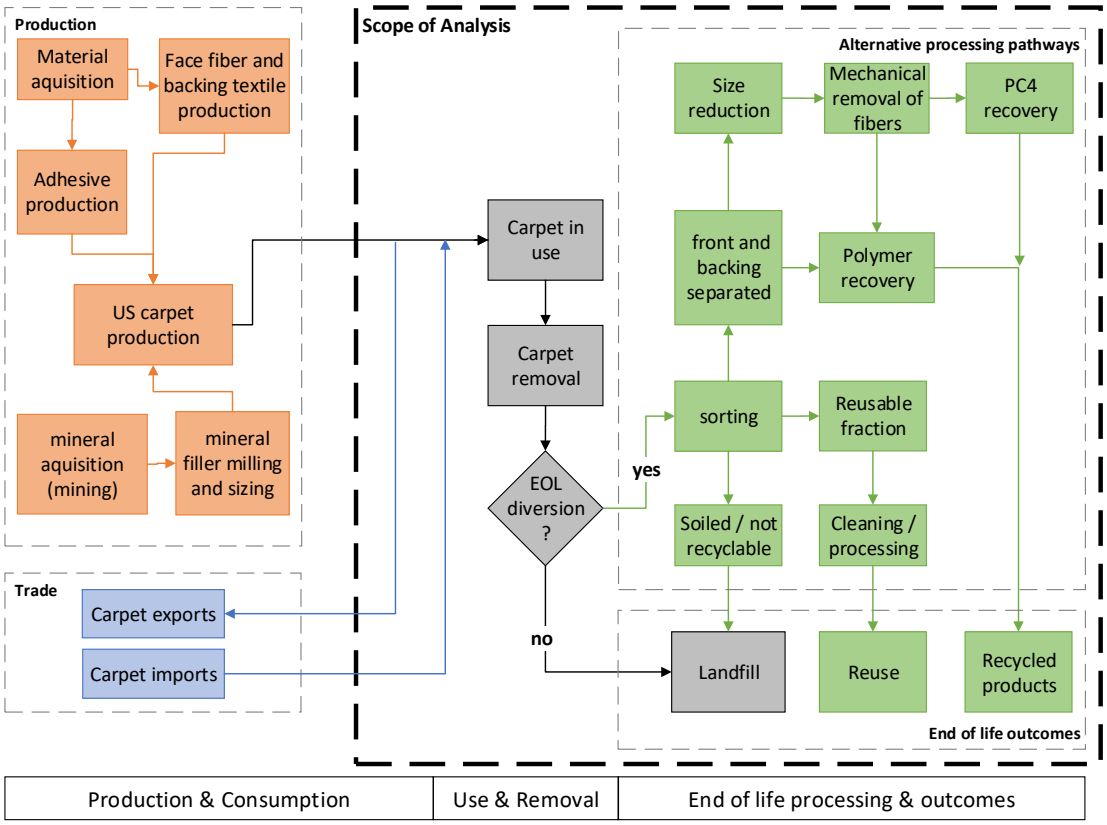

Figure 2.2. System diagram showing carpet production, use, and end of life (EOL) phases. EOL outcomes are considered in this analysis, but specific processes are not. Here, EOL pathway processes are shown as examples of potential pathways (e.g., mechanically recycling for material separation and reuse), but are not exhaustive of all EOL processing pathways.

This analysis considers carpet flows in the United States (US) for carpeting produced from 1950-2018. We examine tufted carpet, as it has been 97% or more of the annual production since 1973. This analysis considers US domestic production, imports, and exports of carpeting to quantity annual stock change and uses a lifespan distribution to quantify annual removals from stock. Natural fibers make up a

small amount of US carpeting, but are considered as a flow in this analysis. The EOL outcomes are modeled from 2002 on, the earliest year of EOL data available. As the efficiency of EOL processing methods vary by recycler and carpet type, the material flows in the PCC are quantified without consideration of a specific processing methods. However, mechanical recycling is shown in **Figure 2.2** as an example of one such method.

2.2.1.2.Data utilized

2.2.1.2.1. Carpet production

Carpet production, imports, and exports are the initial flows into the system considered. Production data from 1950-1959 was collected from carpet industry reports published by the Wharton School of Finance and Commerce [109]. The data for production from 1950 to 1959 did not include the type of front fiber nor backing material and, thus, the constituent flows during these years are not modeled. For data from 1960 to 2010, the US Census Bureau published quarterly or annual reports on US carpet production, including production by carpet fiber composition (Appendix A, **Table A.1**), are leveraged. From 2010 to 2018, annual sales reported by CARE are used as a proxy for production (Appendix A, **Table A.1**). CARE also reports the annual breakdown of the recycled carpet by polymer type. While sales likely under-estimate the actual amount of carpet produced, both the CARE sales data and US Census Bureau data is available for 2008 and 2009 facilitated a comparison across reporting schemes. In these years, the CARE sales data are within 7% of the US Census Bureau carpet production data. Over the 68 years of data collected, reported statistic and categories changed. This variation in reporting led to occasional gaps in composition data. In these cases, the missing data were interpolated or extrapolated linearly (Appendix A, **Table A.3**).

Import and export data for tufted carpets was collected from the USA Trade Online database [112] (Appendix A, **Table A.2**). As imports and exports averaged ~5% of carpet flows during the years modeled, we assume that trade did not affect average fiber composition. Due to a lack of trade data prior to 1977,

percentages of import and export from 1978 were assumed to be the consistent in the preceding years (Appendix A, **Table A.3**). Averages composition data is used to calculate the flow of constituent materials. Calculated as the 1968-2008 averages from US Census production data, we use 1.46 kg/m^2 as the unit mass of face fiber and 4.27 kg/m^2 as the average unit mass of carpet. From composition data in Realff [113] and the average mass fractions of backing textile, PC4, and face-fibers are assumed to be 10%, 44%, and 47.5%, respectively (Appendix A, **Table A.4**).

2.2.1.2.2.Carpet lifespan

To determine the lifespan distribution for carpet, a semi-systematic review of the literature was performed using Google Scholar with search terms: "carpet LCA", "carpet lifespan", and "average lifespan of carpet." The lifespan of the carpet varied in the literature depending on analysis, application, and carpeting type. In use service life estimates were collected from 14 publications (data is summarized in Appendix A, **Table A.5**) to create lifespan distributions of carpeting. Examples of values reported in literature to inform the in-use distributions include:

- Bowyer et al. [71] evaluates carpets compared to other floorings estimating lifespans of 11 and 25 y for polymer and wool carpets, respectively.
- Stephan and Athanassiadis [80], in an evaluation of non-structural material flows in Melbourne, Australia, use lifespans of 10 y for both wool and polymer carpets.
- Junnila et al. [114] considers polymer carpet in a life-cycle assessment European office buildings to have a 4 y lifespan.
- Outhred [115] recommends apartment landlords to assume a 5 y replacement rate in their cost analysis.
- The national home builders association (a US organization) suggests a lifespan of 8-10 y for home owners [116].

2.2.1.2.3.Carpet end of life

The reutilization of carpeting materials at their EOL is dependent on appropriate diversion from landfilling. Data on EOL outcomes for diverted PCC were collected from CARE annual reports from 2002-2019 (Appendix A, **Table A.1**). CARE relies on industry surveys to collect data [117], these data are also used by the US Environmental Protection Agency (EPA) to quantify carpet diversion from landfills [118].

2.2.1.2.4. Potential material markets

To contribute our discussion on material markets, we compare the material flows from EOL carpet to the production of similar virgin materials. We focus on substituting recycled materials for virgin material production because reuse and recycling are show in the literature as the lowest impact EOL pathways. Whether the carpet is reused or recycled, it would decrease the need for additional virgin materials. Polymer flows from carpet disposal are compared to US virgin polymer production. Annual polymer production data from 1995 to 2014 for nylon, PP, and PET was collected from Commodity Resource Bureau reports (see Appendix A, **Table A.7**). Annual PC4 removal is compared to resources used in Portland cement, another limestone-based product, production from 1994 to 2019. Namely, limestone is used in two primary ways during Portland cement production: (1) as a mineral feedstock to produce clinker, a solid precursor to Portland cement; and (2) for inter-grinding during finish milling of clinker to produce a Portland-limestone cement [119]. Data for annual cement and limestone for cement are show in Appendix A (**Table A.5**).

Recycling/reusing these materials could lead to reductions in the environmental burdens both by avoiding landfilling and by avoiding virgin material production impacts [95]. The potential to mitigate environmental impacts from virgin material production is quantified with life-cycle inventories: US LCI Database [120] for US production of PP and PET polymers [121], and for US cement production [122], and from the ecoinvent 3.0 database [123] for nylon 6 and nylon 6,6 production in Europe (note: a US model was not available) [124].

2.2.1.3.Quantifying stocks and flows

2.2.1.3.1. Material flows into and out of stock

The apparent consumption, annual in-use stock, and annual disposals of carpet were determined to inform material flows. Annual apparent consumption, or flow of carpet into use, is calculated using **Equation 2.1** where, for year "i", v_i is the apparent consumption (mass), p_i is the production mass, z_i is the imported mass, and x_i is the exported mass.

$$v_i = p_i - x_i + z_i \qquad \textbf{Equation 2.1}$$

The mass of material constituents in carpet are modeled on an annual basis because the average carpet composition varies over time. The flow of materials into stock, $[Mass\ Material]_i$, is calculated as a mass fraction of the carpet annual consumption with **Equation 2.2**; where $[Mass\ \%]_i$ is the mass fraction for the constituent of interest (e.g., nylon or PC4). The removal of materials from stock can be modeled using the carpet lifespan distribution and the annual flows into stock. The mass of carpet removed from stock "n" years after consumption is determined using **Equation 2.3**, where r_n is the percentage of carpet removed after "n" years and $d_{n,i}$ is the mass of carpet consumed in year "i" that is removed "n" years later. Development of the r_n values is discussed below. The mass of carpet constituents removed is modeled in the same way by substituting v_i with $[Mass\ Material]_n$ in **Equation 2.3**.

$$[Mass\ Material]_i = [Mass\ \%]_i * v_i \qquad \textbf{Equation 2.2}$$

$$d_{n,i} = r_n \cdot v_i \qquad \textbf{Equation 2.3}$$

With this production-based accounting, the total mass of material removed (d_k) from stock in a year of interest (i.e., year "k") can be calculated with **Equation 2.4**. The same process is used to calculate

the removals from stock by material type, $[Mass\ Material]_n$. In this analysis, MATLAB is used to compute the annual disposal in matric form as illustrated in **Figure 2.3**.

$$d_k = \sum_{i=1}^{k-1} d_{k,i} = d_{k,1} + d_{k,2} + \cdots + d_{k,k-1,} \qquad \textbf{Equation 2.4}$$

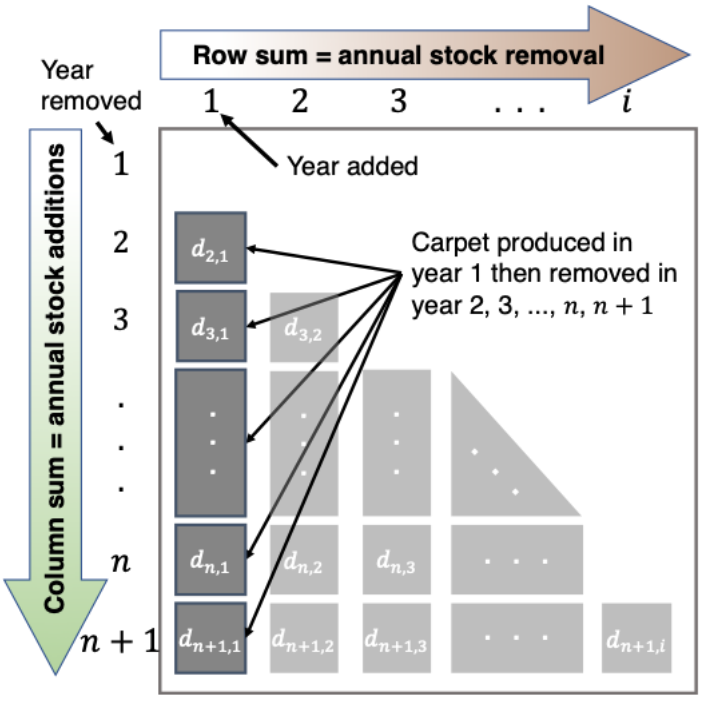

Figure 2.3. Illustration of matrices created to model the total amount of material removed from the stock annually. The notation $d_{n,i}$ indicates materials added to stock in year i and removed from stock in n.

Finally, the annual stock can be calculated using **Equation 2.5**; where $[stock]_k$ is the stock of carpet in year "k". For other materials, the stocks are calculated by replacing v_k and d_k with the analogous value for the material stock being modeled. For the first year modeled, the previous year's stock, $[stock]_{k-1}$, is assumed to be zero.

$$[stock]_k = [stock]_{k-1} + v_k - d_k \qquad \textbf{Equation 2.5}$$

2.2.1.3.2.Carpet lifespan distribution

The lifespans used in literature were tallied to form a frequency distribution (see **Figure 2.4**). For works that used a range for service life, each integer in the range was counted as one possible value: e.g., a reported range of 8 to 10 y would be represented as 8, 9, and 10 y lifespan values (3 counts). To perform a scenario analysis, the role of an increased or decreased lifespan on disposal rates was explored. Namely, a shorter lifespan distribution was created by reducing the life by 3 years and a longer lifespan distribution was created by adding 3 years to the initial distribution (modeled lifespan) (see **Figure 2.4**). These lifespan distributions were used to calculate the percentage of carpet removed from stock at different ages (disposal rate), indicated by r_i in **Equation 2.3**.

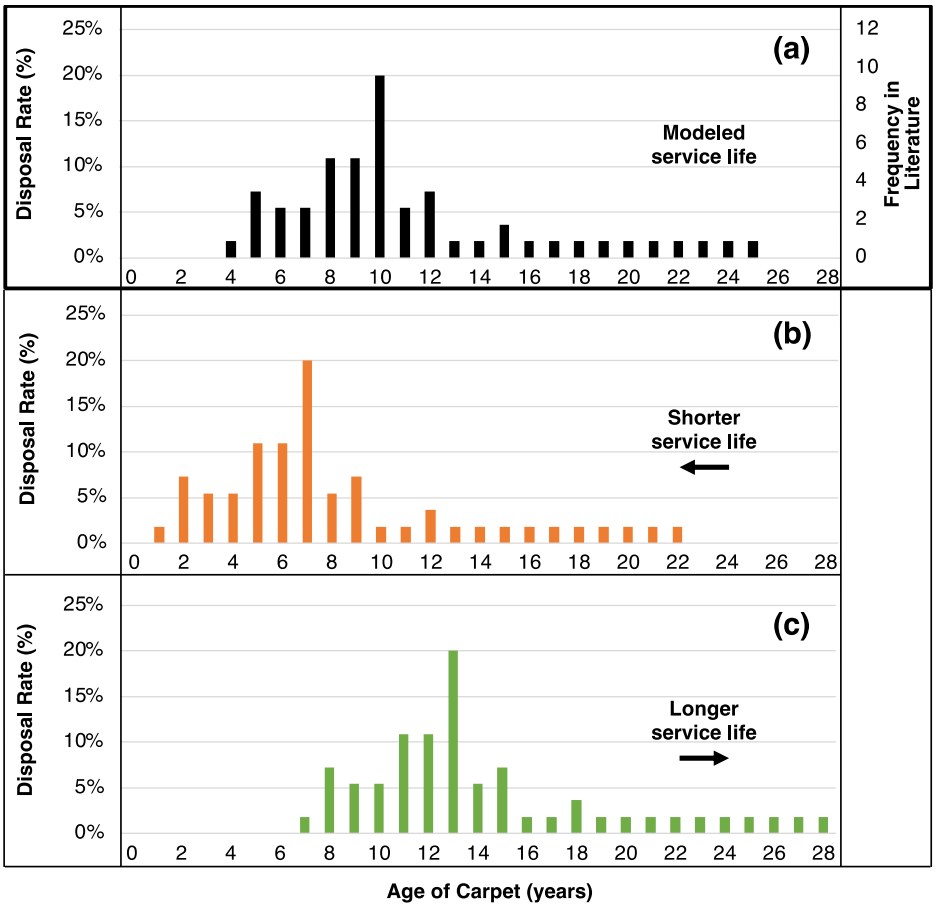

Figure 2.4: Disposal rates calculated from carpet lifespans used in literature: (a) collected values from literature; (b) shorter lifespans (reduced by 3 y); (c) longer lifespans (increased by 3 y).

2.2.1.3.3.Carpet end of life

The main EOL outcomes for collected PCC are: (1) recycling or reuse; (2) waste-to-energy (WTE) (e.g., via combustion); or (3) higher temperature industrial process energy (e.g., cement kiln fuel). In addition to these EOL pathways, some CARE reports also quantify material that is collected and then landfilled after diversion (presumably because it could not be processed with one of the pathways). We assume the mass of carpet that is not diverted is landfilled or lost to the environment. To quantify the mass of carpet not collected, the total mass of EOL outcomes reported by CARE was subtracted from the mass of discards modeled for each year.

2.2.1.4. Examining benefits of resource use in potential material markets

Flows for PC4, nylon, PP, and PET, the four most prevalent materials from EOL carpet, are compared to virgin material production flows as an illustration of potential material reuse sinks. The masses of the recycled material flows are quantified as percentages of the total virgin material production to demonstrate the available supply of the EOL material flow. To calculate percentages, the recycled material mass is divided by the production mass of the virgin material for the same year and multiplied by 100%.

We extend this comparison by quantifying the potential avoidable environmental impacts by scaling the EOL material flows with LCI data. Pathways for utilizing EOL carpet flows remain variable (e.g., different pathways and mechanisms for extracting materials, need for additional processing based on material type, varying reuse application). Herein, only the environmental impacts from avoiding the virgin material production are quantified. The TRACI impact scheme is used with LCI data and factored by the mass of the material flow. For flows greater than the virgin production mass, the maximum mass for substitution was modeled as 100% of the virgin material mass. Impact categories for global warming potential (GWP, CO_2-eq), respiratory effects ($PM_{2.5}$-eq), ozone depletion (CFC-11-eq), smog (O_3-eq), acidification (SO_2-eq), eutrophication (N-eq), carcinogenics (CTUh), non-carcinogenics (CTUh),

ecotoxicity (CTUe), and fossil fuel depletion (MJ surplus) are quantified with TRACI 2.1 [125].

2.2.2. Results

2.2.2.1. Carpet in the United States

The flow of carpeting in the United States since 2002 is shown in **Figure 2.5**a. Since 2002, over 52 Mt of carpet has been removed with stock with ~50 Mt being landfilled or lost to the environment. Yearly diversion from landfills ranged from 1% to 5.5%. The largest magnitude of reused or recycled carpet was ~135 kt in 2012, reflective of ~4.2% of removed carpet. After dropping in 2013 and 2014, the percentage of reused or recycled carpet rebounded to ~4.3% (~92 kt) in 2019. Coinciding with this shift, the percentage of carpet use for WTE or kiln fuel has decreased since 2014. It would be expected that this change in EOL processing would decrease environmental impacts of diverted carpet [94], [95]. This figure shows that there is a large untapped flow of materials that needs to be diverted to meet upcoming regulatory targets.

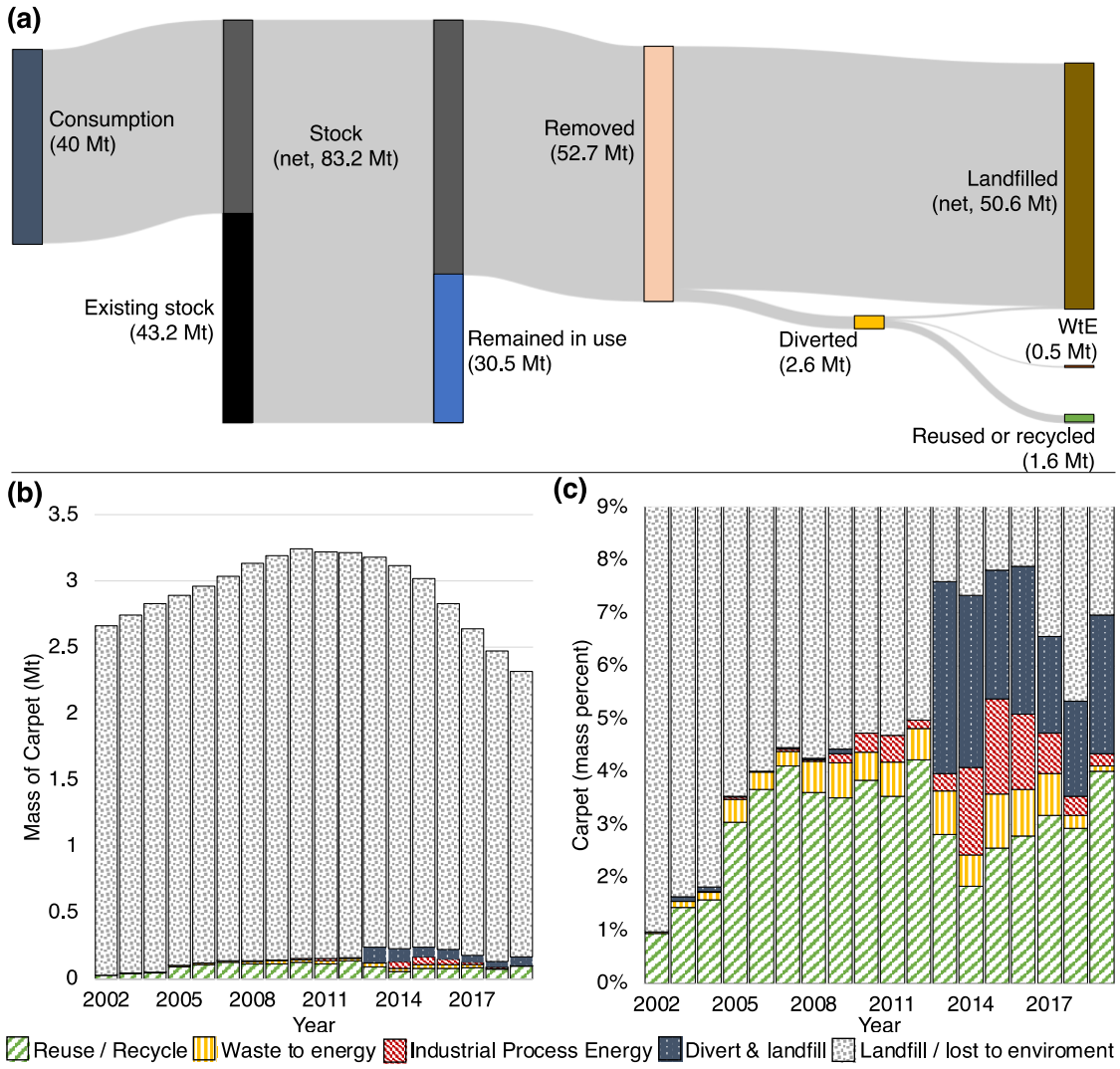

Figure 2.5. Carpet flows and EOL outcomes from 2002-2019. (a) Shows the sum of carpet flows from 2002-2019. (b) Shows EOL outcomes by mass of carpet. (c) Shows EOL outcomes by mass percent. Divert & landfilled is carpet that is collected, but then landfilled. Incineration data reported in 2015 is included in the Divert & landfill amounts for that year. *Note: y-axis in (c) is trimmed to show the fraction for non-landfill EOL outcomes, Landfill/ lost to the environment is only partially shown and sums to 100%.*

2.2.2.2.Carpet production, stock and material removal

Quantifying flows by material type is important for identifying suitable markets for diverted and recycled materials. Figure **2.6** shows modeled carpet stock and carpet disposal relative to production. Carpet production peaked in 2006 / 2007, but nearly halved in 2008 to 2010, likely coinciding with the Great Recession beginning in 2008 [110], with production rates remaining well below 2006 levels. As anticipated, disposal of carpet mirrors carpet production, albeit delayed (*Figure* **2.6***b*). The delay is approximately 10

years, resulting from ~54% of carpet having an 8-12y lifespan. The peak carpet stock, in 2006, is equivalent to ~50% of the combined residential and commercial building stock square footage (excluding agricultural, warehouse, and manufacturing stocks) [126], [127]. The decrease in stock during 2008-2012 likely fails to capture actual consumer behavior during a recession; however, lower stock values in subsequent years, despite improved economic conditions, is consistent with expectations [110]. Notably, there is only production data through 2018; as such modeled carpet disposal after this time do not include new input from carpet produced after 2018.

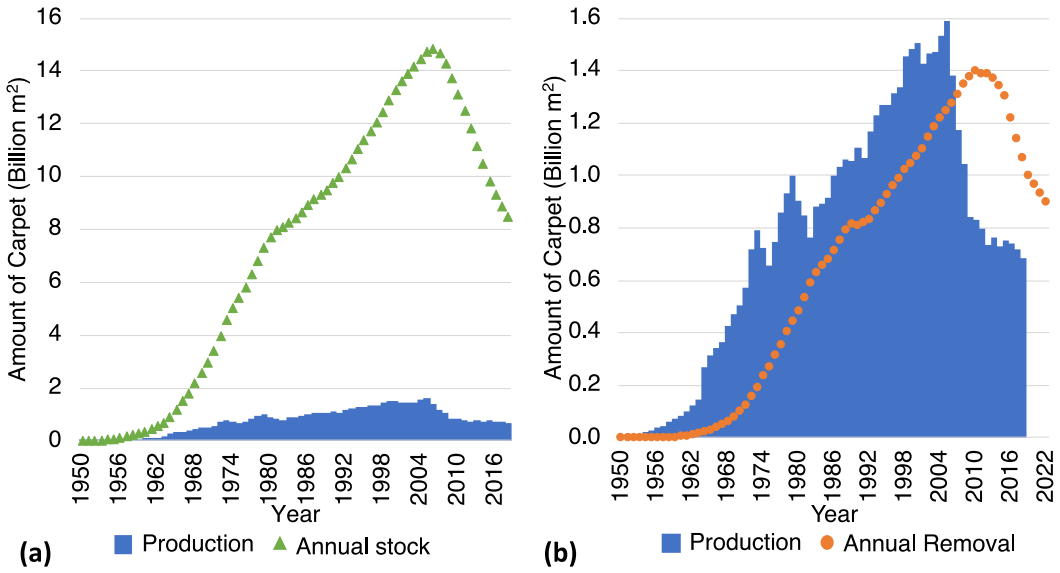

Figure 2.6. Tuft carpet production, removal from stock (disposal), and in-stock model: (a) Annual in-stock average and tuft carpet production data, and (b) annual discards and tuft carpet production data. Brackets show the range based on the two lifespan distributions.

As the material flows are calculated using an average annual mass percentage, the shapes of the disposal flows mirror that of the carpet removal. Figure **2.7** shows the carpet produced by fiber type (Figure **2.7**a) and the mass of front-fiber and textile backing materials disposed of by year (Figure **2.7**b). Both plots show that nylon is the dominant fiber type in disposed carpet, followed by PP and PET. Other fibers, including non-polymer fibers, were dominant from 1964 to the 1970's; however, the introduction of nylon fibers around 1960 led to synthetic polymers becoming the dominant material for carpet production [109].

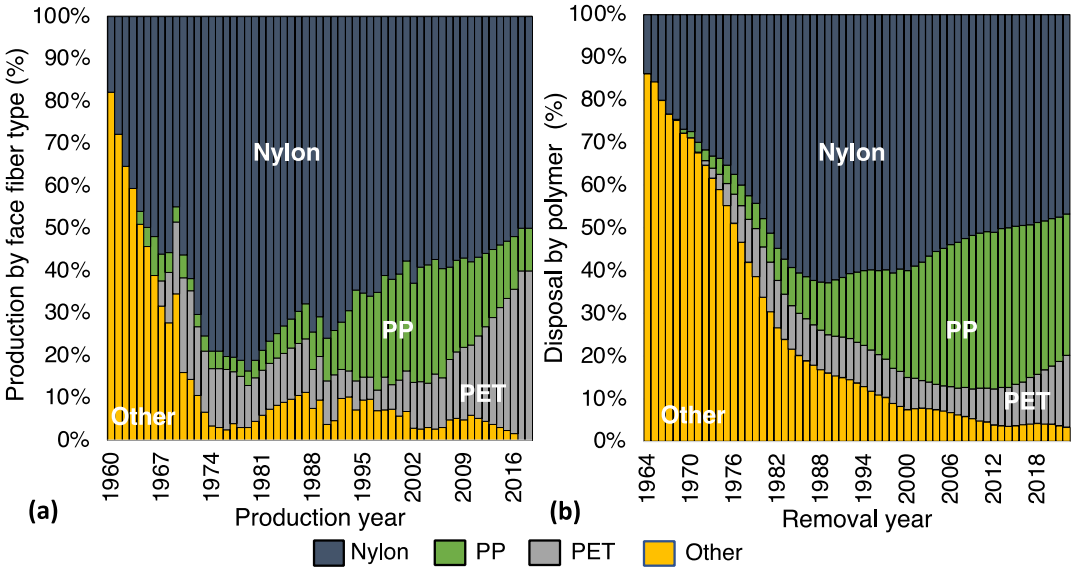

Figure 2.7. (a) Percentage of carpet made with each face fibers (Nylon, PP, PET, and other fiber) by year produced and (b) composition of fiber and textile-backing material disposals, by year. The category of "Other" includes non-polymer materials.

The mass of fiber and textile materials is show by removal year (**Figure 2.8**). Approximately 33 Mt of nylon, 16 Mt of PP, and 5.5 Mt of PET from carpet have been disposed of between 1954 and 2022. The largest amounts of nylon and PP were disposed of in 2010 and 2013, respectively. The year with the greatest nylon disposals is also the year with the largest total discards. The increase in disposed PP corresponds with the increased use of PP as backing textiles. As was anticipated for the scenario analysis with modified lifespans, the disposal masses shifted by the same number of years the lifespan distribution was adjusted. The shorter lifespans led to faster removal with the peak removal reached 3 y sooner and the longer lifespan shifted the peak back 3 y. The total magnitude of the removal remained largely unchanged.

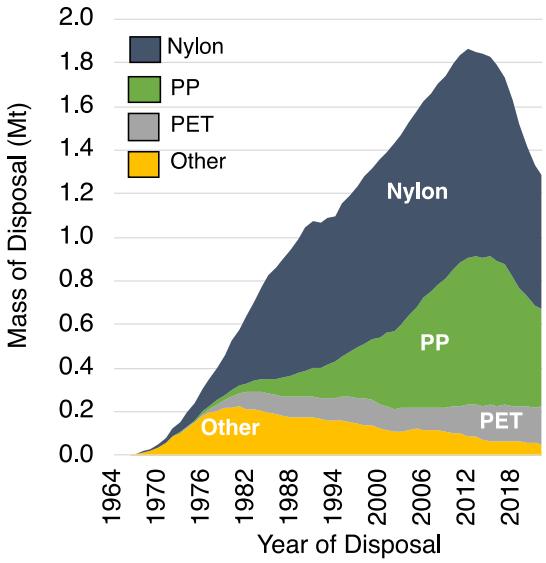

Figure 2.8. Annual fiber and textile material removal by type.

The annual PC4 in-stock and amount of PC4 disposed were modeled using average mass fractions (**Figure 2.9**). As of 2018, PC4 stock measures approximately 15 Mt. In total, approximately 49 Mt of PC4 is estimated to have been disposed of between 1954 and 2022, with the largest amount (~1.4 Mt) removed in 2010. In 2022, the disposal is expected to be ~1 Mt. As with polymer disposals, shorter lifespan shifted the removals forward 3 y and the longer lifespan shifted the curve backwards by 3 y, with little change to the magnitude of removed material.

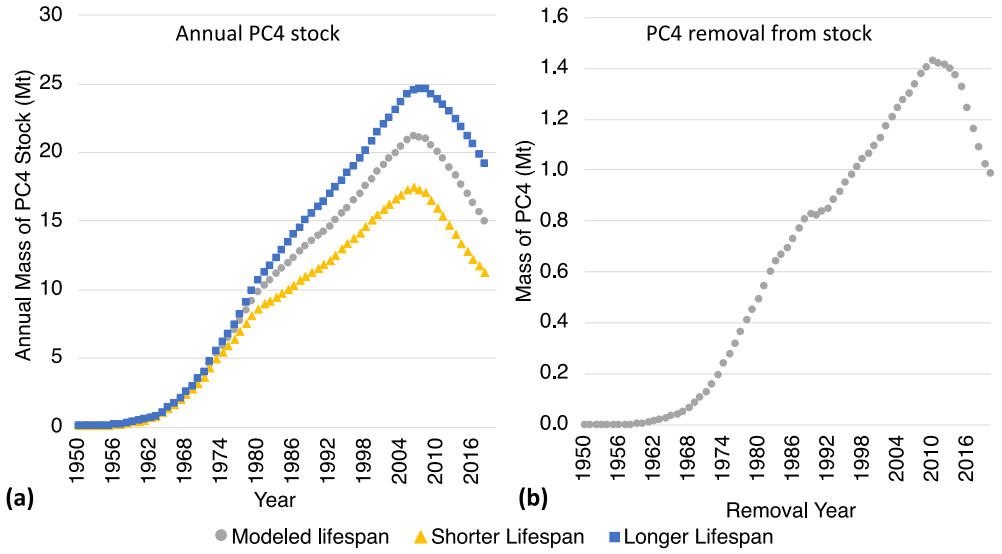

Figure 2.9. Model for annual mass of PC4 in-stock and annual PC4 discards. (a) shows impact of lifespan on stock (b) shows removals for the modeled lifespan.

2.2.3.Discussion

These findings show, annual removals from stock ranged from ~2.7-3.3 Mt between 2002-2008. These results are in agreement with some of the literature (e.g., 2-3.5 Mt estimate by Moody and Needles [73] and 2-3 Mt estimate by Wang [74]). The findings are notably higher than others (~1.5 times the 2 Mt estimated by McNeil et al. [89] and approximately twice the ~1.6 Mt of PCC estimated for 2012 by CARE [128]). While it is possible that carpet disposals during this time were delayed due to the recession, even under the lengthened lifespan distribution our model shows disposal flows ~1.5 times the size of CARE's sales-based disposal predictions. Since an MFA uses a mass balance to consider all flows in and out of the system, these findings could indicate that current industry methods are under-estimating EOL carpet flows and over-estimating the success of recycling programs.

From a circular economy perspective, if similar material performance can be achieved, nylon and PP from carpet disposal could substitute a notable amount of virgin production. As shown in **Figure 2.10**a, the mass of nylon from carpet discards exceeded the production of nylon in the US in all years studied, with the highest discarded mass, in 2009, exceeding 200% of production. Removed PP mass (**Figure 2.10**b)

ranged from 5-10% of PP production, with increased rates in recent years likely from PP being the predominant textile backing material. Removal of the third most common polymer, PET (**Figure 2.10**c), after 1997 were less than 1% of US production; as such, they would not constitute a large replacement potential. Yet it must be emphasized that textiles are not used in isolation within carpets; rather backing materials (e.g., PP) and PC4 are substantial fractions of carpet mass. Findings from this work, which address the multiple materials present in carpet disposals, are critical for valorizing EOL carpet and to maximize material recovery.

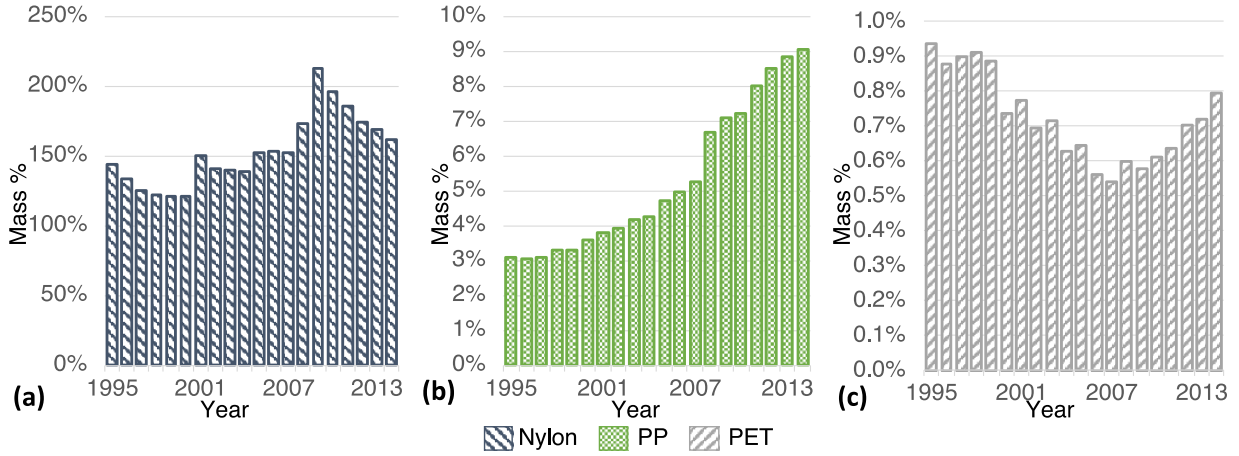

Figure 2.10. Mass of polymer discards show as a percentage of annual US production of virgin polymers (a) Nylon, (b) PP, and (c) PET. *Note: y axis changes across all three plots.*

Given the prevalence of trace materials and remnant polymers [72], PC4 has found fewer value-added markets compared to fiber and textile materials. Current research has focused on PC4 as a constituent for various civil infrastructure materials [72], [129]. The low mass fraction of PC4 removed relative to clinker production and inter-ground limestone consumption (**Figure 2.11**) demonstrates the possibility of using PC4 in cement-based materials or in other limestone-based application as a low level additive would be unlikely to shift material performance. The findings of this work show that, between 2009 and 2011, PC4 mass from carpet disposal was equivalent to approximately 90% of limestone mass used for cement finish milling and over 1.5% of limestone used for clinker production. With reductions in carpet disposals,

these percentages have decreased recent years, now at approximately 30% of limestone used in finish milling and just under 1% of the mass of limestone used in clinker production. Despite being a relatively small fraction of virgin limestone used for clinker, this represents a large resource savings given the scale of limestone consumption (~100 Mt in 2019) [130].

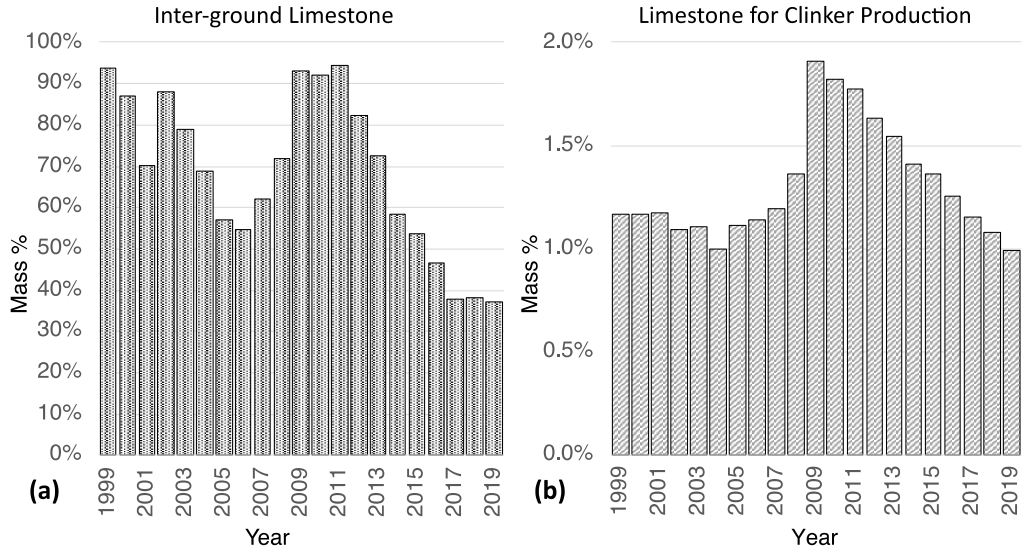

Figure 2.11. Mass of PC4 discards show as a percentage of annual US consumption of virgin limestone for (a) finish milling during cement production and (b) clinker production for cement. *Note: y-axis changes.*

To demonstrate potential environmental benefits from using EOL carpet resources as substitutes for virgin material production, we examine the environmental impacts from producing the comparable material. **Figure 2.12** shows the annual potential GWP, respiratory, and fossil fuel depletion impacts from virgin material production that could be avoided. The remaining impacts from the TRACI weighting scheme are presented in Appendix A (**Figure A.1**). While it is unlikely to recover all resources and fully offset the impacts of virgin material production, an initial estimate indicates potential benefits of recycling carpets (note: impacts from recycling, transport, or process emissions are not considered; comparisons are drawn exclusively on the potential mass-replacement basis). Across the three environmental impact categories, nylon substitution could lead to the highest impact reduction: approximately 4.7 Mt $CO_{2\text{-eq}}$, 1.1 kt $PM_{2\text{-eq}}$, and 8.7 TJ annually. This is because nylon is the second largest material flow evaluated and virgin nylon

production has the highest production impact in these categories. Substitution of PP is the second highest average reduction potential for fossil fuel depletion (~5.4 TJ, annually), and the use of PC4 as a partial substitution for clinker in cement (i.e., the use of PC4 as an additive, similar to inter-ground limestone in Portland-limestone cement blends, which lower clinker demand [72]) is the next highest reduction potential for GWP (~1.65 Mt CO_2-eq, annually) and respiratory effects (~.5 kt $PM_{2.5}$-eq, annually). The reuse of all four material flows from PCC could lead to reductions of up to 7.5 Mt CO_2-eq emissions, 2 kt $PM_{2.5}$-eq respiratory effects, and 15 TJ of energy each year in the US.

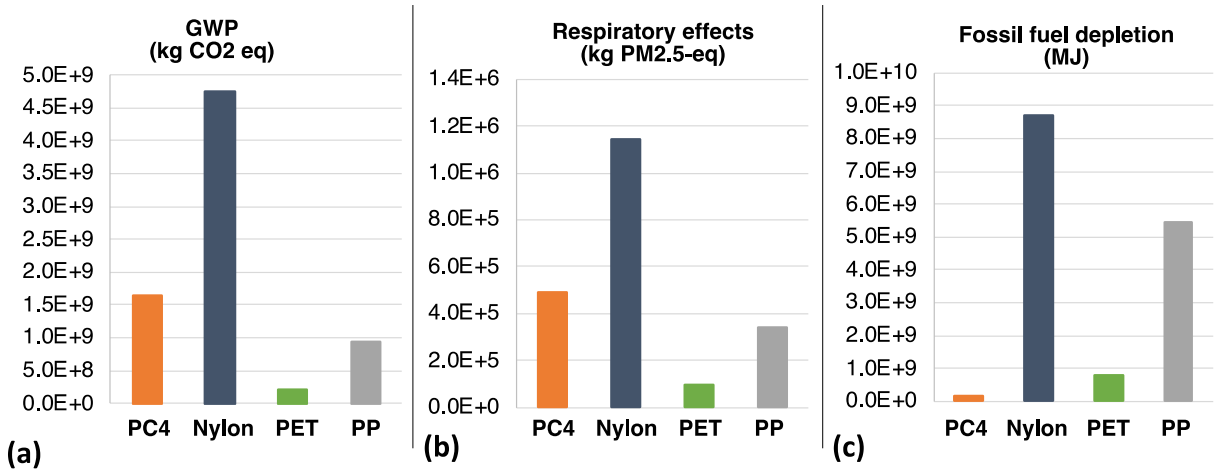

Figure 2.12. Average annual impacts from virgin material production that could be avoided by substituting with recycled carpet products: PC4 (substituted for cement production) between 1999-2019 as well as nylon, PET, and PP substituted for virgin polymer production from 1995-2014.

Importantly, these reductions reflect only avoidable impacts from virgin material production and not the net-reduction in environmental impacts from the diverted and processed post-consumer materials. As such, it is important for decision makers to understand the environmental impacts and economic costs associated with recycled material recovery, transportation, and treatments to determine if using these recycled polymers can deliver actual environmental benefits at reasonable economic cost. **Table 2.1** summarized initial considerations around the additional environmental impacts and economic cost reported in literature for material processing. However, decision makers should verify these impacts and costs for the given region, time period, and scope relevant to a specific process and use case being considered.

Notably, the additional environmental impacts from recycling and transportation could limit the potential environmental impact savings. For example, the average transport distance for onsite quarried materials at a Portland cement plant is 2 km by conveyor [122] or 46 km by truck for concrete production [131]. The average industrial byproduct for Portland cement production is transported 198 km by road; however, these materials comprise less than 10% of the Portland cement feedstocks [122]. As such, transporting PC4 to a Portland cement facility could lead to larger impacts from transportation. The actual impacts reduction would depend on the transportation distance, the local energy grid, and the recycling process. Additionally, the impact allocation method used to assign portions of these environmental impacts from recycling-related processes to the different recycled products (e.g., polymer, PC4). As carpets vary in composition and the value of these different polymer types differ, the actual environmental impacts assigned to PC4 could differ greatly depending on the allocation method selected.

Table 2.1. Summary of potential environmental impacts and economic cost considerations for PC4 reuse in Portland cement and/or concrete production.

Source	**Potential impact or cost**
Carpet recycling emissions	• For Nylon carpeting: 0.06 kg CO_2-eq / kg and 0.42 MJ/ kg (modeled in 2018 in the US) [96]. • Process based impacts, such as particulate matter or water use, should be expected, and will vary depending on the particulate emissions control put in place. • Reuse avoids landfill impacts (and transportation to landfill), which should be considered.
Transport emissions	• Truck transportation per ton-km: 1.69×10^{-4} kg GHG emissions, 2.26×10^{-8} PM_{10}, 2.6×10^{-8} $PM_{2.5}$, and 1 MJ energy demand in the United States [36].
Processing emissions	• Processing PC4 after separations would contribute to additional impacts via increased energy demands and likely process-based impacts (e.g., NO and particulate matter from industrial heat treatments and polymer combustion [113], particulate emissions from conveyance, particulate emissions and water demands for sieving and dust control) • Avoids quarrying impacts from virgin limestone production.
Economic costs	• Virgin limestone is cheap and abundant ($12.88 / ton [132]). • Recycling subsidies for PC4 are ~$375 / ton ($0.17/lb) (polymer subsidies range from ~$110-551 / ton depending on type and form) [133]. • Portland cement production is often co-located with the limestone quarry (lower transport costs). • Average 2021 truck transportation cost ~$0.40/ ton-km and rail transport was ~$0.08 / ton-km [134]. • Costs for energy, facilities, and labor would be an additional expense.

Regarding potential economic costs, PC4 recycling in California is economically incentivized with pricing subsidies. Currently the program administered by CARE provides a subsidy of ~$374/ton of PC4 that is recovered and diverted from landfills [133]. This subsidy could make PC4 more economically attractive despite the additional costs associated with transport (~$0.40 / ton-km by truck or ~$0.08 / ton-km by rail [134]), additional labor, and/or further PC4 processing expenses. Adopting additional filler materials for concrete or blended cement production may also require capital investments for handling equipment and storage facilities at the concrete production site. Additionally, if treatment of the PC4 is required to remove harmful compounds or improve the material performance, additional capital investment may be required. Replacing a portion of virgin limestone consumption with PC4 could extend the life of a quarry site and reduce localized, onsite impacts. Notably, these subsidies have changed over time and only reflect incentives for California. These tradeoffs between capital needs and operating costs should be considered together with regional cost considerations to determine the viability of PC4 adoption as a limestone replacement.

2.3.As-received PC4 characterization and evaluation in concrete

Construction of building and infrastructure systems is the largest consumer of materials in the United States [135]. There is continued expected growth in construction demand [136], [137] and with it, demand for infrastructure materials. There are many materials that are used in construction practice, including metal alloys [138], [139], plastics [140], and cement-based materials [141]. Portland cement is the primary binder in concrete, which is typically composed of a hydraulic Portland cement binder, water, and aggregates. Of the common construction materials, concrete is the most consumed by mass and has a relatively long in-use service period once constructed [141], [142]. These factors suggest that waste minerals, even if used in small fractions, could be incorporated into concrete in large quantities and, in doing so, be kept from entering waste streams for long periods of time.

The components in built systems have varying lifespans, which leads to material waste flows occurring at different times. A prime example of this service-life effect is the difference between the lifespan of carpet in a building and the concrete building components. A piece of carpet could be in-use for less than a fifth of the in-use period of concrete [143]. While materials such as carpets may not comprise a large mass of buildings, their high component embodied energy and the frequency of replacement could lead to their being a significant contributor to the total embodied energy of a building over its life cycle [143]. Currently, the United States (US) produces nearly 90 Mt of cement annually [144], with the majority being used in concrete [145]. From the national average cement content per cubic meter of concrete, 270 kg/m^3 [146], it can be estimated that approximately 320 million m^3 of concrete are produced every year. Approximately 821 million square meters of carpet is used in the US annually, based on sales in 2017 [147]. Each year, total discards of carpet are estimated at 1.5 Mt of carpet [147], less than 2% the mass of cement production. Due to this low relative mass fraction, there is a potential to use waste streams from one building component, carpets, in another, concrete, to increase the potential for construction materials to contribute to the circular economy, in which material loops are closed to extract maximum utility.

For decades, the exploration of using waste streams in concrete to reduce landfilling materials and, in certain cases, improve the properties of concrete has been an active area of study. It is well known that several industrial by-products, such as coal fly ash and blast furnace slag, have pozzolanic and/or cementitious properties that can benefit the performance of concrete [148]. The incorporation of other waste streams into concrete mixtures have been studied with various effects on material performance. For example, studies in literature range from replacing aggregates with crushed glass bottles and used tires [149], [150] to fillers produced from waste ceramic powder [151], [152] and marble dust [153]. Previous research on the utilization of carpet waste in concrete has focused on the use of plastic fibers [103]. The focus of these studies has been using carpet fiber to bridge concrete crack and improve factors such as concrete tensile performance and toughness (e.g., [103]). Classically, carpet backing has been considered to have no significant use and has been the major part of carpet waste being sent to landfills [103]. While initial investigation has been performed on the properties of carpet backing that could contribute to the performance of concrete, these studies have been limited [154]. The rising demand for Portland-limestone cements, which use 5 to 15% limestone blended with Portland cement [155], could lead to a notable market for the utilization of the calcium carbonate from post-consumer carpet backing if it is found to contribute to adequate concrete performance. Further, the increased use of blended cements, such as these, could act as a mechanism to mitigate greenhouse gas (GHG) emissions by lowering the overall clinker content in a set volume of concrete [156].

The objective of this work is to provide a foundation for understanding the functionality of using recycled calcium carbonate ($CaCO_3$) from deconstructed carpet— Post-consumer Carpet Calcium Carbonate (PC4)— as a constituent in concrete production. Limestone is used as a raw material for Portland cement production; however, there are other common uses for limestone in concrete, namely: (i) as a mineral admixture; and (ii) as aggregate. If PC4 can be used as a mineral admixture that can partially reduce cement demand while providing the same performance as Portland-limestone cement, there could be environmental benefits, most notably a reduction in GHG emissions. If PC4 can be used as aggregate,

benefits could be obtained if there are improvements in concrete performance or if there is a reduction in impacts through a reduction in landfilling of PC4 and the need to excavate and transport limestone rock. Thus, this work examines the effects of using PC4 to offset use of Portland cement or fine aggregates. Comparisons for the influence on material properties from using PC4 were drawn to conventional limestone fines (LS) as a partial replacement and a concrete mixture containing neither PC4 nor LS. Properties assessed in this work include the coefficient of thermal expansion, drying shrinkage, workability, flexural strength, compressive strength, void volume, and specific gravity. Additionally, changes in the associated GHG emissions of each mixture were quantified by performing environmental impact assessments of the concrete mixtures studied.

2.3.1.Materials and Methods

For this work, PC4 from recycled nylon 66 carpet was obtained from Circular Polymers located in Lincoln, California on March 14, 2019. From the recycling processes implemented at the plant, the PC4 was obtained with 99.39% passing a No. 40 mesh (420 um) and 64.47% passing a No. 100 mesh (150 um). To remove long remnant fibers, the PC4 was sieved through a No. 40 sieve (420 um). Comparisons were made with mixtures using LS obtained from Blue Mountain Minerals located in Columbia, California that had a fine gradation with 99.8% passing a No. 120 (125 um) mesh and 95.8% passing a No. 200 (75 um) mesh. To assess the effects of using PC4 relative to a typical concrete blend and relative to use of ground limestone, concrete mixtures were batched. The Portland cement used was ASTM Type II/V, obtained from Lehigh Southwest Cement Co in Stockton, CA. The fine aggregate was alluvial concrete sand sourced from Esparto, California. Two sizes of coarse aggregates were used, an intermediate gravel aggregate and a larger, crushed gravel aggregate, both obtained from Esparto, California (aggregate, PC4, and LS gradations are given in Appendix B, **Table B.1**).

This work examined how PC4 can act as a partial replacement for Portland cement or fine aggregate. For this assessment, two partial replacement levels were examined, namely 5% and 15% by

mass. These replacement levels were selected because they are currently used in Portland-limestone cements. The same replacement levels were considered for both the partial replacement of Portland cement and the partial replacement of fine aggregates. Control group blends were used for comparison, namely: 0% replacement, 5% replacement with LS, and 15% replacement with LS. The mixture proportions and mixture nomenclature used are shown in **Table 2.2**.

Table 2.2. Mixture proportions for concrete and mortar specimens

Concrete Mixture Proportions (units in kg/m^3)									
	Binder			Aggregates					
Mixture Name	Portland Cement	PC4	Limestone	5 mm	10 mm	25 mm	PC4	Limestone	Water
PC	411	0	0	516	382	763	0	0	193
C-PC4-5	390	21	0	505	382	763	0	0	193
C-PC4-15	349	62	0	482	382	763	0	0	193
C-L-5	390	0	21	514	382	763	0	0	193
C-L-15	349	0	62	510	382	763	0	0	193
FA-PC4-5	411	0	0	491	382	763	26	0	193
FA-PC4-15	411	0	0	439	382	763	77	0	193
FA-L-5	411	0	0	491	382	763	0	26	193
FA-L-15	411	0	0	439	382	763	0	77	193
Shrinkage and Setting Time Mortar Mixture Proportions (units in kg/m^3)									
	Binder			Aggregates					
Mixture Name	Portland Cement	PC4	Limestone	5 mm	10 mm	25 mm	PC4	Limestone	Water
PC	411	0	0	516	0	0	0	0	193
C-PC4-5	390	21	0	505	0	0	0	0	193
C-PC4-15	349	62	0	482	0	0	0	0	193
C-L-5	390	0	21	514	0	0	0	0	193
C-L-15	349	0	62	510	0	0	0	0	193
FA-PC4-5	411	0	0	491	0	0	41	0	193
FA-PC4-15	411	0	0	439	0	0	123	0	193
FA-L-5	411	0	0	491	0	0	0	41	193
FA-L-15	411	0	0	439	0	0	0	123	193

Concrete was batched using a MulitQuip MC64SE concrete mixer. Aggregates were mixed for 2 minutes before adding Portland cement and PC4 or LS, where applicable. Mixing then commenced for an additional 2 minutes prior to the inclusion of water. Water was gradually added as constituents were mixed for 3 additional minutes. Blended mixtures were allowed to sit for 3 minutes followed by a final mixing of 2 minutes. Batches were then molded. After 1 day, specimens were demolded and placed in a conditioning chamber set at 25°C and a relative humidity of 95%. Compressive strength testing was performed on

cylinders measuring 100 mm X 200 mm (4 X 8 inches); flexural strength tests were performed on prisms of 100 X 100 X 300 mm (4 X 4 X 12 inches); coefficient of thermal expansion test specimens were cut from 100 mm X 200 mm (4 X 8 inch) cylinders; density, permeable air voids, and porosity tests were performed on 100 mm X 200 mm (4 X 8 inch) cylinder specimens.

For the setting time and shrinkage experiments, mortar was prepared separately from the concrete mixtures, but the same replacement levels were considered. The mortar mixtures were batched in Hobart A200 dough mixer. To make mortars, fine aggregates were dried out in an oven at 120°C, then allowed to cool before mixing. Sand and powder were combined in the mixing bowl and mixed for 1 minute. After 1 minute, water was gradually added, and the mixture was mixed for 2 more minutes. The mixture was allowed to sit for 1 minute and finally mixed for 2 minutes before being molded. Shrinkage prism specimens were cast with dimensions of 25 mm X 25 mm X 285 mm (1 X 1 X 11.2 inches). Setting time mixtures were tested inn 154 mm X 154 mm (6 X 6 inch) cylinders forms.

2.3.1.1. Slump, Air Content, and Unit Weight

The partial replacement of aggregates and cement with mineral admixtures can have a significant influence on the fresh properties of concrete [157]. These fresh properties can affect the ability to easily place the concrete or inform the need to use certain chemical admixtures. For this reason, several fresh-state properties of the concrete mixtures were assessed. To determine the effects concrete workability, slump was measured following ASTM C143 [158]. To determine the effects of PC4 on air content and density, the air content in the fresh concrete was assessed following ASTM C231 [159] and the unit weight of the fresh concrete mixtures was assessed following ASTM C138 [160].

2.3.1.2. Setting times

To evaluate the effects of PC4 on setting time for the mixtures, experimental investigation of initial

and final set were performed following ASTM C403 [161]. For each mixture, three specimens were produced for testing. As the mortars set, the resistance to penetration was measured using an Acme Penetrometer and the initial and final set times were determined.

2.3.1.3. Isothermal calorimetry

The heat flow from hydration of the binder mixtures was evaluated to examine the effect of PC4 on the initial hydration. As with the concrete and mortar tests, comparisons were drawn to a control binder with no mineral admixture and to mixtures with LS. For the binder containing PC4 and for the binder containing LS, the powder components were made with 5% and 15% mass replacement of Portland cement with each mineral admixture, respectively. Binders were proportioned such that the total mass of the paste mixture was 5g, with a 0.47 water-to-binder ratio. Reference samples were made to match the heat capacity of the paste mixtures using inert silica sand. Samples were tested in a TAM Air Isothermal Microcalorimeter (TA instruments) at 30°C using glass admixture ampules and a syringe-and-paddle mixing apparatus that allows for water addition as well as paste mixing within the calorimeter. Powder mixtures were weighed into the ampoules and distilled water was loaded into a syringe, the syringe tips were dried, and then dipped into silicon grease to prevent water from prematurely interacting with the powder. The ampoules were loaded into the calorimeter sample chamber with a corresponding reference sample added to the reference chamber. After the samples equilibrated to the chamber temperature, the baseline was measured, and the signal was corrected automatically by the accompanying software package. Water was then injected into the first sample, the time of injection was marked, and the paste was mixed for approximately 90 seconds. This process was then repeated for each sample.

2.3.1.4. Compressive strength

It is known that mineral additions like limestone filler can induce early hydration in concrete mixtures and can lead to a dilution effect which lowers compressive strength at later ages relative to a

Portland cement mixture without limestone [162]. For this reason, compressive strength was determined for each of the concrete mixtures at several curing ages, namely, after 7, 14, 28, and 56 days of curing. Experiments were performed on a SoilTest CT-950 load frame following ASTM C39 testing procedures [163]. Cylinder specimens were capped on either end with neoprene-padded aluminum cap and specimens were loaded under force control. Five specimens were tested for each mixture at each of the four ages. Ultimate strength of the concrete mixtures was determined based on the average maximum load reached before softening or failure occurred.

2.3.1.5. Flexural Strength

Flexural strength was determined by performing three-point bend tests after 28 days of curing using a MTS Testline Component load frame managed by an MTS TestStarIIs controller following ASTM C293 testing procedures [164]. Three specimens were tested from each mixture and average ultimate flexural strength was determined.

2.3.1.6. Coefficient of Thermal Expansion

Coefficient of thermal expansion is known to have significant effects on the feasibility of utilizing concrete mixtures in systems that undergo changes in temperature, such as roadways [165]. To assess the effects of PC4 and limestone on Portland cement-based mixtures, this work followed AASHTO T336 testing procedure [166]. Using 100 mm X 200 mm (4 X 8 inch) cylinders, specimens for testing were cut to have a length of 177.9 ± 2.54 mm (7 ± 0.1 inches). One concrete specimen was tested for each of the mixtures after curing for 42 days. Experiments were performed at the University of California Pavement Research Center.

2.3.1.7. Shrinkage

To determine how replacement of Portland cement or fine aggregates with PC4 affects drying

shrinkage, mortar specimens were cast to have the same binder content and replacement ratios as the concrete mixtures tested. Following ASTM C157 testing procedures [167], specimens were removed from molds after 1 day of curing and placed in a conditioning chamber set at 25°C and 50% relative humidity. Three mortar prisms were cast for each mixture. The length change of each mortar specimen was measured at 0, 14, 21, and 28 days and the average length changes were reported.

2.3.1.8. Bulk Density, Void Volume, and Absorption

Density, absorption, and voids in each of the concrete mixtures were assessed following ASTM C642 testing procedures [168]. One 101.6 mm X 203.2 mm (4 X 8 inch) cylinder specimen from each concrete mixture was tested after curing for 28 days. To determine oven-dry weight, specimens were dried at 100-110°C and weighed every 24 hours until less than 0.5% weight fluctuation between two successive measurements were achieved. Specimens were then submerged in water and weight measurements of the specimens after surface drying were taken every 24 hours until less than 0.5% weight fluctuation between two successive measurements occurred. Specimens were then placed in water and boiled for 5 hours. The boiled specimens were allowed to cool for 14 hours before being submerged in water using a specific gravity bench to determine the apparent weight. Finally, the surface was dried and the specimens were weighed once more. Water absorption, void volume, apparent density, and bulk density were determined using the formulae stipulated in ASTM C642 [168].

2.3.1.9. Estimating Greenhouse Gas Emissions from Producing Concrete Mixtures

Noting that mineral admixtures can facilitate reductions of cement content in concrete, which can in turn lower GHG emissions, a preliminary assessment of changes to GHG emissions from using ground limestone or PC4 in concrete was examined in this work. For each of the mixtures (proportions in **Table 2.2**), GHG emissions were modeled using the GreenConcrete LCA Webtool developed at the University of California Berkeley [169]. Within this tool, 100-year global warming potentials were used to draw

comparisons. Production was modeled as occurring in California, including all constituent production and mixture batching. For each constituent requiring electricity during processing and for concrete batching, the average California grid mix for 2018 was used [170]. For modeling the production of cement clinker, the California average kiln fuel mix for 2017 was used [171]. Cement production was modeled in the GreenConcrete Tool following the most common production modes in the US [172]. Specifically, the raw material processing was modeled as dry ball milling and preheater/precalciner processing. The clinker was modeled as being cooled through a reciprocating grate cooler and finish milled in a ball mill. For each of the concrete constituents, transportation by truck was selected since it is the predominant mode throughout the cement and concrete production process in the US [131], [172]. Transportation distances are the average for each constituent provided in reports published by the Portland Cement Association [131], [172]. Namely, these distances were modeled as 146 km for cement, 61 km for fine aggregate, 43 km for coarse aggregate, and 43 km for LS. Water was considered to be available on site with negligible energy resources necessary for its acquisition. Because PC4 is a residual waste product of the carpet recycling process, the impacts from PC4 removal from carpet were allocated to the recycled plastic product. As such, no GHG emissions were modeled from the production of PC4. However, transportation of PC4 to the concrete batching site was considered. This PC4 transportation was modeled as 197 km by truck, based on the US average distance for post-industrial product transport for use in concrete [131].

2.3.2. Results

2.3.2.1. Slump, Air Content, and Unit Weight

The incorporation of PC4 influenced slump, air content, and unit weight of concrete (see **Table 2.3**). Partial replacement of Portland cement with PC4 and 5% replacement of fine aggregate with PC4 increased concrete slump by 5 to 27%. However, a 15% replacement of fine aggregate resulted in a 64% decrease in slump. The partial replacement of cement with PC4 had similar effects on slump as partial replacement with LS. This similarity suggests that, like the LS, a filler effect or a net increase in water to

Portland cement ratio could have contributed to an increase in workability. The same reduction in workability was noted when 15% of fine aggregate was replaced with PC4 and LS relative to the Portland cement mixture (without any PC4 or LS). However, noting the slump increased at 5% fine aggregate replacement, there is an apparent varying effect of the PC4 based on the concentration. The carpet backing from which PC4 is produced from is known to contain polymer fibers and latex adhesives [79], [173], [174]. It is possible that remnant compounds from the backing, such as latex and microfibers, are affecting surface interactions and, possibly, contribute to the noted differences.

Table 2.3. Slump, air content, and unit weight of fresh concrete mixtures and the average compressive strength, flexural strength, and coefficient of thermal expansion of hardened concrete specimens.

	Fresh Properties Measured			**Hardened Properties**		
Mixture Name	Slump, mm	Air Content, %	Unit Weight, kg/m^3	f_c', MPa (range)	f_r', MPa (range)	CTE, microstrain / °F (range)
PC	140	6	2431	43.8 (4.1)	6.89 (0.12)	7.08 (0.03)
C-PC4-5	165	12.5	2161	26.8 (5.5)	4.29 (0.52)	7.15 (0.01)
C-PC4-15	146	16	2087	14.4 (1.4)	3.17 * (0.10)	7.16 (0.03)
C-L-5	152	1.8	2835	46.5 (4.1)	3.18 (0.19)	7.28 (0.02)
C-L-15	165	1.2	2739	44.8 (2.7)	3.84 (2.12)	7.05 (0.07)
FA-PC4-5	178	11	2609	24.9 (4.1)	4.46 (0.47)	7.25 (0.05)
FA-PC4-15	51	9.5	2649	22.6 (1.6)	4.06 (0.51)	7.11 (0.03)
FA-L-5	114	1.5	2846	44.2 (5.2)	2.93 (0.32)	6.93 (0.05)
FA-L-15	51	1.4	2860	43.6 (3.3)	3.25 (0.41)	7.15 (0.07)

'*' indicates only two specimens tested; f_c' = 28-day compressive strength; f_r' = 28-day flexural strength; CTE = 42-day coefficient of thermal expansion. Values in '( )' indicate the range between values used to calculate the reported average

The use of PC4 did not consistently affect the air content or unit weight of fresh concrete in the same manner as the LS. The PC4 consistently increased air content relative to the control mixtures. This change could be a function of the size and air content of the PC4 particles. Additionally, any remnant latex

could contribute to increased air entrainment during mixing. The use of LS had the opposite effect, leading to a consistent reduction in air content. The LS also increased the concrete unit weight relative to the Portland cement mixture. Both parameters indicated that the finer LS particles likely increased particle packing. While the PC4 increased air content, the replacement of Portland cement with PC4 led to a reduction of unit weight and the replacement of fine aggregate with PC4 led to an increase in unit weight. These results suggest that the PC4 may improve gradation when used as a fine aggregate replacement, but not when used as a partial cement replacement. These differing effects based on constituent replaced could be due to the gradation of PC4, which is coarser than the LS.

2.3.2.2. Setting time

The inclusion of PC4 resulted in an increase to both the initial and final setting times relative to the mixtures containing no PC4 (see **Figure 2.13**). Compared to the Portland cement mixture, the replacement of cement with PC4 led to a 64-123% increase in initial set time and a 74-117% increase in final set time. While 5% fine aggregate replacement did not lead to as large a change to setting times as the 5% Portland cement replacement, 15% fine aggregate replacement with PC4 resulted in 2.5- and 3-times greater initial and final setting times than the Portland cement mixture, respectively. As a result, all of the PC4 mixtures studied here exceed the 375 min final setting time stipulated by code [148]. Under certain scenarios, it is possible that the increase in initial setting time offered by the PC4 could improve the window during which the concrete can be adequately mixed and placed. However, the delay in when mechanical strength begins to develop could affect the use of PC4 in certain applications. For example, the delayed setting time would hamper the use of PC4 in applications when a load needs to be applied to the concrete quickly or it could increase the time between which concrete is poured and formwork can be removed.

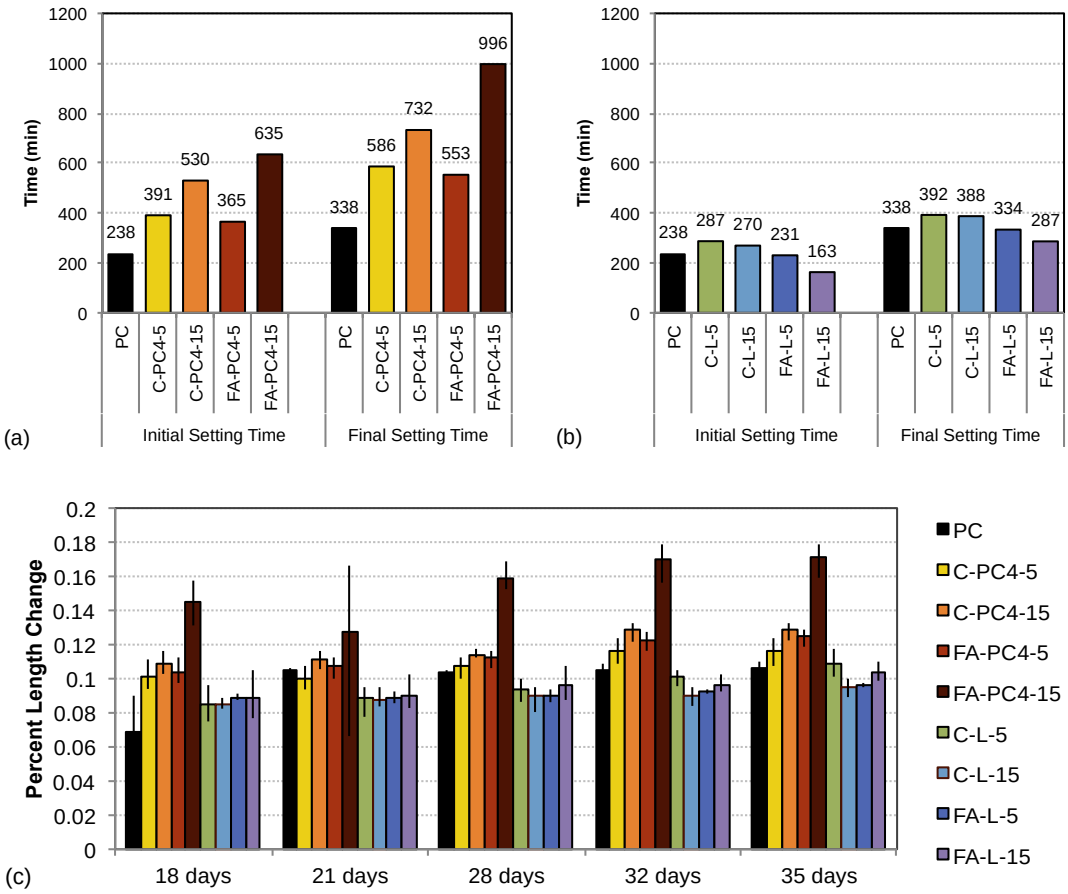

Figure 2.13. Initial and final setting times for (a) mixtures containing PC4 and (b) mixtures containing limestone relative to mixture PC (a control without PC4 or limestone replacement) and (c) shrinkage of specimens over a two-week period as shown by percent change in length

The use of LS in the concrete mixtures resulted in smaller changes in setting times than the use of PC4. Cement replacement with LS increased initial and final setting times relative to the Portland cement mixture, but by less than the use of PC4, namely by 13-21% and 15-16%, respectively. This shift in final setting times also resulted in the mixtures containing LS as a partial cement replacement exceeding final set time limits. It is possible that these shifts were caused by the reduction in Portland cement, which the LS partially compensates for by improved cement dispersion and hydration. The larger particle size of PC4, however, may not be as effective at cement particle dispersion. The use of LS as a partial replacement for fine aggregates reduced both initial and final setting times by up to 31% and 15%, respectively. This change could result in these LS mixtures being more difficult to handle, but it would lead to the earlier onset of strength development.

2.3.2.3.Isothermal Calorimetry

The partial replacement of cement with either PC4 or LS showed little effect on the early age heat flow of the binders (Appendix B, **Figure B.1**). The PC, C-L-5, and C-L-15 binders all reached maximum heat flow approximately 8 hours after the introduction of water into the powder. This was followed by C-PC4-5 with a delay of approximately 30 minutes, a 6% increase in time. The C-PC4-15 binder was offset from the first three mixtures by approximately 2 hours, a 25% increase in time; however, the peak heat flow of C-PC4-15 was approximately the same as the binders with 5% replacement and the binder with neither PC4 nor LS. The C-L-15 paste had a small, ~3%, decrease in heat flow at the peak compared to the other mixtures. This decrease for the C-L-15 is consistent with mixtures reported in literature with similar levels of Portland cement replacement with LS and it is also similar to the results for cement replacement with fly ash [175], [176]. The 2-hour shift for C-PC4-15 is also similar to the delays shown with fly ash replacement [175], [176].

2.3.2.4. Compressive Strength

Each of the concrete mixtures studied showed an increase in compressive strength over time, ranging from a 27% to 48% increase between measurements taken at 7 days and 56 days (**Figure 2.14**). The largest increase in strength was exhibited by FA-L-5 and the smallest was exhibited by the FA-PC4-15. The mixtures containing PC4 had significantly lower compressive strength than the control mixtures (based on a T-test analysis, $p < 0.001$ for all ages). The PC4 mixtures varied from 10.4 MPa at 7 days for C-PC4-15 to 28.7 MPa at 56 days for FA-PC4-15. At 28-day and 56-day ages, all LS mixtures had higher compressive strengths than the Portland cement mixture. While the compressive strength for mixture C-L-5 differed significantly from the Portland cement mixture at 28- and 56-days ($p = 0.036$ and 0.015, respectively), the other mixtures containing LS did not ($p = 0.285$ and 0.655, $p = 0.667$ and 0.448, and $p = 0.867$ and $p = 0.056$ for mixtures C-L-15, FA-L-5, and FA-L-15 at each age, respectively).

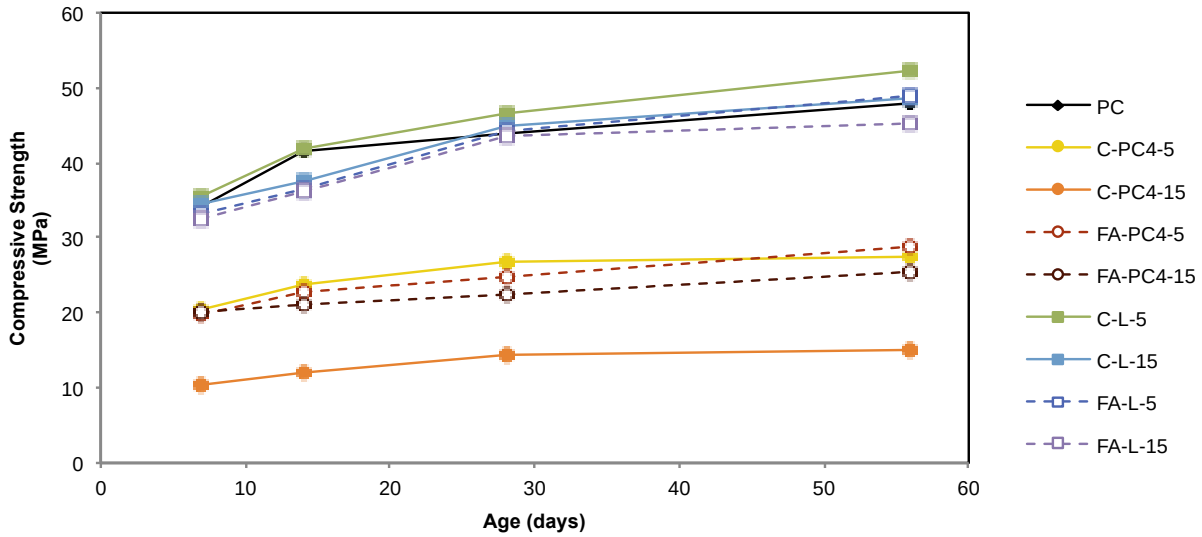

Figure 2.14. Compressive strength development of concrete mixtures containing PC4 or limestone relative to a mixture with neither

In general, LS replacement appeared to either improve or have negligible effects on compressive strength, while PC4 replacement led to notable decreases in compressive strength at all ages and replacement levels tested, a 30 to 60% reduction in strength relative to the Portland cement mixture. For the LS mixtures, most of the strength development occurred at early ages (i.e., below 28 days). This trend was true for the PC4 mixtures with the partial replacement of Portland cement. However, similar strength development was noted between 7 to 28 days and between 28 to 56 days for the PC4 mixtures with fine aggregate replacement. The inclusion of LS can contribute to early age strength development and a dilution effect that influences later age strength development [162]; however, the effects of such mineral additions can have varying influence on mechanical properties depending on a variety of other factors [177]. In addition to these contributing factors, the PC4 could have a different internal microstructure than LS or remnant coating, such as latex, both potential artifacts of the carpet manufacturing process [79], [173], [174]. Styrene-acrylic ester copolymer latex, even in low concentrations, has been shown to significantly reduce the compressive strength of cement mortars [178]. Possibly, the remnant latex polymers in PC4 behaved similarly in the mixtures tested. Such artifacts could lead to flaws at the interface between matrix and inclusions or flaws within the inclusions, which may affect strength. Further study, regarding the chemical and microstructural properties of PC4 should be conducted to assess such parameters.

2.3.2.5.Flexural Strength

Both PC4 and LS decreased flexural strength at 28 days (see **Table 2.3**) relative to the Portland cement mixture. The partial replacement of fine aggregate with PC4 had the least effect on flexural strength, resulting in a 35% reduction. The greatest reduction in flexural strength was noted for the 5% replacement of fine aggregates by LS, but when considering specimen variability, the reduction in flexural strength noted for this mixture was similar to that for several others. The use of LS has been shown in past work to lead to varying effects on different mechanical properties, dependent on factors such as gradation, composition, and water-to-binder ratio [162], [177], [179]. However, the consistent reduction in mechanical properties from PC4 could be a function of a dilution effect or inherent flaws within the particles themselves, acting as either crack initiation or weak points that facilitate propagation of failure through the concrete specimens.

2.3.2.6. Coefficient of Thermal Expansion

The partial replacement of cement or fine aggregates with either PC4 or LS had limited effect on the coefficient of thermal expansion (see **Table 2.3**). The Portland cement mixture, with neither PC4 nor LS, had a coefficient of thermal expansion of approximately 7 microstrain / °F. The use of PC4 in the concrete mixtures had a 0 to 3% increase in the coefficient of thermal expansion; the use of LS had between a 2% reduction and a 3% increase in the coefficient of thermal expansion. These variations resulted in all mixtures having coefficients of thermal expansion within a normal range for conventional concretes [165] and indicates these mixtures would behave similarly under typical temperature conditions.

2.3.2.7. Shrinkage

In most cases, the inclusion of PC4 exhibited a larger impact on drying shrinkage than the inclusion of LS (**Figure 2.13**). Mixtures with higher weight fractions of PC4 generally exhibited 3 to 110% greater arithmetic mean shrinkage than PC, depending on age and mixture. The exception to this trend was the C-PC4-5 at 21 days, where, considering the variability present, the change in length appears comparable to

the Portland cement mixture. The inclusion of LS filler predominantly exhibited the opposite effect on drying shrinkage. With the exception of early age measurements, the mixtures with LS filler generally exhibited smaller length changes than the Portland cement mixture (3 to 15% lower change in length). The exception to this trend was the C-L-5 mixture at 35 days, which had comparable shrinkage as the Portland cement mixture. It is known that geometry, moisture, and material properties all affect the drying shrinkage of cement-based materials. Given that the moisture and geometry are controlled, the changes observed are potentially caused by the material properties of the LS and PC4 used. The LS, with a higher modulus of elasticity, can reduce drying shrinkage [148]. However, the opposite is observed for PC4 inclusion, suggesting the less-dense PC4 could lead to a lower modulus elasticity and, thus, lead to the increased drying shrinkage observed.

2.3.2.8. Bulk Density, Void Volume, and Absorption

Inclusion of PC4 consistently increased concrete absorption and void volume, while reducing bulk density (see **Figure 2.15**). As a partial Portland cement replacement, PC4 increased absorption by 28-34% and void volume by 7-11%, while reducing bulk density by ~10%. As a replacement of fine aggregate, PC4 increased absorption by 28-38% and void volume by 20-50%, while reducing bulk density by ~10%. While this notable increase in voids and absorption could lead to less desirable attributes in a reinforced concrete system by facilitating additional ingress of moisture, the ability to form a less dense, more permeable concrete could be desirable in other applications requiring lighter or permeable concretes.

The partial replacement of Portland cement and fine aggregate with LS did not have as large of an effect as the PC4, but trends of increased absorption and void volume were still noted. Despite these changes, bulk density remained relatively consistent to the Portland cement mixture. The partial replacement of Portland cement with LS led to a 13-16% increase in absorption and a 15-24% increase in void volume, whereas the partial replacement of fine aggregates resulted in a 1-19% increase in absorption and a 4-23% increase in void volume relative to the Portland cement mixture. It is possible the shifts noted

from the use of LS are associated with both the density of the LS and its effect on particle packing; however, the trends noted from the use of PC4 suggest that it is not consistently contributing to the same effects. As discussed above, the variability from the PC4 replacement could be attributed to the gradation of PC4 modifying the overall gradation of the mixture, dependent upon which constituent the PC4 replaces.

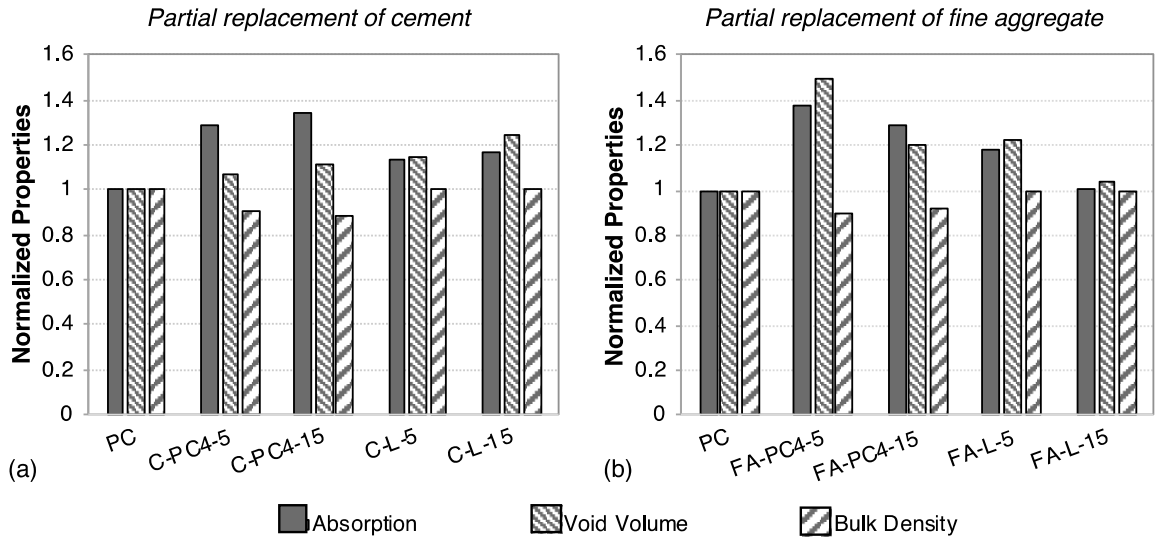

Figure 2.15. Absorption, void volume, and bulk density for concrete mixtures normalized to the Portland cement mixture without either PC4 or quarried limestone for (a) partial cement replacement and (b) partial fine aggregate replacement

2.3.2.9. Greenhouse Gas Emissions

The GHG emissions were examined for each mixture to understand possible reductions in emissions that could be achieved through utilizing this material waste stream. When PC4 and LS were used as partial Portland cement replacements, reductions in GHG emissions were found (**Figure 2.16**). These findings were expected as the cement production is responsible for the majority of the GHG emissions from concrete production. For mixtures where cement is replaced with 5 or 15% PC4 or LS by mass, the GHG emissions were approximately 5 and 15% lower, respectively, reflecting the mass replacement of the high-emitting cement. Mixtures with PC4 used for cement replacement provided slightly larger reductions than the LS replacement. However, the differences between the use of PC4 and the use of LS were less than 0.1% and can be considered negligible within the confines of this type of environmental impact assessment.

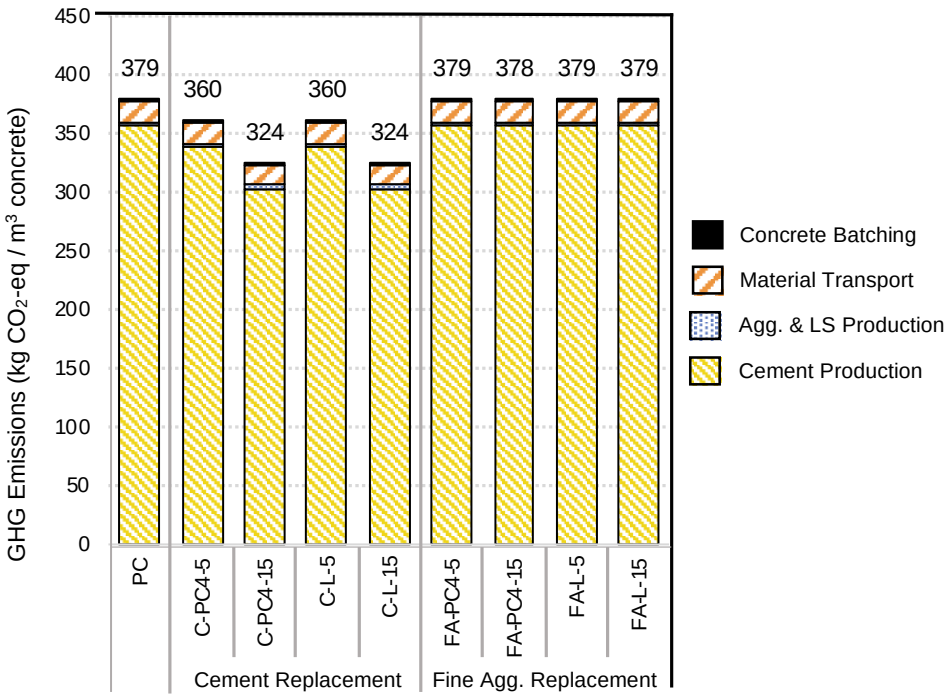

Figure 2.16. Estimated GHG emissions (kg CO_2-eq/m^3 of concrete) for mixtures produced evaluated by major process for production

For the mixtures in which PC4 and LS were used as partial fine aggregate replacement, marginal differences in GHG emissions were noted compared to the PC mixture. The replacement of 5 and 15% of fine aggregate with LS led to negligible increases in GHG emissions compared to PC4 replacement. This minute increase was a function of the additional emissions from limestone excavation and processing. Though, since the cement content— the primary contributor to concrete GHG emissions— is the same as that of the control for all mixtures with fine aggregate replacement, changes to GHG emissions from the use of either LS or PC4 were small.

2.4. PC4 Treatment, characterization and evaluation in mortars

The United States (US) has produced over 5 trillion square meters of carpet since 1950 (by summing data in ref. [1–4]). Unlike many materials (e.g., metal alloys and concretes mixtures), carpets are a relatively transient part of buildings [5] with lifespans between 4 to 25 years [6,7]. Waste carpet amounted to 3.2% of California landfill volume in 2008 [8] and on average 2% of landfill volume in the entire US [9]. Post-consumer calcium carbonate from carpet (PC4, a mix of CaCO3 and remnant backing material) is ~38-50% of the recycled carpet mass. As PC4 is predominantly CaCO3, it could fulfill a similar role as limestone (LS) in Portland-limestone cement (PLC) concretes. Further, the use of PC4 in concrete could serve the circular economy, in which resources are used as many times as possible to extract maximum utility and lower environmental impacts.

Ground LS is included in mixtures either in PLC, produced by inter-grinding LS with clinker [10], or as a filler added during mixing [11]. Cement-based materials with LS can reach similar compressive strengths with less cement clinker [11–13] and is accepted in standards [12,14]. The literature generally agrees that higher LS binder contents can result in lower compressive strengths (often for replacement >15% [10,12,15], though this varies) and the differences in strengths are more acute at greater ages. Improved compressive strengths are often attributed to the filler effect and increased nucleation [12], whereas compressive strength reductions are attributed to the dilution affect from decreased cement content [11,12].

Using PC4 as a mineral filler could lead to dual environmental benefits. First, benefits can come from partially closing the loop on a post-consumer waste flow and extracting additional utility from this mineral resource. Second, PC4 as a Portland cement replacement can reduce some of the estimated 8-9% of anthropogenic CO2 emissions [16,17] from concrete [18]. Over 70% of greenhouse gas (GHG) emissions in concrete come from cement production [19]. Lowering the high emitting portions of cement reduces GHG emissions from concrete [20]. In addition to GHG emissions reductions and material reuse benefits,

reusing waste materials could sequester potentially harmful compounds that would otherwise leach at a disposal site [21]. As in the case of fly ash and slag, their use with cement can sequester heavy metals [22,23]. Similarly, antimony (Sb) found in PC4 may be sequestered in cement-based materials [18]. Leaching Sb could lead to human health concerns if it enters drinking water supplies [24,25]. Limiting Sb migration is important for any future PC4 application.

Studies using PC4 as a fine aggregate or as a mineral filler in concrete show PC4 could lead to large reductions in the mechanical performance of concrete [72]. Namely, strength loss of 30-60% was noted, relative to mixtures with LS filler [72]. Concrete with PC4 had increased wet air-content, increased permeable air-voids once hardened, decreased density, and increased set-time, indicating PC4 changed the microstructure of the concrete [72]. These changes in properties from using untreated PC4 were hypothesized to be deleterious effects driven by the remnant latex polymer and impurities (i.e., fibers, dirt, hair) affecting the paste microstructure, which would restrict the applications of the material.

Herein, treated PC4 is evaluated as an inert filler material. Noting limits of this material when not treated, this work evaluates different strategies to engineering PC4 to mitigate these affects and improve PC4 performance as a mineral filler and partial cement replacement. It is hypothesized that effective treatment of PC4 could lead the material to behave similarly to ground virgin LS in cement-based materials.

2.4.1.Methods

2.4.1.1. Materials, PC4 preparation, and chemical properties

To examine effects of PC4 in cement-based systems, mixtures were produced with Type II/V Portland cement (BASALITE Concrete Products; Dixon, CA). Silica-sand was acquired from the Esparto quarry (Esparto, CA). PC4 was acquired from Circular Polymers (Lincoln, CA). For all mortars and pastes, distilled water was used as the mixing water.

Four preparations of PC4 were considered in this work (shown in **Table 2.4**). First, PC4 was sieved through a #40 sieve to match the PC4 used in previous work (*preparation 1*) [72]. To reduce the particle size and improve the gradation of the PC4, milled PC4 was prepared in a PM200 planetary ballmill (Retsch; Haan, Germany) using 3 mm Zirconium grinding medium in a Zirconium grinding jar (*preparation 2*). To remove potential remnant latex, plastic fibers, and other contaminants, PC4 was oxidized in a Model 750-58 air-muffle furnace (Fisher; Waltham, MA). Two temperatures were selected for oxidization: 600°C (*preparation 3*), which has been shown to reduce concentrations of persistent organic contaminants (in one hour, polybrominated diphenylethers decreased >99% and perfluorinated compounds decreased >80%) [180], and 900°C (*preparation 4*), similar to the calcining stage in clinker production.

Table 2.4. Treatments / preparations for post-consumer calcium carbonate from carpet

Material	Treatments/ preparations
PC4-S	PC4 sieved through # 40 (420 um) sieve to remove remnant fiber (as in [72])
PC4-M	PC4 milled for 20 minutes at 300 RPM, to passed through #200 (74 um) sieve
PC4-600	PC4 oxidized for 6 hours at 600°C
PC4-900	PC4 oxidized for 6 hours at 900°C

Characteristics of treated PC4 were examined herein via two methods. First, the loss on ignition (LOI), likely oxide content, trace elements, and mineralogy were determined by ACT laboratories (Ancaster, Canada). Likely oxide content was estimated through inductively coupled plasma optical emissions spectrometry (ICP-OES) using an 700 Series ICP-OES machine (Agilent; Santa Clara, CA). LOI was determined by placing two grams of a sample in a furnace at 1000°C for 2 hours. Next, mineralogy and phases were determined through semi-quantitative XRD analysis with an internal standard method by mixing samples with a known amount of corundum. Samples were then analyzed in a D8 Endeavor (Bruker; Billerica, MA) with a Cu anode. Crystalline minerals were identified using the PDF-4/Minerals ICDD database and amounts quantified via the Rietveld method using the known quantity of the internal standard.

2.4.1.2.Mixture proportions and batching

Mortar mixtures were produced using the proportions listed in **Table 2.5**. Herein, binder refers to

the combined mass of the cement and any mineral additive. A control mixture with only PC (CTRL) as the binder was designed with a water-to-binder ratio of 0.47 and a binder-to-sand ratio of 2.5. A second set of control mixtures with LS filler as 5 and 15% replacement of PC by mass were also considered. Finally, PC4 mortars for testing were designed with 5 and 15% replacement, by mass, for each PC4 treatment scenario. Replacement rates of 5 and 15% were selected to represent the lower and upper limits for LS content for PLCs in ASTM C595 [58].

Table 2.5. Mixture nomenclatures and constituent proportions for the Portland cement-only mixture as well as mixtures with 5 and 15% replacement of Portland cement with Limestone or post-consumer calcium carbonate from carpet

Mixture Type	Mixture Proportions (kg constituent / m^3 mortar)				
	Portland Cement	PC4	Limestone	Sand	Distilled Water
CTRL	564	0	0	1410	265
5%LS	535	0	28	1408	265
15%LS*	478	0	84	1405	264
5%PC4	533	28	0	1401	263
15%PC4*	471	83	0	1385	260

*Note: the mass differences to make 1 m^3 of 15%LS versus 15%PC4 are due to the difference in density between the post-consumer calcium carbonate from carpet (PC4) and limestone (LS) powder

Mortar mixtures were produced in a Hobart A200 dough mixer (Hobart; Troy, OH) following the mixing procedure and times prescribed in ASTM C109 [181]. Cube mortar specimens were prepared in 50.8 cm x 50.8 cm (2 x 2 inches) molds. For leaching analysis and SEM imaging, 50.8 cm x 101.6 cm (2 x 4 inches) cylinders were cast from the same mortar mixtures. Cast specimens were cured at 25°C and >90% humidity for 1 day prior to being removed from the molds, after which they continued to be cured under the same conditions until compressive strength testing at 7 and 28 days. Specimens for leaching were kept in the molds at 25°C and >90% humidity until just before leaching, to prevent premature leaching in the high humidity environment. Bulk leaching of all specimens was performed simultaneously with well cured specimens (ages >42 days).

2.4.1.3. Compressive strength

Compressive strength testing was performed following ASTM C109 [181]. Cubes were tested using

a CT-950 load frame under force control and an externally calibrated load-cell which allowed measurements to the nearest 44 N-force (10 lbs-force). The compressive strength of the mortars was compared based on the average strength of five specimens at each age.

2.4.1.4. Isothermal calorimetry

To assess both the potential for improved cement hydration and the occurrence of additional hydration reactions, isothermal calorimetry was performed on paste samples. As with the effects of LS, it was anticipated that treated PC4 would improve the particle dispersion of cement and thus improve hydration. Additionally, it was anticipated that the PC4 oxidized at 900°C, would lead to additional CaO increasing the cement hydration reactions that occur. A control paste sample (5g) was proportioned with a water to binder ratio of 0.47. Paste samples were produced with 5 and 15% cement replacement with LS and each of the PC4 preparations.

To capture the initial hydration, samples were mixed in-situ. Powders were weighed into 20mL glass ampoules; distilled water was measured into a syringe and stirring apparatus. The tips of the syringe were dipped in silicon grease to prevent premature water introduction into the powder. The uncombined powder and water samples were loaded into an Isothermal calorimeter (TA Instruments; New Castle, DE) at 25°C and allowed to come to equilibrium. Then the included software package was used to take baseline readings. After collecting a baseline, the water was injected into the powder, the time of injection was recorded, and the mixture was stirred for 1.5 minutes. After 7 days (168 hours), data collection was stopped, and data were corrected with the baseline readings using the software package. Replicates of the calorimetry was performed measuring heat flow over 7 day (168 hours) for verification. An additional replicate of each mixture was tested over 4 days (96 hours) to allow for higher resolution data collection.

2.4.1.5. Scanning electron microscopy (SEM)

To investigate the effect of the mineral additives on the mortar microstructure, backscatter SEM imaging of samples was performed. Mortar cylinders for the PC control mixture and 15% replacement mixtures were cut into thin sections and mounted in epoxy. The SEM specimens were partially polished and then stored in ambient conditions. A day before testing, epoxy mounted specimens were given the final polish, carbon coated, and then stored in a vacuum jar to prevent interaction with gaseous CO_2. SEM of mortar sections was performed in a Cameca SX-100 Electron Microprobe at the UC Davis Electron Microprobe Laboratory.

2.4.2. Results and discussion

2.4.2.1. Chemical and X-ray Diffraction

To compare how the treatments altered the composition of the PC4, likely oxides were estimated (**Table 2.6**). Additionally, the mineralogy (**Table 2.7**) and concentrations of certain trace elements (**Table 2.8**) were evaluated. The mineralogy determined through semi-quantitative XRD analysis showed the sieved (PC4-S) and milled (PC4-M) PC4 to be predominantly calcite ($CaCO_3$) and dolomite ($CaMg(CO_3)_2$). The oxides analysis of PC4 (**Table 2.6**) indicated large quantities of Ca (75.69-78.42%) and Mg (12.18-12.57%). Notably, compared to virgin LS (amorphous content below detection level), a high fraction (21.2%) of the PC4-S was found to be amorphous. The reduction of amorphous content found in the PC4-M may be attributed to the finer sieve size reducing the concentration of remnant organic materials (e.g., polymer fibers, pet hair). There was greater reduction of amorphous content for the heat-treated PC4-600 and PC4-900 compared to both PC4-S and PC4-M. The furnacing of PC4 for 6 hours likely removed polymer coatings (such as latex) and other materials smaller than the 200-mesh sieve used for the milled PC4 (such as nano-plastics), thus contributing to the reduction of amorphous material shown **Table 2.7**. A reduction of remnant latex and other organic materials would be expected to benefit PC4 as a filler material.

Table 2.6. Chemical Analysis and likely oxides of Type II/V Portland cement, Limestone Powder, and each preparation of post-consumer calcium carbonate from carpet (n = 1)

Oxides Mass %, (Detection Limit)	**II/V Cement**	**Limestone**	**PC4-S**	**PC4-M**	**PC4-600**	**PC4-900**
SiO_2 (*0.01%*)	21.36%	2.17%	5.96%	6.08%	5.39%	4.86%
Al_2O_3 (*0.01%*)	4.61%	0.43%	1.63%	1.68%	1.59%	1.49%
Fe_2O_3(T) (*0.01%*)	3.64%	0.20%	0.89%	0.88%	0.89%	1.33%
MnO (*0.001%*)	0.17%	0.01%	0.04%	0.04%	0.04%	0.05%
MgO (*0.01%*)	2.77%	8.66%	12.18%	12.57%	12.26%	12.20%
CaO (*0.01%*)	66.22%	88.38%	76.28%	75.69%	77.36%	78.42%
Na_2O (*0.01%*)	0.15%	0.02%	1.89%	1.93%	1.47%	0.85%
K_2O (*0.01%*)	0.63%	0.07%	0.45%	0.45%	0.40%	0.27%
TiO_2 (*0.001%*)	0.24%	0.02%	0.35%	0.35%	0.31%	0.27%
P_2O_5 (*0.01%*)	0.21%	0.04%	0.32%	0.32%	0.29%	0.27%

S = Sieved, M = Milled, 600 = oxidized at 600°C, 900 = oxidized at 900°C, PC4 = Post-consumer calcium carbonate from carpet

In addition to lower amorphous content, the temperature treated PC4 also showed reductions in dolomite. While decomposition is dependent on conditions beyond temperature (e.g., the composition of the flue gas [182], [183] and composition and moisture content of the material [182], [184]), dolomite decomposition can begin at temperatures as low as 350°C [184]. This process can result in either a full decomposition into CaO or a partial decomposition into calcite [185], which could also be a contributing factor to the increase in calcite for the PC4-600 material. Decomposition of calcite occurs at higher temperatures, typically around 650°C [182], [184]. The decrease in calcite and corresponding increase in lime in the PC4-900 is consistent with the decomposition of dolomite and calcite as well as formation of lime and periclase [185]. Notably, the high lime content of PC4-900 holds promise as a CaO source in tertiary-blends by allowing for higher levels of cement replacement.

Table 2.7. Minerology of materials (n = 1)

	II/V Cement	Limestone	PC4-S	PC4-M	PC4-600	PC4-900
Calcite	0.8%	77.4%	49.3%	51.8%	86.2%	1.5%
Dolomite	-	20.6%	26.3%	28.2%	-	1%
Quartz	0.3%	0.8%	2.0%	1.5%	2.6%	-
Muscovite	-	0.4%	0.9%	1.9%	0.9%	-
Talc	-	0.8%	-	-	-	-
Chlorite	-	tr	0.3%	0.7%	-	-
Larnite	2.9%	-	-	-	-	3.6%
Hatrurite	63.9%	-	-	-	-	-
Brownmillerite	12.2%	-	-	-	-	-
Periclase	1.2%	-	-	-	5.1%	13.9%
Lime	-	-	-	-	0.4%	61.9%
Portlandite	-	-	-	-	-	9.3%
Gypsum	1.6%	-	-	-	-	-
Amorphous	17.1%	-	21.2%	15.9%	4.8%	8.8%

'-' indicates none detected, 'tr' below sensitivity threshold (<0.1%), S = Sieved, M = Milled, 600 = oxidized at 600°C, 900 = oxidized at 900°C

To determine the effects of treatments on undesirable trace elements, the concentrations of Ba, Sr, Y, Sc, Zr, Be, and V were quantified (**Table 2.8**). The trace element concentrations of Ba, Sr, Zr, and V in the PC4 were larger than the virgin LS. However, the amount in the LS and all PC4 materials were all lower than those in the II/V Portland cement. Thus, either replacement level would still represent a net reduction of the trace element compared to mixtures with only PC. The reduction of PC4 LOI with heat treatment, and its further decrease at higher temperature, is consistent with the expectation of reduced organic materials and the decomposition of the dolomite and calcite (**Table 2.8**).

Table 2.8. Trace Elements and Loss on Ignition (LOI) (n = 1)

	Detection Limit	II/V Cement	Limestone	PC4-S	PC4-M	PC4-600	PC4-900
Ba (ppm)	2	157	10	48	54	64	82
Sr (ppm)	2	716	270	275	272	369	585
Y (ppm)	1	13	6	2	3	3	5
Sc (ppm)	1	5	< 1	< 1	< 1	< 1	1
Zr (ppm)	2	68	2	23	31	26	37
Be (ppm)	1	1	< 1	< 1	< 1	< 1	< 1
V (ppm)	5	65	< 5	5	< 5	7	15
LOI (%)	0.01	2.47	43.04	52.24	52.07	36.62	0.56

S = Sieved, M = Milled, 600 = oxidized at 600°C, 900 = oxidized at 900°C, PC4 = Post-consumer calcium carbonate from carpet

2.4.2.2.Compressive strength

The average 7- and 28-day compressive strengths are presented in **Table 2.9** and **Figure 2.17**. Similar to prior work on the effect of sieved PC4 in concrete, the use of PC4-S in the mortar mixtures led to notable reductions in compressive strength. Namely, replacement of cement with 5% PC4 and 15% PC4 resulted in approximately 40 and 56% reductions in strength at 7 days as well as 45 and 57% reductions at 28 days, respectively. Milling PC4 (PC4-M), with the intent of improving particle dispersion, resulted in mortars with the same or lower compressive strengths as the PC4-S. Noting that remnant latex could be affecting the microstructure of the mixtures and thus contribute to the lower compressive strengths, milling, which did not remove such compounds, may have increased the distribution of these impurities in the mixture and caused the observed loss in compressive strength.

Table 2.9. The average 7- and 28- day compressive strengths of mortar specimens, average of 5 specimens at each age. Values in brackets is the standard deviation of the averaged values (n = 5)

	CRTL	**LS**		**PC4-M**		**PC4-S**		**PC4-600**		**PC4-900**	
Replacement %	**-**	**5%**	**15%**	**5%**	**15%**	**5%**	**15%**	**5%**	**15%**	**5%**	**15%**
7-Day Strength	38.34 *(4.82)*	36.34 *(2.68)*	35.38 *(2.28)*	20.92 *(2.05)*	17.39 *(1.03)*	22.96 *(1.24)*	16.85 *(0.84)*	41.74 *(2.33)*	34.06 *(1.66)*	40.90 *(1.77)*	24.03 *(1.18)*
28-Day Strength	56.73 *(2.25)*	59.44 *(4.67)*	53.03 *(4.05)*	33.84 *(5.14)*	24.93 *(1.74)*	31.04 *(1.72)*	24.28 *(1.01)*	55.51 *(5.12)*	52.31 *(3.05)*	54.31 *(4.67)*	31.77 *(2.87)*

The thermal treatment of PC4 resulted in notable benefits to compressive strength compared to the sieving and milling. The 5%PC4-600 mixture exhibited the highest average 7-day compressive strength of all the mixtures tested, 9% greater than the CTRL mixture and 15% greater than 5%LS mixture. These results indicate that PC4-600 can lead to desirable mechanical performance, similar to the LS mortars evaluated. The 15%PC4-600 mixture had an average compressive strength that was 11% lower than the CTRL and was 6% lower than the 15%LS mixture. Of note, the 5%PC4-900 mixture exhibited only slightly lower strength than the 5%PC4-600 mixture at both 7 and 28 days (~2% and 6% lower, respectively). However, the 7- and 28-day compressive strengths for the 15%PC4-900 mixture were 42 and 43% lower than the 15%PC4-600 mixture and 37% and 33% lower than the CTRL mixture. These reductions may be

a result of the deleterious effects from paste mixtures with large amounts of hydrating free lime [186].

For the specimens tested, 5% or 15% mass replacements of cement with PC4 oxidized at 600°C or 5% replacement with PC4 oxidized at 900°C show promise for improving the performance of PC4 in cement-based materials. However, while outside the scope of this work, future studies should consider the durability implications of using oxidized PC4 as a virgin LS substitute. Depending on PC4 application, PC replacement levels, and the desired lifetime, a multitude of durability characteristics could be examined.

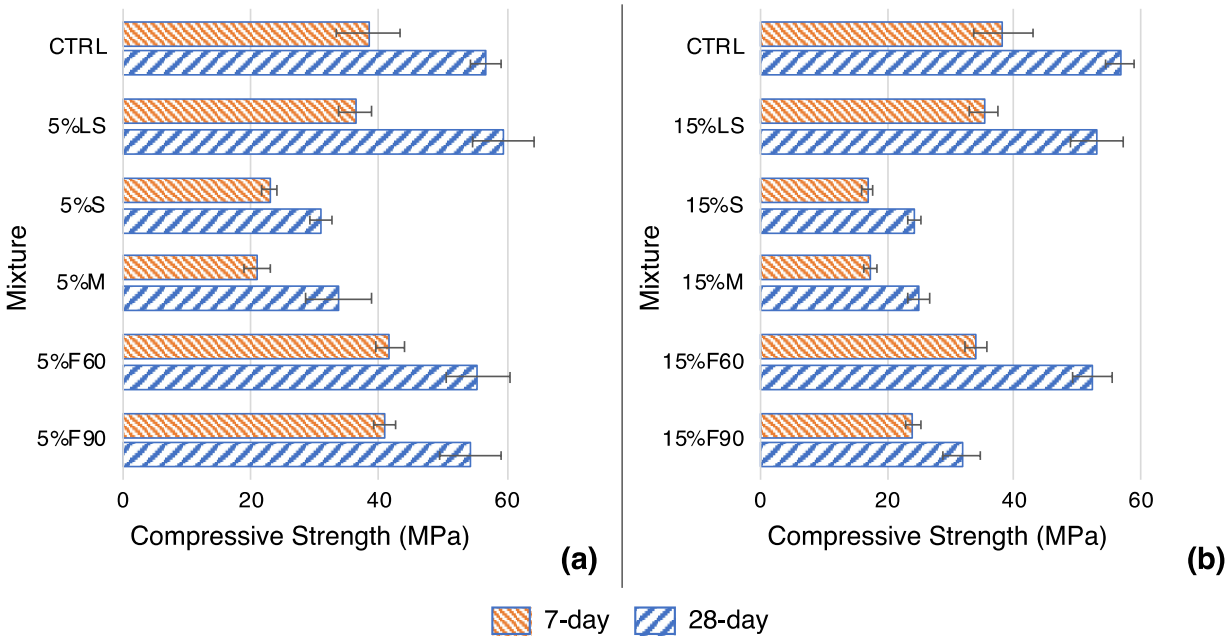

Figure 2.17. The average compressive strength at 7 to 28 days of mortar specimens, average of 5 specimens per age. (a) Shows CTRL mixture and specimens with 5% replacement and (b) shows CTRL mixture and specimens with 15% replacement. Bars show standard deviation. (n = 5)

2.4.2.3. Isothermal calorimetry

Isothermal calorimetry was performed to assess how replacement materials and rates could change the heat of hydration of cement-based materials. The heat flow over time is shown in **Figure 2.18**. The results showed that the 5%LS paste and 5%PC4-600 paste both led to a negligible decrease in time of the peak heat flow (approximately 26 minutes) (Figure **2.18**a and b). The LS led to a slight decrease in hydration

peak (~1%) and the PC4-600 led to a slight increase (~1.5%). The use of PC4-900 led to an approximately 11% increase in peak heat flow. However, the time of the peak was approximately the same as the CTRL. The increased heat flow from the oxidized PC4 was likely caused by the increase lime content and energy released from the hydration of the additional CaO [187], [188], which is similar to cement-lime mixtures in literature [189]. Similarly, the peak heat flow increased by 24% for the 15%PC4-900 paste. The 15%PC4-600 paste led to a decrease in heat flow, which could have been caused by a reduction in reactive compounds in the paste due to the decrease in PC; this heat flow is similar to the behavior of the 15%LS paste both in peak heat flow and time of peak heat flow.

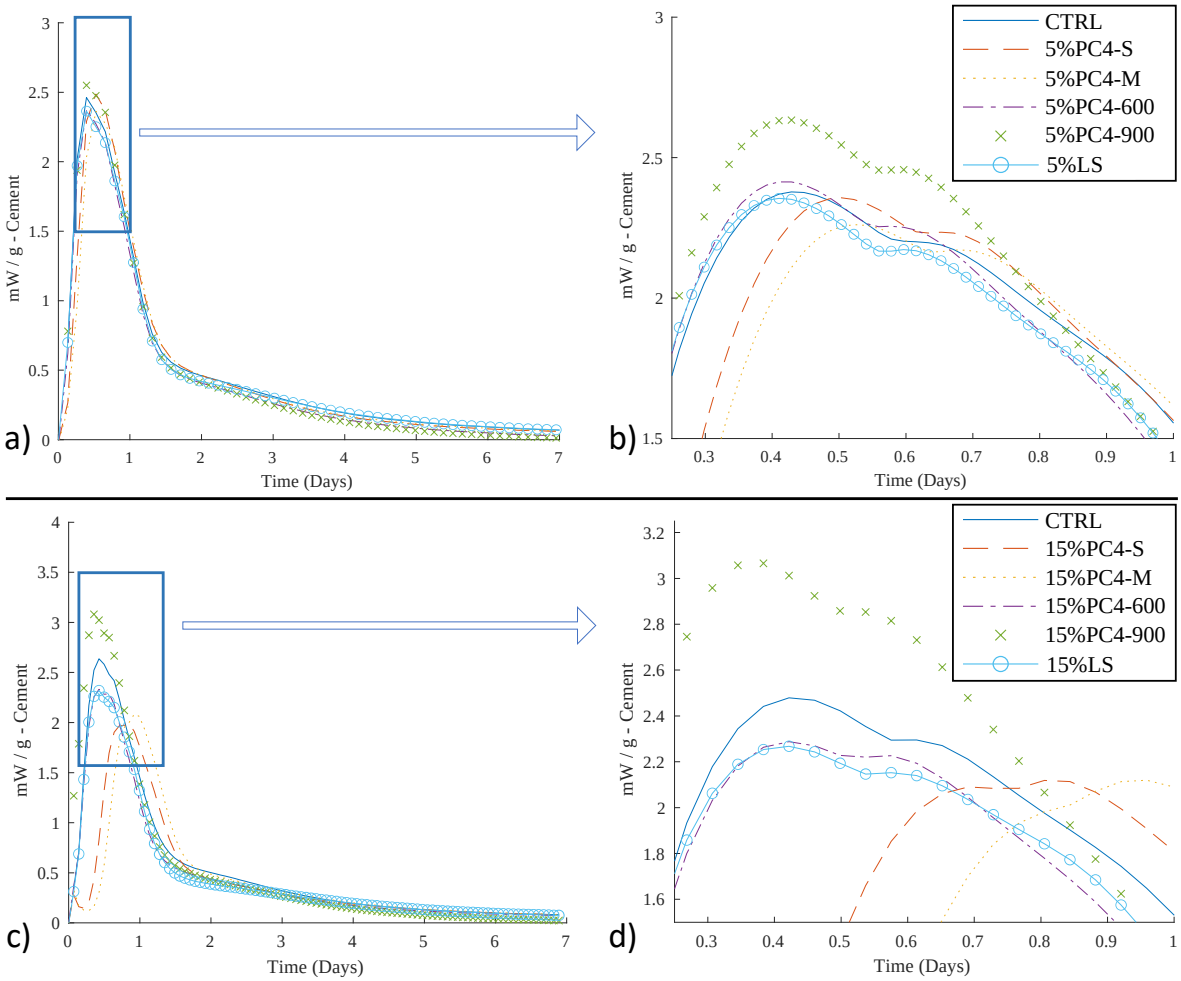

Figure 2.18: Composite figure of Isothermal Calorimetry over 7-day and 1-day timespans. Panels a) and b) are 5% cement replacement. Panels c) and d) are for 15% cement replacement. Panels, a) and b), show 7-day heat flow. Panels b) and d) show 1-day heat flow.

The PC4-S and PC4-M both led to increases in time to peak (1.8 hours and 2.2 hours, respectively), and the 5%PC4-S led to a ~1% decrease in heat flow. Contrary to the expectation that milling PC4 would increase and speed cement hydration through better particle dispersion, the 5%PC4-M paste led to an approximately 4.8% decrease in heat flow at the peak. Similarly, the 15%PC4-M led to ~17% decrease in peak heat flow and a 12.8-hour delay in the time to the peak heat flow. The hydration delay suggests that the remnant impurities, possibly latex, could be acting as a retardant. Furthermore, milling may have increased the dispersion or surface area of the impurities, shifting the interaction with the cement.

2.4.2.4. Scanning Electron Microscopy

Backscatter SEM micrographs were used to examine the microstructure of the mortars (Figure **2.19**). All the mortar specimens exhibited cracking which is likely from drying from ambient storage and water removal during specimen preparation. The CTRL (Figure **2.19**a) and 15%LS (Figure **2.19**b) mortars show drying cracks, with the 15%LS mortars showing visible grains of LS and some small voids. Unlike the CTRL and LS mortars, the mortars with PC4-S (Figure **2.19**a) and PC4-M (Figure **2.19**d) exhibited large circular voids in addition to the drying cracks. These voids are consistent with previous reports of PC4 increasing the amount of entrained air in wet concrete and permeable air voids in cured concrete [72]. The mortars with PC4-600 (Figure **2.19**e) and PC4-900 (Figure **2.19**f), which have reduced amounts of latex polymer, displayed much smaller voids compared to the PC4-S and PC4-M mortars. This change in microstructure likely contributes to the substantial reduction in compressive strength recorded for the PC4-S and PC4-M mortars.

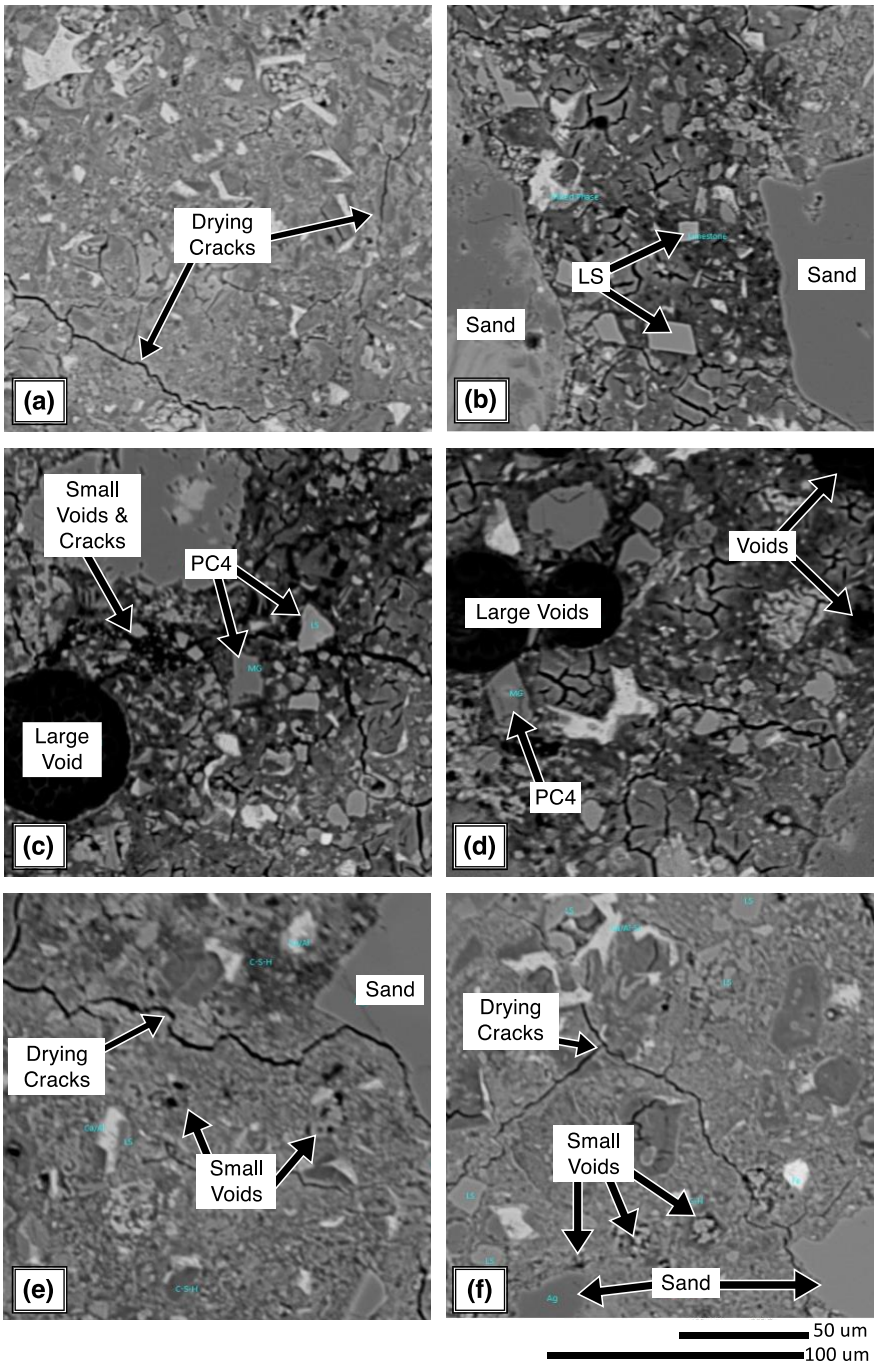

Figure 2.19. Representative backscatter Scanning Electron Microscope (SEM) micrographs of mortar sections with notation for: (a) CTRL; (b) 15%LS; (c) 15%PC4-S; (d) 15%PC4-M; (e) 15%PC4-600; and (f) 15%PC4-900 mixtures.

2.5.Summary

2.5.1. Material Flow of PC4

Cumulatively, approximately 1.4 billion m^2 of carpet has been disposed of in the US since 1954. This disposed material constitutes 33 Mt of nylon, 16 Mt of PP, 5.5 Mt of PET, 7 Mt of other textile and fiber material, and ~47 Mt of PC4. Notably, analysis of such resource flows from disposed carpet, particularly the large quantify of PC4 from carpet backing, have been poorly addressed in the literature. Relative to the US domestic production of polymers and utilization of limestone in cement production, these discarded resources from carpet use represent a significant fraction of virgin material demand, or in the case of nylon, exceed national production. Annually, less than 6% of PCC is reused, recycled, or used for energy recovery. The remaining ~94% of PCC represents a large, untapped material resource, and a lack of useful diversion has limited advancements towards a circular economy. We note that the EOL flows quantified here are 1.5-2 times larger than those estimated by industry. Cumulatively, the impacts from producing the same mass of virgin materials would include 7.5 Mt CO_2-eq in of greenhouse gas emissions, 2 kt $PM_{2.5}$-eq in respiratory effects, and 15 TJ of fossil fuel depletion annually. However, net-impact reductions including processing and transportation need to be guide EOL decision making.

Therefore, future studies should develop life-cycle inventories for carpet recycling to validate and quantify resource recovery to offset burdens of virgin material production. Investigations should explore scenario analysis to identify the best pathways for recycling. Such work is necessary to avoid unintended consequences of EOL processes. In the investigation of resource recovery, shifts in material performance from using these recovered materials and the environmental impacts and technoeconomic feasibility of recycling methods that limit changes in material performance, such as depolymerization pathways, should be considered to inform decisions by industry, policy makers, and other stakeholders. These pathways could expand the performance and functional application of post-consumer resources. The findings from this work and from future studies that can build from these findings are critical to limit the inefficient utilization of material resources and to drive best practice in recycling programs.

2.5.2.Material properties of PC4 in cement-based materials

In this work, we address how a waste mineral stream from the building industry can be utilized in the production of cement-based materials. Specifically, this work examines how the mineral components in carpet could be used to reduce demand for virgin materials in cement-based materials. The development of new, environmentally sustainable materials and practices is of great societal necessity. The utilization of minerals that are readily available and recycled from the same industry could be a significant mechanism in improving environmental sustainability. Currently, however, the understanding of how the calcium carbonate used in carpets can influence the material attributes of concrete is extremely limited. A foundation of how these recycled mineral waste streams influence cement-based material performance is critical in addressing waste-minimization strategies and routes to reduce dependence on virgin-mineral resources.

This research serves as a contribution toward understanding the viability of Post-Consumer Carpet Calcium Carbonate (PC4) for use in concrete. In this work, 5 and 15% mass replacements of Portland cement as well as 5 and 15% replacements of fine aggregate with PC4 were examined. To draw comparisons with commonly used materials, the effects of using these mixtures were assessed relative to control mixtures with Portland cement as the only powder in the binder as well as the same mass replacements with limestone. Fresh and hardened concrete properties were assessed. Key findings from this work include:

- The use of PC4 as an inclusion in concrete, either as a partial cement replacement or as a partial fine aggregate replacement, increases initial and final set times by up to 167% and 195%, respectively;
- The use of PC4 can lead to a lower density concrete (~10% decrease) that is more porous (11% increase in air voids) than a mixture with only Portland cement as the binder or only conventional aggregates;
- PC4 lowers the strength of concrete mixtures by up to 60%; however, this may not be of concern for low strength applications;

- PC4, when used to replace cement, can lead to reduction up to 15% in GHG emissions. However, such benefits should be weighed in the context of any shifts in necessary performance.

In future studies, the effects of any variability between PC4 batches, such as those that might occur as a function of the carpet fiber type, age of carpet, or recycling process, should be examined. Additionally, the effects of PC4 on other durability properties of concrete should be assessed. Future work should address possible beneficial traits that might occur from the low-density PC4 mixtures, such as changes in thermal conductivity. Despite these areas for further investigation, this work provides insight into the feasibility of utilizing PC4 as a constituent in concrete. Noting the importance of decreasing the impact of concretes, the need to minimize waste streams, and the value of immobilizing wastes in a long-service life material, such as concrete, these findings suggest there is a potential market for PC4 in cement-based materials. Due to alterations in material properties noted from this work, it is possible that PC4 would be best utilized in low-strength applications, such as pavers. However, with further study and refinement of processing methods, it is possible that additional uses for PC4 in cement-based materials can be elucidated.

2.5.3. Properties of Treated PC4 in cement-based materials

In this work, thermal and mechanical treatments were used to process PC4 with the goal of improving the consistency of PC4 and its contributions to strength in cement-based materials. In doing so, this study provides a novel attempt to overcome limitations found in prior investigations regarding use of PC4 as a mineral constituent in concrete, which suggested that residue carpet backing additives resulted in concrete with both reduced density and strength. For the first time, heat treatments of PC4 at 600°C and 900°C were evaluated to remove remnant fibers and coating from the PC4 for cement-based mortars. Additionally, a milling treatment on the PC4 was evaluated to alter the mineral gradation with the goal of improving the dispersion and hydration of cement particles. Notable results include:

- PC4 oxidized at 900°C showed decreases in both amorphous phases and calcite with an increase in lime and periclase formation;
- Contrary to the hypothesis that M-PC4 would improve the strength of mortars through increased cement hydration, 5%PC4-M and 15%PC4-M mortars had approximately the same strength as the use of PC4-S at the same replacement levels. Further, 5% and 15% cement replacement PC4-M decreased the heat of hydration by approximately 5% and 17%, respectively, and delayed time to peak by 2.2 and 12.8 hours, respectively;
- The mixtures with 5% and 15% cement replaced with PC4-600 led to negligible reductions in 28-day compressive strength compared to the 100% PC control;
- The 5%PC4-900 mortar had 6% lower average strength than the 5%PC4-600 mortar.

This work is an important step in understanding treatment methods that can drive beneficial reutilization of waste flows in cement composites. Findings demonstrate that 5% or 15% mass replacements of cement with PC4 oxidized at 600°C or 5% replacement with PC4 oxidized at 900°C show promise for improving the performance of PC4 in cement-based materials.

CHAPTER 3

Rice hull ash and rice straw ash as supplementary cementitious materials

Author Note

This chapter is comprised of portions from the following peer-review journal articles. The author is grateful for the expertise and advice provided by co-authors.

i. **P.R. Cunningham**, L. Wang, P. Thy, B.M. Jenkins, S.A. Miller. *Effects of Leaching Method and Ashing Temperature of Rice Residues for Energy Production and Construction Materials*. ACS Sustain Chem ENG. (2021). https://doi.org/10.1021/acssuschemeng.0c07919.

ii. **P.R. Cunningham,** L. Wang, S. Nassiri, P. Thy, J.T. Harvey, B.M. Jenkins, S.A. Miller. *Evaluating the viability of regional supplemental cementitious materials: the performance and potential supply of rice straw and rice hull ashes*. Under review. (Anticipated 2024).

3.1. Introduction

Industrial symbiosis across food, energy, and materials production industries could contribute to meeting rising energy and materials demands [3], [190], while simultaneously improving the environmental sustainability of these industries. In particular, the use of residual biomass from the cultivation of rice – a prevalent food crop grown around the world – could be well suited to benefit the agricultural, energy, and construction material industries. In this work, rice straw and hulls (husks) are evaluated as a means to valorize agricultural biomass residue, generate electricity, and partially replace greenhouse gas (GHG) intensive Portland cement in construction materials. Specifically, pre-combustion leaching methods that benefit energy production are evaluated as a means to simultaneously improve rice hull ash (RHA) and rice straw ash (RSA) properties for cement-based material applications.

The potential for benefits from synergistic bio-ash engineering are well exemplified when studying individual regions, like California, which is the state with the second largest production of Portland cement in the United States [191]. The most popular supplementary cementitious material (SCM) in California is fly ash (FA) from coal-fired power plants. Currently, California uses approximately one million tons of FA annually [67] (equivalent to approximately 15% of the mass of Portland cement (PC) produced in the state [192]). However, as California does not combust coal as a primary energy source, this FA is imported from other regions. The nearest import sources of FA for the state have either recently been decommissioned or are currently facing issues of economic and environmental viability. Conversely, alternative energy supplies have been gaining prominence: 86 waste-to-energy power plants (including 32 biomass-to-energy plants) comprised approximately 3% of instate energy production in 2019 [193], and this energy is largely considered carbon neutral [194]. By 2050, it is projected that the demand for cement in California will increase by 65% beyond 2015 levels [195], [196] and, with it, the demand for SCMs is expected to rise. At the same time, the state had the second highest annual electricity demand in the United States in 2018 at approximately 1 EJ [197]. As an agriculture-intensive state, California has a large amount of residual biomass, with an estimated potential availability of RHA and RSA of approximately 400,000 tons annually [148], [198], [199]. This availability, coupled with the demand for both energy resources and SCMs, is a strong motivator for improving our understanding of achievable co-benefits from methods to support energy generation and the use of rice-based ashes in concrete. This example is pertinent to many other areas around the world. Regions in India and China are struggling with managing rice residues [200], [201]. These countries are currently the two largest producers of cement in the world and could similarly benefit from a combined avenue for residue management: the production of energy and an SCM source [202], [203], [204], [205].

3.2. Material flow analysis of rice hull and rice straw ash

The beneficial aspects of SCMs must be considered within the context of the substantial size of the demand for cement and concrete. Globally, approximately 4 gigatonnes (Gt) of cement are produced each year [119], and over 30 Gt of concrete are consumed annually [142]. Without significant abatement to reduce consumption [37], cement demand is projected to increase by 30% by 2050 [206]. There have also been escalating demands for SCMs. Over the past 30 years use of such materials in blended cements has increased by 10% [207], with additional amounts incorporated during concrete batching [208]. As demand for cement and SCMs grows, and the supply of industrial-byproduct SCMs is declining [67], alternative SCMs are necessary. Many alternative SCMs and fillers have been proposed, including biomass ashes [209], [210], [211], ground waste glass [67], [210], [212], ground limestone filler [67], [210], [213], and mineralized CO_2 from carbon capture and storage systems [214], [215]. To be feasible, these SCMs must be available in suitable quantities, be cost-competitive, and provide suitable performance.

As an important source of food and nutrition [216], rice is cultivated across the world [217] and rice biomass residues are particularly promising as a bio-derived SCM. The United States (US) is the 13th largest producer of rice in the world, accounting for approximately 1% of 2022 global rice production [218], [219]. China and India each produced about 27% and 25%, respectively, of global rice production in 2021 while also accounting for 54 and 8% of global PC production [219], [220]. In rice cultivation, residue hulls and straw do not have as strong of a market as milled rice. Rice hulls can be used for energy generation and the resulting ashes to be used as an SCM in concrete [209]. While other waste reduction strategies have been proposed for rice residues [221]; in practice, there are limited value-added applications [222], [223]. Rice biomass could play an important role in energy generation [224], and the resulting ash could be an SCM in these regions if suitable performance and supply can be achieved.

To understand the role of these ashes as regional SCMs, the potential annual production of RHA and RSA in the US is modeled in six rice-producing US states and avoidable GHG impacts by reducing

virgin PC production is quantified. The results of this work can guide post-combustion decision-making for rice-based biomass ashes and inform initial supply chain decisions for identifying and implementing biomass ash as a regional SCM.

3.2.1.Methods and Materials

3.2.1.1. Quantifying rice biomass and potential ash production

To understand the potential supply of RSA and RHA, as well as potential GHG emissions reduction through their use to replace PC at scale, both a materials flow analysis and an environmental impact assessment were conducted. The focus of these assessment was on US production, with particular attention given to states that produce large amounts of rice (i.e., Arkansas, California, Louisiana, Mississippi, Missouri, and Texas).

To quantify the potential production of RHA and RSA from 2017-2022, magnitudes of rice cultivation, weight fractions of hull and straw relative to paddy, and ash content that could be recovered for post-combustion use as an SCM were assessed (system shown in **Figure 3.1**). As there are few value-added options for rice biomass ashes, competition with alternative pathways for rice straw and rice hull was not considered.

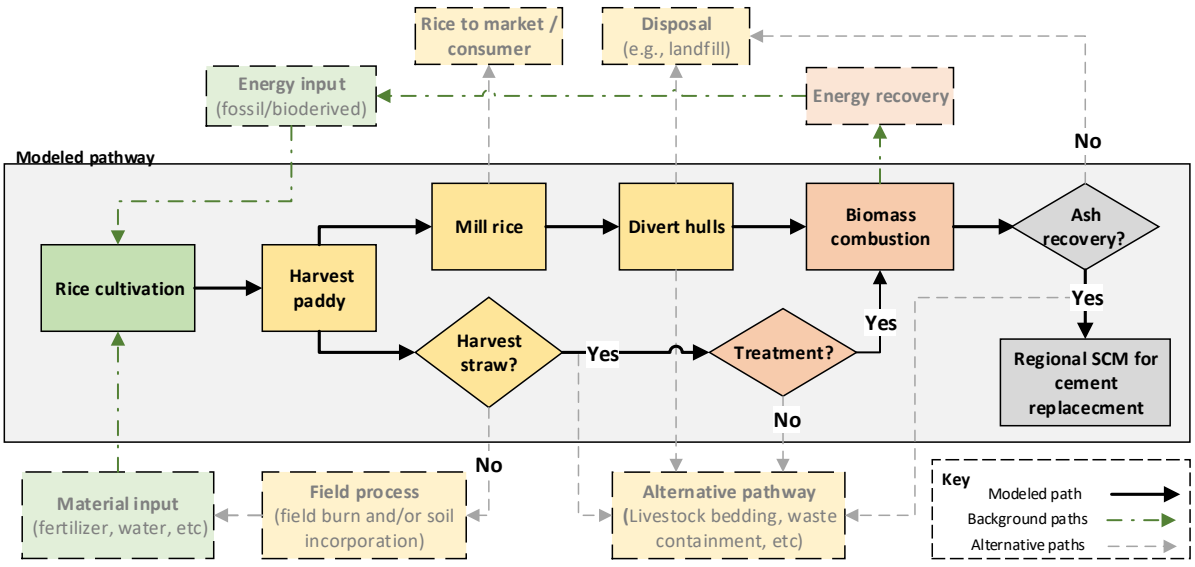

Figure 3.1. The system modeled showing the material flow of rice biomass from cultivation, harvest, separation, combustion, and ash recovery for use as an SCM. External processes (i.e., energy generation, rice production for food) and alternative pathways for rice-biomasses are also shown. Treatment can include post-combustion processes to aid the combustion stage, e.g., milling and leaching of biomass straws.

Rice hull masses were calculated with **Equation 3.1**, where $[rice\ hull]$ is the annual rice hull generation, $[rice\ yield\ per\ area]$ is the annual average rice yield per unit area, $[planted\ area]$ is the total planted area, and $[fraction\ hull]$ is the mass fraction of hull relative to the total rough (unprocessed) rice. Rice straw yields were modeled using **Equation 3.2** where, $[rice\ straw]$ is the annual rice straw removable, $[planted\ area]$ is the planted area in the region, and $[straw\ yield]$ is the straw harvested per unit area. The yield used in this work was selected to mitigate nutrient depletion (**Table 3.1**), though twice that yield is possible with greater nutrient loss [223].

$$[rice\ hull] = [rice\ yield\ per\ area] * [planted\ area] * [fraction\ hull] \qquad \textbf{Equation 3.1}$$

$$[rice\ straw] = [planted\ area] * [straw\ yield] \qquad \textbf{Equation 3.2}$$

The annual potential ash generation was modeled using **Equation 3.3**, where x is rice hull or rice straw biomass, ash_X is the annual ash production for biomass type x, $biomass_X$ is the mass (dry basis) of the type x biomass produced annually (i.e., the hulls or straw from **Equation 3.1** or **Equation 3.2**), and

$[ash\ content]_x$ is the ash content of biomass type x (dry basis).

$$ash_X = biomass_x * [ash\ content]_x \quad \textbf{Equation 3.3}$$

Rice cultivation data were collected from US Department of Agriculture rice production statistics [225]. The average ash contents of rice hull and straw samples in the Phyllis2 database were used to model ash yields [226]. To encompass variations in ash, a range representing one standard deviation increase or decrease in ash content was used. To assess the cement replaced potential by RHA and RSA, the modeled annual production potential of ash was compared to the annual cement deliveries to end customers in each of the 6 states (including inter-state transfers) and the total apparent consumption of PC in the US [220], [227]. Values and assumptions are shown in **Table 3.1** and Appendix C.

Table 3.1. Model assumptions and data sources

Parameter	Value	Comments & Source
Annual planted acres of rice (2017-2021)	Varies from 2017-2021	~2.5M acres ($10.24x10^5$ Hectare) in 2021, 2017-2021 values in Appendix C. From USDA [225].
Annual rice yield per acre (2017-2021)	Varies from 2017-2021	7,709 lbs/acre (8.6 Mg/hectare) in 2021, 2017-2021 values in Appendix C. From USDA [225].
Ratio of rice hull mass to rice harvested	0.2	Approximating values from [228], [229], [230] for typical hull mass as a fraction of rough rice.
Rice hull ash content by mass (percent)	19.56%	Mean value from 8 samples by the Phyliss2 biomass database [226].
Rice hull ash content by mass, 1 standard deviation (percent)	2.45%	Calculated from 8 samples by the Phyliss2 biomass database [226].
Rice straw yield per acre (US & State)	3.36 metric ton / hectare (1.5 US short-ton / acre)	Value from [223] and [231], recommended harvesting rate to mitigate additional fertilizer need.
Rice straw ash content by mass	18.13%	Mean value from 20 samples by the Phyliss2 biomass database [226].
Rice straw ash content by mass, 1 standard deviation	3.50%	Calculated from 20 samples by the Phyliss2 biomass database [226].
US kiln fuel mix	See Appendix C.	Modeled in OpenConcrete [36] based on [202].
State-level electricity grid mix	Varies by state	Modeled in OpenConcrete [36] based on [232]. All values in Appendix C.
State-level kiln type mix	Varies by state	Modeled in OpenConcrete [36] based on [172]. All values in Appendix C.
2021 US Portland cement consumption	210 Mt	USGS reported apparent consumption of Portland cement in 2021 [227].
2021 State-level Portland cement consumption	Varies by state	USGS reported 2021 cement deliveries to end user for each State [220].
2021 Portland cement production (global & by country)	Varies by country	USGS reported [220], global production and production in countries with >1% of rice production.
2021 rough rice production (global & by country)	Varies by country	USDA reported [219], global production and production in countries with >1% of rice production.

3.2.2.2.4.2. Regional potential for cement replacement and modeling impact reduction

To illustrate the potential for RSA and RHA substitution to reduce GHG emissions (kg CO_2-eq) by replacing PC, ash and cement production were quantified for six states: Arkansas, California, Louisiana, Mississippi, Missouri, and Texas, as well as for the US average. GHG emissions impact from PC production was modeled from a cradle-to-gate perspective using the OpenConcrete Tool [36]. State-level production impacts were quantified using the state average kiln efficiency and state average electric grid mix. The kiln fuel mix for each state was modeled as the US average. US average GHG impacts for PC production were made using the US average electricity grid mix, US average kiln fuel mix, and US average kiln efficiency. Inputs for the OpenConcrete tool are summarized in **Table 3.1**, above.

Potential emissions avoided through the replacement of PC with RSA or RHA were calculated using **Equation 3.4**, where $I_{avoidable}$ is the annual maximum potential avoidable GHG emissions, M_{ash} is the potential ash generation (from **Equation 3.3**), and $I_{unit\ PC}$ is the impact per unit mass of PC.

$$I_{avoidable} = M_{ash} * I_{unit\ PC} \qquad \textbf{Equation 3.4}$$

3.2.3.Results: At-scale potential as a supplementary cementitious material

To assess resource availability and potential to reduce GHG impacts, the maximum potential flows of RHA and RSA were modeled and compared to the consumption of PC within the US (**Figure 3.2a-b**). The GHG emissions from producing PC in 6 US states and the RSA and RHA available to offset these emissions when used as an SCM were used to understand the magnitude of potentially avoidable emissions (**Figure 3.2c-d**). Notably, these replacement levels may not be feasible in all applications. The percentage of PC replacement possible is largely driven by the amount of PC consumed (**Figure 3.2a**). For example, California is the second largest producer of rice in the US [225], but as the second largest consumer of PC [227], rice-based ashes could only replace ~2% of PC (**Figure 3.2b**). In Texas, the largest consumer of PC

in the US, rice-based ashes are limited to ~0.5% of PC mass. In regions with lower PC consumption, there is higher in-state replacement potential on a fractional basis, with mass fractions of ~6-7% in Mississippi, ~4-5% in Missouri, ~9-10% in Louisiana, and ~50-60% in Arkansas. By mitigating the production of PC by partially replacing it, the implementation of biomass ashes as a SCM could yield large reductions in regional GHG emissions (**Figure 3.2c**).

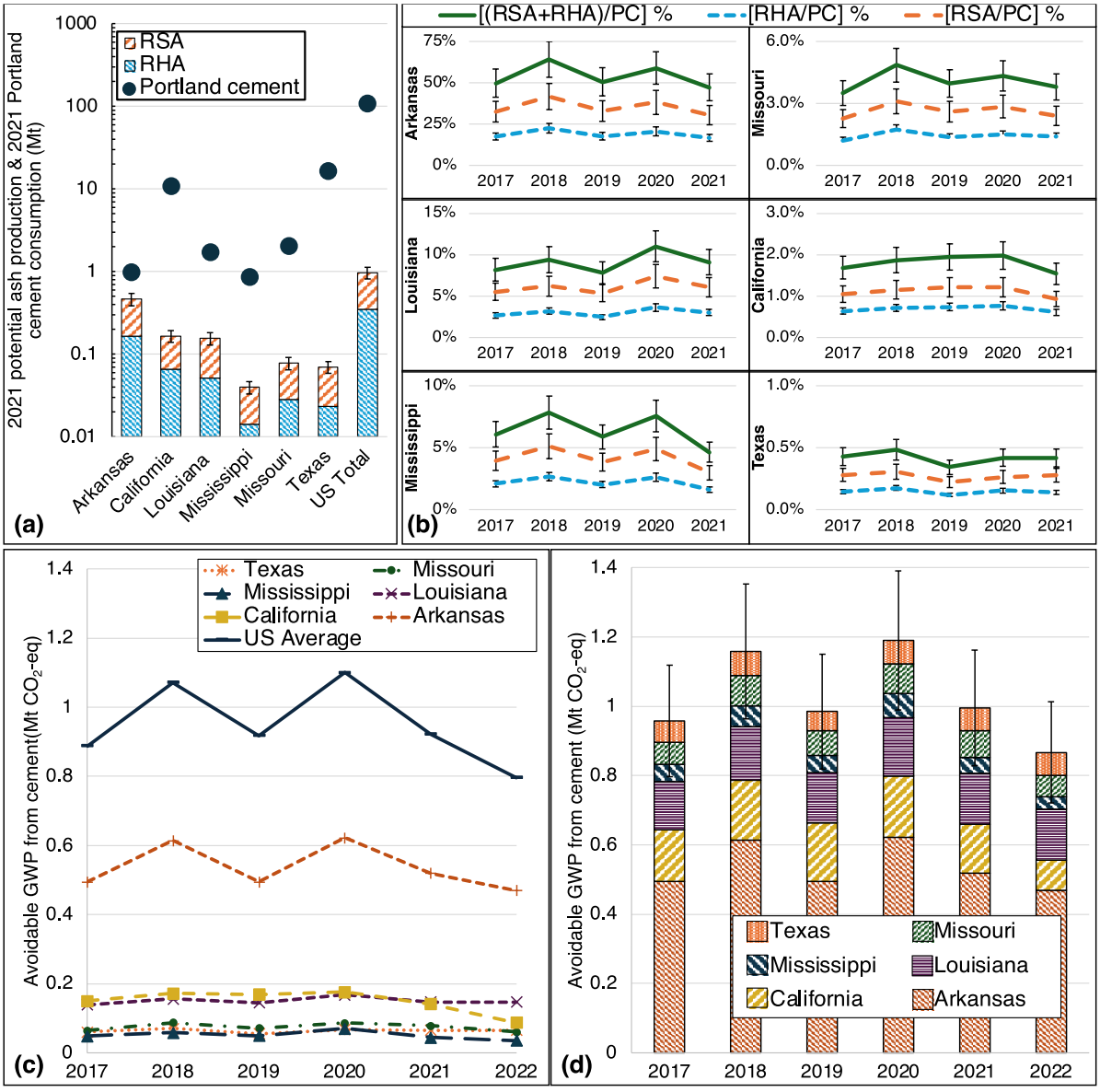

Figure 3.2. The Portland cement replacement potential of rice hull ash and rice straw ash in Arkansas, California, Louisiana, Mississippi, Missouri, Texas, and the US total. (a) Potential 2021 rice hull ash and rice straw ash production and 2021 Portland cement consumption (*note, log scale*). (b) State-level rice hull ash and rice straw ash generation as a percentage of Portland cement consumption. (c) GHG emissions from avoidable Portland cement consumption. (d) Avoidable GHG emissions via reducing Portland cement consumption. Bars indicate the range of one standard deviation increase or decrease of ash content.

The largest regional potential replacement is in Arkansas, where the approximately 0.5 Mt CO_2-eq reduction potential modeled is equivalent to ~3% of Arkansas's 13 Mt CO_2-eq of 2021 industry-related GHG emissions [233]. Notably, 50-60% cement replacement is more than typical with rice biomass ashes [209]. Realizing these reductions may require exporting ashes to other regions. Regional import is often done with conventional SCMs (e.g., coal fly ash and GBFS imports to California) [54], [234]. Regional economic considerations and concrete specifications are often deciding factors in SCM shipments and use locations. After Arkansas, the next largest reduction potentials are in Louisiana (0.13-0.16 Mt CO_2-eq) and California (0.08-0.17 Mt CO_2-eq), which both produce similar masses of rice biomass ash. Benefits to emissions reduction at the state level (**Figure 3.2d**) reflect a slightly higher potential to avoid GHG impacts than the US average (**Figure 3.2c**), which is a function of replacing cement produced with the higher-impact energy grids and lower kiln efficiencies that are present in the US Gulf region [172]. As the cumulative reduction from these ashes (1.2 Mt CO_2-eq in 2020) is only 1.8% of the total US cement industry GHG emissions (66.4 Mt CO_2-eq in 2020) [235], RSA and RHA may be most suitable as regional SCMs.

3.2.4. Discussion: Potential for Rice straw ash and rice hull ash to replace Portland cement

As GHG emissions from the cement and concrete industry are under increased scrutiny, the potential for agricultural-based SCMs is a growing interest [69]; however, the best utilization of these regional resources requires further examination. In the case of rice-based resources, the mass of harvestable rice straw is nearly twice that of rice hulls. This magnitude of residues means if RSA is used as an SCM, there would be greater resource availability to support increased adoption beyond niche applications. Further, compared to other countries globally, the US has a moderate share of global rice production (~1% in 2021) [218], [219]. The largest rice-producing nations are also large PC producers (**Figure 3.3**). In 2021, China and India each produced 27% of global rice production (**Figure 3.3a**) and accounted for ~54 and 8% of global PC production in the same year (**Figure 3.3b**). Indonesia and Bangladesh were the next large rice producers with shares of 7% each. Yet, they produce less PC (1.5 and 0.8%, respectively). As such, rice-biomass ashes could replace a notable fraction of PC in certain regions around the world.

To this end, additional research is needed to address the potassium in RSA that can foul biomass energy kilns if the straw is not treated to remove it prior to combustion. This research should include investigation of the GHG emissions from pre-combustion treatment and transportation of straw prior to combustion to quantify the net impact from processes through the supply chain. These may vary greatly depending on treatment technology and transportation distances and modes.

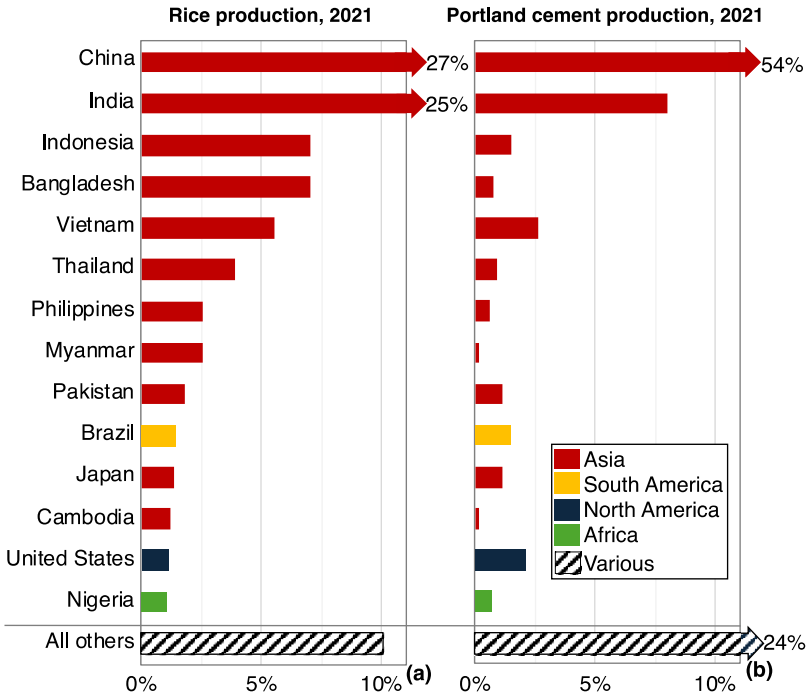

Figure 3.3. (a) Rough rice and (b) Portland cement production as fractions of 2021 global production (e.g., 7.6×10^8 tonnes rice and 4.3×10^9 tonnes of Portland cement) in countries with 1% share or more of global rough rice production in 2021 (calculated from [219], [220]).

For RHA and RSA to be adopted as SCMs, they not only needs to perform suitably, but also needs to meet cost and environmental impact requirements. Initial considerations for additional environmental impacts, economic costs, and spillover effects to crop production are summarized in **Table 3.2**. Importantly, decision makers should be guided by economic and environment analyses that are specific to the time and context being considered. Initial investigations suggest that rice straw may require additional precombustion treatment which would likely lead to higher environmental impact than from combusting untreated rice hulls. For transportation, similar comparisons may be drawn to coal fly ash or, potentially,

ground blast furnace slags which both require transportation from the industrial production facility where they are generated to the concrete production site. Likewise, if RHA and RSA are byproducts of energy production, then a similar allocation method as applied to coal fly ashes may be appropriate for allocating combustion impacts to RHA and RSA ashes. Importantly, removing rice straws could drive additional environmental impacts related to farm impacts and fertilizer needs. Growers may be required to purchase fertilizers which in turn may contribute additional economic costs and increase environmental impacts associated with rice growing. Recent analysis suggests that rice hull-energy can be produced at costs below the market rate. Thus, RHAs could be available at low-cost. This demonstrates the initial promise for RHA to be a byproduct SCM, like coal fly ash. The potential for acceptable environmental and cost performance of RHA and RSA compared to conventional SCMs still requires formal verification with environmental impacts assessment and techno-economic assessment methods.

Table 3.2. Summary of potential environmental impacts and economic cost considerations for PC4 reuse in Portland cement and/or concrete production.

Source	Potential impact or cost
Combustion impacts	• If byproducts of energy generation, impact may be allocated between the products. Potentially, similar allocation strategies as with coal fly ash may be suitable. • Biomass pretreatment, if required to minimize slagging and fouling may add additional environmental burdens.
Transport impacts	• Truck transportation per ton-km: 1.69×10^{-4} kg GHG emissions, 2.26×10^{-8} PM_{10}, 2.6×10^{-8} $PM_{2.5}$, and 1 MJ energy demand [36]. • Conventional SCMs are transported ~146 km (by truck) [131]. In some areas (e.g., California) SCMs are imported from other regions and countries to meet demand [234].
Processing impacts	• Post-combustion milling model in literature as requiring 67.7 kWh/ton [236], [237]. • Additional impacts (e.g., particle matter emissions) are anticipated from conveyance and milling.
Cost-constraints	• Rice hull energy production costs: $0.07/kWh (lower than market price in California, modeled in 2022) [238]. RHA could be available as a low-cost residue. • Conventional coal fly ash average price: ~$93/ton (in 2023 in US) [239]. • As with conventional SCMs, RHA and RSA transported from an industrial production facility to the concrete production facility is required. • Costs for post-processing facilities, leachates, and labor would be an additional cost.
Impacts to agriculture	• May require fertilizers or other means of nutrient recovery depending on rice straw harvesting rate [223]. • Could increase costs to crop growers and drive additional environmental impacts associated fertilizer production, transportation, and application [240], [241].

3.3. Pre-combustion leaching treatments of rice hull and rice straw

In this work, ashes produced from rice hulls and straw are evaluated as a SCM for cement-based building materials. The use of SCMs is a common practice for improving performance-aspects of concrete and reducing environmental impacts. While RHA could be a substitute for more common SCMs and improve concrete performance [242], these improvements are not always consistent [209]. Previous studies have shown combustion conditions have a strong effect on the production of reactive RHA [148], [211], [243]. Achieving high amorphous silicate content in the RHA through low temperature combustion has been favored for the production as SCMs. While lower temperatures are not commonly desirable for energy generation, gasification methods could be implemented to gain reasonable energy returns at these lower temperatures [244]; however, any resulting bioash may require additional processing to remove carbon and make it suitable for use in cement-based materials [245].

Pioneering work on the combustion of rice hulls to produce a silicate material for cement replacement was performed by Mehta in the 1970's [242], [246], which sparked significant subsequent investigation. Recent studies on the use of RHA as an SCM have found ash produced under controlled combustion conditions can replaced 5-30% of cement and yield higher strength materials [169], [209], [247], [248], [249], [250], [251]. For example, Vigneshwari *et al.* examined RHA as a replacement for silica fume, a highly reactive SCM, in concrete mixtures [248]. The authors found that at low combustion temperatures, namely 500-700°C, an ash with predominately amorphous silica is formed, and that ash can increase concrete compressive strength by up to 28% when it is used as a 30% replacement of the cement. Similar findings have been noted elsewhere. Sandhu and Siddique reviewed RHA use in self-consolidating concretes and found that RHA replacement of cement up to 15% provided higher strength [249]. Work done by He *et al.* and Thomas suggested a maximum strength is achieved at 20% replacement [247], [250]; however, Thomas noted that greater than 10% replacement of cement with RHA can lead to workability issues [247]. Gursel *et al.* evaluated RHA-FA-limestone cement blends and found RHA improved later age strength development as well as durability properties, while significantly reducing emissions from material

production [237]. Despite robust literature on RHA in concrete, RSA is not as commonly considered as an SCM, owing in part to its chemical composition, which includes higher potassium levels. The potential increased alkali metal concentrations could lead to undesirable concrete properties, such as deleterious effects on durability.

Pre-combustion leaching treatments, developed originally to benefit energy production, could have a co-benefit for producing cement-based materials by removing less-desirable compounds biomass ashes. Specifically, treatments prior to combustion, such as leaching, can reduce the presence of chlorides and alkali metals in addition to reducing agglomeration because of melting and fouling during combustion [240], [252], [253], [254], [255], [256]. Industrial-scale leaching may be accomplished under controlled, commercial operations; though, treatment of leachate adds additional costs for operators [255]. More affordable in-field water leaching has proven feasible for treating rice straw and allows for direct recovery of nutrients back into the field; however, it is more variable in final quality and is weather dependent with higher concomitant economic risks [240]. To the best of our knowledge, systematic examination of the influence of leaching pretreatments on the viability of RHA and on RSA in cement-based materials has not been performed.

To determine avenues for industrial symbiosis in which biomass leaching is used to benefit both energy conversion and materials production, further research is needed. This study investigates the use of select biomass pretreatment methods for processing rice-based residues for bioenergy and cement-based materials production, while providing an initial assessment of environmental sustainability factors for both industries. Based on experimental and analytical techniques: (1) the effects of leaching protocols and ashing temperature on ash properties are identified, (2) the mechanical properties of mortar mixtures formed with rice ashes from direct combustion methods are established, and (3) changes in environmental impacts for energy and material production from leached and unleached biomass are quantified. In doing so, this work provides both a systematic analysis from multiple engineering perspectives and a critical initial step into

the consideration of agricultural resources to support varied applications. Research in this area has a strong potential to contribute to advancement of the circular economy, in which maximum value is extracted from resources and they are maintained in use for as long as possible.

3.3.1. Materials and Methods

3.3.1.1. Materials

To produce treated and untreated ashes for analysis and mortar production, rice hulls and rice straw samples were acquired in August 2019, from Northern California suppliers. Rice hulls were provided by Farmer's Rice Cooperative in Sacramento, California which, after processing, stores hulls in covered bins at ambient conditions [257]. Rice straw was acquired from Windmill Feed in Woodland, California and was stored in unprotected outdoor conditions prior to acquisition, which likely subject the feedstock to precipitation during the winter season. Both feedstocks were from the 2018 harvest. To examine the effects of using the rice-based ashes on cement-based materials, mortars were produced using natural quartz-sand from Esparto, California (with a 99.95% passing rate through a #4 sieve) and ASTM Type II/V Portland Cement (PC), from Lehigh Southwest Cement Company in Stockton, California.

3.3.1.2. Biomass Pretreatment

Prior to ashing, rice straw was milled and portions of the hull and straw biomass were leached to simulate pretreatment leaching for energy production. The rice-straw was milled to facilitate handling and lab-scale leaching. For the straw, a hammermill with 1-1/4" (32 mm) diameter round-hole screen was used to reduce the majority of the straw to lengths less than 25 mm prior to leaching and ashing. As hulls are relatively small in size, no milling was performed. The size gradations of the straw and hulls were measured prior to leaching via a sieve analysis resulting in over 59.5% of rice straw passing through a 3/8" (9.5 mm) mesh sieve and 95.3% passing a 1" (25.4 mm) mesh. For rice hulls, 99.8% passed through a #4 mesh (4.76 mm) and 32.9% passed through a #8 mesh (2.38 mm) (size distribution give in Appendix D, **Table D.1**).

The effects of leaching were examined through the use of two solutions: (i) tap water; (ii) 0.5 M phosphoric acid (H_3PO_4) solution (made from 85 wt.% phosphoric acid, ACS reagent grade). These solutions were selected for their reported ability to remove alkali metals from rice-based feedstock [254], [258]. Comparisons were drawn to biomass that was combusted without leaching pretreatment, i.e. unleached. Bulk leaching was performed in low-density polyethylene containers using 15 L of leaching solution per kg of biomass (air-dry basis, moisture content given in Appendix D, **Table D.2**) to simulate potential industrial leaching [259]. This ratio is reported to be the smallest ratio that minimized the volume of leaching solution while maintaining agitatable biomass [260]. Biomass was leached for a period of 5.5 hours and agitated every 30 minutes by manually stirring. Afterwards, the biomass solids were dewatered through manual compression between two mesh strainers over the leaching vessel and then oven dried for 2 days at 100°C.

For unleached and leached feedstock, moisture, ash, volatile matter, and fixed carbon contents were assessed. For leached biomass, moisture content was determined after dewatering by oven drying at 103±2°C for 24 hours following ASTM E871 [261]. Volatile content was determined using ASTM E872 on oven-dried samples in covered crucibles in a Fisher Model 750-58 air-muffle furnace at 950°C [262]. Ash content was determined using ASTM E1755 in the furnace at 575ºC for 8 hours [263]. Fixed carbon content was determined by subtracting the percentages of volatile matter and ash from 100% dry basis.

3.3.1.3. Biomass Ashing

To produce ash, biomass was oxidized in air under controlled temperatures at for 600°C, 850°C and 1100°C in a Fisher Model 750-58 air-muffle furnace. Ashing at 600°C was selected to approximate temperatures found in literature that led to performance improvements for ash in concrete [246], [248]. The 1100°C condition was chosen to approximate temperatures at which the literature suggests that ash should

be less-reactive [264] and the 850°C condition was selected as the midpoint between the two to test for non-linear effects. These temperatures are also in the range of many commercial furnace exit or reactor temperatures for biomass boilers and thermal gasifiers.

For RSA, a two-stage procedure started with straw torrefaction at 250°C for 40 minutes to remove most of the volatiles and prevent ignition. After torrefaction, straw was oxidized, without ignition, at each of three final temperatures but for different lengths of time to complete the oxidation, namely at 600°C for 8 hours, 850°C for 4 hours, or 1100°C for 1 hour. To produce RHA, a modified procedure was used to mitigate carbonaceous ash production. For 600°C RHA, hulls were ashed at 600°C for 8 hours, this was the only stage for production of 600°C RHA. For the remaining two temperature conditions, a first stage heating to 600°C for 8 hours was used. After the initial 600°C, the ashes were oxidized at either 850°C for 4 hours or 1100°C for 1 hour. The ash identifications were assigned based on feedstock treatment method and oxidation temperature where "S" or "H" represent straw or hulls; "U", "W", or "A" signify untreated (unleached), water-leached, or H_3PO_4-solution (acid)-leached; and "600", "850", or "1100" is the final oxidation temperature in degrees Celsius. For example, S-U-850 represents untreated straw oxidized at 850°C.

3.3.1.4. Mixture Proportions and Mortar Batching

Bioash-cement mortars were made to determine the impact of treatment on the performance of cement-based materials. Control mortars were designed to contain 100% PC as the cementitious binder. Bioash-cement mortars were proportioned using with ashes replacing 15% of the PC. Bioashes were used in their original form without any additional treatment (e.g., leaching, milling of ash). For all mixtures, the sand-to-binder ratio, where the binder is the combined mass of PC and ash, was set at 2.50 and water-to-binder ratio fixed at 0.59. Specimens were cured at 25°C and ≧ 95% relative humidity.

3.3.1.5. Leachate Chemical Analysis

The composition of the leachates after the leaching process were measured to quantify the amount of soluble salts and micronutrients removed from the feedstock. Measurements were adjusted for background concentrations in the leaching water and acid. While amorphous silicates, sodium, and calcium can also contribute to desirable gels in cements [194], [209], the presence of other compounds, such as high levels of potassium, chlorides, or carbon can lead to undesirable performance. Soluble salts and micronutrient concentrations, K, Ca, Mg, Na, Zn, Cu, Mn, and Fe, were measured following EPA Method 200.7 using inductively coupled plasma atomic emission spectrometry [265], [266].

3.3.1.6. Ash Analysis

The elemental composition of each ash was analyzed and the oxide compositions were estimated to determine the effects of leaching condition and ashing temperature. The specific gravity of each ash was quantified by pycnometer method using an AccyPyc II 1345 Pycnometer (Micromeritics Corp., Norcross, GA). Chemical analysis for major elements, selected trace elements, and loss on ignition, were performed for PC and all ashes. The materials were assessed using inductively coupled plasma optical emission spectroscopy (ICP-OES) to estimate oxide composition (Agilent Model 700 Series ICP-OES, Agilent, Santa Clara, CA) [267]. Both methods were carried out by Activation Labs, Ancaster, Ontario, Canada.

3.3.1.7. Concrete Compressive Strength of Mortars

Compression strength was tested on 50 mm diameter x 100 mm long (2 inch x 4 inch) cylinder mortar specimens after 7, 28, and 56 days of curing. Compression tests were conducted on a Soiltest CT-950 (Soiltest, Evanston, IL) load frame following an adaptation of ASTM C39 testing procedures [163], where cylinder specimens were capped both ends with neoprene-padded aluminum caps and then loaded under force control. The average maximum load before failure of five replicate specimens of each mixture, tested at each age, was used to determine the compressive strength.

3.3.2. Environmental Impact Assessment

3.3.2.1. Goal and Scope of Assessment

Environmental impact assessments were performed to quantify the potential environmental benefits of using rice-biomass to produce energy and cement-based materials relative to conventional resources. The literature suggests there could be environmental benefits from the production of electricity from rice straw and hulls [201], [268]. Similarly, rice-based ashes may reduce several environmental impacts from cement-based materials production [237]. In this research, two environmental impacts were examined: greenhouse gas (GHG) emissions and embodied energy. GHG emissions were weighted using the IPCC 100a scheme from 2013 [269]. Embodied energy was compared using the cumulative energy demand method of calculation published by Simapro [270]. The role of treatment methods for the rice biomass, as well as impacts of rice ash relative to other constituents in mortar, were assessed to inform targeted improvements in reducing environmental burdens for the energy and materials systems.

Two primary products from the rice biomass were considered in this work: electricity and an SCM. To investigate the biomass as an energy resource, the GHG emissions per MJ of electricity produced from rice-based feedstocks were compared to several fossil fuel resources. For the SCM, three units of comparison were employed: (1) GHG emissions of rice-based ashes were compared directly to PC on a per kg basis; (2) the use of rice-based ashes in mortars was explored based on the production of one cubic meter of mortar (comparisons drawn for GHG emissions and embodied energy); (3) the use of rice-based ashes in mortars was examined by weighting GHG emissions per cubic meter of mortar as a ratio of compressive strength achieved by the mixture at 28 days.

The scope of this analysis is outlined in **Figure 3.4**. Impacts associated with transportation, treatment methods for the biomass prior to ashing, energy generation, and the production of mortar (including impacts from other constituents) were assessed. In this analysis, both rice straw and rice hulls

were considered to be agricultural residues and no impacts from cultivation were considered. Impacts from biomass were allocated to the electricity generation. Impacts were attributed to the ash only after electricity generation, namely, only impacts from transportation impacts. Stages after mortar production and impacts generated from the treatment or conversion of waste, e.g. disposal or recovery of leachates, as well as potential offsets from using the biomass for energy production were not considered in this assessment.

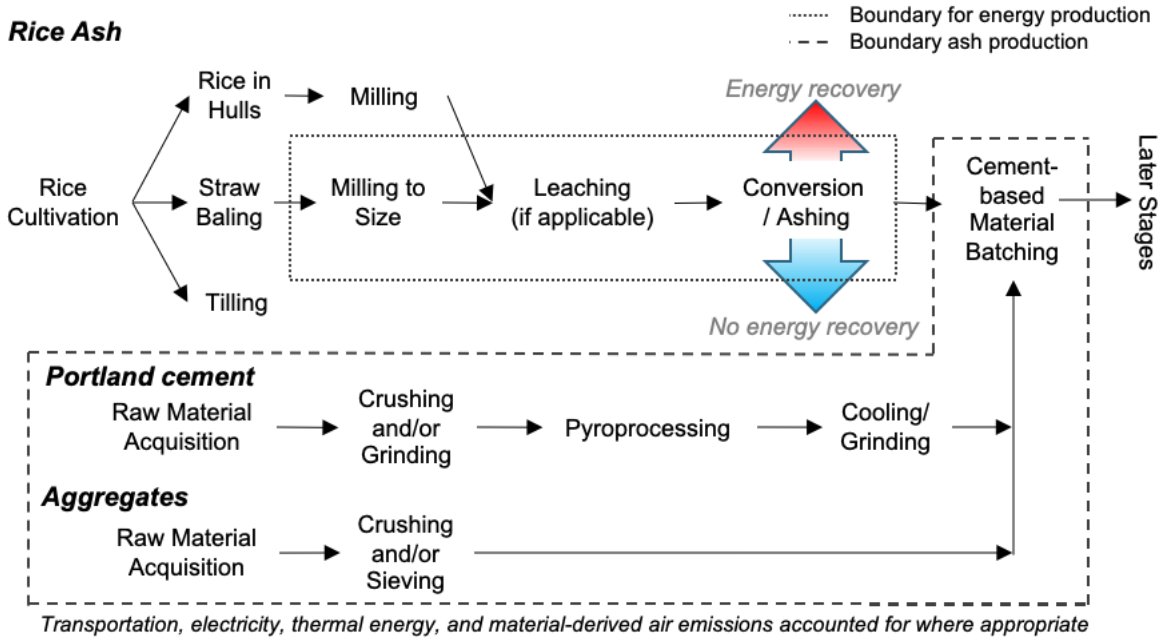

Figure 3.4. Process flow diagram depicting the boundary of the assessment

3.3.2.2. Inventory Models

Relevant inventory quantities for the environmental impact assessment were based on treatment methods and mortar outlined in the Materials and Methods section. These quantities include those for leaching water, acid solution, ashing, and mortar mixture proportions. Additionally, the quantity of feedstock biomass needed to produce the ash for each mortar mixture was determined by using measured ash yields and properties (Appendix D, **Table D.3**). Water for leachate and for mortar batching was modeled as requiring no necessary energy input. These quantities were supplemented with values from the literature. An inventory of the materials, energy demand, quantities, and models used are stipulated in **Table 3.3**.

Table 3.3. Inventory model assumptions and values

Biomass treatment, electricity generation and ash production			
Input	Quantity	Reference for Quantity	Impact Model
Biomass feedstock yields and properties	Multiple values, varies by ash type	This study, see Appendix D* Table S4	Not considered
H_3PO_4	15.35 kg H_3PO_4 : 1 kg biomass for acid leachate	This study	No impacts for water; phosphoric acid from ecoinvent [271]
Water leachate to biomass ratio	15 kg water : 1 kg biomass	This study, Yu [260] and Yu, et al. [259]	No impacts for water
Energy to mill rice straw	0.244 MJ / kg biomass	Gursel et al. [237]	2017 2017 California average electricity grid mix [272]
Emissions from bioenergy production	Material input based on 17.209 MJ / kg (LHV*) and 25% efficiency	Argonne National Laboratory [273]; Biomass Energy Resource Center [274]	Biomass combustion emissions, from NREL [120],*
1 MJ of electricity from bituminous coal, diesel, and natural gas (for comparisons)	-	-	NREL [120],*
Mortar constituent production (for inputs for ash production, see above)			
Input	Production Method	Reference for Method	Impact Model
Cement production	Preheater-precalciner kiln, US average kiln fuel mix	Miller and Myers [2]	UCB Green Concrete Tool [169];* 2017 California average electricity grid mix [272]
Fine aggregate production	Quarried, crushed and/or ground	UCB Green Concrete Tool [169],*	
Mortar batching per cubic meter	-		
Transportation			
Input	Distance	Reference for Distance	Impact Model
Biomass (field to production site)	30 km	Bakker and Jenkins [240]	Truck (transportation) emissions from NREL [120],*
Cement raw materials to kiln	25 km	Marceau et al. [172]	
Cement / bioash to batching site	130 km	Marceau et al. [131]	
Aggregates to concrete batching site	88 km	Marceau et al. [131]	

*NREL = National Renewable Energy Laboratory; UCB = UC Berkeley; LHV = lower heating value.

3.3.3. Results and Discussion

3.3.3.1. Leachate and Biomass Properties

To determine how leaching can facilitate the removal of compounds that are potentially detrimental to energy production and cement-based materials, the soluble cations in the water and acid leachate were tested (Appendix D, **Table D.2**). Compared to the water leachate, examination of the acid leachate showed a 49% increase in potassium leached from hulls, but a 45% decrease in potassium removal from straw. This difference in leaching can be attributed to the variability in the solubility of inorganic compounds from

various biomass source in different solvents coupled with the likely exposure of straw to precipitation during storage over the winter season. For example, the concentration of water-soluble potassium varied from 58-86% in rice straws examined by Baxter et al., with as little as 2-8% of the potassium being acid-soluble [275]. While water leaching removed more potassium from the straw than the acid solution, the use of acid leaching improved removal of most other soluble elements examined. However, the changes in Ca, Mg, Na, Zn, Cu, Mn, and Fe were small and unlikely to affect the ash behavior in concrete mixtures.

As anticipated, the leaching techniques applied in this work affected the ash content, volatile matter, and fixed carbon of the biomass (Appendix D, **Table D.3**). The differences between water-leached and unleached biomass were small. For rice straw and hulls, water leaching led to approximately 4 and 5% decrease in ash content, 3 and 4% increase in volatile matter, and 5 and 8% decrease in fixed carbon compared to unleached biomass, respectively. Phosphoric acid was selected for leaching, because past studies indicated that high alkali-removal could be achieved while maintaining high ash content [254], which is consistent with the results of this work. Acid leaching reduced volatile matter in rice hulls by 13% and in the rice straw by 29%, but increased fixed carbon 26% and 50%, respectively. Compared to water leaching, increased amounts of ash from acid leaching could lead to a larger supply for replacing cement; however, the potential losses in recoverable energy will impact the feasibility of using the leached biomass for both energy production and cement replacement.

3.3.4. Ash Properties

Properties of the ash were evaluated to provide insights into how leaching affects the chemical composition, which can influence the performance of bioash-cement materials. Both different leaching solutions and different ashing temperatures altered the composition of the ashes produced. Notably, acid leaching led to high amounts of phosphorus remaining in the feedstock: 43-46% and 12-13% P_2O_5 for straw and hull ash, respectively. This increase in P_2O_5 is important to consider when evaluating the bioash-cement mortars performance and the ashing behavior of the biomass. However, in order to compare ash to ash, the

composition has been scaled by setting the P_2O_5 fraction of the acid-leached biomass ash to the average P_2O_5 percentage of the unleached biomass ash and then scaling a total of 100% (**Table 3.4**).

Table 3.4. Ash composition, by percent, of rice-based ashes, Type II/V PC, and average compositions reported in the literature scaled so total sums to 100%. (n=1)

Ash ID		SiO_2	Al_2O_3	Fe_2O_3(T)	MnO	MgO	CaO	Na_2O	K_2O	TiO_2	P_2O_5
Type II/V Cement		22.40	3.86	3.61	0.046	2.32	66.78	0.05	0.57	0.187	0.17
S-U-600		84.14	0.25	0.53	1.047	1.33	1.62	0.52	9.82	0.015	0.72
S-U-850		86.70	0.19	0.54	0.918	1.30	1.39	0.47	7.80	0.011	0.67
S-U-1100		87.74	0.17	0.43	0.933	1.31	1.72	0.45	6.65	0.011	0.58
S-W-600		94.01	0.15	0.44	0.141	0.54	0.54	0.02	2.93	0.007	1.22
S-W-850		90.02	0.19	0.49	0.985	1.15	1.71	0.34	4.60	0.011	0.49
S-W-1100		90.37	0.16	0.18	0.970	1.11	1.72	0.45	4.61	0.010	0.41
S-A-600[d]		94.04	0.74	0.27	0.339	0.45	0.74	0.18	2.59	0.016	0.64*
S-A-850[d]		90.95	0.65	3.89	0.394	0.40	0.63	0.13	2.29	0.012	0.64*
H-U-600		93.40	0.17	0.35	0.138	0.61	0.56	0.06	3.29	0.009	1.40
H-U-850		94.90	0.07	0.15	0.175	0.46	0.60	0.05	2.55	0.005	1.04
H-U-1100		94.17	0.08	0.15	0.178	0.46	0.59	0.08	3.15	0.005	1.13
H-W-600		96.76	0.06	0.11	0.141	0.39	0.60	0.05	1.39	0.004	0.48
H-W-850		95.85	0.07	0.21	0.159	0.52	0.67	0.06	1.60	0.004	0.85
H-W-1100		95.55	0.13	0.15	0.148	0.36	0.53	0.03	2.52	0.008	0.58
H-A-600[d]		97.82	0.43	0.08	0.036	0.08	0.13	0.00	0.24	0.005	1.17*
H-A-850[d]		97.06	0.80	0.50	0.048	0.09	0.11	0.00	0.22	0.003	1.17*
Lit Hull Ash [a, b]	Max	95.60	2.00	0.14	-	0.20	3.21	0.21	3.71	0.02	0.46
	Min	91.42	0.78	0.03	-	0.01	0.20	0.10	1.20	0.02	0.42
Lit Straw Ash [a, c]	Max	95.60	2.00	0.88	-	2.50	3.21	0.96	16.60	0.09	8.87
	Min	72.20	0.10	0.03	-	0.01	0.20	0.10	1.20	0.01	0.43

[a] "-" refers to values not commonly reported in the literature, [b] range of values based on 3 hull ash composition reported in Phyllis 2 [226], [c] range of values based on 14 straw ash composition reported in Phyllis 2 [226], [d] "*" indicates P_2O_5 percentage assumed based on the average for straw or hull of the unleached ash for recalculating oxides composition

Both leaching methods increased the percentage of SiO_2 for both feedstock types. Compared to unleached samples, water leaching led to increases in silica of 3-10% in RSA and 1-3% in RHA as SiO_2 is not removed by water to the same extent as other constituents (dilution effect). For acid-leached samples, silica increased 4-10% in RSA and 3-4% in RHA. The SiO_2 percentage in unleached RHA and RSA and leached RSA are within the range reported by the *Phyllis 2* database [226] and in the literature [209], [260]. The leached RHA SiO_2 concentrations were, at most, 2% higher than the maximum reported by *Phyllis 2* [226]. The increase in SiO_2 fraction for both acid and water leached RHA and RSA could be beneficial to

an ash for use in cement-based materials if it is reactive. Both leaching methods also decreased the K_2O fraction of the ashes, with the acid leaching being more effective at reducing the K_2O fraction: up to 74% for RSA and 93% for RHA, both ashed at 600°C. For unleached RHA and RSA, ashes prepared at a higher temperature had lower K_2O fractions. The K_2O percentage for RSA is on the lower end of the range reported by *Phyllis 2* [226].

The untreated feedstock compositions of rice hulls and rice straw differ, which informs composition of their respective ashes. Hulls typically have an overall higher ash content than straw, and the SiO_2 content in RHA often exceeding 90-95% of the ash, which is consistent with the findings in this work. RSA typically contains greater amounts (15%) of potassium with SiO_2 concentrations of around 75%. These concentrations vary depending on geographic location, soil type, and agronomic practice (e.g., fertilization and other inputs). The higher starting concentrations of SiO_2 and lower concentrations of K_2O in the ash of the untreated straw used here, compared with typical concentrations for California rice production, suggest that some pre-leaching occurred due to precipitation either prior to harvest or during uncovered storage over the winter season prior to acquisition for these experiments [240], [256], [259]. Such factors influencing variability may also be present among materials reported in the *Phyllis 2* database.

In addition to composition, the ashes were evaluated for trace elements, loss on ignition, and relative density. Chlorides and the trace elements Ba, Sr, Zr, and V were detected in some ashes (Appendix D, **Table D.4**). Elements Sc and Be were not detected (detection limit 1 ppm for both) in the ashes, but they were detected in the PC. Yttrium was only detected in the PC and the acid leached RSA ashed at 850°C with the concentration in ash at the detection limit of 1 ppm, which is lower than the 11 ppm of Y detected in the PC. For all trace elements detected in the ash, the concentrations are lower than those detected in the PC and thus unlikely to lead to a degraded performance compared to typical cement-based materials. The results indicate that higher temperatures and leaching decrease the amount of chlorides present in the ash,

which agrees with other reports in the literature [259], [276], [277]. For the ashes tested, the Cl values are low regardless of treatment or ashing temperature and thus are unlikely to impact concrete in most applications. The highest value was 1.52% Cl for S-U-600, which, if used to replace 15% of cement as done in this study, would lead to a Cl content of 0.22% for the binder. This level is below the maximum concentration recommended in ACI 318-14 for normal concretes with moderate exposure conditions [278]. For all other ashes, with measured values of 0.14% and lower, the binder Cl concentration would likely be below maximum for high-exposure conditions.

3.3.5. Compressive Strength of Mortars

Despite the potential performance benefits in cement-based materials from increasing the silica fraction and reducing potassium in ash, the average compressive strengths (5 replicates) indicate that the leaching methods used resulted in a loss of compressive strength at early ages (**Table 3.5**). Mortars made with S-U-600 had nearly the same (1% lower) average strength as the control at 7 days; however, S-W-600 exhibited a 17% loss in strength and S-A-600 exhibited a 45% loss in strength at that same age. Similarly, at 7-days, H-U-600 resulted in only a moderate loss of strength (5% lower), while H-W-600 and H-A-600 resulted in reductions of approximately 27% and 21%. The largest reduction in compressive strength at 7 days was observed in RSA-mortars produced with acid-leached biomass. While milling of ash and assessing the effect of particle size on the reactivity of the leached and unleached biomass ash was outside the scope of this work, milling RHA [148], [279] or inter-grinding RHA and cement [242] is shown in the literature to improve the consistency of bioash or bioash-cement blends and improve hydration [280]. Milling of RHA has also been suggested as a means to improve the reactivity of ashes produced at higher temperatures [281] and may be a topic for future study to examine if leached ash can be tailored to improve performance in cement-based materials at early ages.

At later ages, both leaching methods led to improved strength for mortars with RHA produced at 600°C or 850°C, with most strengths being higher or comparable to mortars with ash from unleached

biomass at 28- and 56-days. After 28 days of curing, mortars containing unleached ash prepared at 600°C lowered compressive strength by 1-5% compared to the control, and after 56 days, mortars with leached rice hull ash prepared at 600°C had 5-6% lower compressive strengths compared to the control. The high strength from the acid leached hulls, with increased P_2O_5 content, is notable as the literature suggests that P_2O_5 should lead to reduced compressive strengths at these levels [282]. It is possible that the acid-leaching increased the fraction of amorphous silicates, which would improve reactivity and could have compensated for the increase in P_2O_5. If the additional P_2O_5 could be removed, potentially through improved leaching protocols or treatments to the ash, the acid-leached biomass may lead to additional gains in compressive strength at later ages.

Table 3.5. Average compressive strengths (MPa) of mortars at 7, 28, and 56 days by ash feedstock, leaching condition, and ashing temperature and strength of the control mixture (n=5)

Ashing Temperature		600°C			850°C			1100°C		
Age (Days)		7	28	56	7	28	56	7	28	56
Straw	Unleached	27.9 (2.5)	37.1 (2.5)	39.5 (3.4)	22.4 (2.1)	29.6 (1.9)	32.9 (1.9)	23.7 (1.3)	31.6 (1.9)	31.4 (1.8)
	Water Leached	23.3 (1.4)	28.3 (5.7)	34.0 (2.0)	20.8 (0.8)	27.0 (1.7)	27.7 (2.1)	17.6 (0.8)	25.9 (1.3)	31.4 (1.0)
	H_3PO_4 leached	15.6 (0.5)	22.2 (0.5)	27.4 (1.1)	20.8 (0.8)	31.4 (1.3)	34.7 (1.8)	-	-	-
Hulls	Unleached	26.8 (1.8)	34.2 (2.4)	38.8 (1.3)	21.1 (1.2)	27.2 (0.9)	29.0 (1.9)	19.8 (1.3)	29.2 (1.7)	32.7 (3.6)
	Water Leached	20.6 (0.9)	31.4 (1.8)	39.7 (1.4)	19.8 (0.8)	27.7 (2.1)	31.4 (1.8)	16.7 (0.5)	23.5 (1.3)	28.1 (1.0)
	H_3PO_4 Leached	22.2 (0.5)	34.5 (1.3)	40.2 (1.0)	19.3 (1.3)	27.7 (0.9)	32.3 (2.5)	-	-	-
Control Mortars		28.1 (1.0)	38.2 (3.4)	42.1 (3.3)						

Values in parenthesis are the standard deviations for the mortar samples tested, "-" indicates no mortars produced for these conditions

Siliceous SCMs, like RHA and RSA, frequently create a delayed contribution to strength gain [148]. For mixtures containing RHA, both small increases and decreases in 7-day compressive strength have been reported in the literature [248], [279] with low early-strengths attributed to slower hydration of RHA-cement mixtures [248], possibly due to RHA absorbing free water [280]. Most of the mortars studied herein exhibited the greatest increase in strength between 7 and 28 days (ranging from 18% to 35% increase

in strength), consistent with continued pozzolanic reactions after the initial cement hydration [279], [283]. Lower gain in strength was observed from 28 to 56 days (ranging from a negligible change to 21% increase in strength). While many milled-ashes have been reported to improve cement-based materials at later ages [242], [247], [248], [251], non-milled ashes have exhibited lower strengths (approximately 20%) in literature compared to cement-only materials [279]. Notably, as mentioned earlier, the ash produced from water and acid leached biomass exhibited large gains in strength at later ages, suggesting a possible effect on the pozzolanic nature of these ashes.

Two-way ANOVA analyses for unleached ash at 7, 28, and 56 day ages reveal that, for 7-day compressive strength, both ashing temperature ($f(3.4) = 32.7$, $p = 1.4 \times 10^{-7}$) and feedstock type ($f(4.3) = 10.6$, $p = 3.3 \times 10^{-3}$) are significant variables. For 28- and 56-day compression strengths, the temperature remains a significant variable ($f(3.4) = 28.8$, $p = 4.2 \times 10^{-7}$ and $f(3.4) = 19.9$, $p = 7.9 \times 10^{-6}$, respectively). However, for 28- and 56-day ages we cannot reject the null hypothesis for feedstock type ($f(4.25) = 2.31$, $p = 0.14$ and $f(4.25) = 0.17$, $p = 0.68$, respectively), suggesting that feedstock type has a diminished impact on compressive strength at later ages. The ashing temperature dependence of compression strength corresponds to expectations from the literature that higher ashing temperatures lead to greater quantities of less reactive crystalline silica and thus lower strengths [209].

3.3.6. Environmental Impact Assessment

Environmental impact comparisons were made for two products: (i) use of rice-biomass as an electricity resource; and (ii) rice-ashes as a partial PC alternative (**Figure 3.5a** and **b**). Results suggest that treatment methods could play a significant role in the viability of rice-biomass as a low environmental impact energy resource. Compared to the fossil fuel electricity resources examined, rice-based electricity could lead to 90-95% reductions in GHG emissions. However, the acid-leached biomass would result in net GHG emissions greater than from fossil-based resources due to the emissions associated with producing

acid for the leaching solution. While not in the scope of this analysis, if the leaching solution could be recycled for multiple leaching cycles or recovered in another way, larger reductions in GHG emissions could be achieved for energy generated from acid-leached biomass. As pre-combustion impacts are assigned to electricity production, all ashes have significantly lower GHG emissions than PC, suggesting they may be promising alternatives from an environmental impact perspective.

To further examine the implications of using rice-based ashes as an SCM, environmental impacts of mortar mixtures were assessed. **Figure 3.5c** and **d** show a breakdown of the contributions to the net GHG emissions and total energy demand for the mortar mixtures examined in this work. The production of PC is the largest contributor to both GHG emissions and embodied energy in these mortars. The GHG emissions attributed to RHA in cement-materials reported here are lower than in other work [237], as the ashes studied did not undergo additional treatment (e.g. milling), thus the environmental impacts of the ash simply reflect their necessary transportation. As such, use of rice-ash to offset high-impact PC drives the GHG emissions and reductions are in the range of 10 to 15%, reflecting the mass of cement replaced. If ashes were used to replace other concrete constituents, the change in GHG emissions would differ dependent on the material the rice-based ash replaces and the quantity of the replacement rate in the mixture being studied. Noting that each biomass type, leaching method, and ashing temperature led to different compressive strengths, comparisons were also drawn using a ratio of GHG emissions per cubic meter of mortar divided by the 28-day compressive strength of said mixture (**Figure 3.6**). These comparisons allow one to weigh tradeoffs of environmental impact and performance. In the mixtures evaluated, a lower ratio indicates a higher compressive strength and/or a lower impact relative to the other mixtures, both of which are desirable. Since the impacts prior to ashing are assigned to energy production, the resulting bioash-cement mortars all have approximately the same impact. Thus, the value in **Figure 3.6** for bioash-cement mortars are hyperbolic in the compressive strength ($y = 469.8/x$) due to the constant GHG emissions per cubic meters assumed.

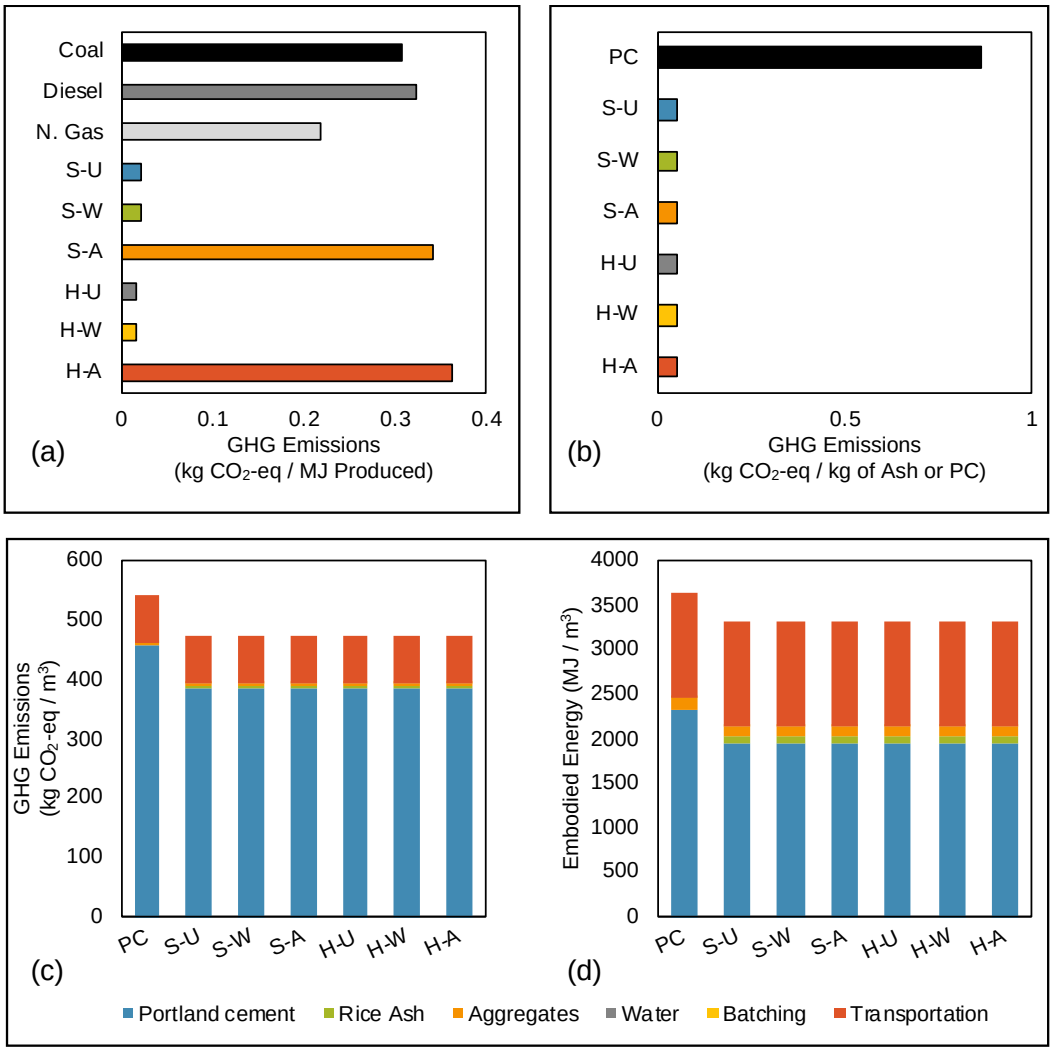

Figure 3.5. Comparison of greenhouse gas (GHG) emissions for (a) rice-based energy relative to fossil-fuel energy where "N. Gas" is natural gas, (b) cement relative to rice-ash, and impacts per m3 of mortars by ash leaching condition by (c) GHG and (d) embodied energy.

While this study shows that mortars made with PC and ash would result in lower GHG emissions relative to the PC mortar, only three alternatives led to a better combination of GHG emissions and compressive strength than the control PC mortar: (i) unleached rice straw ash produced at 600°C; (ii) unleached rice hull ash produced at 600°C; and (iii) acid-leached rice hull ash produced at 600°C. These findings suggest that even with loss in mechanical strength, there is a potential for the rice-based ash mortars tested in this work to contribute to a desirable combination of properties to mitigate environmental burdens if performance constraints can be met.

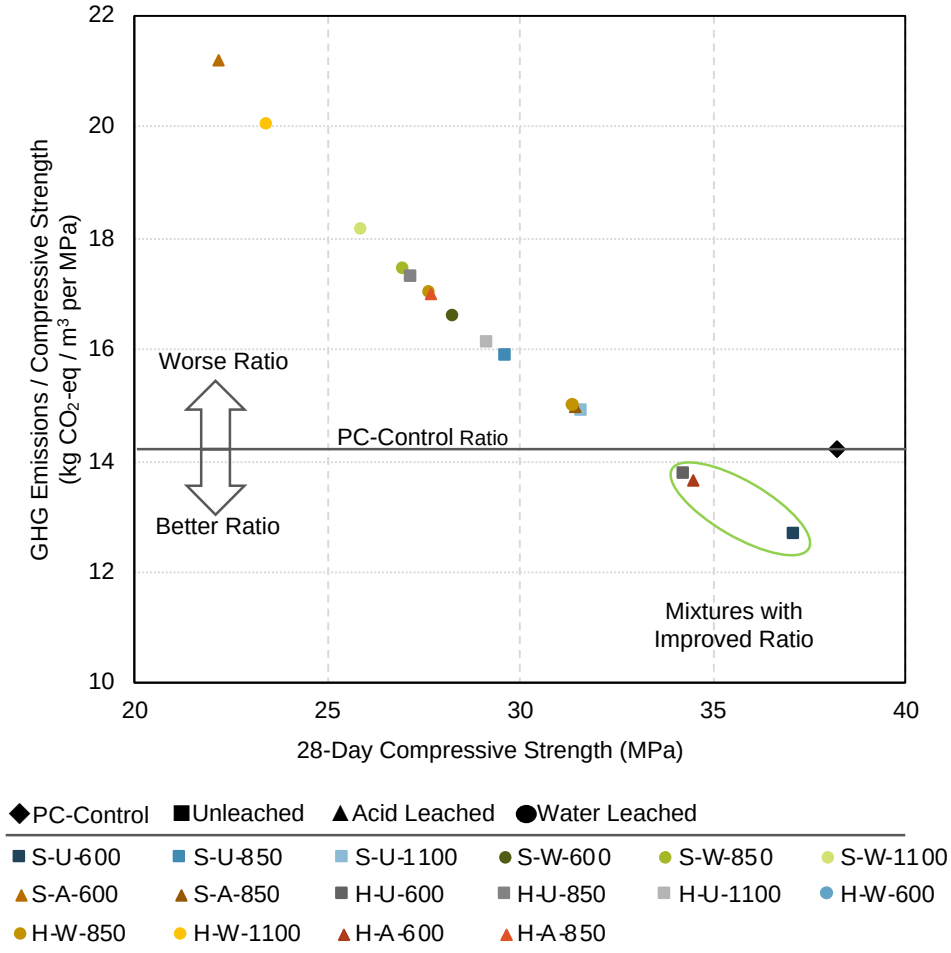

Figure 3.6. Greenhouse gas emissions relative to 28-day compressive strength for each of the mortars tested.

3.4. Post-combustion treatment of rice hull and rice straw ash

Producing concrete emits significant amounts of GHG emissions, driven by the use of PC, the hydraulic binder used in concrete [284]. These emissions are predominantly from limestone decarbonation and the energy resources required to produce clinker [285]. The process of producing PC and other emissions throughout the concrete value chain lead to approximately 8% of annual global CO_2 emissions [41]. Such impacts will be exacerbated by continued demand for cement-based materials, especially in developing regions [286]. The use of SCMs to partially replace Portland cement is a key route to lowering GHG emissions [3]. Conventionally, coal fly ash from coal combustion and ground granulated blast furnace slag (GBFS) from iron/steel production have been used as SCMs. The generation of these industrial byproducts is decreasing as the electrical energy and steel industries reduce their GHG emissions, while the demand for SCMs continues to increase and, together, intensify the need for alternative SCMs to replace cement [67], [210].

The use of RHA as an SCM has garnered interest in the US [287], [288], as well as other regions globally [289], [290]. RHA is a byproduct of combusting residue hulls from rice milling, often for energy production [209]. RHA as an SCM has been well studied in the literature [242], [248], [291], with a high silica content (60-90%) and relatively low CaO content (0-4%) [209], [226]. This composition can contribute to desirable hydration products in cement-based materials [292]. RHA can replace cement in concrete and lead to similar or improved mechanical properties at later ages (typ. ≥ 28-days) [247], [249], [250]. RHA preparation conditions and optimal replacement rates vary across studies [209]. The reactivity of RHA largely depends on the oxidization temperature which drives the amorphous silica content, with beneficial characteristics often observed at lower temperatures (typ. 500-800°C) [209], [293]. Lower temperatures may limit the energy returns [209], [211], [244]. Leaching pre-combustion treatments, typically used to prevent slagging and reactor fouling in energy production [253], [254], were evaluated to create synergies between biomass energy production and desirable SCMs. Leaching in water or phosphoric

acid solution increased the SiO_2 content, decreased some alkali oxides (e.g., K_2O) that contribute to fouling [293]. However, combustion temperature remained significant in relation to the compressive strength of the material [293].

Expanding biomass combustion to produce rice straw ash (RSA) could increase energy generation and biomass ash for regional SCM applications. As large fractions of the rice straw are not collected during harvest and instead remain on the field [240], there has been less exploration into valorization of this resource [222], [294]. Wang et al. [295] showed RSA is reactive in calcium-silicate-hydrate gels while investigating RSA blended with PC and mine tailings as a mining backfill material. Roselló et al. [296] found a high pozzolanic reactivity when evaluating RSA. Cunningham et al. [293] showed that the ash oxidation temperature affected the performance, but that leaching biomass prior to combustion did not cause significant changes in PC mortars with 15% RSA replacement. Other works have identified 10% RSA as a suitable replacement rate [297], [298], noting the loss of compressive strength at replacement rates greater than 10-20% [298], [299].

In this work, RHA and RSA are investigated as regionally available SCMs. Post-combustion milling and SCM blending strategies to modify the performance of RHA sourced from industrial biomass energy combustion and laboratory produced RSA were investigated. The efficacy of these treatments is evaluated to overcome limitations associated with industrial energy combustion noted in literature. Two strategies for improving RHA and RSA as mineral admixtures are explored: (1) to assess the effects of grinding the ashes, (2) to blend the RSAs with another SCM (i.e., ground granulated blast furnace slag, GBFS) to increase clinker replacement rate. Attention is given to the change in ash composition and mechanical performance between ash and control mortar mixtures. The results of this work can guide post-combustion decision-making for rice-based biomass ashes and using biomass ash as a regional SCM.

3.4.1.Materials and Methods

3.4.1.1. Materials and binder constituents

Mortar specimens were produced to experimentally evaluate RSA and RHA. Mixtures were made with Type II/V PC (Basalite Concrete Products, Dixon, California); silica-sand acquired from the Esparto quarry (Esparto, California); and GBFS acquired from Lehigh-Hanson Cement (Stockton, California). RHA from 2014 and 2020 energy production was acquired from Wadham Energy Biomass Facility (Williams, California). The ashes were three fly ashes collected in a baghouse from 2014 (F14a and F14b) and 2020 (F20), and a bottom ash from 2020 (B20). As rice straw is not combusted locally for energy production, RSA was produced at laboratory scale with locally sourced straw (Windmill Feed, Woodland, California). Rice straw was milled in a hammermill with a 1.25-inch (32 mm) diameter round-hole screen. Rice straw was torrefied at 250°C for 40 minutes, to prevent premature ignition, and then oxidized for 6 hours at 500°C. Treatments considered for the ashes were untreated (U-), milled (M-), or blended with GBFS (10%Ash-30%GBFS) (ash IDs provided in **Table 3.6**). Milled ash was prepared to pass through a #200 sieve (74um) by milling in a planetary ball mill at 300 RPM for 45 minutes using 3 mm Zirconium grinding medium in a Zirconium grinding jar.

Table 3.6. Treatment and ash sample nomenclature

Ash Conditions			Ash ID	
Feedstock	**Ash fraction**	**Production Year**	**Untreated**	**Milled**
Rice Straw	Laboratory ash	2022	U-RSA	M-RSA
Rice Hull	Rice fly ash	2014	U-F14a	M-F14a
		2014	U-F14b	M-F14b
		2020	U-F20	M-F20
	Rice bottom ash	2020	U-B20	M-B20

The chemical compositions of the binder materials were evaluated for likely oxide composition, trace elements, loss on ignition (LOI), and amorphous content by Activation Labs (Ontario, Canada). Composition, expressed as common oxides, and trace elements were determined using inductively coupled plasma optical emissions spectroscopy (ICP-OES). Trace elements were evaluated to understand how co-blending changes the prevalence of these elements. The relative amorphous content was determined by X-

ray diffraction using an internally mixed coronium standard to determine the phase abundance. In this method, the relative amounts of identifiable crystalline phases were summed and subtracted from 100% to quantify the amorphous content. LOI was determined by measuring the mass loss of a 2g sample in an air-atmosphere furnace at 1000°C for 2 hours.

3.4.1.2. Mortar mixture preparation

To be an effective SCM, the RHA and RSA need to provide similar performance. To experimentally evaluate RHA- and RSA-mortars, cubes of 50.8cm x 50.8cm (2 x 2in.) were prepared following the mixing procedure and times in ASTM C109 [181]. Mortars were cured at 25°C and >90% humidity for 1 day before being demolded and then continued to cure in the same conditions until testing. Mortar mixtures were prepared with a water-to-binder (w/b) ratio of 0.59 and a silica sand-to-cementitious material ratio of 2.5 for all mixtures. Additional RHA mixtures were prepared with w/b = 0.47. As RSA production was limited in scale, only mortars with w/b = 0.59 were prepared. Five variations of mixtures were produced: (1) a control mixture with 100% PC; (2) a control mixture with 30% GBFS and 70% PC; (3) a mixture with 15% untreated ash and 85% PC; (4) a mixture with 15% milled ash and 85% PC; and (5) a mixture with 10% untreated ash, 30% GBFS, and 60% PC (the same replacement ratios Gursel *et al.* [237] tested for RHA-Coal Fly Ash-PC mixtures). Due to the higher water requirement for untreated RHA, 15% untreated ash mortars with a w/b = 0.47 were not workable and, thus, not tested. (Mixture proportions in Table **3.7**).

3.4.1.3.Compressive strength

To determine if any of the treatments improved consistency of RHA performance, the 7- and 28-day compressive strengths of RHA-cement mortar cube specimens were tested following the procedure in ASTM C109 [181]. Cubes were tested using under force control until failure. Five specimens at each age were used to determine the average compressive strength of the mortar and the standard deviation between the compressive strengths of the same mortar mixture. Additional comparisons were made between mortars

with the same feedstock (i.e., rice hull or rice straw) and the same w/b ratio (i.e., 0.47 or 0.59) using a one-way ANOVA analysis to identify significant changes in the mean difference across the group of similar samples. The Tukey HSD test (Tukey test) was used to compare the values pairwise to identify significant differences between mortar mixtures. ANOVA and Tukey tests were performed with R [300] and the R stats package [301].

Table 3.7. Mortar mixture composition and proportions for compressive strength testing

Mixture Names	w/b ratio	Constituent Proportions (kg per cubic meter of concrete) *				
		PC	Silica sand	RHA/RSA	GBFS	Water
w/b = 0.59						
CTRL	0.59	528	1321	0	0	312
30%GBFS	0.59	370	1321	0	158	312
15% Untreated (U-)	0.59	444	1306	78	0	308
15% Milled (M-)	0.59	444	1306	78	0	308
10%Ash-30%GBFS	0.59	315	1311	52	157	309
w/b = 0.47						
CTRL	0.47	564	1410	0	0	265
30%GBFS	0.47	395	1411	0	169	265
15% Milled (M-)	0.47	474	1393	84	0	262
10%Ash-30%GBFS	0.47	336	1399	56	168	263

* PC - Portland cement; RHA - Rice hull ash; RSA - Rice straw ash; GBFS – Ground granulated blast furnace slag; Water - Distilled water

3.4.2. Results

3.4.2.1. Chemical composition of ashes

The composition of the RSA, RHAs, GBFS, and PC is presented in **Table 3.8**. The RHAs were 94-96% SiO_2. These values are similar to the untreated RHA produced from northern California rice hulls reported in Cunningham *et al.* [293] and are also within the ranges reported in literature [209], [226]. The RSA SiO_2 contents were 76-78%, and these ashes also had notable potassium contents (~12% K_2O). For RSA, all the oxide compositions except for Na_2O were within commonly reported ranges [293]. The maximum Na_2O value was larger than the 3.06-3.39% range reported [258]. While Na_2O content is not restricted in ASTM C150 [302], regional standards do place limits on Na_2O and other alkali content. For

example, the California Department of Transportation restricts alkali (as Na_2O equivalent) to a maximum of 3% due to durability concern [303]. This content could be reduced via pre-combustion treatments of the rice straw biomass, such as leaching [258], [293]. Rice straw leaching treatments could also provide co-benefits to the energy-generation process by reducing alkali-metals and Cl that can lead to slagging during combustion [258], [304], which currently preclude their use by commercial biomass energy plants, while reducing Cl and other alkalis to acceptable levels for PC binders [293]. The PC and GBFS chemical compositions display CaO as the predominant oxide with a relatively large amount of SiO_2. For the cement, the amount of Al_2O_3, Fe_2O_3, and MgO are all within the allowable limits in ASTM C150 [302].

Table 3.8. Oxide composition of rice hull ashes, rice straw ashes, ground granulated blast furnace slag, and Portland cement (n = 1)

		SiO_2 (%)	Al_2O_3 (%)	Fe_2O_3 (%)	MnO (%)	MgO (%)	CaO (%)	Na_2O (%)	K_2O (%)	TiO_2 (%)	P_2O_5 (%)
Detection Limit		0.01	0.01	0.01	0.005	0.01	0.01	0.01	0.01	0.001	0.01
Untreated	F14a	94.14	0.22	0.18	0.182	0.39	0.66	0.11	3.50	0.012	0.59
	F14b	94.96	0.17	0.16	0.148	0.33	0.53	0.08	3.09	0.010	0.53
	F20	96.26	0.06	0.10	0.106	0.21	0.34	0.07	2.54	0.003	0.31
	B20	96.16	0.08	0.10	0.107	0.23	0.38	0.06	2.59	0.005	0.29
	RSA	76.37	0.42	0.54	0.316	2.18	2.21	4.25	12.52	0.023	1.16
Milled	F14a	94.10	0.24	0.18	0.182	0.39	0.67	0.11	3.53	0.013	0.59
	F14b	95.12	0.16	0.14	0.141	0.32	0.51	0.10	3.05	0.009	0.44
	F20	96.09	0.07	0.09	0.108	0.23	0.36	0.07	2.64	0.003	0.35
	B20	95.90	0.09	0.10	0.114	0.25	0.40	0.07	2.71	0.005	0.36
	RSA	78.55	0.35	0.42	0.266	1.80	1.82	4.09	11.73	0.017	0.95
GBFS		33.10	15.38	0.43	0.244	8.31	39.79	0.36	0.43	1.964	0.03
PC		22.62	3.78	3.58	0.082	2.16	66.89	0.08	0.54	0.183	0.11

The differences between untreated and milled ashes were limited. When comparing the same ashes, differences in likely oxide composition across treatments were less than 0.5% in RHAs. Differences for RSA were larger, with an approximately 2% difference in SiO_2 content, potentially caused by the fractioning and sampling of ash for milling. All other oxides had less than a 1% difference between milled and untreated conditions. Lower amounts of SiO_2 would mean less SiO_2 available for the pozzolanic reaction with PC hydration products that contributes to the strength of the cement-based material [33].

The amorphous content and trace element analysis (**Table 3.9**) show the amorphous content varied little between the untreated and milled ashes. The greatest differences measured for amorphous content were a 1.3% increase in amorphous content in M-F20 (vs. U-F20) and a 1.2% decrease in amorphous content in M-B20 (vs. U-B20). These shifts may be related to the energy from ball milling changing the crystalline and amorphous structure of the ashes [305], [306]. For the other ashes, amorphous content before and after milling varied by ≤ 0.6%. The trace elements in the PC were at least 6 times larger for Ba, 48 times larger for Sr, 1.5 times larger for Y, and 11 times larger than V. Thus, using RHAs as a partial replacement for PC would lower the overall content of these elements. Differences for Ba and Sr between analogous untreated and milled RHA were at most 2 ppm. For the milled condition, Zr increased, but this reflects unavoidable trace contaminants introduced from the Zr milling materials. Zr contents for all the milled ashes remained lower than that of the commercially available GBFS. The LOI of GBFS is negative, which indicates a mass increase from oxidation during LOI testing (which could occur from oxidation of sulfur species [307]).

Table 3.9. Trace elements, loss on ignition (LOI) and amorphous content of mortar constituents (n = 1)

		Ba (ppm)	Sr (ppm)	Y (ppm)	Sc (ppm)	Zr (ppm)	Be (ppm)	V (ppm)	LOI (%)	Amorphous (%)
Detection Limit		2	2	1	1	2	1	5	0.01	0.1
Untreated	U-F14a	26	22	-	-	3	-	-	9.47	98.0
	U-F14b	20	17	-	-	5	-	-	9.92	97.6
	U-F20	12	12	-	-	4	-	7	9.72	96.3
	U-B20	13	12	-	-	4	-	5	11.11	97.6
	U-RSA	93	106	3	-	22	-	8	9.69	93.3
Milled	M-F14a	28	22	3	-	60	-	-	9.33	97.8
	M-F14b	20	16	7	-	89	-	6	9.78	97.7
	M-F20	13	12	1	-	22	-	7	9.36	97.6
	M-B20	14	13	4	-	54	-	-	10.31	96.4
	M-RSA	71	82	12	-	172	-	6	11.3	93.9
GBFS		604	686	62	28	317	9	72	-1.36	n.t.
Cement		172	1069	11	4	70	-	83	2.23	n.t.

'- 'denotes measurement below detection limit, 'n.t.' denotes samples not analyzed

3.4.2.2.Compressive strength

The ternary mixture 10%RSA-30%GBFS had a higher 7-day average then the corresponding RHA mixtures, but the lowest 28-day strength of the ternary blends (**Figure 3.7** and Table **3.10**). For all other mixtures, the RSA average compressive strength was within the same range as analogous RHA mortars. At 7-days, the U-RSA compressive strength was approximately 2% larger than the M-RSA mortar (**Figure 3.7**). Compared to the 7-day compressive strength of CTRL, U-RSA and 30%GBFS were 18% lower, and the M-RSA 7-day strength was 20% lower. At 28-days, the mortar mixtures with SCMs experienced greater rates of strength development than the CTRL, but the mixtures with RSA remained, on average, lower strength than the CTRL. U-RSA and M-RSA mixtures had 11% lower and 4% lower strength than the CTRL. The M-RSA compressive strength was 8% larger than the U-RSA mixture. This delayed strength gain may be attributed to a delayed pozzolanic reaction during binder hydration and development [293]. At 7-days, the 10%RSA-30%GBFS mixture had 14% lower strength than the U-RSA mixture. At 28-days, 10%RSA-30%GBFS performed similarly to the U-RSA mixture. These findings suggest additional material optimization and appropriate application selection could enable a low-clinker-content ternary cement blend.

A one-way ANOVA was used to compare the RSA, the CTRL, and the 30%GBFS mixtures. Results at 7-days show the difference in mean compressive strengths is statistically significant ($F(2.87) = 14.67$, $p = 9.53\text{x}10^{-6}$). Pairwise comparisons of the mixtures using the Tukey test (tabulate values for pairwise comparisons provided in the Supplemental Information, Part 2) indicate that the mean variations between the CTRL mixture and all other mixtures are statistically significant ($P = 1.4\text{x}10^{-3}$; $0.4\text{x}10^{-3}$; $0.3\text{x}10^{-5}$; $1.4\text{x}10^{-3}$ for mixtures 30%GBFS, U-RSA, M-RSA, 10%RSA-30%GBFS, respectively; $\alpha = 0.05$). Differences in the 7-day compressive strengths between the non-CTRL mixtures with each other are not statistically significant (all $P > 0.05$). Thus, the reduced mechanical strength at 7-days for mixtures with replacement led to meaningful variations in the average compressive strength. This indicates that RSA and GBFS have less beneficial contributions to the compressive strength compared to the PC at 7-days. Comparing 28-day compressive strengths shows a statistically significant difference: $F(2.86) = 2.90$, $p =$

0.047 ($\alpha = 0.05$). However, the Tukey test does not show statistically significant variation between mixtures compared pairwise (P ranges from 0.099 – 0.999, all P > 0.05). Together, these results suggest that the RSA and GBFS materials may have a slower contribution to the strength development, but comparable performance is achievable by 28-days.

Table 3.10. Average compressive strength and standard deviation at 7- and 28-days (n = 5).

w/b	Treatment	Untreated Ash (U-)		Milled Ash (M-)		10%Ash-30%GBFS	
	Age (Days)	7	28	7	28	7	28
0.59	CTRL	38.9 (2.8)	43.2 (4.8)	--	--	--	--
	30%GBFS	31.7 (0.8)	43.7 (2.2)	--	--	--	--
	F14a	33.2 (2.0)	43.7 (3.0)	33.3 (0.7) *	45.1 (3.4)	25.5 (0.4)	44.1 (0.6)
	F14b	32.4 (1.5)	40.6 (1.9)	33.6 (3)	49.8 (3.1)	23.9 (1.3)	39.3 (3.1)
	F20	27.2 (2.4)	38.0 (2.4)	28.6 (3.1)	39.6 (3.9)	22.5 (1.4)	40.6 (1.0)
	B20	19.8 (1.2)	29.3 (1.8)	24.6 (1.4)	35.6 (2)	19.8 (1.9)	32.5 (3)
	RSA	31.7 (2.6)	38.4 (3.6)	30.8 (2.7)	41.5 (1.5)	27.2 (1.1)	37.7 (2.6)
0.47	CTRL	52.4 (3.3)	64.6 (1.8)	--	--	--	--
	30%GBFS	45.1 (2.7)	66 (6.6)	--	--	--	--
	F14a	--	--	48.9 (3.1)	67.3 (2.9)	38.4 (0.4)	52.7 (5.4)
	F14b	--	--	54.6 (1.6)	73.9 (2.3)	40.6 (1.4)	62.3 (1.7)
	F20	--	--	46.0 (4.2)	55.8 (7.9)	32.7 (1.8)	51.8 (0.6)
	B20	--	--	41.1 (4.7)	56.7 (4.8)	29.8 (2.5)	45.1 (3.9)

Note: value in brackets "( )" is the standard deviation; *n =4 for milled F14a at 7-days, all others n = 5

Compared to the CTRL mixture, the untreated RHA mortars with a w/b ratio of 0.59 had 2-15 MPa (5-43%) lower strength at 7-days and 8-24 MPa (16-44%) lower strength at 28-days. At both ages, U-F14a had the highest strength among the untreated RHA-mortars (2 and 8 MPa lower strength than the 0.59 w/b ratio CTRL at 7- and 28-days, respectively). The 7-day strength of the 0.47 w/b U-F14a was 3 MPa lower, and the 28-day strength was 3 MPa higher than CTRL. Milling the RHA improved compressive strength, with reductions of 2-10 MPa (5-30%) at 7-days and 7-17 MPa (5-32%) at 28-days for w/b = 0.59. These tighter ranges in strength suggest that milling could improve RHA performance as an SCM. At the 0.47 w/b

ratio, milling RHA led to an increase of 2 MPa (4%) for M-F14b RHA mortars at 7-days compared to CTRL. Strengths decreased by 3-11 MPa (6-21.21%) for the other milled ashes at 7-days compared to CTRL. Compared to untreated ash mortars at 28-days, M-F14a increased 3 MPa (4%), M-F14b increased 9 MPa (15%), M-F20 decreased in strength by 9 MPa (13%), and M-B20 decreased by 8 MPa (12%). For 10%Ash-30%GBFS mortars, strengths decreased by 11-23 MPa (22-43%) at 7-days and by 2-19 MPa (3-30%) at 28-days, compared to CTRL.

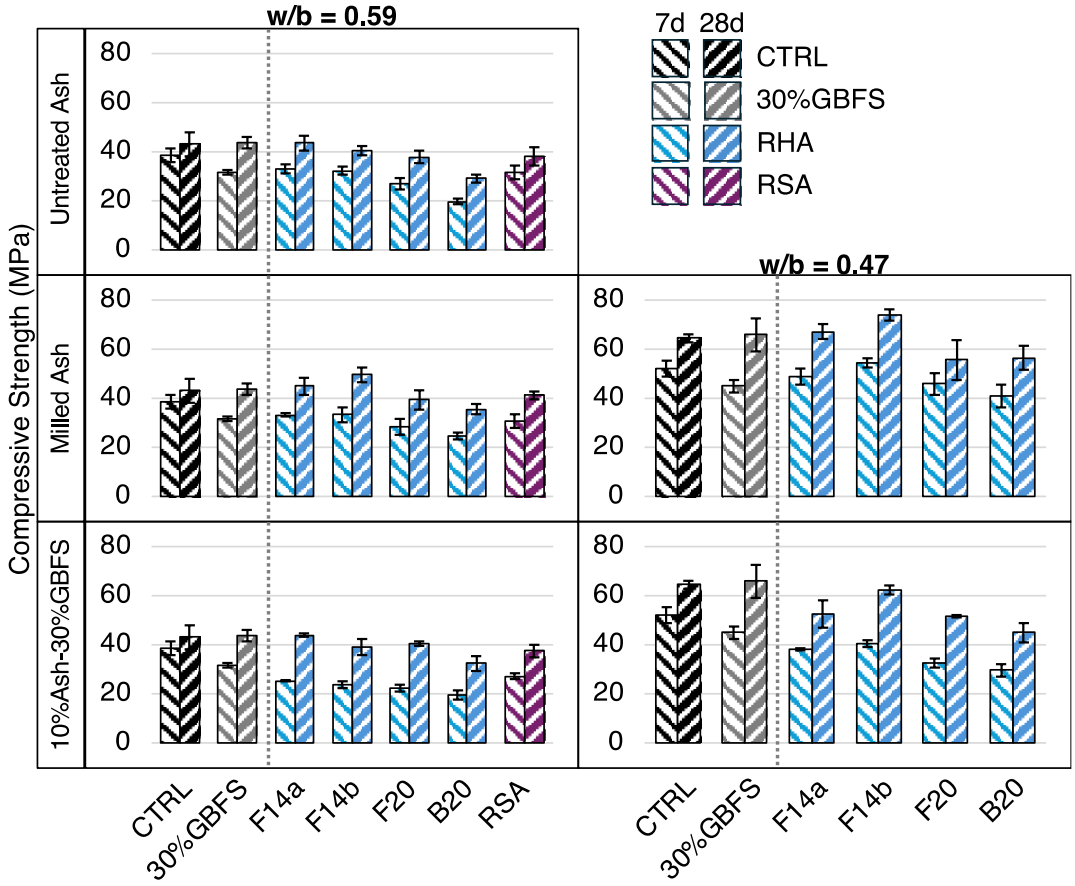

Figure 3.7. Average compressive strength of mortar mixtures. Brackets show the standard deviation across compressive strengths. (n = 4 for milled F14a at 7-days, for all others n = 5)

In several cases, RHA led to equivalent or higher compressive strengths than the CTRL mixture. An AVOVA showed the 28-day compressive strengths of 0.47 w/b RHA mixtures differed significantly ($F(2.12) = 30.56$, $p = 2.1 \times 10^{-10}$; $\alpha = 0.05$). The Tukey test did not identify significant differences between

the CTRL and the M-F14a, M-F20, M-B20, M-F14b, and 10%F14b-30%GBFS mortars (P ranged from 0.12 – 0.99, all P > 0.05, α = 0.05). The 28-day strength did vary significantly between the CTRL and 10%F14a-30%GBFS, 10%F20-30%GBFS, and 10%B20-30%GBFS mortars (P ranged from $1.0x10^{-5}$-$1.6x10^{-2}$, α = 0.05), indicating that lowering the PC content in these RHA mixtures led to meaningful reductions in the compressive strength. This result is consistent with literature showing high GBFS content leads to slower development of early-age strength [308], [309]. For the RHA mixtures with w/b = 0.59, 28-day compressive strengths also differed significantly ($F(1.899) = 14.07$, $p < 2.0x10^{-16}$; α = 0.05). Pairwise comparisons via the Tukey test identified that the significance or lack of significance compared to the CTRL were consistent across ash type. The difference between the CTRL and mortars made with B20 was significant ($P = 3.8x10^{-7}$ - $2.4x10^{-2}$), indicating that the bottom RHA led to meaningfully lower compressive strengths at 28-days. Differences between CTRL and mixtures made with the F14a, F14b, or F20 ashes were not significant (P = 0.99-1.00; for F14a mortars; P = 0.38-0.98, for F20 mortars; and P = 0.09-0.98 for F14 mortars). Targeting fly RHA over bottom RHA, may lead to a higher performance SCM.

3.5. Summary

3.5.1. Material Flow

In this work, a material flow analysis of rice hull and rice straw generation from 2017-2022 in the United States and the potential annual RHA and RSA generation was performed. The analysis showed that, while generation was relatively small nationally, the regionally generated flows in 6 rice producing states could be sizable compared to Portland cement consumption. Key findings include:

- The potential replacement as a percentage of PC consumption varied from ~0.5% in Texas to up to 60% in Arkansas, not accounting for interstate transfers.
- Replacement of PC with RSA and RHA could yield up to 1.2 Mt CO_2-eq of avoidable GHG impacts, equivalent to 1.8% of 2020 emissions, from PC production in the US.

If biomass can be combusted with reasonable energy returns, these opportunities for PC replacement with RSA and RHA in the United States may also be possible in other rice producing regions around the world. Importantly, potential emissions reductions should be considered in light of an life cycle assessment that includes the environmental impacts of biomass pre-treatment (e.g., leaching), post-combustion processing, and transportation. Future work could also consider, via technoeconomic assessment, the costs associated with ash production relative to conventional SCMs.

3.5.2. Pretreatment

With growing energy and material resource demands worldwide, pathways to advance environmental sustainability through industrial symbiosis could be a critical means to improving the circular economy. In this work, we examine the effects of rice-biomass pretreatment and ashing temperature the use of ash in cement-based materials to support a critical step in understanding a potential symbiotic relationship. Through experimental and analytical techniques, this research provides context for the

influence of such treatments on ash properties, on strength development in cement mortars containing rice ash, and on potential shifts in environmental impacts. Some key findings from this work include:

- Feedstock leaching was shown to remove more than 90% of chloride and up to 93% of potassium, while increasing silica concentration by 1-10% in ash.
- While leaching methods did not benefit early-age strength of cement-based mortars, higher rates of strength development were noted for ashes produced from leached biomass, leading to mortars with comparable strength to the control mixture at 56 days.
- Agreeing with the literature, this work further supports the dependency of rice ash reactivity on ashing temperature, where more reactive ashes were noted at 600°C.
- Environmental impact assessment results showed the use of refined chemicals in leaching, such as the acids explored in this work, could drive net GHG emissions in rice-based energy production.
- When considering ash as a residue from energy generation, reductions in emissions for cement-based mortar production were shown to be approximately equal to the cement replacement rate (~10-15% lower emissions in this study).
- When impacts are considered in tandem with the compressive strength of the mortars, untreated hulls produced at 600°C, untreated straw produced at 600°C, and acid leached straw produced at 600°C all provided reduced impacts.

While this research provides a valuable initial step in understanding potential industrial symbiosis for rice energy generation and infrastructure materials production, further research is needed. Such future studies should identify the effects of ash treatment requirements for ash produced from different combustion equipment as well as the stage at which treatment is performed (e.g., leaching of ash in addition to or in place of biomass leaching) to improve to ash properties and consistency. Future consideration of co-

products, such as nutrient reclamation from leachates or recycling leachates for reuse, could improve the extent to which these products may mitigate costs and decrease environmental impacts. Future study should also consider additional conversion or ashing methods, such as gasification or biochemical conversion of rice-based biomass, to simultaneously benefit energy and materials production. Additionally, the ability of alternative pretreatment methods, such as an alkali [310] or acid digestion and enzymatic hydrolysis[311] to valorize feedstock for energy and cement-based material production should be considered, and the influences of all these processes evaluated for potential economic consequences.

3.5.3. Post-treatment

To abate the impacts from concrete and cement production, additional SCM resources are needed. Using rice straw ash (RSA) could nearly triple the amount of rice biomass ash available to use as an SCM in the US, with potential to mirror this in other rice producing countries. This work evaluates rice hull ash (RHA) and RSA performance under three post-combustion processing conditions: (i) untreated, (ii) milled to decrease particle size, and (iii) mixed with GBFS to form a ternary blend. Key findings include:

- For w/b = 0.59, the 28-day compressive strengths of the fly RHA mixtures did not differ significantly from the 100% PC control.
- For w/b = 0.59, the mixtures made with bottom RHA led to a 17-32% reduction in 28-day compressive strength that was significant from the 100% PC control. Additional treatments could be considered to valorize this ash fraction.
- The 28-day compressive strength of RSA mixtures (w/b = 0.59) did not differ significantly from the 100% PC control.

This work shows that less-studied RSA, in performing similarly to industrially produced RHA, holds promise as an SCM. Future work addressing expanded mechanical and durability performance of

RSA composites is important to understand the viability of widespread RSA SCM adoption. Additionally, as the higher alkali composition of rice straw necessitates pre-combustion treatment for improved energy generation, designing regional systems for RSA valorization (e.g., rice-straw processing and combustion systems for concurrent energy and biomass SCM generation) could further improve the synergistic benefits of these agricultural residues as value-added products.

CHAPTER 4

Material comparison incorporating mechanical performance, resource availability, and environmental impacts

4.1.Introduction

The significant global greenhouse gas (GHG) emissions from concrete production are directly related to large amount of concrete used globally [206]. Shifting these systematic environmental impacts requires changes across concrete production, design, and use are [37]. This need for change is especially true as geographical regions continue to develop and are expected to increase their regional demand for construction materials [312]. At global [3], [37], [313] and national [38] levels, cement-decarbonization roadmaps identify reducing clinker content by partially replacing Portland cement (PC)— or by replacing the clinker within Portland cement— with mineral admixtures, i.e., supplementary cementitious materials (SCMs) or mineral fillers (herein, fillers), as a key strategy to enabling GHG emissions reduction. Enabling the glo transition to lower-GHG emitting cement-based materials requires suitable mineral admixtures that lower GHG emissions, meet performance needs, and are available in large enough quantities [314].

Using mineral admixtures in concretes is already a common strategy to reduce the clinker content in the United States (US). In addition to the benefit of reducing GHG impacts, SCMs can also contribute to the strength development of cement-based materials and can provide valuable benefits to the durability and longevity of these building materials [284], [314], [315]. Traditional SCMs are often byproducts of industrial processes, namely, coal fly ash (referred to herein as fly ash) from coal-based energy production, ground blast furnace slag (GBFS) from pig iron production (with much of that iron feeding into steel production), and silica fume from the ferrosilicon and silicon alloy industry [316]. Notably, the coal-energy and steel production industries are also significant contributors to global GHG emissions and must

decarbonize to avert the worst-case climate change scenarios [317], [318]. As these carbon-intensive industries shift production systems to lower-emissions alternatives, the generation of byproduct SCMs is also expected to decrease. Simultaneously, the demand for SCMs for cement-based materials is expected to increase. These coupled effects have already led to regional scarcities of traditional SCMs and growing interest in finding alternative mineral resources with enough supply and availability [54], [67].

For a material to be a suitable alternative mineral admixture it must also allow for comparable (or improved) performance relative to traditional cement-based materials. The effects of alternative materials on concrete performance are often compared experimentally. To aid in direct comparison informed by environmental impacts, efforts have been made to include material performance consideration in functional units during life cycle assessment. For example, Panesar et al. [319] combines volume, compressive strength, and chloride permeability to produce functional units of varying complexities. Such comparisons, however, highlight the challenges of capturing the function of concrete materials. In similar efforts, others have proposed concrete-specific environmental impact comparison indices to allow for the comparison of the environmental impacts of different cement-based materials based on engineering constraints and a declared unit (i.e., m^3 material). For example, Miller et al. [320] proposed indices to compare materials based on member (i.e., column, beam, or panel) and controlling design property (e.g., compressive strength, thermal conductivity, and chloride diffusion).

In this chapter, industrial ecology methods for environmental impact assessment, material flow analysis, and comparison indices are used to evaluate different mineral resources in cement-based materials. First, the recent supply of traditional SCMs and fillers is compared to the potential supply of alternatives. Additionally, projections for the future supply of industrial byproduct SCMs are modeled to understand how shifting production technologies could change the availability of traditional SCMs. Then, a harmonized environmental impact assessment is performed on the mortar mixtures investigated in previous chapters. As a simplification of the analysis presented herein, indices informed by compressive strength are used to

compare mixtures (using a comparison index proposed by Miller et al. [320]). Finally, an assessment framework is built that provides a system-level perspective, using supply-informed comparison to reflect potential binder production as well as the environmental impacts of mixtures at set compressive strengths. This supply-informed comparison is performed using mineral admixture generation in 2021 as well as projections from 2035 to 2050. These findings provide a new perspective on mineral admixture use at the national (US) scale and underlines the need to identify alternative mineral flows as traditional SCM generation decreases in the near future.

4.2.Current and projected generation of supplementary cementitious materials

4.2.1.Motivation

To incorporate material supply as a consideration for material comparison, the potential generation of post-consumer carpet calcium carbonate (PC4), rice hull ash (RHA), and rice straw ash (RSA) modeled in Chapter 2 and Chapter 3 was compared to the historical generation and use of conventional SCMs and fillers.

4.2.2. Methods and Data

4.2.2.1. Generation and use of traditional SCMs and fillers

Using data collected from industry reports and data reported by the USGS, the historic use of fly ash, limestone, GBFS, silica fume, and metakaolin clays in the US and globally were quantified. The use of traditional SCMs in cement-based materials was collected to assess the historic flows of SCMs for comparison. For industrial byproducts (i.e., GBFS, silica fume, and fly ash) data were collected for both total byproduct generation and the mass of material used in cement-based materials. For mined and manufactured SCMs and fillers (metakaolin clays and limestone, respectively), the reserves of these materials is expected to be significantly large and there is little concern at present about escalating demands for these materials [321], [322]. Data sources and methods are summarized in **Table 4.1**.

Table 4.1. Data sources for traditional mineral admixture generation and use in cement and concrete

Material	Values & calculations	Source
Ground blast furnace slag (GBFS)	Calculated from reported sales, assuming 99.8% used	[323]
Coal fly ash	Reported values	[324]
Silica fume	Caltrans modeled generation	[54]
Metakaolin clay	Reported values for calcined clays, assuming 100% use in concrete	[325]

4.2.2.2. Trends in the future generation of traditional SCMs

Projected coal combustion data and steel production data were used to estimate potential future supplies of fly ash and various iron and steel slags. Namely, we examine the future generation of fly ash

from coal combustion as well as consider total coal combustion products (CCPs). We project future GBFS, basic-oxygen furnace (BOF) steel slag, and electric arc furnace (EAF) slag availability. We note that different ashes and coal combustion products as well as different slags have different properties that may limit the applicability for use as SCMs. However, noting the interest in alternative SCM supply flows, herein, each of these resources was considered.

Future fly ash generation was modeled under three coal-combustion scenarios compiled from the US Energy Information Agency (EIA) using EIA projected total coal combustion in the US [326]. The three coal-combustion scenarios are the 2023 Annual Energy Outlook (AEO) reference scenario, low-cost zero-carbon technology scenario, and high-cost zero-carbon technology scenario [326] that are generated by the EIA using a macro-economic model [327]. The high-cost technology scenario assumes no change in the cost of zero-carbon electricity generation technology (e.g., renewable and nuclear energy) and the low-cost technology case assumes a 40% reduction in cost by 2050 [328].

Fly ash generation is projected from mass fractions for fly ash components and CCPs, which are calculated from the average historical fly ash and CCP yields reported by the American Coal Ash Association (ACAA) [324] and corresponding historical coal combustion reported by the EIA [329]. The modeled results are compared alongside historic data reported by the ACAA [324]. Coal combustion byproduct generation is calculated as shown in **Equation 4.1** where $M_{cp,i}$ is the mass of the generated byproduct, cp, (i.e., fly ash or total CCPs) in year i, $M_{coal,i}$ is the mass of coal combusted in year i, and α_{cp} is the average mass ratio of the combustion product cf (i.e., either fly ash or total CCPs). Values, assumptions, and historic generation data are summarized in **Table 4.2**.

$$M_{cp,i} = M_{coal,i} * \alpha_{cf} \qquad \textbf{Equation 4.1}$$

Table 4.2. Data and sources for modeling future supply of fly ash and total coal combustion products (data for 2010-2022)

Value	Data / model	Source / method
Mass ratio, average fly ash content of coal	5.54%	Calculated from annual coal combustion data and fly ash generation (below)
Mass ratio, average total coal combustion product (CCP) content of coal	13.90%	Calculated from annual coal combustion data and total product generation (below)
Annual total coal combustion product (CCP) generation (2010-2022)	Varies, (62-118 Mtons)	Reported, [324]
Annual fly ash generation (2010-2022)	Varies, (24-61 Mtons)	Reported, [324]
Annual fly ash for cement and concrete (2010-2022)	Varies, (11-17 Mtons)	Reported, [324]
Annual mass of coal combustion (2010-2022)	Varies, (432-951 Mtons)	Reported, [329]

Herein, GBFS from blast furnaces (BF), BOF slag, and EAF slag are modeled under three projection scenarios: (1) A constant production rate to 2050; (2) a linear decrease in production totaling 5% by 2050, as shown by [330]; and (3) a linear increase in steel production totaling 12% by 2050, as suggest by [331]. All steel production scenarios included a linear shift in steel production technology from BOF to EAF with 2050 steel production split between 10% BOF and 90% EAF (compared to approximately 30% BOF and 70% EAF today), based on the target set by IEA [68]. As with coal byproducts, iron and steel byproducts were calculated using mass ratios. For iron and steel by products, these data were reported by the World Steel Association [332] and the IEA [68] for slag generation per ton of steel. This model assumed simplified steel production pathways of either coupled BF-BOF or coupled direct reduced iron (DRI)-Steel Scrap-EAF. However, possible combination of production systems can contain different permutations of these systems. In this model steel slags (either BOF slags or EAF slags) encompass both the slag derived from the BOF or EAF process and the ladle slags from later-stage steel refinement. Values and assumptions are summarized in **Table 4.3**.

To model the projected generation of the three slags, **Equations 4.1 - 4.4** are used where $M_{BOF,i}$; $M_{BF,i}$; and $M_{EAF,i}$ are the masses of BOF slag, GBFS, and EAF slag generated in year i. $M_{steel,i}$ is the mass

of steel production in year i. $y_{BOF,i}$ and $y_{EAF,i}$ are the production ratio of steel in either a BOF or EAF in year i. Finally, α_{BOF}; α_{BF}; and α_{EAF} are the mass ratio of slag generation to crude steel production for BOF slag, BF slag, and EAF slag.

Table 4.3. Data and sources for modeling future supply of blast furnace and other steel slags

Parameter	Value	Source / method
Crude Steel production (2012-2023)	Varies, (72.7-88.7 MMt)	USGS [333]
Share, BOF production (2012-2023)	Varies, (28.0-40.9%)	USGS [333]
Share, EAF production (2012-2023)	Varies, (59.1-72.0%)	USGS [333]
Share, BOF/EAF by 2050	10% BOF / 90% EAF	Assumed from [68]
Share, BOF/EAF 2020-2049	linear increase from 2019 to 2050 (via linear interpolation)	interpolated
Mass ratio, Slags from BF & BOF	400 kg /tonne crude steel	World Steel [332]
Mass ratio, slag from BOF	125 kg/tonne crude steel	IEA [68]
Mass ratio, slag from BF	275 kg/tonne crude steel	calculated from previous (400kg-125kg = 275kg)
Slag EAF	170 kg/tonne crude steel	World Steel [332]

$$M_{BOF,i} = M_{steel,i} * y_{BOF,i} * \alpha_{BOF} \quad \textbf{Equation 4.2}$$

$$M_{BF,i} = M_{steel,i} * y_{BOF,i} * \alpha_{BF} \quad \textbf{Equation 4.3}$$

$$M_{EAF,i} = M_{steel,i} * y_{EAF,i} * \alpha_{EAF} \quad \textbf{Equation 4.4}$$

4.2.3.Results and Discussion

4.2.3.1. Traditional SCMs and fillers

Recent trends in SCM and filler use and the potential material generation from 2017-2021 for fly ash, GBFS, metakaolin, and silica fume is shown in comparison to the alternative resources presented in this dissertation: PC4, rice hull ash (RHA), and rice straw ash (RSA) material flows (each modeled in earlier chapters) (**Figure 4.1**). Kaolin clays that are calcined (making metakaolin) for use in concrete are only a small portion (~7%) of the kaolin clay used in 2021 [334]. However, as a mined material with expansive reserves [321], the actual maximum potential flow is expected to be significantly larger. Herein, kaolin clay

production is expected to be restricted by clay mining and calcining production capacity and, thus, is scaled to the maximum kaolin mined in a given year. As such, metakaolin potential is estimated at over 400% the 2021 kaolin clay production, if the systems for calcining clays can be expanded appropriately. To account for anticipated mass reductions from calcination, the collected kaolin clay generation data was dived by 1.15 (from [62]). Conversely, 99.8% of the GBFS between 2017-2021 was used in binder applications [335]. Silica fume was the smallest flow considered, as it is a byproduct of the smaller ferrosilicon industry, the flow is relatively small compared to other industrial by-products [54]. However, silica fume is highly reactive, meaning it is often used in smaller mass rates than other SCM materials [316]. Of the materials considered, fly ash is the largest flow. However, only a third of generated fly ash was used in cement and concrete applications. With a total utilization rate of ~60-70% depending on year, just under one third of fly ash is not diverted for beneficial use.

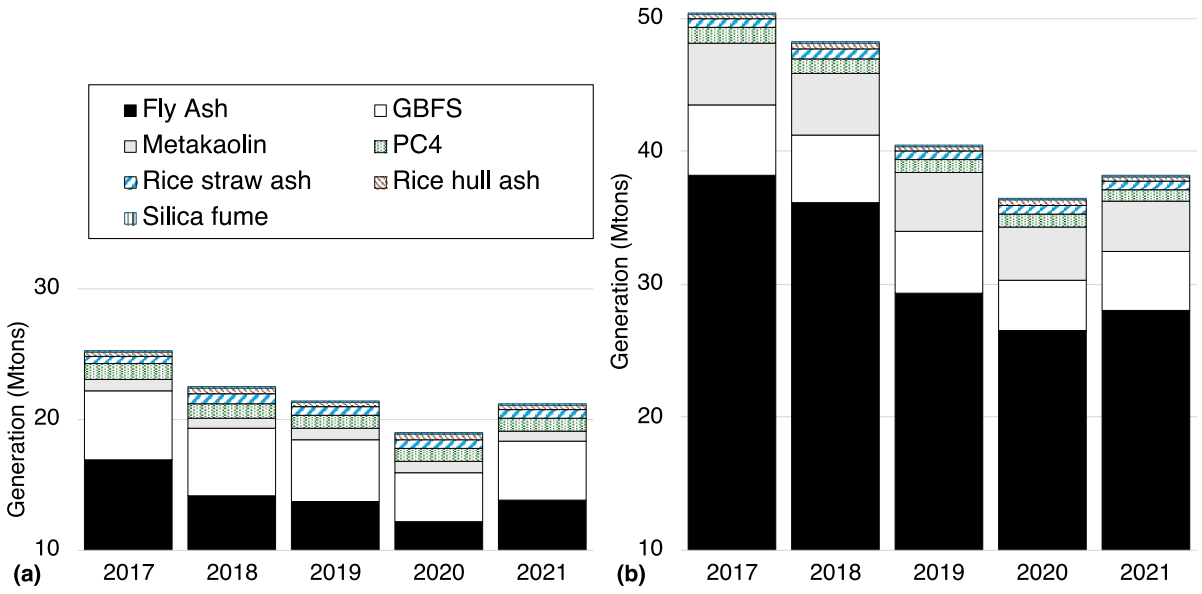

Figure 4.1. The maximum modeled generation of alternative SCMs (post-consumer carpet calcium carbonate (PC4), rice hull ash (RHA), and rice straw ash (RSA)) from 2017-2021 compared to traditional SCM generation showing (a) the reported and modeled actual traditional SCM use in concrete and cement and (b) the reported and modeled maximum potential SCM use in concrete and cement.

Alternative mineral admixtures, together with expanding the use of industrial byproducts, lead to a

potential SCM and filler generation from 2017-2022 that is estimated to be nearly twice that of actual mineral admixture uses in the US during the same period. Of the potential flows modeled in earlier chapters, PC4 is the largest at 0.9-1.1 Mtons per year between 2017-2021 (similar in size to actual metakaolin use of ~0.8 Mtons, **Figure 4.1a**). This is followed by RSA (0.6-0.7 Mtons) and RHA (0.3-0.4 Mtons). While not visualized here, cement replacement using metakaolin could be further expanded via ternary cement blends with metakaolin and limestone (i.e., LC3's). With metakaolin comprising two-thirds of the replacement materials (i.e., 30% metakaolin and 15% limestone [336]), blending metakaolin and limestone would result in a material flow approximately 1.5 times the mass of the metakaolin shown here.

4.2.3.2. Projected SCM supply

While current flows show SCM generation to be large compared to reported use in the US, the threat that climate change poses to society is pushing carbon-intensive industries, such as energy generation and steel production, to shift production technologies. These changes in production technology will affect future trends in SCM generation and reduce the availability of the commonly used fly ash and GBFS. Projected trends for the generation of fly ash and of total CCP are shown in **Figure 4.2.** Fly ash generation is expected to decrease 30-55% between 2025 and 2030, across all scenarios considered (**Figure 4.2a**). After 2030, the decrease results in an additional 18-70% from 2030 (a 44-87% decrease from 2025) by 2050. By 2030, under the reference scenario, fly ash generation is expected to decrease below the historical uses of fly ash in cement-based materials (8.9 Mtons). As with fly ash, total CCPs also decrease as coal combustion decreases (**Figure 4.2b**). With the generation of 25-39 Mtons by 2030, total CCPs generation under the reference scenario remains above 2021 fly ash generation. This combined CCPs flow is likely less reactive than fly ashes; however, if beneficiation of CCPs can be performed at acceptable cost with minimal environmental impacts, it could lead to a symbiotic relationship that allows for the sequestration of potentially environmentally harmful CCP and benefits to the cement-based materials [337], [338], [339].

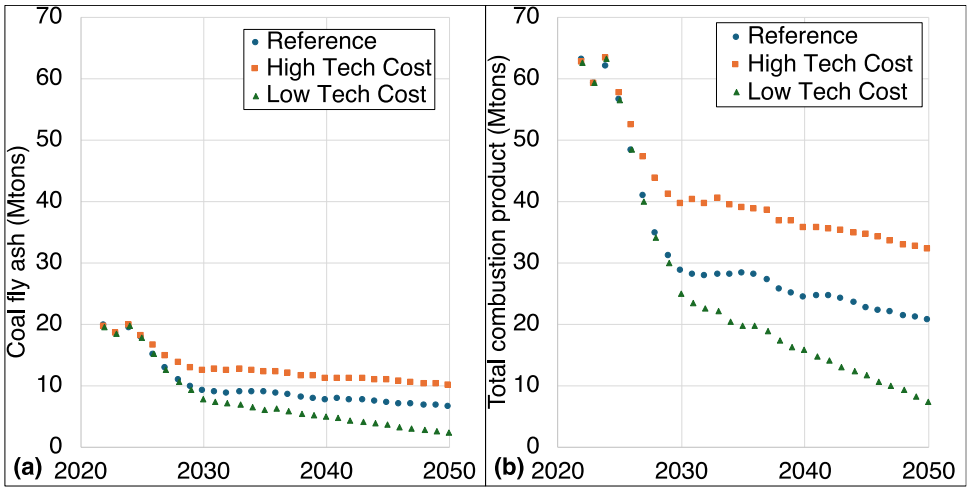

Figure 4.2. Projected changes in the United States in the generation of (a) coal fly ash and (b) total solid combustion products under the IEA AEO 2023 reference scenario (Reference), high cost of zero-carbon technology scenario (High Tech Cost), and low cost of zero-carbon technology scenario (Low Tech Cost).

When considering GBFS, trends must reflect that this SCM is a byproduct of pig iron production using blast furnaces, and in the US, this iron is used predominately to produce steel [333]. Here, the projected change between 2020-2050 in the generation slags from iron and steel production was modeled under shifting steel production technology from coupled BF-BOF systems to EAF production using scrap steel and DRI as feedstocks (**Figure 4.3**). We note, the processes tied to these different furnaces results in different characteristic of the slag, which can impact their efficacy as SCMs [210], [340].

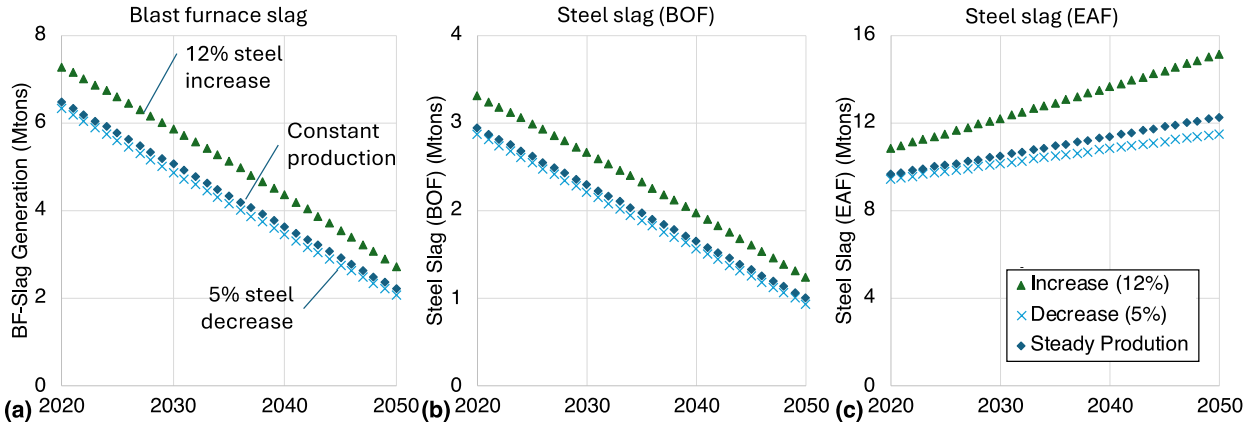

Figure 4.3. Projected trends in the United States for the generation of (a) blast furnace slags from 2020-2050 compared to the generation of (b) steel slags from basic-oxygen furnaces and (c) steel slags from electric arc furnaces under increased steel production (12%), decreased steel production (5%) or constant production.

In all steel production scenarios, the generation of GBFS is projected to decrease by 11-13% from 2025 to 2030. As steel production transitions to 90% EAF, annual GBFS generation is expected to decrease by half (54-58%) to 2.0-2.7 Mtons in 2050 (**Figure 4.3a**). This decrease in BF usages is modeled with a concurrent reduction in BOF use. As such, BOF steel slag generation is projected to reduce in the same proportions as GBFS (**Figure 4.3b**). While this GBFS and BOF steel slags are expected to decrease, the increased use of EAF systems is projected to increase EAF slag production (here reflecting both the ladle and EAF slag together) by 15-24% from 2025 to 2050 (~9-15 Mtons by 2050). From 2020, the generation of EAF slags is modeled as increasing by 15-24% from 2030 to 2050 (**Figure 4.3c**). This trend suggests a possible strategy to offset the reduction in GBFS generation could be to valorize and utilize slags associated with the EAF processes. Currently, steel slags (both BOF and EAF) are predominately used as road base (44.8%), fill (12.9%), and asphalt concrete (12.4%) [341]. If slag from EAF processes can be engineered with suitable SCM performance, this could add value to the EAF-steel production system and provided additional benefits to the production of lower-impact cements and concrete mixtures.

4.3. Mixture comparison via harmonized environmental impacts and experimentally determined compressive strengths

4.3.1.Motivation

Comparison indices allow for the rapid comparison of different products or processes based on key performance and design factors. For concretes mixtures and other structural materials, these indices are commonly used for comparing environmental impacts with the added context of engineering or material properties. In this chapter, the environmental impacts assessments of mixtures from Chapter 2 and Chapter 3 are harmonized to reflect consistent input modeling assumptions using US average environmental impacts for production. The environmental performance of these mixture is then compared using a compressive-strength informed comparison index.

4.3.2.Methods and data

4.3.2.1. Environmental impact harmonization

In the preceding chapters, the environmental impacts of different mixtures with fixed mixture proportions are quantified using a cradle-to-gate methodology with different production assumptions for the concrete mixtures, transport distances, and energy grids. To enable consistent impact modeling and comparison to conventional SCMs, lifecycle inventories (LCI) from the OpenConcrete Tool [36] were used to model the impacts from thermal energy demand, electric energy demand, and transportation using consistent energy mixes. For this quantification, the US average fuel mix, electricity mix, and kiln efficiency reported in the OpenConcrete Tool [36] were used.

The GHG emissions for RHA, RSA, and PC4 were harmonized by adopting the allocation of all process-based emissions to the primary products, as in the previous works (i.e., [72], [293]), and only the energy requirements for transporting and processing RHA, RSA, and PC4 are allocated to these materials. RSA and RHA GHG emissions are quantified using the electric energy demand reported for milling [237],

[293] and the US average electricity mix in the OpenConcrete tool. Consistent with the methodology in [72], PC4 is modeled as a residue of carpet recycling and only transportation impact are considered.

Transportation for all materials are assumed to be by truck (the predominant mode of transportation for concrete constituents [131]). PC is modeled with the US average transportation distance of 43 km [131], and all SCMs and fillers, including RHA, RSA, and PC4, are modeled as being transported 146 km, the average distance for industrial byproduct mineral admixtures [131]. Fine aggregate is modeled with a transportation distance of 61 km, by truck [131]. A system diagram for assessment of mortar- and cement paste-based environmental impacts is shown in **Error! Reference source not found.**. To quantify the total GHG emissions of mortar mixtures (kg CO_2-eq / m^3), **Equation 4.5** is used, where I is the total impact of a mixture, m_k is the mass of constituent k in 1 m^3 of cement-based material (i.e. mortar or paste), i_k is the per-unit-mass environmental impact of constituent k, d_k is the transportation distance of constituent k by truck, $i_{transport}$ is the transportation GHG emissions per unit mass of material, and $i_{batching}$ is the GHG emissions for batching 1 m^3 of material.

$$I = \sum_{k=1}^{n} m_k * i_k + m_k * d_k * \ i_{transport} \ + \ i_{batching} \qquad \textbf{Equation 4.5}$$

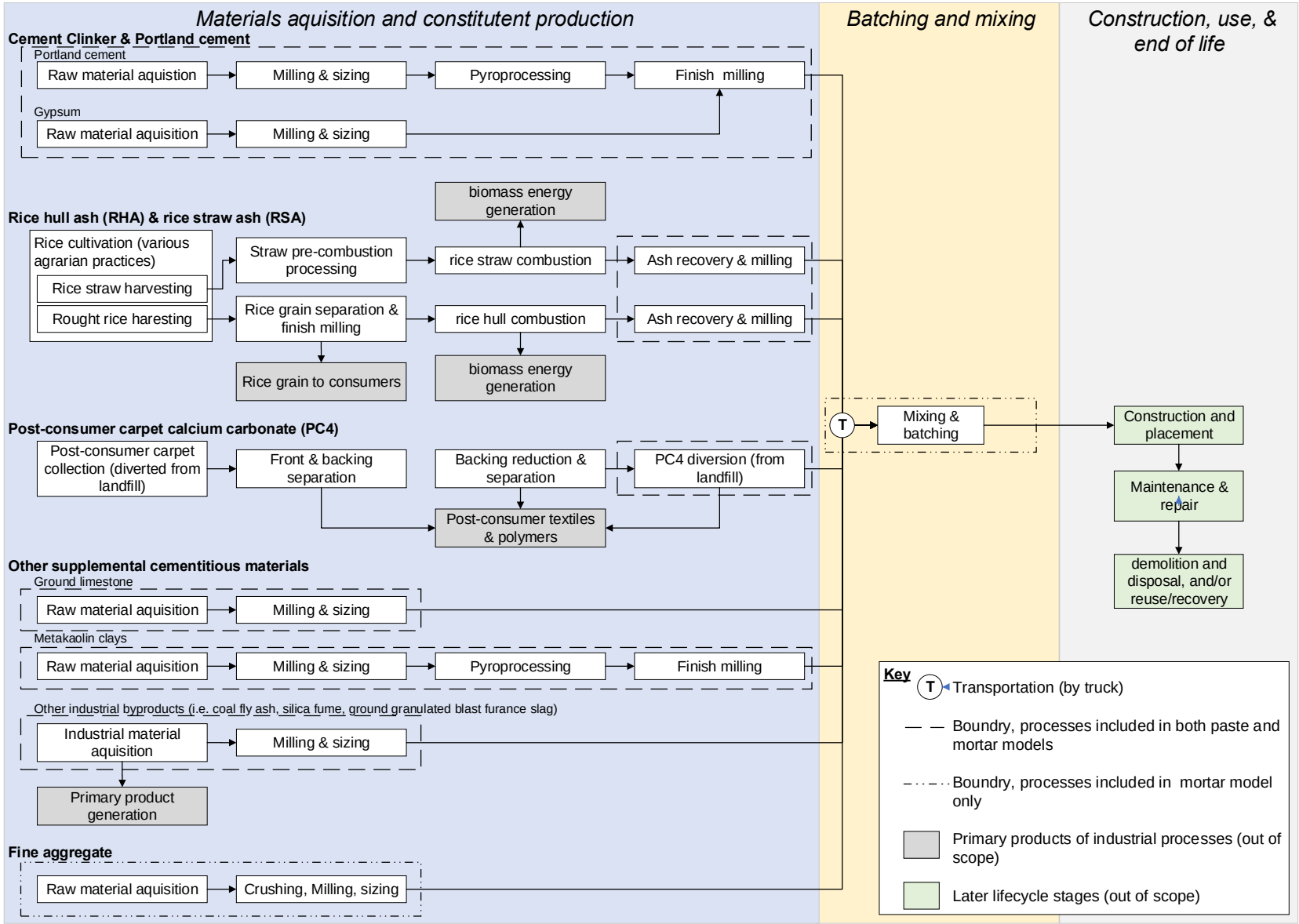

Figure 4.4. System for producing pastes and mortars with Portland cement, traditional mineral admixtures, post-consumer carpet calcium carbonate, rice hull ash, and rice straw ashes. Water is not depicted in the system as no impacts were assigned.

4.3.2.2.Compressive strength harmonization

In Chapter 2 and Chapter 3, the average compressive strength of mortars is reported for either cube (50.8 mm x 50.8 mm) or cylinders (50.8 mm diameter and 101.6 mm height) specimens. To address size effects from different geometries and enable comparing compressive strengths, equations proposed by Yi et al. [342] were applied account for the dimensional effects. These equations were developed by Yi et al. by applying linear regressions to experimentally acquired mechanical testing data from specimens of the same concrete mixture, but with different specimen shapes (e.g., cubes, prisms, cylinder) and varying specimen dimensions for the different shapes evaluated . [342]. The equations were arranged to solve directly for the general compressive strength of cube (see **Equation 4.6**) and cylinder specimens (see **Equation 4.7**). Where f_{cu} and f_{cy} are the specimen specific cube and cylinder compressive strengths (in MPa), respectively; $d_{cu}$is the length of the cube specimen (in cm); d_{cy} is the diameter of the cylinder specimen (in cm); and f_c. Is the general compressive strength (in MPa).

$$f_c = f_{cu} * \frac{1}{\frac{1.17}{\sqrt{1 + {d_{cu}}/{2.6}}} + 0.62} \qquad \textbf{Equation 4.6}$$

$$f_c = f_{cy} * \frac{1}{\frac{0.49}{\sqrt{1 + {d_{cy}}/{2.6}}} + 0.81} \qquad \textbf{Equation 4.7}$$

4.3.2.3. Compressive strength-informed comparison index

Common comparison indices allow for the comparison of the environmental impacts of a cement-based mixtures informed by performance and/or engineering design properties of the material. Here, the method shown in Miller et al. [320] and adapted in [39], [293] is used as a compressive strength-informed comparison index. As show in **Equation 4.8**, this index is assembled by dividing the environmental impact

under consideration, I (in this case, GHG emissions), by the compressive strength of the material.

$$X_{axial} = \frac{I}{f_c}$$

Equation 4.8

This index can then be used to rank and graphically compare mixtures (as shown in Miller et al. [320], Cunningham et al. [293] and Cunningham and Miller [39]) to select the best combination of environmental impact and strength for mixtures of varying performance (assuming a linear relationship between these materials is appropriate for the application, as is assumed here). For other material applications, where compressive strength is not the governing design factors, additional materials properties could be incorporated with environmental impact models following a similar methodology. As demonstrated in Miller et al. [320], this methodology can also be extended to other material properties and design performance considerations. For example, bending, thermal conductivity, carbonation, or beam deflection. Thus, making this comparison strategy especially useful for making material selection in the context of different structural design decisions.

4.3.3. Results and discussion

4.3.3.1. Environmental impact harmonization

The harmonized environmental impacts and the environmental impacts of mortar mixture production are shown in **Figure 4.5**. As shown in **Figure 4.5a** and **Table 4.4**, PC has the highest GHG emissions, on a unit mass basis, of common concrete constituents. This finding is expected as PC often contributes the majority of GHG emissions to concrete mixtures. Notably, the average transportation impacts (modeled as by truck), make up a very small portion of the impacts compared to the production of concrete constituents.

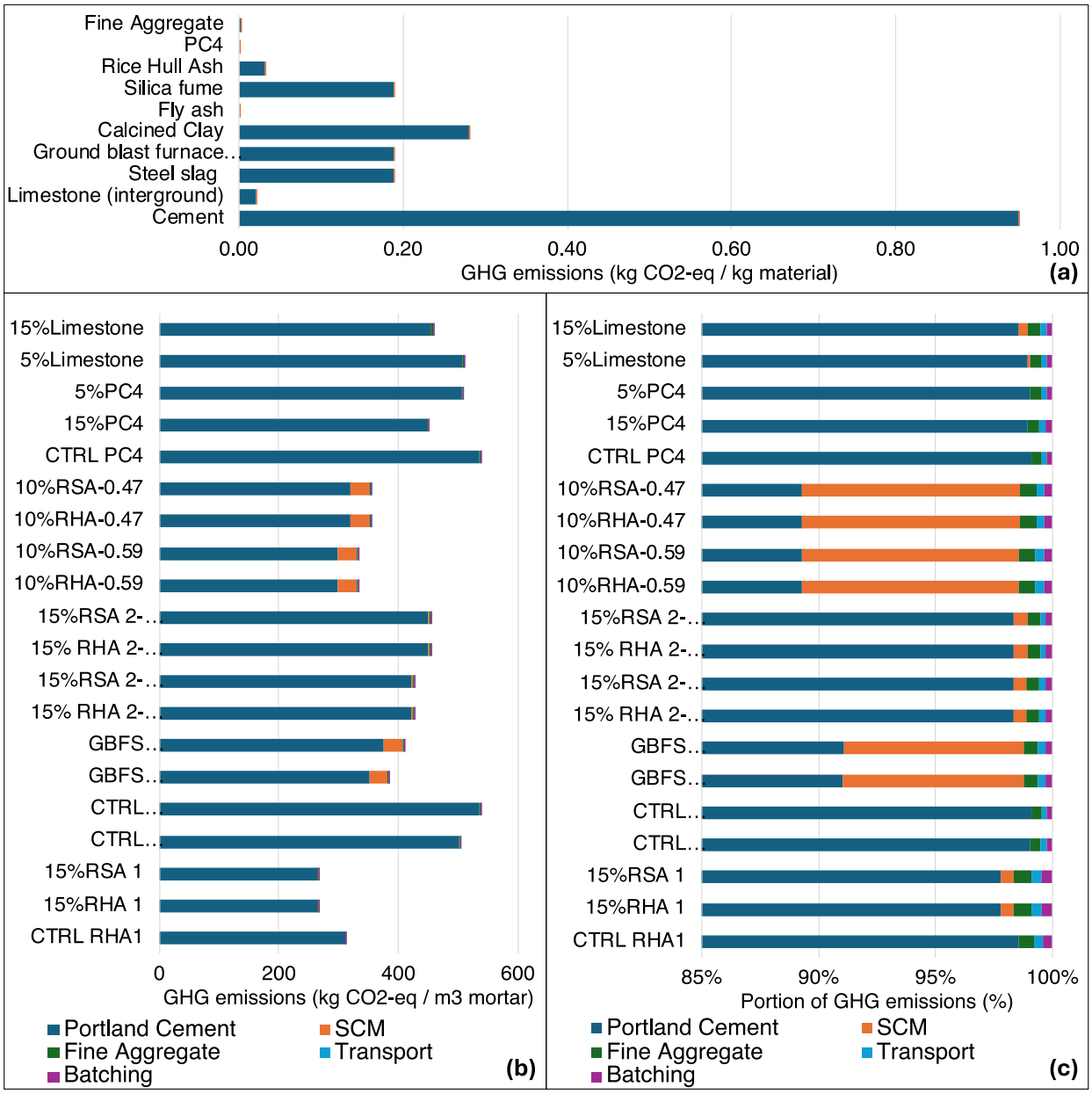

Figure 4.5. Harmonized GHG emissions (kg CO_2-eq) impacts (a) by constituent as modeled in the OpenConcrete tool [36] and (b) for mortar mixtures proportions for experimental works (kg CO_2-eq / m^3), and (c) the percentage of GHG emissions by material constituent and for mixture batching.

The harmonized environmental impacts of mixtures (from Chapter 2 and Chapter 3) are shown in **Figure 4.5b**, and demonstrate, as expected, that PC is the largest contributor to the GHG emissions of the mixtures modeled. PC contributed more than 90% of the GHG impacts for all mixtures (**Figure 4.5c**) and more than 95% of GHG emissions for mixtures with <30% mass replacement of PC. Mass replacement with mineral admixtures led to GHG emission reduction rates that correspond approximately with the mass

replacement rates (**Figure 4.5b**), as is also observed in earlier chapters of this dissertation. PC4 and limestone mixtures with 5% PC replacement had a ~5% reduction in GHG emissions. RHA and RSA mixtures with 40% PC replacement (i.e., 10% with ash and 30% with GBFS) showed a 34% reduction in GHG emissions and mixtures with 15% replacement had a 14-16% reduction in GHG emissions.

Table 4.4. Harmonized GWP by constituent modeled in the OpenConcrete tool [36]

US average impacts	GWP impacts (kg CO_2-eq /kg material)
Portland Cement (PC)	9.49E-01
Limestone	2.05E-02
Steel slag	1.88E-01
Ground blast furnace slag (GBFS)	1.88E-01
Metakaolin / calcined clays	2.80E-01
Fly ash	2.47E-05
Silica fume	1.88E-01
Rice hull/Rice straw ashes (RHA/RSA)	3.17E-02
Post-consumer calcium carbonate (PC4)	2.47E-05
Sand	1.75E-03
Batching (impact/m^3) *	1.23E+00

*Batching impact is per m^3 material, all impacts other per kg material

4.3.3.2.Compressive strength harmonization

The average compressive strengths for experimentally tested mixtures, harmonized to adjust for dimensional effects, are shown in **Figure 4.6**. The mixtures from Chapter 3 are shown in **Figure 4.6a** and **Figure 4.6b**, and mixtures from Chapter 2 are shown in **Figure 4.6c**. These harmonized data allow for direct comparison between mixture designs across studies. For example, the compressive strengths differ for the w/b=0.59 CTRL mixtures in **Figure 4.6a** and **b**, which is likely caused by the higher sand-to-binder ratio used in the pre-combustion leaching of the ashes (to reduce the amount of lab-produced ash required to make the mortars) resulting in different cement contents in the CTRL mixtures. As similar trend can be noted between the w/b=0.47 CTRL mixtures for **Figure 4.6a** and **c**, where differing sand-to-binder ratios have changed the total cement content of the mixture. These harmonized average compressive strengths mixtures are further evaluated in the next section in the comparisons index.

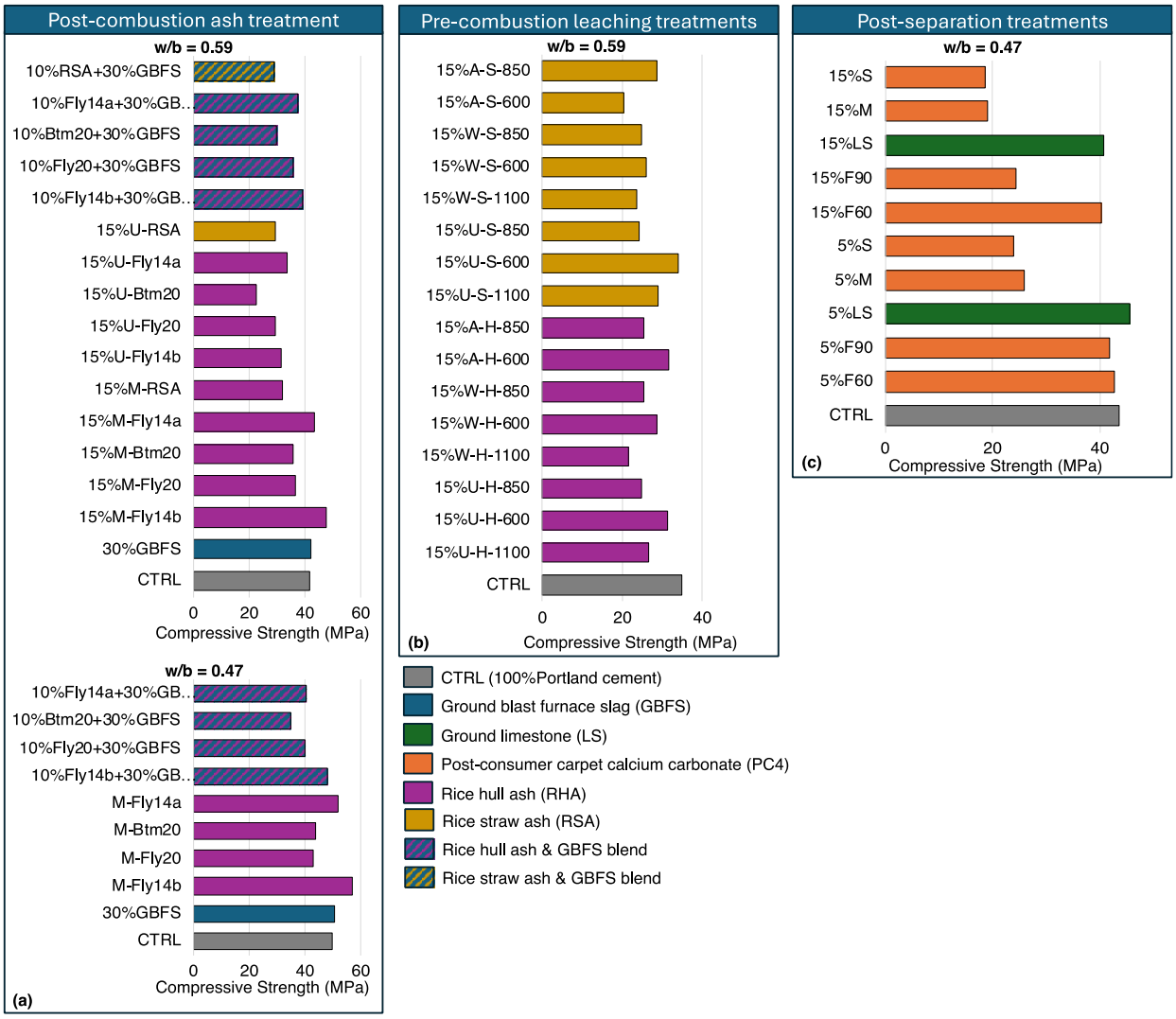

Figure 4.6. Harmonized compressive strengths by mixture type for mixtures from (a) post-combustion treatment of rice biomass ash (Chapter 3), (b) Pre-combustion biomass treatment (Chapter 3), and (c) PC4 processing (Chapter 2).

4.3.3.3. Performance-based comparison index

The different mixtures are compared using the X_{axial} index in **Figure 4.7**. For this index, lower values indicate a lower environmental impact, a higher compressive strength, or a both. Traditional, 100% PC mixtures in this work have an X_{axial} average of 11 kg-CO_2/MPa (ranging from 9-12 kg-CO_2/MPa). Of the mixtures with SCM cement replacement, 27 mixtures have values <11 kg-CO_2/MPa and 24 mixtures had index values >11 kg-CO_2/MPa (**Figure 4.7a**). For mixtures with required compressive strengths <40 MPa, the mixtures with a w/b=0.59 could lead to lower index, as they have less cement due to a higher

water content and partial cement replacement (**Figure 4.7a**). However, post-treated rice ashes led to higher indexes, likely due to a combination of having a higher-impact SCM (compared to limestone, GBFS, and PC4) and having varying influences on the compressive strength results relative to 100% PC mixtures. Notably, rice hull bottom ashes and untreated PC4 led to low compressive strengths, with X_{axial} values approximately twice those of CTRL mixtures. This finding suggests that these mixtures offer less performance for the GHG emissions associated with material production.

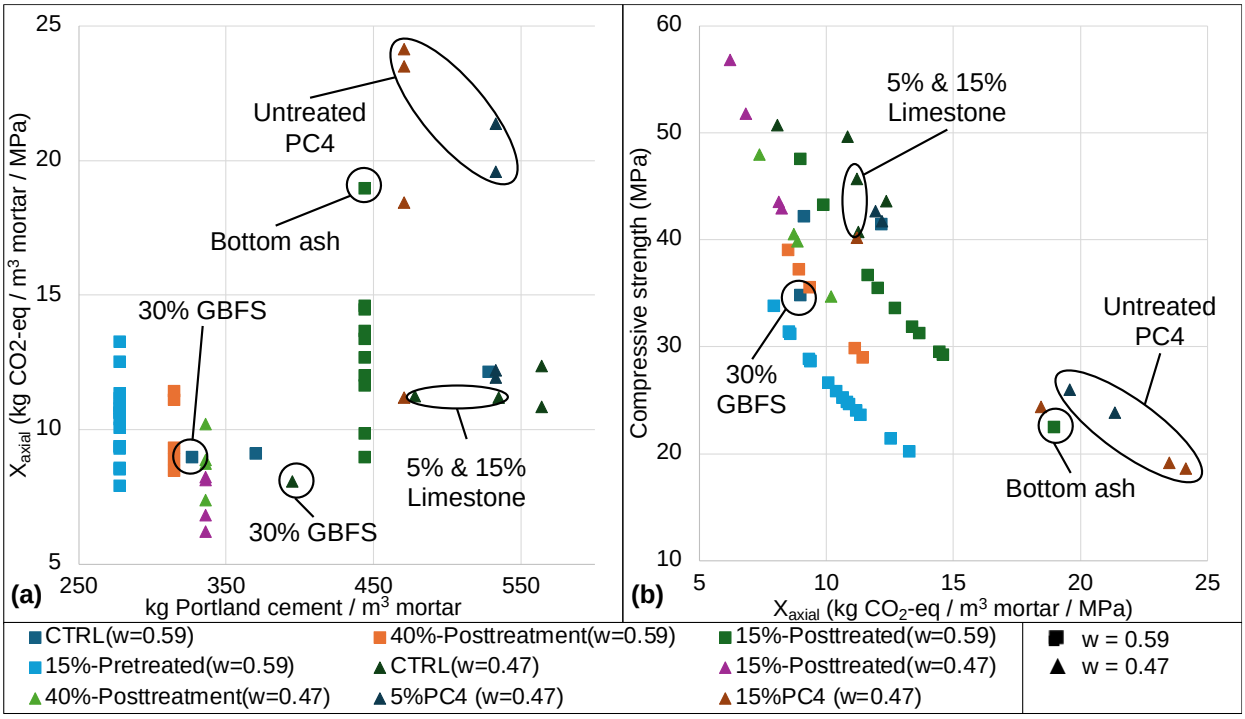

Figure 4.7. Comparison index X_{axial} for different mixtures plotted in (a) with the Portland cement content of the mixture and (b) with the compressive strengths of the mixtures to allow for selecting mixtures based with a required compressive strength and the lowest impact for the given strength.

4.4. Supply-informed comparisons of supplementary cementitious materials

4.4.1. Motivation

Concrete is the most used building material by mass [343]. Due to the large material supplies required to make cement-based materials, candidate materials need to be available in enough supply to be adopted by the industry and make meaningful contributions to environmental impact reduction from a system perspective [314], [344]. In this work, a framework is demonstrated to provide a system level perspective for assessing mineral admixtures using the supply of the material and the potential GHG emissions of paste made with the mineral admixture. For these supply-informed comparisons, the mass of paste that could be produced with the SCM or filler is modeled to achieve a fixed compressive strength and the corresponding environmental impacts associated with producing the paste is quantified.

4.4.2.Assembling supply-informed material comparisons

4.4.2.1. Equations for quantifying paste proportions, material supply, and environmental impacts

Importantly, different mineral admixtures have different contributions to the strength of cement-based materials, which limit the range of PC replacement. Required material performance characteristics, such as compressive strength of the mixture, could restrict the amount of SCM or filler that can be used. To quantify the amount of paste that can be produced with a given SCM or filler, the contribution of the mineral admixture to the strength development and the impact on replacement rate should be considered. To account for compressive strength and determine possible mixture proportions, a modified Bolomey equation was used. The Bolomey equation, first proposed by Bolomey in 1925 [345], is similar to the volume-based Feret's rule [346] or mass-ratio-based Abrams' rule [347], which both addresses changing mixture proportions [33]. In the Bolomey equation, (**Equation 4.9**), f_c is the compressive strength; m_{PC} is the mass of cement; m_w is the mass of water; h is the volume of air; and k_B and a are fitting constants.

$$f_c = k_B \left(\frac{m_{PC}}{m_w + h} - a \right) \qquad \textbf{Equation 4.9}$$

A binding equivalence factor for each mineral admixture (or cementing efficiency factor), as proposed by Oner et al. (e.g., [348], [349]), is used to account for differing contributions to the material strength. Binding equivalence enables quantifying a mass equivalence to cement for each of the SCMs or fillers, wherein PC would have a binding equivalency factor of 1. The equivalent cement mass can be found as shown in **Equation 4.10**, where in the equivalent mass of PC (m_{PC-eq}) is equal to the mass of PC (m_{PC}) plus the mass of mineral admixture (m_{MA}) multiplied by the binding equivalence (E_{MA}). Declared binding equivalency and cementing efficiencies can vary. For example, the binding equivalency concept outlined in European standards prescribes different factors for the same mineral admixture (e.g., for fly ash, France allows for E_{MA} of 0.6 [350], [351], while the British standard restricts fly ash E_{MA} to 0.4 [352]). Further, this standard also allows differences for BE based on region and replacement rates [352]. As such, these binding equivalence factors are not universal equivalency. However, this approach also allows for a framework that is amendable to regional contexts and conventions so a practitioner can adopt appropriate binding equivalence factors.

$$m_{PC-eq} = m_{PC} + m_{MA} * E_{MA} \qquad \textbf{Equation 4.10}$$

The method shown by Oner [349] is used to incorporate binding equivalency, as shown in **Equation 4.11**, where the variables are defined as they are above and $m_{C'}$ is mass of PC with the same binding equivalency as the actual mass of the mineral admixtures. Thus, $m_{C'}$ can be computed using **Equation 4.12** (all values as previously defined).

$$f_c = k_B \left(\frac{m_{PC} + m_{C'}}{m_w} - a \right) \qquad \textbf{Equation 4.11}$$

$$m_{C'} = m_{MA} * E_{MA} \qquad \textbf{Equation 4.12}$$

To enable comparisons of materials with equivalent mechanical performance, the compressive strength is fixed and the constituent proportions (i.e., water-to-binder ratio and replacement rate) are allowed to vary. **Equation 4.13** is arranged to solve for the cement content using discrete values for w/b ratio, compressive strength, and mass of the mineral admixture. With these values, the paste proportions to achieve a fixed compressive strength can be calculated.

$$m_{PC} = \left(\frac{f_c}{k_B} + a\right) * (m_w + h) - m_{C'} \qquad \textbf{Equation 4.13}$$

Finally, to allow for directly solving the equation, these variables are substituted into the equation as shown in **Equation 4.14**, where m_{c_o} is some initial PC mass to design from, w is the mass ratio of water-to-equivalent PC content, and r is a mass replacement ratio (i.e., where mineral admixture mass replacement is $m_{MA} = m_{c_o} * r$). Notably, m_{c_o} is not representative of the actual cement content, but instead allows for the computation of reasonable masses of mineral admixtures and water based on the ranges defined above.

$$m_{PC} = \left(\frac{f_c}{k_B} + a\right) * \left(m_{c_o} * w + h\right) - \left(m_{c_o} * r * E_{MA}\right) \qquad \textbf{Equation 4.14}$$

In this framework, the production of paste (i.e., the combination of PC, water, and mineral admixture) was quantified to understand the effect of changing w/b and replacement ratios. Of the mixture proportions, the mass of SCM or filler is modeled as constrained to material supply and the supply of water and PC is modeled as unrestricted. From the calculated proportion of mineral admixture in a mixture and known resource supply of mineral admixture, a scaling factor (SF_{MA}) is calculated with **Equation 4.15**, where S_{MA} is the supply of mineral admixture and m_{MA} is the mass of SCM. This factor is then used to quantify the total mass of paste using **Equation 4.16**, where the total mass of paste (m_{paste}) is the sum of the masses of PC (m_{cement}), mineral admixture (m_{MA}), and water (m_{water}) multiplied by the scaling factor (SF_{MA}).

$$SF_{MA} = S_{MA}/m_{MA}$$ **Equation 4.15**

$$m_{paste} = (m_{cement} + m_{MA} + m_{water}) * SF_{MA}$$ **Equation 4.16**

For the corresponding environmental impacts of the paste, **Equation 4.17** is used, where i_{cement} is the per unit mass impact of PC, i_{MA} is the per unit mass impact of the mineral admixture, and i_{water} is the per unit impact of water. Note, because paste is not representative of the full concrete product, environmental impacts associated with mixing and batching were not included. The environmental impacts associated with water use were assumed to be negligible ($i_{water} = 0$) in the comparisons quantified here as PC contributes the majority of GHG emissions from concrete mixtures. However, in scenarios where water use is of greater concern (e.g., in locations with water scarcity), this impact could be incorporated as shown in the equations. Additionally, impacts beyond GHG emissions could be incorporated using the same equation.

$$I_{paste} = \frac{(m_{cement} * i_{cement} + m_{MA} * i_{MA} + m_{water} * i_{water})}{(m_{cement} + m_{MA} + m_{water})}$$ **Equation 4.17**

4.4.2.2.Data and assumptions

The harmonized environmental impacts in **Table 4.4** were used to model the GHG emissions per kg of paste. The control mixture proportions and harmonized compressive strengths (**Figure 4.6**) were used along with **Equation 4.9** to determine values for the Bolomey equation constants of a = 0.532 and k_B = 15.238 MPa. To quantify PC content, a starting m_{c_o} of 400 kg was assumed with w ranging from 0.25 to 0.6, and r and E_{MA} values were defined individually for each SCM and filler. Minimum replacement mass was modeled as 1% for silica fume and 10% for all other mineral admixtures. The lower minimum for silica fume was selected to account for the lower maximum replacement modeled for silica fume (following limitation suggested in [316], [352]) and allow for more mixture permutation to be modeled in this smaller range. A maximum GBFS replacement of 50% was assumed to be consistent with literature [309], [353].

Future slags from EAF processes were modeled as behavior similarly to GBFS. Metakaolin replacement was limited to 35% due to potential workability concerns at higher replacement rates and due to literature showing performance reduction at 40% and greater replacement [354] with marginal additional reacted kaolin in excess of 30% replacement [355]. A 35% replacement rate for fly ash was selected to represent a maximum replacement rate, as informed by [352]. Though, we note that this represents a moderately high fly ash replacement rate [356]. RHA and RSA were assumed to have similar values, based on performance reported in literature [293]. A maximum replacement rate of 20% was used, informed by a reported minimum of 12% RHA [54], though literature has reported performance losses in excess of 20% RHA [209]. A maximum replacement rate for limestone was set at 15%, based on maximum rate allowed in blended cements [65]. PC4 as a filler was assumed to have the same replacement rate as virgin limestone as shown in [357]. The equivalency factors and maximum replacement rates adopted for this demonstration are described in **Table 4.5**. As discussed previously, appropriate factors for binding efficiencies and suitable replacement rates can vary by region and context. As discussed above, binding efficiencies and maximum replacement parameters may be modified to better reflect local convention.

Table 4.5. Binding efficiencies of mineral admixtures used in model

Material	BE value	Modeled max replacement
Ground blast furnace slag (GBFS)	0.9 [a]	50%
Electric arc furnace (EAF) slag	0.9 [b]	50%
Metakaolin	0.9 [b]	35%
Coal fly ash	0.6 [a]	35%
Rice hull ash (RHA)	0.6 [c]	20%
Rice straw ash (RSA)	0.6 [c]	20%
Limestone	0.4 [d]	15%
Post-consumer carpet calcium carbonate (PC4)	0.4 [e]	15%
Silica Fume	2.0 [f]	10%

[a] value used by from EN 206-1 [351, p. 20]; [b] modeled as similar to GBFS; [c] assumed equivalent to fly ash;
[d] assumed high BE at low replacement rate, [e] assumed same as limestone; [f] value reported in British standard [352]

Two categories of mineral admixture resource availability data were used to quantify supply-informed indices. The first takes a historic perspective by observing modeled and reported use of

conventional SCMs and fillers in 2021 and comparing that to the potential supply of PC4, RSA, and RHA available in the same year. The values for GBFS, fly ash, and kaolin clay are collected from the results in section **4.2** as summarized in **Table 4.6**. This work assumes limestone, as a key feedstock in PC production, would be available in a much supply as the PC production. As such, limestone was assumed to be available in the same magnitude as the PC it would replace (i.e., 1:1 relationship between PC production and limestone SCM supply). This estimate is conservative for the annual production of limestone as the mass of limestone required to make PC is larger than the PC produced; namely, for 95% clinker PC, we assume nearly 1.15 kg of limestone is needed to produce 1 kg of PC (1.785 kg $CaCO_3$ per kg of CaO at an estimated 65% weight fraction in PC).

Table 4.6. 2021 Mineral admixture supply values for determining cement, water, and mineral admixture masses per kg paste

Material	Generation (Metric ton)	Reported / Potential, Source
Ground blast furnace slag (GBFS)	7.60×10^6	Reported use, [323]
Coal fly ash	1.38×10^7	Reported use, [358]
Silica Fume	1.0×10^6	Approximate, value from [54]
Metakaolin	3.71×10^6	Estimated, from [334] and [62]
Rice hull ash	3.28×10^5	Potential, modeled in Chapter 3
Rice straw ash	6.08×10^5	Potential, modeled in Chapter 3
Post-consumer carpet calcium carbonate (PC4)	9.51×10^5	Potential, modeled in Chapter 2
Limestone	1.20×10^8	Potential, assumed to be similar to 2021 cement demand

The second category considers the potential maximum material flow reported and modeled for conventional and candidate SCMs and fillers in 2021, 2035, and 2050, to compare the supply and impact reduction potential of different mineral admixtures. As limestone and kaolin clays are mined materials with very large values of reserves [321], [322], the potential maximum flow of these materials could be significant if production is rapidly increased. Due to the uncertainty associated with the generation of mined mineral admixtures, they are excluded from the analysis of projected flows. RHA and RSA potential availability are driven by rice cultivation for food production (and thus the residues used to make these ashes) will remain constant as populations increase to 2050 is used. PC4 is also modeled as a constant generation rate between 2021-2050. As a byproduct of recycling, PC4 generation is a delayed phenomenon

at the EOL phase of carpet (after typically 8 years of use, but ranging from 2-24 years [315], [359]). We note, for PC4, there is further complexity due to consumer trends, which makes future carpet selection and deselection (when carpet is replaced with a different type of flooring material) [110], [315], even from an economic perspective, challenging to accurately forecast [360]. All values shown in **Table 4.7**. Paste mixture proportions, the mass of potential paste generation, and the GHG emissions of the paste was modeled using MATLAB [361]. Comparisons of potential paste production at a given GHG emissions per kg paste was plotted using base r [300], tidyvers [362], and ggforce [363].

Table 4.7. Reported and assumed mineral admixture usage compared to the potential flow of candidate materials (all masses in metric tons).

Year	2021	2035	2050
Ground blast furnace slag (GBFS)	7.60×10^6	5.11×10^6	2.72×10^6
Electric arc furnace (EAF) slag	8.10×10^6	1.29×10^7	1.51×10^7
Coal fly ash	2.82×10^7	8.79×10^6	6.42×10^6
Rice hull ash	3.28×10^5	3.28×10^5	3.28×10^5
Rice straw ash	6.08×10^5	6.08×10^5	6.08×10^5
Postconsumer carpet calcium carbonate	9.51×10^5	9.51×10^5	9.51×10^5

4.4.3.Results

The possible 2021 production of paste with candidate materials compared to pastes made with traditional mineral admixtures at compressive strengths of 20, 40, and 60 MPa are shown in **Figure 4.8**. As expected, lower strength concretes allow for higher replacement ratios and, thus, with less PC they have lower modeled GHG emissions (**Figure 4.8a)**. However, higher replacement with a restricted mineral admixture resource also means lower potential paste masses. As strength thresholds increases, the amount of replacement rates that can achieve these strengths decrease and the lowest possible GHG emissions for the mixture increases **Figure 4.8b** and **c**. Of course, higher PC content (modeled as unconstrained) also means more paste can be produced. Notably, increasing strength requirements has marginal impact on the maximum GHG emissions of the mixtures and, maximizing paste mass does not mean maximizing GHG emissions. This result is, in part, because the paste mass includes the contribution to water while the

environmental impact assessment assumes negligible GHG emissions from water. Thus, increasing w/b ratio leads to increased paste production and lowers the paste GHG emissions on a kg paste basis. At the 60 MPa strength parameter (**Figure 4.8c**), the lowest GHG emissions possible are further truncated and the maximum GHG emissions again increases for the mixtures.

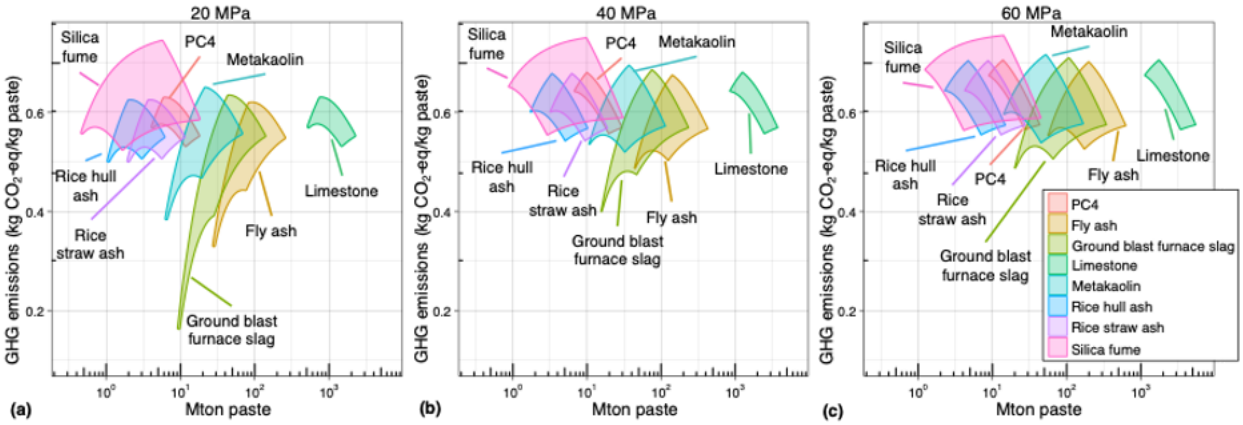

Figure 4.8. Comparison of potential mass of paste (mineral admixture, Portland cement, and water) production in 2021 and the potential global warming potential (in kg of CO_2-eq) for different compressive strengths. Fly ash, GBFS, and metakaolin use represents actual reported usage. PC4, limestone, rice hull ash, rice straw ash, and silica fume based on modeled and assumed values for maximum potential production for (a) 20 MPa binder, (b) 40 MPa binder, and (c) 60 MPa binder.

Across the strengths considered, paste with silica fume resulted in the largest GHG emissions modeled (the lowest being 0.52 kg CO_2-eq/kg paste) compared to other paste mixtures with mineral admixtures. Silica fume mixtures also had only moderate possible mass flows (at most 4 Mtons paste). This finding reflects the low maximum replacement rate. While silica fume is highly reactive with a binding efficiency 200% times that of PC, the maximum replacement rate modeled is 10% and the generation of silica fume is small compared to the other SCMs and fillers. These two factors limit the paste mass produced with silica fumes. For low-strength mixtures (20 MPa), GBFS can replace PC at larger rates with GHG emissions as low as 0.16 kg CO_2-eq /kg paste. This SCM is followed by fly ash with the lowest modeled impact of 0.33 kg CO_2-eq /kg paste. Notably, these two minimums also correspond with the minimum paste masses for GBFS and fly ash mixtures (9 Mtons and 28 Mtons, respectively). At higher strengths, the lowest GHG emissions compared to other mineral admixtures become less drastic, with the lowest modeled

impacts of 0.40 kg CO_2-eq/kg paste for GBFS and 0.48 kg CO_2-eq/kg paste for fly ash at 40 MPa. At 60 MPa, the minimum impacts further increase 0.5 kg CO_2-eq/kg paste for GBFS and 0.52 kg CO_2-eq/kg paste for fly ash. Metakaolin, with a similar binding equivalency as GBFS, allows for the third lowest minimum GHG impacts between 0.38-0.54 kg CO_2-eq/kg paste depending on strength. Limestone, modeled as having as large of a supply as PC, can produce the largest amount of paste (~2 $x10^3$ - $5x10^3$ Mtons depending on strength), and from a systems level, the large availability of limestone is promising.

In comparing the RHA, RSA, and PC4 to other materials, all three combined could produce higher amounts of mortar at lower GHG emissions than silica fume. However, metakaolin, GBFS, and fly ash, all had a higher paste production potential than these alternative materials with similar GHG emissions. Together these alternative materials have the potential to produce large amounts of paste at higher PC replacement rates. With increase paste production and lower GHG emissions (i.e. higher PC replacement) they could contribute to system while reductions in GHG emissions for the cement and concrete industry.

To understand how shifting material flows could impact the potential mass of paste that can be produced and the associated GWP, comparisons were produced for 2021, 2023, and 2050 at 60 MPa (**Figure 4.9**), figures showing comparisons for 20, 40, and 60 MPa in the same year are provided in Appendix F. The maximum paste production with fly ash and GBFS is expected to decrease from 1.2 $x10^3$ Mtons and 0.3 $x10^3$ Mtons in 2021 to 0.3 $x10^3$ Mtons and 0.2 $x10^3$ Mtons in 2035, respectively. In 2050 this further reduces to 2 $x10^2$ Mtons with fly ash and 1 $x10^2$ Mtons with GBFS in 2050. These changes in fly ash and GBFS generation further emphasize the need for alternative mineral admixtures and the potential role for the alternative materials investigated in this work. However, at current production rates, these alternative flows are still in lower national supply compared to the decreased supply of fly ash and GBFS. While there may be a role for RHA, RSA, and PC4 as materials for smaller geographical regions, this finding also suggests an opportunity for identifying alternative materials with larger material availability.

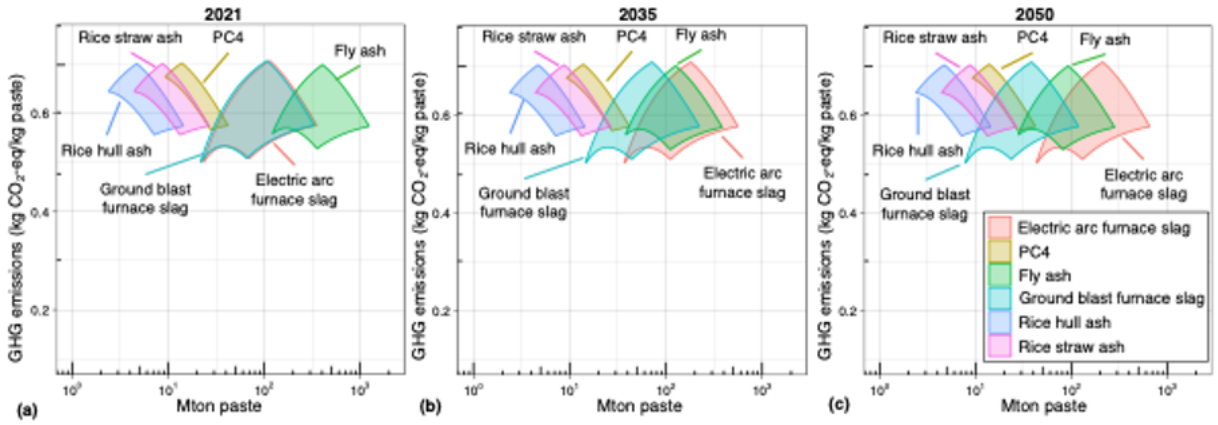

Figure 4.9. Potential maximum mass of paste (mineral admixture, Portland cement, and water) production for 60 MPa calculated from modeled and reported maximum mineral admixture generation each year: (a) for 2021, (b) for 2035, and (c) for 2050.

In addition to the material flows investigated in this chapter, EAF slag was included in this comparison of paste materials with projected flows. As production system shift, especially for GBFS, the production of EAF slags will increase. If similar performance to GBFS can be achieved, pastes with EAF slags could be produced in similar masses to current fly ash and GBFS flows: 3 x10^2 Mtons in 2021, 5 x10^2 Mtons in 2035, and 6 x10^2 Mtons in 2050. While not modeled here, a similar argument could be made for processing and engineering other CCPs. If these less-reactive materials can be engineered for suitable performance with minimal additional GHG emissions, they could become useful mineral admixtures with supplies that rivals the levels of present-day fly ash and GBFS generation.

4.5. Summary

4.5.1. Current and projected generation of mineral admixtures

Historically, SCM and filler generation has exceeded their use in concretes. When candidate materials are included, the supply of mineral admixtures generated in the US from 2017-2022 is approximately twice that of actual usage. Notably, the potential generated mass of candidate RHA, RSA, and PC4 materials (from chapter 2 and chapter 3), are relatively small compared to traditional mineral admixtures in the US. However, modeling projections of traditional industrial byproduct SCMs reflect a potential reduction in the supply of these materials. Notable findings include:

- Projected SCM generation from coal combustion is expected to sharply decrease 30-55% by 2030, and continue to decrease further by 2050;
- Total coal combustion product generation is estimated at 25-40 Mtons in 2030 and 7-32 Mtons by 2050;
- Changing steel production systems are expected to reduce blast furnace slag production by ~10-13% between 2025 and 2030 and by a total of 54-58% by 2050;
- The generation of EAF slag is projected to increase by 15-24% to 9-15 Mtons in 2050.

While steel slags and coal combustion byproduct materials are less reactive, if these materials can be engineered for improved performance with minimal additional GHG emissions, they could represent a large potential material flow for cementitious materials.

4.5.2. Mixture comparison via harmonized environmental impacts and experimentally determined compressive strengths

The environmental impacts of mortar mixtures for different works are compared using a compressive-strength informed index. To inform this index, the experimentally determined average

compressive strengths are harmonized to account for different specimen geometries, and the environmental impacts are quantified using harmonized lifecycle inventories to represent the US average production of the mortars. Key findings from this assessment include:

- As is consistent with literature, PC contributes the most to the GHG emissions of the mixtures;
- Partial cement replacement with mineral admixtures reduced the environmental impacts at approximately the same rate as the mass replacement rate in the modeled mixtures;
- The lowest reduction in GHG emissions (compared to analogous PC-only mixtures) was achieved by the mixtures with the highest replacement rates;
- Multiple mixtures provided lower comparisons index values, indicating a better ratio of GHG emissions to compressive strength;
- The modeled mixtures with the highest index were also the mixtures with the greatest reduction in compressive strength relative to analogous mixtures made with only PC.

Together, comparison of mixture with harmonized performance and environmental impact assessment can enable the selection of mixtures with the lowest environmental impacts for a required performance characteristic. Thus, this method can be useful for evaluating materials on a performance level as well as for design and engineering material selection.

4.5.3. Supply-informed comparisons of supplementary cementitious materials

In this work a methodology for assembling supply-informed comparisons of different SCM materials is proposed. These comparisons are performed with two perspectives: (1) based on reported actual use of traditional mineral admixtures and potential generation of alternative materials; and (2) based on projected trends in industrial byproduct SCM generation. Key findings include:

- Lower compressive strength requirements allow for higher amounts of PC replacement and the lowest GHG emissions as well as the smallest paste production masses;
- High PC replacement becomes less feasible as strengths requirements increase;
- RHA, RSA, and PC4 can produce more paste with similar GHG emissions as silica fume, but the potential paste production at similar GHG emissions is less compared to GBFS, metakaolin, fly ash, and limestone;
- Future projections show large reductions in the potential paste production from fly ash and GBFS; however, the paste production potential at similar GHG emissions remains higher than the RHA, RSA, or PC4 materials in both 2030 and 2050;
- EAF slag generation is expected to increase in the future with potential paste production exceeding fly ash and GBFS in 2035 and 2050.

There is need for mineral admixtures that can offset the projected reductions in fly ash and GBFS generation. While PC4, RSA, and RHA can contribute to offsetting these materials and may be particularly useful in smaller regions, the generation EAF slag is projected to be of similar quantity to those of fly ash and GBFS. Notably, use of these slags will require engineering and valorization efforts to achieve required material performance and characteristics. However, the significant projected supply of EAF makes it a promising future candidate for experimental investigation.

CHAPTER 5

Conclusions

Supplementary cementitious materials (SCMs) and mineral fillers (fillers) remain an important resource for reducing the clinker content of Portland cement systems. As the need to lower the greenhouse gas (GHG) emissions from the cement and concrete industry has grown, so too has the demand for mineral admixtures. This resource shift has led to changes in the supply of mineral admixtures and localized scarcities in certain regions. To formulate a framework to assess alternative materials, this dissertation evaluated two residue flows as alternative, Portland cement-replacing mineral admixtures and explored the potential symbiotic relationships from diverting residue materials into beneficial use in cement-based materials.

5.1. Summary and key conclusions

5.1.1. Post-consumer carpet calcium carbonate

Chapter 2 evaluated postconsumer carpet calcium carbonate (PC4), from end-of-life carpet backing, as an alternative mineral filler. PC4 was experimentally characterized, its effects on performance of cement-based materials were investigated, and industrial ecology methods were employed to evaluate the material flow and GHG emissions of PC4 in cement-based materials. When PC4 was used as a filler to partially replace Portland cement in concrete, PC4 produced a lower density material with increased air content. This increase coincided with up to 60% lower compressive strengths and large increases to the initial (167%) and final (195%) set times. As such, incorporating untreated PC4 led to deleterious effects on both fresh and hardened properties of the cement-based materials. Concurrently, Portland cement replacement was shown to reduce GHG emissions at a rate that was roughly equivalent to the mass replacement rate. As such, if the performance of PC4 can be better tailored for cement-based materials, environmental benefits could be achieved from this material.

To improve the performance of PC4, three strategies were evaluated: (1) milling PC4 to decrease particle size; (2) heat-treating PC4 at 600°C to remove latex and other remnant polymers; and (3) heat-treating PC4 at 900°C to remove remnant polymers and mimic a pre-calciner stage. Experimental evaluation showed PC4 treated at 600°C and 900°C improved PC performance for mixtures with 5% Portland cement replacement. Notably, 15% replacement with PC4 furnaced at 600°C exhibited similar performance to mixtures with 15% virgin limestone replacement. These results suggest mixture optimization of PC4 furnaced at 900°C, to balance the CaO content of the binder, may yield additional benefits to performance. Microstructural analysis via SEM micrographs showed heat treatments reduced the observable large voids in mortars, likely due to the absence of latex leading to less air entrainment.

This chapter demonstrated a pathway to process PC4 as a filler material that leads to reduced waste in the environment and the valorization of a large and previously under-used material flow. A material flow analysis showed that over 1.4 billion m^2 of carpeting has been disposed of since 1954. From 2002-2019, less than 6% of the carpet constituents, by mass, were recovered with the remaining materials being landfilled or lost to the environment. This end-of-life material included over 61.5 Mt of fiber and textile materials, including 33 Mt of nylon, 16 Mt of polypropylene, and 5.5 Mt of polyethylene terephthalate. Additionally, an estimated 47 Mt of PC4 was disposed of in the same period. Annual generation of PC4 was estimated to be equivalent to ~1% of the mass of virgin limestone used for clinker production or ~30% of the mass of inter-ground limestone.

5.1.2. Rice hull ash and rice straw ash

Chapter 3 identified synergies from the biomass energy generation and construction material production. Specifically, rice hull ash (RHA) and rice straw ash (RSA) were evaluated a reactive SCMs for cement-based material production. As with the previous chapter, a material flow analysis to quantify supply and an environmental impact assessment to assess GHG emissions were conducted. These results were

coupled with experimental analysis of pre-combustion biomass leaching and post-combustion ash processing on the mechanical performance of cement-based materials made with RHA and RSA.

The use of RSA and RHA to partially replace Portland cement was evaluated. A regional flow assessment was used to compare generation on a national (United States - US) and state-level for six states with rice cultivation. Findings showed the potential quantities of RSA were twice that of RHA. While these ashes together amount to only ~1% of annual US cement consumption, these ashes could replace sizeable fractions of cement production in certain regions. In Arkansas, Louisiana, and Mississippi, the potential state-level generation of rice biomass ashes were equivalent to approximately 60%, 10%, and 6% of the mass of Portland cement use in those states, respectively. In California and Texas, the states with the largest consumption of Portland cement, replacement would be limited to 2% and 0.5%, respectively. This finding suggests that rice biomass ashes could be a regionally desirable SCM if ash generation is scaled and the ashes can provide acceptable performance in Portland cement-based materials.

The influence of pre-combustion leaching (to reduce slagging and fouling during combustion in bioenergy generation) of rice straw and rice hull on the resulting ash was investigated. Water leaching and phosphoric acid leaching were shown to reduce the concentration of K and Cl, which could have benefits to concrete durability. Findings showed comparable compressive strengths for mixtures using either RHA or RSA as partial cement replacement and that the temperature of oxidization was a significant parameter driving material performance. An environmental impact assessment showed that acid leaching without leachate recovery led to high GHG emissions for energy generation, but if impacts were allocated to energy generation, the use of the remaining ashes would result in GHG emissions reductions with the same magnitude as the mass replacement level. Ash made from unleached rice hulls, unleached rice straw and acid leached rice hulls (all oxidized at 600°C) provided lower GHG emissions per unit strength than the 100% Portland cement mixture.

To examine the effects of post-combustion strategies, four RHAs from industrial energy generation and one laboratory-produced RSA were evaluated to produce bioash-Portland cement binder mixtures. Results indicated that without leaching, the alkali content of the RSA can exceed standards set for binder applications. In evaluating the compressive strengths, bottom RHA significantly reduced the compressive strength compared to the control (17-32% reduction at 28-day). However, fly RHA and RSA mixtures did not differ significantly from the control mixtures. Experimental findings indicate that with appropriate pre-leaching and post-combustion treatment as well as concrete mixture design, mixtures with 15% RHA or 15% RSA replacement can perform similarly to 100% Portland cement control mixtures at 28-days. Cumulatively, this chapter demonstrates the potential for rice hull and rice straw to support regional biomass energy generation where in the ashes are then recovered to act as SCMs, partially replacing Portland cement and lowering GHG emissions.

5.1.3.Mineral admixture generation and environmental impact-informed comparisons

In Chapter 4 an investigation of these resources was used to establish a framework for assessment of different mineral admixtures for use in cement-based materials. The developed framework allows for comparison of the modeled GHG emissions and the potential production mass of paste materials under consistent mechanical performance requirements (fixed compressive strengths) using input from experimental evaluations of performance, environmental impact assessment, and material flow analysis. In this work, recent mineral admixture production and use was compared to projected generation potential of PC4, RHA, and RSA materials. The future generation of ground blast furnace slag (GBFS) and coal fly ash (herein, fly ash) were modeled under changing steel production and energy production systems to understand future availability of traditional SCMs and fillers. Harmonized environmental impact assessments were conducted for cradle-to-gate production of the mortar mixtures evaluated in Chapter 2 and Chapter 3 and were applied in a compressive strength-informed comparison index. Finally, an assessment framework was developed to provide a system-level perspective for mineral admixture availability in the US and GHG emissions reduction potential from their use, wherein the potential supply

of paste made with different mineral admixtures and the associated GHG emissions of the pastes were compared for 2021 mineral admixture use, maximum mineral admixture supply in 2021, and projected supply of mineral admixtures in 2035 and 2050.

The historical mineral admixture generation and use and the projected generation of fly ash and GBFS highlight the need for alternative materials to meet the continued demand for Portland cement-replacing materials. The results show that fly ash generation is projected to decrease by 30-55% between 2025 and 2030. GBFS generation is expected to reduce but at a slower rate: 10-13% between 2025 and 2030 and 54-58% by 2050. As GBFS generation decreases, electric arc furnace (EAF) slag generation is expected to increase by 15-24% by 2050. While generation of coal combustion products (CCPs) was projected to decrease, the total CCPs were projected to have a combined mass of 7-32 Mt in 2050. EAF slag and total CCPs are expected to have different properties and performance characteristics than GBFS and fly ash, respectively, but they represent a material flow on a similar scale to GBFS and fly ash SCMs.

To compare mixture designs, a harmonized environmental impact assessment was performed for the mortar mixtures evaluated in Chapters 2 and 3. Findings agreed with earlier conclusions that replacement with PC4, RHA, and RSA each reduced GHG emissions at approximately the same degree as the rate of Portland cement replacement. A compressive strength informed comparison index showed multiple mixtures provide lower GHG emissions per unit strength compared to mixtures with only Portland cement. These multi-objective comparisons can be tailored to performance parameters and/or environmental impacts that are of interest during the engineering and design stages.

To build an assessment framework, system-level comparisons were made for the potential mass of paste that could be produced with a given mineral admixture, while controlling for consistent material performance. Under current production levels, the amount of paste that can be produced with PC4, RHA, and RSA was similar to that of silica fume, but with lower GHG emissions. At low strengths, replacement

rates for fly ash and GBFS were relatively high and allowed for lower GHG emissions compared to the other mixtures. These GHG emissions reductions decreased at higher strengths. For future mineral admixture availability, a large decrease in the potential paste production with either GBFS or fly ash was noted. However, both fly ash and GBFS maintained higher paste production rates in 2050 than PC4, RSA, and RHA, again, suggesting these alternative materials may be desirable at a regional in scale. At a national scale, EAF slags were shown to potentially support the same volume of paste as GBFS in 2021 (assuming similar performance), exceeding fly ash by 2035. Based on resource availability, EAF slags could be an area for continued investigation as an industrial byproduct SCMs. However, similar material performance (likely via processing) and lower-GHG emissions must be verified.

5.2. Directions for future research

This work establishes key metrics that must be examined in the consideration of alternative mineral admixtures. The alternative SCMs and fillers analyzed, RHA, RSA, and PC4, showed potential to reduce the GHG emissions of cement-based materials, but the complementary assessments conducted showed further work is needed to improve performance and considerations must be made to address the ability for utilization of mineral admixtures at scale. Based on these findings, opportunities for future research into PC4, RSA, and RHA materials, and promising pathways for identifying and developing other alternative materials are presented.

5.2.1. On post-consumer carpet calcium carbonate

The generation of PC4 from carpet recycling is likely to continue as the carpet industry in under pressure across the US to divert carpet from landfills. Significant efforts have been made in literature to model the polymer recycling network and supply chain from carpet. However, little consideration has been made for the PC4 fraction. Building on the national-level material flow analysis present here, a regional-level material flow analysis to project localized PC4 generation would be useful in designing recovery and valorization systems for PC4 (e.g., use as a filler). Additional durability testing of temperature-treated PC4 in cement-based materials could be studied as could the effects of PC4 property variation between carpeting material type and recycling process. Variations in PC4 would be expected from different recycling facilities (ideally, from facilities using different recycling technologies) and from different processing times (e.g., different points in the year). Yet, treatment methods such as the heating method explored herein may be able to limit the effects of such variations if the PC4 were to be used as a filler. Together, this knowledge would improve our understanding of the consistency and availability of PC4.

The potential applications for PC4 are not limited to use as a mineral filler. PC4 could substitute for a portion of virgin limestone as a cement kiln feedstock. This use of PC4 could reduce dependency on landfilling and limestone quarrying, thus improving resource circularity. Recovery of latex from PC4 could

also be investigated, which may reduce the need for heat treatment of the PC4, improve the performance of PC4 without heat treatment as a filler, and yield latex for reuse (e.g., as a chemical admixture or in other products). The strategy of using PC4 as both a mineral filler and a chemical admixture could also be investigated via techno-economic and experimental investigations, though the PC4 dosage would likely need to be much smaller than the ratios used in this work. While separate from producing cement-based materials, the material flow analysis of PC4 in the US identified significant quantities of nylon, PET, and polypropylene. The use of these recovered plastics is under evaluation by others, but future work could also consider mechanisms such as chemical recycling instead of downcycled into lower-grade applications (potentially reducing reliance on production of virgin plastic materials).

5.2.2. On rice straw and rice hull ashes from energy generation

RHA and RSA generation were shown to be benefited by using hull and straw residues to produce energy and then diverting the ash for use as an SCM. While rice hulls typically exhibit low alkali content, rice straw had higher fractions of alkalis, which could pose challenges to both energy recovery and concrete durability. Focusing on use of these ashes as SCMs in concrete, future work should address potential shifts in long-term material performance via experimental analysis and computational modeling with comparisons to traditional binder systems. Both methods could be used to project longevity, which could then inform a cradle-to-grave lifecycle assessment of the RHA and RSA in cement-based materials. Future work could investigate the potential for leachate, resulting from leaching to remove alkalis prior to combustion, as a resource (e.g., a K-rich fertilizer). Alternatively, if an alkali solution is used for leaching, the remnant solution may be diverted into material production processes. Another possible avenue for investigation could be into alternatives to leaching treatments. For example, blending different biomass fraction (i.e., rice straw and rice hulls) could be used to reduce the overall alkali content of the biomass feedstock for combustion. This blending may provide other benefits, such as increasing the feedstock supply for a combustion facility, decreasing overall alkali content to reduce slagging during combustion, and decreasing the alkali concentration in the ash for anticipated improvements to the durability of bioash-

cement materials. These combined ashes would also need to be evaluated, experimentally characterized, and investigated to ensure appropriate performance as an SCM in cement-based materials.

Alternative uses could also be considered for these biomass materials. In the context of cement-based materials, rice hull and rice straw could be used as a component of the kiln feed which would produce energy and then could be looped into the clinker or cement production system as a silica material source. As with the strategies discussed above, this would require blending to limit the alkali content of the resulting binder material. If appropriate chemical composition and phase development can be achieved, these materials could play a role as a kiln fuel in regions where rice cultivation is prominent.

5.2.3. On trends in supply of mineral admixtures and material comparisons

Investigations could build upon the models initiated here to investigate future supply of commonly used mineral admixture by modeling global supplies. Specific information in context of regional SCM and filler generation, demand, and consumption will also be useful to inform industry stakeholders and policy makers on appropriate action to address these anticipated in challenges in mineral admixture availability.

The emergence of alternative and regionally available mineral admixtures (such as RHA and RSA investigated here) require standards that support utilization of these alternative materials, when safe and appropriate. These changes should be supported by science and rigorous investigation, such as established suitable binding equivalency factors for regionally produced materials that are reflective of the regional building practices. Additionally, future investigations could address how these materials can contribute to regional production systems and quantitatively reduce environmental impacts via techno-economic assessment and environmental impact assessment methods.

Potential mineral admixture production projected in 2050 suggested EAF steel slags and total CCPs will be generated in sizeable quantity. Based on resource availability and chemical composition, these

materials are two potential mineral admixture flows that could be produced at a national scale from alternative industrial byproducts. Importantly, the performance and required post-production treatments for these materials has not been well demonstrated. Future research should investigate byproduct treatment strategies for EAF and CCPs to drive suitable material performance. If the required beneficiation can be achieved with minimal additional environmental impacts (especially if it is easily electrifiable, via controlling slag cooling and/or milling), these materials could help address the resource availability constraints expected from reduced fly ash and GBFS generation. Experimental investigation into these alternatives could include evaluating processing strategies and investigating their performance as mineral admixtures in cement-based materials.

The influence of these partial cement replacements on the durability and longevity of structural materials is another avenue for future research. For example, an experimental investigation could quantify changes in various durability properties. Differences in durability properties, like changing permeable pore volumes and sizes, could have implications for chemical ingress into the cement-based materials. Likewise, lowering clinker contents may decrease the pH of the materials and make the steel reinforcement more susceptible to corrosion. Ashes with higher carbon contents could be of particular concern. Less-stable carbon from these materials may contribute to a further pH decrease or, if these higher-carbon ashes were in direct contact with the steel, they could accelerate localized corrosion and pitting in the reinforcement. Lower durability could lead to a reduced lifespan and/or require more frequent maintenance. Notably, this change in lifespan has implications for the life cycle impacts of the material. Thus, quantifying the change in lifespan (e.g., modeling chemical ingress and corrosion to then inform replacement and maintenance) would enable modelling the overall environmental impacts using a life cycle assessment methodology. These works could be complimented by technoeconomic assessment to verify comparable costs, and environmental impact assessment to verify actual reductions to the GHG emissions and avoid unintended consequences to cost or environmental impact from using alternative materials.

References

[1] K. C. Curry, “Cement [Advance Release],” in *2018 Minerals Yearbook*, Reston, VA: US Geological Survey, 2022.

[2] S. A. Miller and R. J. Myers, “Environmental Impacts of Alternative Cement Binders,” *Environ. Sci. Technol.*, vol. 54, no. 2, pp. 677–686, 2020, doi: 10.1021/acs.est.9b05550.

[3] IEA, “Technology roadmap - low-carbon transition in the cement industry,” 2018. [Online]. Available: https://www.iea.org/reports/technology-roadmap-low-carbon-transition-in-the-cement-industry

[4] S. A. Miller and F. C. Moore, “Climate and health damages from global concrete production,” *Nat. Clim. Change*, vol. 10, pp. 439–443, 2020, doi: 10.1038/s41558-020-0733-0.

[5] K. L. Scrivener, V. M. John, and E. M. Gartner, “Eco-efficient cements: Potential economically viable solutions for a low-CO2 cement-based materials industry,” *Cem. Concr. Res.*, vol. 114, pp. 2–26, Dec. 2018, doi: 10.1016/j.cemconres.2018.03.015.

[6] S. A. Miller, A. Horvath, and P. J. M. Monteiro, “Readily implementable techniques can cut annual CO2 emissions from the production of concrete by over 20%,” *Environ. Res. Lett.*, vol. 11, p. 74029, 2016, doi: https://doi.org/10.1088/1748-9326/11/7/074029.

[7] United Nations Environment Programme, *2023 Global Status Report for Buildings and Construction: Beyond foundations - Mainstreaming sustainable solutions to cut emissions from the buildings sector*. United Nations Environment Programme, 2024. doi: 10.59117/20.500.11822/45095.

[8] IPCC, “Mitigation Pathways Compatible with 1.5°C in the Context of Sustainable Development,” in *Global Warming of 1.5°C: IPCC Special Report on Impacts of Global Warming of 1.5°C above Pre-industrial Levels in Context of Strengthening Response to Climate Change, Sustainable Development, and Efforts to Eradicate Poverty*, 1st ed., Cambridge University Press, 2022. doi: 10.1017/9781009157940.

[9] World Meteorological Organization, *State of the Global Climate 2023*. 2024.

[10] USGS, “Cement - Historical Statistics (Data Series 140).” [Online]. Available: https://www.usgs.gov/media/files/cement-historical-statistics-data-series-140

[11] National Bureau of Statistics of China, “1999-2023 Statistics Yearbook, C13-12 Output of Major Industrial Products.” [Online]. Available: https://www.stats.gov.cn/english/Statisticaldata/yearbook/

[12] World Bank, “World Bank national accounts data, and OECD National Accounts data files.” [Online]. Available: https://data.worldbank.org/indicator/NY.GDP.MKTP.CD

[13] A. Favier, C. De Wolf, K. Scrivener, and G. Habert, “A sustainable future for the European Cement and Concrete Industry: Technology assessment for full decarbonisation of the industry by 2050,” ETH Zurich, 2018. doi: 10.3929/ETHZ-B-000301843.

[14] UN Environment Programme, K. L. Scrivener, V. M. John, and E. M. Gartner, “Eco-efficient cements:Potential economically viable solutions for a low-CO2 cement-based materials industry,” DTI/2170/PA, 2017. [Online]. Available: https://wedocs.unep.org/20.500.11822/25281

[15] R. Isaksson and M. Rosvall, “Cement and Concrete-Quality and Sustainability Understanding, defining and measuring opportunities,” in *27nd International Sustainable Development Research Society Conference, Mid Sweden University*, 2021, pp. 13–15.

[16] B. Bruckner, K. Hubacek, Y. Shan, H. Zhong, and K. Feng, “Impacts of poverty alleviation on national and global carbon emissions,” *Nat. Sustain.*, vol. 5, no. 4, pp. 311–320, 2022, doi: 10.1038/s41893-021-00842-z.

[17] G. Myers, “Urbanisation in the Global South,” in *Urban Ecology in the Global South*, C. M. Shackleton, S. S. Cilliers, E. Davoren, and M. J. Du Toit, Eds., in Cities and Nature. , Cham: Springer International Publishing, 2021. doi: 10.1007/978-3-030-67650-6_2.

[18] G. Churkina *et al.*, “Buildings as a global carbon sink,” *Nat. Sustain.*, vol. 3, no. 4, pp. 269–276,

Apr. 2020, doi: 10.1038/s41893-019-0462-4.
[19] V. Göswein *et al.*, "Wood in buildings: the right answer to the wrong question," *IOP Conf. Ser. Earth Environ. Sci.*, vol. 1078, no. 1, p. 012067, Sep. 2022, doi: 10.1088/1755-1315/1078/1/012067.
[20] P. Nepal, C. M. T. Johnston, and I. Ganguly, "Effects on Global Forests and Wood Product Markets of Increased Demand for Mass Timber," *Sustainability*, vol. 13, no. 24, p. 13943, Dec. 2021, doi: 10.3390/su132413943.
[21] D. Safarik, J. Elbrecht, and W. Miranda, "State of Tall Timber 2022," *Counc. Tall Build. Urban Habitat J.*, 2022.
[22] A. Mishra *et al.*, "Land use change and carbon emissions of a transformation to timber cities," *Nat. Commun.*, vol. 13, no. 1, p. 4889, Aug. 2022, doi: 10.1038/s41467-022-32244-w.
[23] F. Pomponi, J. Hart, J. H. Arehart, and B. D'Amico, "Buildings as a Global Carbon Sink? A Reality Check on Feasibility Limits," *One Earth*, vol. 3, no. 2, pp. 157–161, 2020, doi: https://doi.org/10.1016/j.oneear.2020.07.018.
[24] S. Suffian, R. Dzombak, and K. Mehta, "Future directions for nonconventional and vernacular material research and applications," in *Nonconventional and Vernacular Construction Materials*, Elsevier, 2016, pp. 63–80. doi: 10.1016/B978-0-08-100038-0.00003-2.
[25] J.-C. Morel, R. Charef, E. Hamard, A. Fabbri, C. Beckett, and Q.-B. Bui, "Earth as construction material in the circular economy context: practitioner perspectives on barriers to overcome," *Philos. Trans. R. Soc. B Biol. Sci.*, vol. 376, no. 1834, p. 20200182, Sep. 2021, doi: 10.1098/rstb.2020.0182.
[26] J. Fernandes, R. Mateus, and L. Bragança, "The potential of vernacular materials to the sustainable building design," in *Vernacular Heritage and Earthen Architecture: contributions for sustainable development ; proceedings of CIAV 2013, 7th ATP, Versus, Vila Nova de Cerveira, Portugal, 16 - 20 October 2013*, M. Correia, Ed., Leiden: CRC Press, 2014.
[27] D. Gauzin-Müller and N. Favet, *Sustainable architecture and urbanism: concepts, technologies, examples*. Basel ; Boston: Birkhauser, 2002.
[28] D. Gauzin-Müller, "The Ecological Transition of Vorarlberg and Its Implementation in France," in *Bioregional Planning and Design: Volume II*, D. Fanfani and A. Matarán Ruiz, Eds., Cham: Springer International Publishing, 2020, pp. 141–155. doi: 10.1007/978-3-030-46083-9_8.
[29] S. Claude, S. Ginestet, M. Bonhomme, N. Moulène, and G. Escadeillas, "The Living Lab methodology for complex environments: Insights from the thermal refurbishment of a historical district in the city of Cahors, France," *Energy Res. Soc. Sci.*, vol. 32, pp. 121–130, Oct. 2017, doi: 10.1016/j.erss.2017.01.018.
[30] W. Schmidt, N. S. Msinjili, and H.-C. Kühne, "Materials and technology solutions to tackle the challenges in daily concrete construction for housing and infrastructure in sub-Saharan Africa," *Afr. J. Sci. Technol. Innov. Dev.*, vol. 11, no. 4, pp. 401–415, Jun. 2019, doi: 10.1080/20421338.2017.1380582.
[31] US EPA, "Emission Factor Documentation for AP-42, Section 11.6: Portland Cement Manufacturing.," 1994.
[32] S. Ortaboy *et al.*, "Effects of CO_2 and temperature on the structure and chemistry of C–(A–)S–H investigated by Raman spectroscopy," *RSC Adv*, vol. 7, no. 77, pp. 48925–48933, 2017, doi: 10.1039/C7RA07266J.
[33] P. K. Mehta and P. J. M. Monteiro, *Concrete microstructure, properties, and materials*. New York: Mc Graw Hill Education, 2014.
[34] B. Lothenbach, K. Scrivener, and R. D. Hooton, "Supplementary cementitious materials," *Cem. Concr. Res.*, vol. 41, no. 12, pp. 1244–1256, 2011, doi: http://dx.doi.org/10.1016/j.cemconres.2010.12.001.
[35] E. L'Hôpital, B. Lothenbach, K. Scrivener, and D. A. Kulik, "Alkali uptake in calcium alumina silicate hydrate (C-A-S-H)," *Cem. Concr. Res.*, vol. 85, pp. 122–136, Jul. 2016, doi: 10.1016/j.cemconres.2016.03.009.
[36] A. Kim, P. R. Cunningham, K. Kamau-Devers, and S. A. Miller, "OpenConcrete: a tool for estimating the environmental impacts from concrete production," *Environ. Res. Infrastruct. Sustain.*,

vol. 2, no. 4, p. 041001, Dec. 2022, doi: 10.1088/2634-4505/ac8a6d.
[37] GCCA, "The GCCA 2050 cement and concrete industry roadmap for net zero concrete," 2021.
[38] V. Chan, L. Tian, J. Shah, and J. Wagner, "Pathways to Commercial Liftoff: Low-Carbon Cement," 2023.
[39] P. R. Cunningham and S. A. Miller, "Quantitative Assessment of Alkali-Activated Materials: Environmental Impact and Property Assessments," *J. Infrastruct. Syst.*, vol. 26, no. 3, p. 04020021, 2020, doi: 10.1061/(asce)is.1943-555x.0000556.
[40] E. Gartner, "Industrially interesting approaches to 'low-CO2' cements," *Cem. Concr. Res.*, vol. 34, no. 9, pp. 1489–1498, Sep. 2004, doi: 10.1016/j.cemconres.2004.01.021.
[41] G. Habert *et al.*, "Environmental impacts and decarbonization strategies in the cement and concrete industries," *Nat. Rev. Earth Environ.*, 2020, doi: 10.1038/s43017-020-0093-3.
[42] J. L. Provis, "Alkali-activated materials," *Cem. Concr. Res.*, vol. 114, pp. 40–48, Dec. 2018, doi: 10.1016/j.cemconres.2017.02.009.
[43] G. J. G. Gluth *et al.*, "RILEM TC 247-DTA round robin test: carbonation and chloride penetration testing of alkali-activated concretes," *Mater. Struct.*, vol. 53, no. 1, p. 21, Feb. 2020, doi: 10.1617/s11527-020-1449-3.
[44] J. L. Provis *et al.*, "RILEM TC 247-DTA round robin test: mix design and reproducibility of compressive strength of alkali-activated concretes," *Mater. Struct.*, vol. 52, no. 5, p. 99, Oct. 2019, doi: 10.1617/s11527-019-1396-z.
[45] A. Komkova and G. Habert, "Environmental impact assessment of alkali-activated materials: Examining impacts of variability in constituent production processes and transportation," *Constr. Build. Mater.*, vol. 363, p. 129032, Jan. 2023, doi: 10.1016/j.conbuildmat.2022.129032.
[46] K. A. Knight, P. R. Cunningham, and S. A. Miller, "Optimizing supplementary cementitious material replacement to minimize the environmental impacts of concrete," *Cem. Concr. Compos.*, vol. 139, no. February, p. 105049, 2023, doi: 10.1016/j.cemconcomp.2023.105049.
[47] S. A. Miller, A. Horvath, and P. J. M. Monteiro, "Impacts of booming concrete production on water resources worldwide," *Nat. Sustain.*, vol. 1, no. 1, 2018, doi: 10.1038/s41893-017-0009-5.
[48] United Nations Environment Programme, "Global Mercury Assessment 2013: Sources, Emissions, Releases and Environmental Transport.," United Nations Environmental Programme, 2013.
[49] E. Nkhama *et al.*, "Effects of Airborne Particulate Matter on Respiratory Health in a Community near a Cement Factory in Chilanga, Zambia: Results from a Panel Study," *Int. J. Environ. Res. Public. Health*, vol. 14, no. 11, p. 1351, Nov. 2017, doi: 10.3390/ijerph14111351.
[50] P. Van den Heede and N. De Belie, "Environmental impact and life cycle assessment (LCA) of traditional and 'green' concretes: Literature review and theoretical calculations," *Cem. Concr. Compos.*, vol. 34, no. 4, pp. 431–442, 2012, doi: http://dx.doi.org/10.1016/j.cemconcomp.2012.01.004.
[51] R. Mearns and A. Norton, *Social dimensions of climate change: equity and vulnerability in a warming world*. World Bank, 2010. doi: 10.1596/978-0-8213-7887-8.
[52] US EPA, "Human and Ecological Risk Assessment of Coal Combustion Wastes," *Fed. Regist.*, vol. 84, no. 157, p. 409, 2014.
[53] US EPA, "Coal Combustion Residual Beneficial Use Evaluation: Fly Ash Concrete and FGD Gypsum Wallboard - EPA530-R-14-001 - Office of Solid Waste and Emergency Response - Office of Resource Conservation and Recovery," *U. S. Environ. Prot. Agency*, no. February, pp. 1–91, 2014.
[54] S. Sadati and J. Moore, "Final report: supplementary cementitious materials supply look-ahead," California Department of Transportation, 2021.
[55] A. Kunhi Mohamed *et al.*, "The Atomic-Level Structure of Cementitious Calcium Aluminate Silicate Hydrate," *J. Am. Chem. Soc.*, vol. 142, no. 25, pp. 11060–11071, Jun. 2020, doi: 10.1021/jacs.0c02988.
[56] The Portland Cement Association, "All 50 States Give Environmentally Conscious Cement the Green Light; Every state department of transportation and the District of Columbia now permit the use of portland-limestone cement," The Portland Cement Association. Accessed: Apr. 22, 2024.

[Online]. Available: https://www.cement.org/newsroom/2024/04/02/all-50-states-give-environmentally-conscious-cement-the-green-light
[57] A. M. Ramezanianpour and R. D. Hooton, "A study on hydration, compressive strength, and porosity of Portland-limestone cement mixes containing SCMs," *Cem. Concr. Compos.*, vol. 51, pp. 1–13, Aug. 2014, doi: 10.1016/j.cemconcomp.2014.03.006.
[58] ASTM, "C1697: Standard specification for blended hydraulic cements," *Annu. Book Am. Soc. Test. Mater. ASTM Stand.*, vol. 14, pp. 1–7, 2009, doi: 10.1520/C0595.
[59] S. Tsivilis, E. Chaniotakis, G. Kakali, and G. Batis, "An analysis of the properties of Portland limestone cements and concrete," *Cem. Concr. Compos.*, vol. 24, no. 3–4, pp. 371–378, 2002, doi: 10.1016/S0958-9465(01)00089-0.
[60] A. A. Ramezanianpour, E. Ghiasvand, I. Nickseresht, M. Mahdikhani, and F. Moodi, "Influence of various amounts of limestone powder on performance of Portland limestone cement concretes," *Cem. Concr. Compos.*, vol. 31, no. 10, pp. 715–720, 2009, doi: 10.1016/j.cemconcomp.2009.08.003.
[61] A. Marzouki, A. Lecomte, A. Beddey, C. Diliberto, and M. Ben Ouezdou, "The effects of grinding on the properties of Portland-limestone cement," *Constr. Build. Mater.*, vol. 48, pp. 1145–1155, 2013, doi: 10.1016/j.conbuildmat.2013.07.053.
[62] T. Hanein *et al.*, "Clay calcination technology: state-of-the-art review by the RILEM TC 282-CCL," *Mater. Struct.*, vol. 55, no. 1, p. 3, Jan. 2022, doi: 10.1617/s11527-021-01807-6.
[63] F. Zunino and K. Scrivener, "Reactivity of kaolinitic clays calcined in the 650 °C–1050 °C temperature range: Towards a robust assessment of overcalcination," *Cem. Concr. Compos.*, vol. 146, p. 105380, Feb. 2024, doi: 10.1016/j.cemconcomp.2023.105380.
[64] J. Sun, F. Zunino, and K. Scrivener, "Hydration and phase assemblage of limestone calcined clay cements (LC3) with clinker content below 50 %," *Cem. Concr. Res.*, vol. 177, p. 107417, Mar. 2024, doi: 10.1016/j.cemconres.2023.107417.
[65] ASTM, "C595 Standard Specification for Blended Hydraulic Cements," *ASTM Int.*.
[66] D. M. Martinez, A. Horvath, and P. J. M. Monteiro, "Comparative environmental assessment of limestone calcined clay cements and typical blended cements," *Environ. Res. Commun.*, vol. 5, no. 5, p. 055002, May 2023, doi: 10.1088/2515-7620/acccd8.
[67] Caltrans, "Fly Ash: current and future supply. A joint effort between concrete task group of the Caltrans rock products committee and industry," 2016.
[68] IEA, "Iron and Steel Technology Roadmap," Paris, France, 2020. doi: 10.1787/3dcc2a1b-en.
[69] I. H. Shah, S. A. Miller, D. Jiang, and R. J. Myers, "Cement substitution with secondary materials can reduce annual global CO2 emissions by up to 1.3 gigatons," *Nat. Commun.*, vol. 13, no. 1, p. 5758, Sep. 2022, doi: 10.1038/s41467-022-33289-7.
[70] W. Schmidt *et al.*, "Sustainable circular value chains: From rural waste to feasible urban construction materials solutions," *Dev. Built Environ.*, vol. 6, no. August 2020, p. 100047, 2021, doi: 10.1016/j.dibe.2021.100047.
[71] J. L. Bowyer, E. Pepke, K. Fernholz, C. Henderson, H. Groot, and G. Erickson, "Comparison of Environmental Impacts of Flooring Alternatives," 2019.
[72] P. R. Cunningham, P. G. Green, and S. A. Miller, "Utilization of post-consumer carpet calcium carbonate (PC4) from carpet recycling as a mineral resource in concrete," *Resour. Conserv. Recycl.*, vol. 169, Jun. 2021, doi: 10.1016/j.resconrec.2021.105496.
[73] V. Moody and H. L. Needles, *Tufted Carpet: Textile Fibers, Dyes, Finishes, and Processes*. Norwich, New York: William Anderson Publishing, 2004.
[74] Y. Wang, "Carpet Recycling Technologies," in *Recycling in textiles*, 2006, pp. 58–70.
[75] CalRecycle, "Carpet Stewardship Law: Introduction to California's Carpet Stewardship Law." [Online]. Available: https://www.calrecycle.ca.gov/Carpet/Law/
[76] M. Miraftab, "Recycling carpet materials," in *Advances in Carpet Manufacture*, K. K. Goswami, Ed., Cambridge, MA: Elsevier, 2018, pp. 65–77. doi: 10.1016/b978-0-08-101131-7.00005-8.
[77] M. J. Realff, J. C. Ammons, and D. J. Newton, "Robust reverse production system design for carpet recycling," *IIE Trans.*, vol. 36, no. 8, pp. 767–776, 2004, doi: 10.1080/07408170490458580.

[78] M. Miraftab, R. Horrocks, and C. Woods, “Carpet waste, an expensive luxury we must do without!,” *Autex Res. J.*, vol. 1, no. 1, pp. 1–7, 1999, doi: 10.1533/9780857092991.3.173.
[79] M. J. Realff, J. C. Ammons, and D. Newton, “Carpet recycling: Determining the reverse production system design,” *Polym.-Plast. Technol. Eng.*, vol. 38, no. 3, pp. 547–567, 1999, doi: 10.1080/03602559909351599.
[80] A. Stephan and A. Athanassiadis, “Towards a more circular construction sector: Estimating and spatialising current and future non-structural material replacement flows to maintain urban building stocks,” *Resour. Conserv. Recycl.*, vol. 129, no. November 2017, pp. 248–262, Feb. 2018, doi: 10.1016/j.resconrec.2017.09.022.
[81] California State Legislature, “California Public Resource Code, Chapter 20. Product Stewardship for Carpets [42970 - 42983] (Chapter 20 added by Stats. 2010, Ch. 681, Sec. 2.).” Accessed: Jan. 26, 2022. [Online]. Available: https://leginfo.legislature.ca.gov/faces/codes_displayText.xhtml?lawCode=PRC&division=30.&title=&part=3.&chapter=20.&article=
[82] Carpet America Recovery Effort, “Collector Finer Map.” Accessed: Jan. 26, 2022. [Online]. Available: https://carpetrecovery.org/recovery-effort/collector-finder-map/
[83] Carpet America Recovery Effort, “California Drop-off Site Map.” Accessed: Jan. 26, 2022. [Online]. Available: https://carpetrecovery.org/california/ca/
[84] S. Jordan, *HF 1426: Carpet Stewardship Program Establishment; Producer Participation Required*. State of Minnesota House of Representatives, 2021. Accessed: Jan. 26, 2022. [Online]. Available: https://www.revisor.mn.gov/bills/text.php?number=HF1426&type=bill&version=0&session=ls92&session_year=2021&session_number=0
[85] B. Kavanagh, *S5027A: An act to amend the environmental conservation law and the state finance law, in relation to establishing a carpet stewardship program*. New York: The New York State Senate, 2022. Accessed: Jan. 26, 2022. [Online]. Available: https://www.nysenate.gov/legislation/bills/2021/s5027/amendment/a
[86] M. Bush, *SB0345: Carpet Stewardship Act*. Illinois General Assembly, 2021. Accessed: Jan. 26, 2022. [Online]. Available: https://www.ilga.gov/legislation/BillStatus.asp?DocNum=345&GAID=16&DocTypeID=SB&SessionID=110&GA=102
[87] M. Wilde, *House Bill 3271: Relating to carpet; prescribing an effective date*. Oregon: 81st Oregon Legislative Assembly, 2021. [Online]. Available: https://olis.oregonlegislature.gov/liz/2021R1/Downloads/MeasureDocument/HB3271
[88] K. Chu, *AB-1158 Carpet recycling*. California State Assembly, 2018. Accessed: Jan. 26, 2022. [Online]. Available: https://leginfo.legislature.ca.gov/faces/billTextClient.xhtml?bill_id=201720180AB1158
[89] S. J. McNeil, M. R. Sunderland, and L. I. Zaitseva, “Closed-loop wool carpet recycling,” *Resour. Conserv. Recycl.*, vol. 51, no. 1, pp. 220–224, 2007, doi: 10.1016/j.resconrec.2006.09.006.
[90] R. Peoples, “Carpet stewardship in the united states - a commitment to sustainability,” *Recycl. Text. Vol. Woodhead Publ. Ser. Text.*, pp. 38–45, 2006, doi: 10.1533/9781845691424.1.38.
[91] S. Watson, “Environmentally Responsible Carpet Choices,” *Journal of Family and Consumer Sciences*, vol. 97. pp. 27–35, 2005.
[92] B. K. Fishbein, “Carpet take-back: EPR American style,” *Environ. Qual. Manag.*, vol. 10, no. 1, pp. 25–36, 2000, doi: 10.1002/1520-6483(200023)10:1<25::AID-TQEM4>3.0.CO;2-4.
[93] D. Lu, M. Overcash, and M. J. Realff, “A mathematical programming tool for LCI-based product design and case study for a carpet product,” *J. Clean. Prod.*, vol. 19, no. 12, pp. 1347–1355, 2011, doi: 10.1016/j.jclepro.2011.04.004.
[94] J. Morris, “Environmental Impacts From Carpet Discards Management Methods: Preliminary Results (Corrected),” 2010.
[95] US EPA, “Background Document for Life-cycle Greenhouse Gas Emission Factors for Fly Ash Used as a Cement Replacement in Concrete,” United States Environmental Protection Agency, 2003.

[96] J. Sim and V. Prabhu, “The life cycle assessment of energy and carbon emissions on wool and nylon carpets in the United States,” *J. Clean. Prod.*, vol. 170, pp. 1231–1243, 2018, doi: 10.1016/j.jclepro.2017.09.203.
[97] Y. Li, “Life Cycle Assessment of Chemical Processes and Products,” North Carolina State University, 2007.
[98] A. Sotayo, S. Green, and G. Turvey, “Carpet recycling: A review of recycled carpets for structural composites,” *Environ. Technol. Innov.*, vol. 3, pp. 97–107, 2015, doi: 10.1016/j.eti.2015.02.004.
[99] P. Lemieux, E. Stewart, M. Realff, and J. A. Mulholland, “Emissions study of co-firing waste carpet in a rotary kiln,” *J. Environ. Manage.*, vol. 70, no. 1, pp. 27–33, 2004, doi: 10.1016/j.jenvman.2003.10.002.
[100] UK Environment Agency, “Guidance: Using shredded waste carpet in equestrian surfacing: RPS 248.”
[101] C. Mihut, D. K. Captain, F. Gadala-Maria, and M. D. Amiridis, “Review: Recycling of nylon from carpet waste,” *Polym. Eng. Sci.*, vol. 41, no. 9, pp. 1457–1470, 2001, doi: 10.1002/pen.10845.
[102] F. Matejcek, “Thermoplastic fibre carpet waste recovery - effected by shredding waste into pieces laying in layers , heating above m.pt ., pressing and cooling,” 1977
[103] Y. Wang, H. C. Wu, and V. C. Li, “Concrete Reinforcement with Recycled Fibers,” *J. Mater. Civ. Eng.*, vol. 12, no. 4, pp. 314–319, Nov. 2000, doi: 10.1061/(ASCE)0899-1561(2000)12:4(314).
[104] A. Rahimi and J. M. García, “Chemical recycling of waste plastics for new materials production,” *Nat. Rev. Chem.*, vol. 1, p. 46, 2017, doi: 10.1038/s41570-017-0046.
[105] K. A. Thoney, I. Sas, J. A. Joines, and R. E. King, “Logistics of carpet recycling in the U.S.: designing the recycling network,” *J. Text. Inst.*, vol. 111, no. 12, pp. 1724–1734, 2020, doi: 10.1080/00405000.2020.1723257.
[106] A. Jain, G. Pandey, A. K. SINGH, V. Rajagopalan, R. Vaidyanathan, and R. P. Singh, “Fabrication of structural composites from waste carpet,” *Adv. Polym. Technol.*, vol. 31, no. 4, pp. 380–389, Dec. 2012, doi: 10.1002/adv.20261.
[107] M. Biehl, E. Prater, and M. J. Realff, “Assessing performance and uncertainty in developing carpet reverse logistics systems,” *Comput. Oper. Res.*, vol. 34, no. 2, pp. 443–463, 2007, doi: 10.1016/j.cor.2005.03.008.
[108] I. Sas, J. A. Joines, K. A. Thoney, and R. E. King, “Logistics of carpet recycling in the U.S.: designing the collection network,” *J. Text. Inst.*, vol. 110, no. 3, pp. 328–337, 2019, doi: 10.1080/00405000.2018.1480101.
[109] R. W. Kirk, *The carpet industry; present status and future prospects*. Philadelphia, Pennsylvania: Industrial Research Unit, Department of Industry Wharton School of Fiance and Commerce University of Pennsylvania, 1970.
[110] K. Swift and E. Sanchez, “The U.S. Carpet Industry: History, Industry Dynamics, and a Simple Model for Short-Term Forecasting,” *Bus. Econ.*, vol. 52, no. 1, pp. 57–67, Jan. 2017, doi: 10.1057/s11369-017-0023-7.
[111] U.S. Census Bureau, “Current Industrial Reports Series: Rugs, Carpet, and Carpeting 1968-1985, MQ-22Q(68-85),” United States Department of Commerce, Washington D.C., 1986. Accessed: Mar. 05, 2021. [Online]. Available: https://hdl.handle.net/2027/pst.000031323284
[112] U.S. Census Bureau, “USA Trade Online (UTO) Database Import and Export Data for HS-Codes: 5703100000, 5703200000, 5703300000, & 5703900000,” *USA Trade Online Database*. 2020.
[113] M. Realff, “The role of using carpet as a fuel in carpet recovery system development,” 2014.
[114] S. Junnila, A. Horvath, and A. A. Guggemos, “Life-cycle assessment of office buildings in Europe and the United States,” *J. Infrastruct. Syst.*, vol. 12, no. 1, pp. 10–17, Mar. 2006, doi: 10.1061/(ASCE)1076-0342(2006)12:1(10).
[115] David. R. Outhred, “Reserves for Replacement in Apartment Properties,” *Apprais. J.*, vol. 63, no. 1, pp. 69–80, Jan. 1995.
[116] D. Seiders *et al.*, *NAHB / Bank of America Home Equity Study of Life Expectancy of Home Components*. Washington D.C.: National Association of Home Builders (NAHB), 2007.

[117] Carpet America Recovery Effort, "CARE 2019 Annual Report," Dalton, Georgia, 2020.
[118] US EPA, "Durable Goods: Product-Specific Data - Carpet and Rugs," Facts and Figures about Materials, Waste and Recycling. Accessed: Feb. 24, 2022. [Online]. Available: https://www.epa.gov/facts-and-figures-about-materials-waste-and-recycling/durable-goods-product-specific-data#CarpetsandRugs
[119] K. C. Curry and H. G. van Oss, "2017 Minerals Yearbook: Cement," Reston, VA, 2020.
[120] National Renewable Energy Laboratory, "U.S. Life Cycle Inventory Database." [Online]. Available: https://www.lcacommons.gov/nrel/search
[121] Franklin Associates, "Cradle-to-gate life cycle inventory of nine plastic resins and four polyurethane precursors," *Report*, vol. 1, no. 1, p. 572, 2010.
[122] M. L. Marceau, M. A. Nisbet, and M. G. Vangeem, "Life cycle inventory of Portland cement manufacture," 2010.
[123] G. Wernet, C. Bauer, B. Steubing, J. Reinhard, E. Moreno-Ruiz, and B. Weidema, "The ecoinvent database version 3 (part I): overview and methodology," *Int. J. Life Cycle Assess.*, vol. 21, no. 9, pp. 1218–1230, Sep. 2016, doi: 10.1007/s11367-016-1087-8.
[124] H. R., "Life Cycle Inventories of Packaging and Graphical Paper," *Final Rep. Ecoinvent Data V2 0*, vol. No 11, 2007.
[125] J. Bare, "Tool for the Reduction and Assessment of Chemical and Other Environmental Impacts (TRACI) version 2.1," *US Environ. Prot. Agency*, vol. 600/R–12/5, no. August, p. 24, 2012.
[126] Joelle Michaels, "A Look at the U.S. Commercial Building Stock: Results from EIA's 2012 Commercial Buildings Energy Consumption Survey (CBECS)," US EPA 2012 Commercial Buildings Energy Consumption Survey.
[127] M. C. P. Moura, S. J. Smith, and D. B. Belzer, "120 years of U.S. Residential housing stock and floor space," *PLoS ONE*, vol. 10, no. 8, Aug. 2015, doi: 10.1371/journal.pone.0134135.
[128] Carpet America Recovery Effort, "CARE 2012 Annual Report," Dalton, Georgia, 2013. Accessed: Apr. 22, 2020. [Online]. Available: https://carpetrecovery.org/resources/annual-reports/
[129] J. Wright and A. Culick, "Recycled Polyethylene Terephthalate (PET) Carpet (RPC) pilot studies of Civil Engineering Applications," GHD Group, Santa Rosa, CA, Aug. 2019.
[130] USGS, "Cement, advance data release of the 2019 annual tables," US Geological Survey, Reston, VA, 2019.
[131] M. L. Marceau, M. A. Nisbet, M. G. VanGeem, and Portland Cement Association, "Life Cycle inventory of Portland cement concrete," Portland Cement Association, Skokie, Illinois, 2007.
[132] USGS, "Stone (Crushed) - Advance Data Release of 2022 Annual Tables," US Geological Survey, Reston, VA, 2024. Accessed: May 16, 2024. [Online]. Available: https://d9-wret.s3.us-west-2.amazonaws.com/assets/palladium/production/s3fs-public/media/files/myb1-2022-stonec-ert.xlsx
[133] Carpet America Recovery Effort, "CARE California Carpet Stewardship Program 2022 Annual Report," Dalton, Georgia, 2023.
[134] U.S. Department of Transportation, Bureau of Transportation Statistics, "National Transportation Statistics Table 3-21: Average Freight Revenue per Ton-Mile." 2023. [Online]. Available: https://www.bts.gov/content/average-freight-revenue-ton-mile
[135] A. Horvath, "Construction Materials and the Environment," *Annu. Rev. Environ. Resour.*, vol. 29, no. 1, pp. 181–204, Nov. 2004, doi: 10.1146/annurev.energy.29.062403.102215.
[136] H. M. Breunig, T. Huntington, L. Jin, A. Robinson, and C. D. Scown, "Dynamic Geospatial Modeling of the Building Stock To Project Urban Energy Demand," *Environ. Sci. Technol.*, vol. 52, no. 14, pp. 7604–7613, Jul. 2018, doi: 10.1021/acs.est.8b00435.
[137] International Energy Agency, "Energy Technology Perspectives 2017: Catalysing Energy Technology Transformations," IEA, Paris, France, 2017.
[138] American Iron and Steel Institute, "American Iron and Steel Institute: Profile 2014," 2014.
[139] E. L. Bray, "2014 Minerals yearbook: Bauxite and Alumina," US Geological Survey, 2016.
[140] PlasticsEurope, "Use of Plastics: Buildings and Construction." Accessed: Feb. 04, 2012. [Online]. Available: http://www.plasticseurope.org/use-of-plastics/building-construction.aspx

[141] A. Kapur, G. Keoleian, A. Kendall, and S. E. Kesler, “Dynamic Modeling of In-Use Cement Stocks in the United States,” *J. Ind. Ecol.*, vol. 12, no. 4, pp. 539–556, Aug. 2008, doi: 10.1111/j.1530-9290.2008.00055.x.
[142] P. J. M. Monteiro, S. A. Miller, and A. Horvath, “Towards sustainable concrete,” *Nat. Mater.*, vol. 16, no. 7, pp. 698–699, Jul. 2017, doi: 10.1038/nmat4930.
[143] C. Scheuer, G. A. Keoleian, and P. Reppe, “Life cycle energy and environmental performance of a new university building : modeling challenges and design implications,” *Energy Build.*, vol. 35, no. 10, pp. 1049–1064, Nov. 2003, doi: 10.1016/S0378-7788(03)00066-5.
[144] H. G. van Oss, “Mineral Commodity Summaries: Cement,” US Geological Survey, 2019.
[145] F. Xi *et al.*, “Substantial global carbon uptake by cement carbonation,” *Nat. Geosci.*, vol. 9, no. 12, pp. 880–883, 2016, doi: 10.1038/ngeo2840.
[146] ERMCO, “Ready-mixed concrete industry statistics 2015.,” European Ready-mixed Concrete Organization, Brussels, Belgium, 2016.
[147] Carpet America Recovery Effort, “CARE 2017 Annual Report,” Dalton, Georgia, 2018. Accessed: Apr. 22, 2020. [Online]. Available: https://carpetrecovery.org/resources/annual-reports/
[148] P. K. Mehta and P. J. M. Monteiro, *Concrete : microstructure, properties, and materials*. New York: McGraw-Hill, 2006.
[149] A. R. Khaloo, M. Dehestani, and P. Rahmatabadi, “Mechanical properties of concrete containing a high volume of tire–rubber particles,” *Waste Manag.*, vol. 28, no. 12, pp. 2472–2482, Dec. 2008, doi: 10.1016/j.wasman.2008.01.015.
[150] M. Limbachiya, M. S. Meddah, and S. Fotiadou, “Performance of granulated foam glass concrete,” *Constr. Build. Mater.*, vol. 28, no. 1, pp. 759–768, Mar. 2012, doi: 10.1016/j.conbuildmat.2011.10.052.
[151] S. Subaşı, H. Öztürk, and M. Emiroğlu, “Utilizing of waste ceramic powders as filler material in self-consolidating concrete,” *Constr. Build. Mater.*, vol. 149, pp. 567–574, Sep. 2017, doi: 10.1016/j.conbuildmat.2017.05.180.
[152] P. Torkittikul and A. Chaipanich, “Utilization of ceramic waste as fine aggregate within Portland cement and fly ash concretes,” *Cem. Concr. Compos.*, vol. 32, no. 6, pp. 440–449, Jul. 2010, doi: 10.1016/j.cemconcomp.2010.02.004.
[153] I. B. Topçu, T. Bilir, and T. Uygunoğlu, “Effect of waste marble dust content as filler on properties of self-compacting concrete,” *Constr. Build. Mater.*, vol. 23, no. 5, pp. 1947–1953, 2009, doi: 10.1016/j.conbuildmat.2008.09.007.
[154] H. Schmidt and M. Cieślak, “Concrete with carpet recyclates: Suitability assessment by surface energy evaluation,” *Waste Manag.*, vol. 28, no. 7, pp. 1182–1187, Jan. 2008, doi: 10.1016/j.wasman.2007.05.005.
[155] P. D. Tennis, M. D. A. Thomas, and W. J. Weiss, “State-of-the-art report on use of limestone in cements at levels of up to 15%,” Portland Cement Association, Skokie, Illinois, 2011.
[156] V. M. John, B. L. Damineli, M. Quattrone, and R. G. Pileggi, “Fillers in cementitious materials — Experience, recent advances and future potential,” *Cem. Concr. Res.*, vol. 114, pp. 65–78, 2018, doi: 10.1016/j.cemconres.2017.09.013.
[157] O. Esping, “Effect of limestone filler BET(H2O)-area on the fresh and hardened properties of self-compacting concrete,” *Cem. Concr. Res.*, vol. 38, no. 7, pp. 938–944, Jul. 2008, doi: 10.1016/j.cemconres.2008.03.010.
[158] ASTM, “C143/C143M - 15a: Standard Test Method for Slump of Hydraulic-Cement Concrete.” ASTM International, West Conshohoken, Pennsylvania, 2015.
[159] ASTM, “C231/C231M: Standard Test Method for Air Content of Freshly Mixed Concrete by the Pressure Method.” 2010.
[160] ASTM, “C138/C138M - 17a: Standard Test Method for Density (Unit Weight), Yield, and Air Content (Gravimetric) of Concrete.” ASTM International, West Conshohoken, Pennsylvania, 2017.
[161] ASTM, “C403/C403M - 16: Standard Test Method for Time of Setting of Concrete Mixtures by Penetration Resistance.” ASTM International, West Conshohoken, Pennsylvania, 2016.

[162] M. Ghrici, S. Kenai, and M. Said-Mansour, “Mechanical properties and durability of mortar and concrete containing natural pozzolana and limestone blended cements,” *Cem. Concr. Compos.*, vol. 29, no. 7, pp. 542–549, Aug. 2007, doi: 10.1016/j.cemconcomp.2007.04.009.
[163] ASTM, “C39/C39M - 17a: Standard Test Method for Compressive Strength of Cylindrical Concrete Specimens.” ASTM International, West Conshohoken, Pennsylvania, 2017.
[164] ASTM, “C293/C293M - 16: Standard Test Method for Flexural Strength of Concrete (Using Simple Beam With Center-Point Loading),” 2016.
[165] T. Uygunoğlu and İ. B. Topçu, “Thermal expansion of self-consolidating normal and lightweight aggregate concrete at elevated temperature,” *Constr. Build. Mater.*, vol. 23, no. 9, pp. 3063–3069, Sep. 2009, doi: 10.1016/j.conbuildmat.2009.04.004.
[166] American Association of State Highways and Transportation Officials (AASHTO), “T336-15 - Standard Method of Test for Coefficient of Thermal Expansion of Hydraulic Cement Concrete.” Washington, D.C., 2015.
[167] ASTM, “C157/C157M - 17: Standard Test Method for Length Change of Hardened Hydraulic-Cement Mortar and Concrete.” ASTM International, West Conshohoken, Pennsylvania, 2017.
[168] ASTM, “C642-13: Standard Test Method for Density, Absorption, and Voids in Hardened Concrete.” ASTM International, West Conshohoken, Pennsylvania, 2013.
[169] A. P. Gursel and A. Horvath, “GreenConcrete LCA Webtool.” Accessed: Oct. 02, 2020. [Online]. Available: http://greenconcrete.berkeley.edu/concretewebtool.html
[170] California Energy Commission, “2018 Total System Electric Generation.” 2019. Accessed: Oct. 01, 2020. [Online]. Available: https://www.energy.ca.gov/data-reports/energy-almanac/california-electricity-data/2019-total-system-electric-generation/2018
[171] California Air Resources Board, “GHG Current California Emissions Inventory Data: Full Inventory Fuel Combustion Data.” 2019. Accessed: Oct. 01, 2020. [Online]. Available: https://ww3.arb.ca.gov/cc/inventory/data/tables/fuel_activity_inventory_by_sector_all_00-17.xlsx
[172] M. L. Marceau, M. A. Nisbet, M. G. VanGeem, and Portland Cement Association, “Life cycle inventory of Portland cement manufacture,” Portland Cement Association, Skokie, Illinois, 2006.
[173] R. P. Brentin, “Latex coating systems for carpet backing,” *J. Coat. Fabr.*, vol. 12, no. 2, pp. 82–91, 1982, doi: 10.1177/152808378201200202.
[174] M. J. Realff, “Carpet As An Alternative Fuel in Cement Kilns,” Georgia Tech Research Corporation, 2007.
[175] K. De Weerdt, M. B. Haha, G. Le Saout, K. O. Kjellsen, H. Justnes, and B. Lothenbach, “Hydration mechanisms of ternary Portland cements containing limestone powder and fly ash,” *Cem. Concr. Res.*, vol. 41, no. 3, pp. 279–291, Mar. 2011, doi: 10.1016/j.cemconres.2010.11.014.
[176] P. Thongsanitgarn, W. Wongkeo, A. Chaipanich, and C. S. Poon, “Heat of hydration of Portland high-calcium fly ash cement incorporating limestone powder: Effect of limestone particle size,” *Constr. Build. Mater.*, vol. 66, pp. 410–417, Sep. 2014, doi: 10.1016/j.conbuildmat.2014.05.060.
[177] D. Wang, C. Shi, N. Farzadnia, Z. Shi, and H. Jia, “A review on effects of limestone powder on the properties of concrete,” *Constr. Build. Mater.*, vol. 192, pp. 153–166, 2018, doi: 10.1016/j.conbuildmat.2018.10.119.
[178] R. Wang and P. Wang, “Function of styrene-acrylic ester copolymer latex in cement mortar,” *Mater. Struct.*, vol. 43, no. 4, pp. 443–451, May 2010, doi: 10.1617/s11527-009-9501-3.
[179] S. Kenai, W. Soboyejo, and A. Soboyejo, “Some Engineering Properties of Limestone Concrete,” *Mater. Manuf. Process.*, vol. 19, no. 5, pp. 949–961, Oct. 2004, doi: 10.1081/AMP-200030668.
[180] P. G. Green, L. Wong, and T. M. Young, “Executive Summary: ‘Trace organic compounds in Furnace-Treated PC4,’” Department of Civil and Environmental Engineering; University of California, Davis, Davis, CA, 2019.
[181] ASTM, “C109/C109M: Standard test method for compressive strength of hydraulic cement mortars (using 2-in . or [50-mm] cube specimens),” *ASTM Int.*, vol. 04, no. C109/C109M – 11b, pp. 1–9, 2010, doi: 10.1520/C0109.
[182] J. M. Valverde, A. Perejon, S. Medina, and L. A. Perez-Maqueda, “Thermal decomposition of

dolomite under CO2: Insights from TGA and in situ XRD analysis," *Phys. Chem. Chem. Phys.*, vol. 17, no. 44, pp. 30162–30176, 2015, doi: 10.1039/c5cp05596b.
[183] R. M. McIntosh, J. H. Sharp, and F. W. Wilburn, "The thermal decomposition of Dolomite," *Thermochim. Acta*, vol. 165, pp. 281–296, 1990.
[184] S. Zarghami, E. Ghadirian, H. Arastoopour, and J. Abbasian, "Effect of Steam on Partial Decomposition of Dolomite," *Ind. Eng. Chem. Res.*, vol. 54, no. 20, pp. 5398–5406, 2015, doi: 10.1021/acs.iecr.5b00049.
[185] G. Spinolo and U. Anselmi-Tamburini, "Nonequilibrium (Ca,Mg)O solid solutions produced by chemical decomposition," *J. Phys. Chem.*, vol. 93, no. 18, pp. 6837–6843, 1989, doi: 10.1021/j100355a052.
[186] B. Chiaia, A. P. Fantilli, and G. Ventura, "A chemo-mechanical model of lime hydration in concrete structures," *Constr. Build. Mater.*, vol. 29, pp. 308–315, 2012, doi: 10.1016/j.conbuildmat.2011.10.013.
[187] H. Shi, Y. Zhao, and W. Li, "Effects of temperature on the hydration characteristics of free lime," *Cem. Concr. Res.*, vol. 32, no. 5, pp. 789–793, 2002, doi: 10.1016/S0008-8846(02)00714-7.
[188] D. E. Giles, I. M. Ritchie, and B. A. Xu, "The kinetics of dissolution of slaked lime," *Hydrometallurgy*, vol. 32, no. 1, pp. 119–128, 1993, doi: 10.1016/0304-386X(93)90061-H.
[189] M. Fourmentin *et al.*, "Porous structure and mechanical strength of cement-lime pastes during setting," *Cem. Concr. Res.*, vol. 77, pp. 1–8, 2015, doi: 10.1016/j.cemconres.2015.06.009.
[190] IEA, "Data and Statistics." Accessed: Oct. 17, 2020. [Online]. Available: https://www.iea.org/data-and-statistics?country=WORLD&fuel=Electricityandheat&indicator=Electricitygenerationbysource
[191] H. G. van Oss and USGS, "Minerals yearbook: cement," Bureau of Mines, 2012.
[192] H. G. van Oss and USGS, "Mineral Commodity Summaries: Cement," US Geological Survey, 2016.
[193] California Energy Commission, "California Biomass and Waste-To-Energy Statistics and Data." Accessed: Jun. 15, 2020. [Online]. Available: https://ww2.energy.ca.gov/almanac/renewables_data/biomass/index_cms.php
[194] N. Kumar, K. Kupwade-Patil, R. Higuchi, D. P. Ferrell, V. A. Luttrull, and J. G. Lynam, "Use of Biomass Ash for Development of Engineered Cementitious Binders," *ACS Sustain. Chem. Eng.*, vol. 6, no. 10, pp. 13122–13130, 2018, doi: 10.1021/acssuschemeng.8b02657.
[195] International Energy Agency, *Energy Technology Transitions for Industry*. Paris: International Energy Agency, 2009. doi: 10.1787/9789264068612-en.
[196] State of California Department of Finance, "Projections: Population Projections (Baseline 2016)."
[197] California Energy Commission, "Electricity Consumption by County." Accessed: Jun. 25, 2020. [Online]. Available: http://www.ecdms.energy.ca.gov/elecbycounty.aspx
[198] USDA, "National Agriculture Statistics Service, 16 July 2012.US Department of Agriculture," United States Department of Agriculture, 2012.
[199] B. M. Jenkins, L. L. Baxter, T. R. Miles, and T. R. Miles, "Combustion properties of biomass," *Fuel Process. Technol.*, vol. 54, no. 1–3, pp. 17–46, 1998, doi: 10.1016/S0378-3820(97)00059-3.
[200] J. Singh, N. Singhal, S. Singhal, M. Sharma, S. Agarwal, and S. Arora, "Environmental Implications of Rice and Wheat Stubble Burning in North-Western States of India," in *Advances in Health and Environment Safety*, N. A. Siddiqui, S. M. Tauseef, and K. Bansal, Eds., Singapore: Springer Singapore, 2018, pp. 47–55. doi: 10.1007/978-981-10-7122-5_6.
[201] G. Wang, L. Shen, and C. Sheng, "Characterization of biomass ashes from power plants firing agricultural residues," *Energy Fuels*, vol. 26, no. 1, pp. 102–111, 2012, doi: 10.1021/ef201134m.
[202] H. G. van Oss, "Minerals yearbook: cement 2012," US Geological Survey, Reston, VA, 2015.
[203] G. H. van Oss, *Minerals Yearbook: Cement 2015*. US Geological Survey, 2018.
[204] World Bank, "Energy use (kg of oil equivalent per capita)." [Online]. Available: http://data.worldbank.org/
[205] USGS, *Mineral commodity summaries 2020*, no. 703. 2020.
[206] Z. Cao *et al.*, "The sponge effect and carbon emission mitigation potentials of the global cement

cycle," *Nat. Commun.*, vol. 11, no. 1, pp. 1–9, 2020, doi: 10.1038/s41467-020-17583-w.
[207] GCCA, "Getting the numbers right project: emissions report 2019," London, UK, 2019.
[208] ACAA, "Coal ash recycling reaches record 64 percent amid shifting production and use patterns," Washington D.C., 2018.
[209] S. A. Miller, P. R. Cunningham, and J. T. Harvey, "Rice-based ash in concrete: A review of past work and potential environmental sustainability," *Resour. Conserv. Recycl.*, vol. 146, pp. 416–430, Jul. 2019, doi: 10.1016/j.resconrec.2019.03.041.
[210] R. Snellings, "Assessing, understanding and unlocking supplementary cementitious materials," *RILEM Tech. Lett.*, vol. 1, p. 50, Aug. 2016, doi: 10.21809/rilemtechlett.2016.12.
[211] R. Rajamma, R. J. Ball, L. A. C. Tarelho, G. C. Allen, J. A. Labrincha, and V. M. Ferreira, "Characterisation and use of biomass fly ash in cement-based materials," *J. Hazard. Mater.*, vol. 172, no. 2–3, pp. 1049–1060, Dec. 2009, doi: 10.1016/j.jhazmat.2009.07.109.
[212] C. Shi, Y. Wu, C. Riefler, and H. Wang, "Characteristics and pozzolanic reactivity of glass powders," *Cem. Concr. Res.*, vol. 35, no. 5, pp. 987–993, May 2005, doi: 10.1016/j.cemconres.2004.05.015.
[213] J. Péra, S. Husson, and B. Guilhot, "Influence of finely ground limestone on cement hydration," *Cem. Concr. Compos.*, vol. 21, no. 2, pp. 99–105, Apr. 1999, doi: 10.1016/S0958-9465(98)00020-1.
[214] E. Batuecas, F. Liendo, T. Tommasi, S. Bensaid, F. A. Deorsola, and D. Fino, "Recycling CO2 from flue gas for CaCO3 nanoparticles production as cement filler: A Life Cycle Assessment," *J. CO2 Util.*, vol. 45, p. 101446, 2021, doi: https://doi.org/10.1016/j.jcou.2021.101446.
[215] S. Monkman and M. MacDonald, "On carbon dioxide utilization as a means to improve the sustainability of ready-mixed concrete," *J. Clean. Prod.*, vol. 167, pp. 365–375, 2017, doi: 10.1016/j.jclepro.2017.08.194.
[216] D. Zeng *et al.*, "Rational design of high-yield and superior-quality rice," *Nat. Plants*, vol. 3, no. March, pp. 4–8, 2017, doi: 10.1038/nplants.2017.31.
[217] F. Wu, Y. Wang, Y. Liu, Y. Liu, and Y. Zhang, "Simulated responses of global rice trade to variations in yield under climate change: Evidence from main rice-producing countries," *J. Clean. Prod.*, vol. 281, p. 124690, Jan. 2021, doi: 10.1016/j.jclepro.2020.124690.
[218] N. Childs, "USDA rice yearbook," USDA Economic Research Service. Accessed: Jan. 30, 2024. [Online]. Available: https://www.ers.usda.gov/data-products/rice-yearbook/
[219] USDA, "Rice, 2021 rough production," Market and Trade Data: Production, Supply, and Distribution. [Online]. Available: https://apps.fas.usda.gov/psdonline/app/index.html#/app/home
[220] USGS, "Cement 2021 tables - only release," US Geological Survey, Reston, VA, 2021. [Online]. Available: https://d9-wret.s3.us-west-2.amazonaws.com/assets/palladium/production/s3fs-public/media/files/myb1-2021-cemen-ert.xlsx
[221] R. Singh and M. Patel, "Effective utilization of rice straw in value-added by-products: A systematic review of state of art and future perspectives," *Biomass Bioenergy*, vol. 159, p. 106411, Apr. 2022, doi: 10.1016/j.biombioe.2022.106411.
[222] K. L. Kadam, L. H. Forrest, and W. A. Jacobson, "Rice straw as a lignocellulosic resource: collection, processing, transportation, and environmental aspects," *Biomass Bioenergy*, vol. 18, no. 5, pp. 369–389, May 2000, doi: 10.1016/S0961-9534(00)00005-2.
[223] G. A. Nader and P. H. Robinson, "Rice producers' guide to marketing rice straw," *Publication 8425*. University of California Agriculture and Natural Resources, 2010.
[224] L. F. Calvo, M. Otero, B. M. Jenkins, A. Morán, and A. I. García, "Heating process characteristics and kinetics of rice straw in different atmospheres," *Fuel Process. Technol.*, vol. 85, no. 4, pp. 279–291, Mar. 2004, doi: 10.1016/S0378-3820(03)00202-9.
[225] USDA, "U.S. rice acreage, production, and yield," Rice Yearbook. Accessed: Dec. 01, 2023. [Online]. Available: https://www.ers.usda.gov/data-products/rice-yearbook/rice-yearbook/#U.S. Acreage, Production, Yield, and Farm Price
[226] ECN TNO, "Phyllis2, database for (treated) biomass, algae, feedstocks for biogas production and biochar." [Online]. Available: https://phyllis.nl/
[227] A. Hatfield, "Mineral commodity summaries: cement," US Geological Survey, Reston, VA, 2021.

[228] S. Kumar Das, A. Adediran, C. Rodrigue Kaze, S. Mohammed Mustakim, and N. Leklou, "Production, characteristics, and utilization of rice husk ash in alkali activated materials: An overview of fresh and hardened state properties," *Constr. Build. Mater.*, vol. 345, p. 128341, Aug. 2022, doi: 10.1016/j.conbuildmat.2022.128341.
[229] A. N. A. Shakri, K. F. Kasim, and I. B. Rukunudin, "Chemical compositions and physical properties of selected Malaysian rice: A review," *IOP Conf. Ser. Earth Environ. Sci.*, vol. 765, no. 1, p. 012024, May 2021, doi: 10.1088/1755-1315/765/1/012024.
[230] "Anatomy of rice," Riceland Foods. Accessed: Dec. 01, 2023. [Online]. Available: https://www.riceland.com/anatomy-of-rice
[231] T. W. White and F. G. Hembry, "Rice by-products in ruminant rations," *Bulletin No. 771*. Louisiana Agricultural Experiment Station, 1985. [Online]. Available: https://repository.lsu.edu/%0Aagexp/847
[232] US EPA, "Power profiler," eGrid summary tables. [Online]. Available: https://www.epa.gov/egrid/power-profiler#/
[233] US EPA, "Arkansas greenhouse gas emissions from the industrial sector, by category, 2021," Greenhouse Gas Inventory Data Explorer. Accessed: Jan. 27, 2024. [Online]. Available: https://cfpub.epa.gov/ghgdata/inventoryexplorer/#industry/entiresector/allgas/category/current
[234] Caltrans, "Cementitious materials for use in concrete." Accessed: Feb. 22, 2024. [Online]. Available: https://mets.dot.ca.gov/aml/CementitiousList.php
[235] US EPA, "2011-2021 Greenhouse gas reporting program industrial profile: minerals," 2021. [Online]. Available: https://www.epa.gov/ghgreporting/ghgrp-minerals-sector-profile
[236] H. Meryman, "The Emergence of Rice Husk Ash — A Complimentary Cementing Material with Untapped Global Potential," in *Structures Congress 2009*, Austin, Texas, United States: American Society of Civil Engineers, Apr. 2009, pp. 1–10. doi: 10.1061/41031(341)274.
[237] A. P. Gursel, H. Maryman, and C. Ostertag, "A life-cycle approach to environmental, mechanical, and durability properties of 'green' concrete mixes with rice husk ash," *J. Clean. Prod.*, vol. 112, pp. 823–836, 2016, doi: 10.1016/j.jclepro.2015.06.029.
[238] J. W. Ro, P. R. Cunningham, S. A. Miller, A. Kendall, and J. Harvey, "Technical, economic, and environmental feasibility of rice hull ash from electricity generation as a mineral additive to concrete," *Sci. Rep.*, vol. 14, no. 1, p. 9158, Apr. 2024, doi: 10.1038/s41598-024-59615-1.
[239] ChemAnalyst, "Fly Ash Price Trend and Forecast." Accessed: May 18, 2024. [Online]. Available: https://www.chemanalyst.com/Pricing-data/fly-ash-1459
[240] R. R. Bakker and B. M. Jenkins, "Feasibility of collecting naturally leached rice straw for thermal conversion," *Biomass Bioenergy*, vol. 25, no. 6, pp. 597–614, 2003, doi: 10.1016/S0961-9534(03)00053-9.
[241] B. M. Jenkins *et al.*, "Commercial feasibility of utilizing rice straw in power generation," in *Proceedings Bioenergy 2000*, Buffalo, New York, 2000.
[242] P. K. Mehta, "Properties of Blended Cements Made From Rice Husk Ash.," *J Am Concr Inst*, vol. 74, no. 9, pp. 440–442, 1977, doi: 10.14359/11022.
[243] H. Chao-Lung, B. L. Anh-Tuan, and C. Chun-Tsun, "Effect of rice husk ash on the strength and durability characteristics of concrete," *Constr. Build. Mater.*, vol. 25, no. 9, pp. 3768–3772, 2011, doi: 10.1016/j.conbuildmat.2011.04.009.
[244] A. M. Parvez, I. M. Mujtaba, and T. Wu, "Energy, exergy and environmental analyses of conventional, steam and CO2-enhanced rice straw gasification," *Energy*, vol. 94, pp. 579–588, 2016, doi: 10.1016/j.energy.2015.11.022.
[245] N. B. Klinghoffer, M. J. Castaldi, and A. Nzihou, "Influence of char composition and inorganics on catalytic activity of char from biomass gasification," *Fuel*, vol. 157, pp. 37–47, 2015, doi: 10.1016/j.fuel.2015.04.036.
[246] P. K. Mehta, "Elastomeric and plastomeric materials containing amorphous carbonaceous silica," Apr. 20, 1976
[247] B. S. Thomas, "Green concrete partially comprised of rice husk ash as a supplementary cementitious

material – A comprehensive review," *Renew. Sustain. Energy Rev.*, vol. 82, no. July 2016, pp. 3913–3923, 2018, doi: 10.1016/j.rser.2017.10.081.
[248] M. Vigneshwari, K. Arunachalam, and A. Angayarkanni, "Replacement of silica fume with thermally treated rice husk ash in reactive powder concrete," *J. Clean. Prod.*, vol. 188, pp. 264–277, 2018, doi: 10.1016/j.jclepro.2018.04.008.
[249] R. K. Sandhu and R. Siddique, "Influence of rice husk ash (RHA) on the properties of self-compacting concrete: A review," *Constr. Build. Mater.*, vol. 153, pp. 751–764, 2017, doi: 10.1016/j.conbuildmat.2017.07.165.
[250] Z. hai He, L. yuan Li, and S. gui Du, "Creep analysis of concrete containing rice husk ash," *Cem. Concr. Compos.*, vol. 80, pp. 190–199, 2017, doi: 10.1016/j.cemconcomp.2017.03.014.
[251] C. Fapohunda, B. Akinbile, and A. Shittu, "Structure and properties of mortar and concrete with rice husk ash as partial replacement of ordinary Portland cement – A review," *Int. J. Sustain. Built Environ.*, vol. 6, no. 2, pp. 675–692, 2017, doi: 10.1016/j.ijsbe.2017.07.004.
[252] P. Chaivatamaset, P. Sricharoon, S. Tia, and B. Bilitewski, "The characteristics of bed agglomeration/defluidization in fluidized bed firing palm fruit bunch and rice straw," *Appl. Therm. Eng.*, vol. 70, no. 1, pp. 737–747, 2014, doi: 10.1016/j.applthermaleng.2014.05.061.
[253] P. Thy, B. M. Jenkins, C. E. Lesher, and S. Grundvig, "Compositional constraints on slag formation and potassium volatilization from rice straw blended wood fuel," *Fuel Process. Technol.*, vol. 87, no. 5, pp. 383–408, 2006, doi: 10.1016/j.fuproc.2005.08.015.
[254] H. Liu, L. Zhang, Z. Han, B. Xie, and S. Wu, "The effects of leaching methods on the combustion characteristics of rice straw," *Biomass Bioenergy*, vol. 49, pp. 22–27, 2013, doi: 10.1016/j.biombioe.2012.12.024.
[255] B. M. Jenkins, J. D. Mannapperuma, and R. R. Bakker, "Biomass leachate treatment by reverse osmosis," *Fuel Process. Technol.*, vol. 81, no. 3, pp. 223–246, 2003, doi: 10.1016/S0378-3820(03)00010-9.
[256] B. M. Jenkins, R. R. Bakker, and J. B. Wei, "On the properties of washed straw," *Biomass Bioenergy*, vol. 10, no. 4, pp. 177–200, 1996, doi: 10.1016/0961-9534(95)00058-5.
[257] K. Reynolds, "Personal Communication." Farmer's Rice Cooperative, 2020.
[258] P. Thy, C. Yu, B. M. Jenkins, and C. E. Lesher, "Inorganic composition and environmental impact of biomass feedstock," *Energy Fuels*, vol. 27, no. 7, pp. 3969–3987, Jul. 2013, doi: 10.1021/ef400660u.
[259] C. W. Yu *et al.*, "Influence of leaching pretreatment on fuel properties of biomass," *Fuel Process. Technol.*, vol. 128, pp. 43–53, 2014, doi: 10.1016/j.fuproc.2014.06.030.
[260] C. W. Yu, "Leaching Pretreatments for Improving Biomass Quality : Feedstocks, Solvents, and Extraction Modeling (Dissertation)," University of California, Davis, 2012. [Online]. Available: https://www.proquest.com/dissertations-theses/leaching-pretreatments-improving-biomass-quality/docview/1319305674/se-2?accountid=14505
[261] ASTM, "E871-13:Standard Test Method for Moisture Analysis of Particulate Wood Fuels 1," *Annu. Book ASTM Stand.*, vol. 82, no. Reapproved 2013, p. 2, 2013, doi: 10.1520/E0871-82R13.2.
[262] ASTM, "E872-82: Standard Test Method for Volatile Matter in the Analysis of Particulate Wood Fuels," *ASTM Int.*, vol. 82, no. Reapproved 2006, pp. 14–16, 2011, doi: 10.1520/E0872-82R06.2.
[263] ASTM, "E1755: Standard Test Method for Ash in Biomass," *ASTM Int.*, no. Reapproved 2015, 2015, doi: 10.1520/E1755-01R07.2.
[264] D. G. Nair, A. Fraaij, A. A. K. Klaassen, and A. P. M. Kentgens, "A structural investigation relating to the pozzolanic activity of rice husk ashes," *Cem. Concr. Res.*, vol. 38, no. 6, pp. 861–869, 2008, doi: 10.1016/j.cemconres.2007.10.004.
[265] US EPA, "Method 200.7: Determination of Metals and Trace Elements in Water and Wastes by Inductively Coupled Plasma-Atomic Emission Spectrometry," *US Environ. Prot. Agency*, vol. EPA/600/4-, pp. 31–82, 1991.
[266] UC Davis Analytical Laboratory, "SOP 835.03: Solubles: Al, B, Ca, Cd, Cr, Cu, Fe, K, Mg, Mn, Mo, Na, Ni, P, Pb, S, Si, Zn." Accessed: Jul. 27, 2020. [Online]. Available:

https://anlab.ucdavis.edu/analysis/Water/835
[267] J. Diamantopoulos, “Personal Communication,” *Activation Laboratories Ltd.* 2020.
[268] S. M. Shafie, T.M.I.Mahlia, H. H. Masjuki, and B. Rismanchi, “Life cycle assessment (LCA) of electricity generation from rice husk in Malaysia,” *Energy Procedia*, vol. 14, pp. 499–504, 2012, doi: https://doi.org/10.1016/j.egypro.2011.12.965.
[269] Intergovernmental Panel on Climate Change, “IPCC Fifth Assessment Report. The Physical Science Basis,” 2013.
[270] various authors PRé, “SimaPro Database Manual: Methods Library,” Amersfoort, Netherlands, 2019.
[271] H. Althaus *et al.*, “Life cycle inventories of chemicals. Final report ecoinvent data v2.0 No 8.,” 2007. [Online]. Available: http://scholar.google.com/scholar?hl=en&btnG=Search&q=intitle:Life+Cycle+Inventories+of+Chemicals#0
[272] C. E. Comission, “Total System Electric Generation,” CA.gov. [Online]. Available: https://ww2.energy.ca.gov/almanac/electricity_data/total_system_power.html
[273] Argonne National Laboratory, “The Greenhouse Gases, Regulated Emissions, and Energy Use In Transportation Model, GREET 1.8d.1,” Argonne, IL, 2010.
[274] Biomass Energy Resource Center (BERC), “Biomass Energy: Efficiency, Scale, and Sustainability,” Montpelier, Vermont, 2009.
[275] L. L. Baxter *et al.*, “Alkali Deposits Found in Biomass Power Plants Volume II: The Behavior of Inorganic Material in Biomass-Fired Power Boilers—Field and Laboratory Experiences,” 1996.
[276] P. Thy, C. Yu, S. L. Blunk, and B. M. Jenkins, “Inorganic composition of saline-irrigated biomass,” *Water. Air. Soil Pollut.*, vol. 224, no. 7, pp. 1–17, 2013, doi: 10.1007/s11270-013-1617-y.
[277] P. Thy, B. M. Jenkins, S. Grundvig, R. Shiraki, and C. E. Lesher, “High temperature elemental losses and mineralogical changes in common biomass ashes,” *Fuel*, vol. 85, no. 5–6, pp. 783–795, 2006, doi: 10.1016/j.fuel.2005.08.020.
[278] ACI 318-14, *ACI 318-14 - Building Code Requirements for Structural Concrete*. 2014.
[279] J. Alex, J. Dhanalakshmi, and B. Ambedkar, “Experimental investigation on rice husk ash as cement replacement on concrete production,” *Constr. Build. Mater.*, vol. 127, pp. 353–362, 2016, doi: 10.1016/j.conbuildmat.2016.09.150.
[280] K. B. Park, S. J. Kwon, and X. Y. Wang, “Analysis of the effects of rice husk ash on the hydration of cementitious materials,” *Constr. Build. Mater.*, vol. 105, pp. 196–205, 2016, doi: 10.1016/j.conbuildmat.2015.12.086.
[281] M. F. M. Zain, M. N. Islam, F. Mahmud, and M. Jamil, “Production of rice husk ash for use in concrete as a supplementary cementitious material,” *Constr. Build. Mater.*, vol. 25, no. 2, pp. 798–805, 2011, doi: 10.1016/j.conbuildmat.2010.07.003.
[282] R. W. Nurse, “The effect of phosphate on the constitution and hardening of portland cement,” *J. Appl. Chem.*, vol. 2, no. 12, pp. 708–716, 2007, doi: 10.1002/jctb.5010021208.
[283] K. Celik, C. Meral, A. Petek Gursel, P. K. Mehta, A. Horvath, and P. J. M. Monteiro, “Mechanical properties, durability, and life-cycle assessment of self-consolidating concrete mixtures made with blended portland cements containing fly ash and limestone powder,” *Cem. Concr. Compos.*, vol. 56, pp. 59–72, 2015, doi: 10.1016/j.cemconcomp.2014.11.003.
[284] P. Busch, A. Kendall, C. W. Murphy, and S. A. Miller, “Literature review on policies to mitigate GHG emissions for cement and concrete,” *Resour. Conserv. Recycl.*, vol. 182, p. 106278, Jul. 2022, doi: 10.1016/j.resconrec.2022.106278.
[285] S. A. Miller, G. Habert, R. J. Myers, and J. T. Harvey, “Achieving net zero greenhouse gas emissions in the cement industry via value chain mitigation strategies,” *One Earth*, vol. 4, no. 10, pp. 1398–1411, Oct. 2021, doi: 10.1016/j.oneear.2021.09.011.
[286] E. H. Fini, L. Poulikakos, J. de C. Christiansen, W. Schmidt, and M. M. Parast, “Toward sustainability in the built environment: An integrative approach,” *Resour. Conserv. Recycl.*, vol. 172, no. xxxx, pp. 2–5, 2021, doi: 10.1016/j.resconrec.2021.105676.

[287] Caltrans, “Rice hull ash,” in *California Department of Transportation Concrete Technology Manual*, Sacramento, California, 2013, pp. 2–15. doi: 10.3138/9781442689251.
[288] Z. Hossain, A. Elsayed, and K. T. Islam, “Use of rice hull ash (RHA) as a sustainable source of construction material,” Transportation Consortium of South-Central States (Tran-SET), Baton Rouge, LA, LA, 2018. [Online]. Available: http://transet.lsu.edu/completed-research/
[289] W. Schmidt, “Why Africa can spearhead innovative and sustainable cement and concrete technologies globally,” *Proc. Second KEYS Symp. Knowl. Exch. Young Sci.*, no. August, 2016.
[290] N. S. Msinjili, W. Schmidt, A. Rogge, and H.-C. Kühne, “Rice husk ash as a sustainable supplementary cementitious material for improved concrete properties,” *Afr. J. Sci. Technol. Innov. Dev.*, vol. 11, no. 4, pp. 417–425, Jun. 2019, doi: 10.1080/20421338.2018.1513895.
[291] M. S. Meddah, T. R. Praveenkumar, M. M. Vijayalakshmi, S. Manigandan, and R. Arunachalam, “Mechanical and microstructural characterization of rice husk ash and Al2O3 nanoparticles modified cement concrete,” *Constr. Build. Mater.*, vol. 255, p. 119358, 2020, doi: 10.1016/j.conbuildmat.2020.119358.
[292] J. Wang, J. Xiao, Z. Zhang, K. Han, X. Hu, and F. Jiang, “Action mechanism of rice husk ash and the effect on main performances of cement-based materials: A review,” *Constr. Build. Mater.*, vol. 288, p. 123068, Jun. 2021, doi: 10.1016/j.conbuildmat.2021.123068.
[293] P. R. Cunningham, L. Wang, P. Thy, B. M. Jenkins, and S. A. Miller, “Effects of leaching method and ashing temperature of rice residues for energy production and construction materials,” *ACS Sustain. Chem. Eng.*, p. acssuschemeng.0c07919, Mar. 2021, doi: 10.1021/acssuschemeng.0c07919.
[294] J. Ren, P. Yu, and X. Xu, “Straw utilization in China—status and recommendations,” *Sustainability*, vol. 11, no. 6, p. 1762, Mar. 2019, doi: 10.3390/su11061762.
[295] S. Wang *et al.*, “Strength characteristics and microstructure evolution of cemented tailings backfill with rice straw ash as an alternative binder,” *Constr. Build. Mater.*, vol. 297, p. 123780, Aug. 2021, doi: 10.1016/j.conbuildmat.2021.123780.
[296] J. Roselló, L. Soriano, M. P. Santamarina, J. L. Akasaki, J. Monzó, and J. Payá, “Rice straw ash: A potential pozzolanic supplementary material for cementing systems,” *Ind. Crops Prod.*, vol. 103, pp. 39–50, Sep. 2017, doi: 10.1016/j.indcrop.2017.03.030.
[297] A. Pandey and B. Kumar, “A comprehensive investigation on application of microsilica and rice straw ash in rigid pavement,” *Constr. Build. Mater.*, vol. 252, p. 119053, Aug. 2020, doi: 10.1016/j.conbuildmat.2020.119053.
[298] I. S. Agwa, O. M. Omar, B. A. Tayeh, and B. A. Abdelsalam, “Effects of using rice straw and cotton stalk ashes on the properties of lightweight self-compacting concrete,” *Constr. Build. Mater.*, vol. 235, p. 117541, Feb. 2020, doi: 10.1016/j.conbuildmat.2019.117541.
[299] I. Y. Hakeem, M. Amin, I. S. Agwa, M. H. Abd-Elrahman, O. M. O. Ibrahim, and M. Samy, “Ultra-high-performance concrete properties containing rice straw ash and nano eggshell powder,” *Case Stud. Constr. Mater.*, vol. 19, p. e02291, Dec. 2023, doi: 10.1016/j.cscm.2023.e02291.
[300] R Core Team, “R: A language and environment for statistical computing.” R Foundation for Statistical Computing, Vienna, 2023.
[301] R Core Team, “The R stats package,” vol. version 3. Vienna. [Online]. Available: https://www.rdocumentation.org/packages/stats/versions/3.6.2
[302] ASTM, “C150/C150M-22 Standard specification for Portland cement,” *ASTM Int.*, vol. 04, no. 01, 2022, doi: doi.org/10.1520/C0150_C0150M-220150M-22.
[303] Caltrans, *Caltrans 2018 standard of specifications*. California State Transportation Agency, 2018.
[304] N. Zhang *et al.*, “Pretreatment of lignocellulosic biomass using bioleaching to reduce inorganic elements,” *Fuel*, vol. 246, pp. 386–393, Jun. 2019, doi: 10.1016/j.fuel.2019.02.138.
[305] G. C. Cordeiro, L. M. Tavares, and R. D. Toledo Filho, “Improved pozzolanic activity of sugar cane bagasse ash by selective grinding and classification,” *Cem. Concr. Res.*, vol. 89, pp. 269–275, Nov. 2016, doi: 10.1016/j.cemconres.2016.08.020.
[306] H. Li, Y. Chen, Y. Cao, G. Liu, and B. Li, “Comparative study on the characteristics of ball-milled coal fly ash,” *J. Therm. Anal. Calorim.*, vol. 124, no. 2, pp. 839–846, May 2016, doi:

10.1007/s10973-015-5160-5.
[307] Y. Zhang, E. Schlangen, and O. Çopuroğlu, “Effect of slags of different origins and the role of sulfur in slag on the hydration characteristics of cement-slag systems,” *Constr. Build. Mater.*, vol. 316, p. 125266, Jan. 2022, doi: 10.1016/j.conbuildmat.2021.125266.
[308] C. M. Yun, M. R. Rahman, C. Y. W. Phing, A. W. M. Chie, and M. K. B. Bakri, “The curing times effect on the strength of ground granulated blast furnace slag (GGBFS) mortar,” *Constr. Build. Mater.*, vol. 260, p. 120622, Nov. 2020, doi: 10.1016/j.conbuildmat.2020.120622.
[309] E. Özbay, M. Erdemir, and H. İ. Durmuş, “Utilization and efficiency of ground granulated blast furnace slag on concrete properties – A review,” *Constr. Build. Mater.*, vol. 105, pp. 423–434, Feb. 2016, doi: 10.1016/j.conbuildmat.2015.12.153.
[310] Y. S. Cheng, Y. Zheng, C. W. Yu, T. M. Dooley, B. M. Jenkins, and J. S. Vandergheynst, “Evaluation of high solids alkaline pretreatment of rice straw,” *Appl. Biochem. Biotechnol.*, vol. 162, no. 6, pp. 1768–1784, 2010, doi: 10.1007/s12010-010-8958-4.
[311] B. B. Y. Lau, T. Yeung, R. J. Patterson, and L. Aldous, “A Cation Study on Rice Husk Biomass Pretreatment with Aqueous Hydroxides: Cellulose Solubility Does Not Correlate with Improved Enzymatic Hydrolysis,” *ACS Sustain. Chem. Eng.*, vol. 5, no. 6, pp. 5320–5329, 2017, doi: 10.1021/acssuschemeng.7b00647.
[312] Global Alliance for Buildings and Construction, International Energy Agency, and UN Environment Program, “Regional Roadmap for Buildings and Construction in Africa,” 2020. [Online]. Available: https://www.iea.org/reports/globalabc-regional-roadmap-for-buildings-and-construction-in-africa-2020-2050
[313] Global Alliance for Buildings and Construction, International Energy Agency, and UN Environment Program, “Roadmap for Buildings and Construction 2020-2050,” 2020. [Online]. Available: http://globalabc.org/our-work/forging-regional-pathways-global-and-regional-roadmap
[314] M. C. G. Juenger, R. Snellings, and S. A. Bernal, “Supplementary cementitious materials: New sources, characterization, and performance insights,” *Cem. Concr. Res.*, vol. 122, no. May, pp. 257–273, 2019, doi: 10.1016/j.cemconres.2019.05.008.
[315] P. R. Cunningham and S. A. Miller, “A material flow analysis of carpet in the United States: Where should the carpet go?,” *J. Clean. Prod.*, vol. 368, no. June 2022, p. 133243, Sep. 2022, doi: 10.1016/j.jclepro.2022.133243.
[316] R. Siddique, “Utilization of silica fume in concrete: Review of hardened properties,” *Resour. Conserv. Recycl.*, vol. 55, no. 11, pp. 923–932, Sep. 2011, doi: 10.1016/j.resconrec.2011.06.012.
[317] K. Scott *et al.*, “Pathways to Commercial Liftoff: Industrial Decarbonization,” 2023.
[318] International Energy Agency, “Net Zero Roadmap: A Global Pathway to Keep the 1.5C Goal in Reach,” 2023.
[319] D. K. Panesar, K. E. Seto, and C. J. Churchill, “Impact of the selection of functional unit on the life cycle assessment of green concrete,” *Int. J. Life Cycle Assess.*, vol. 22, no. 12, pp. 1969–1986, 2017, doi: 10.1007/s11367-017-1284-0.
[320] S. A. Miller, P. J. M. Monteiro, C. P. Ostertag, and A. Horvath, “Comparison indices for design and proportioning of concrete mixtures taking environmental impacts into account,” *Cem. Concr. Compos.*, vol. 68, pp. 131–143, 2016, doi: http://dx.doi.org/10.1016/j.cemconcomp.2016.02.002.
[321] USGS and K. J. Simmons, “2021 Clays Mineral Commodity Summaries,” 2022.
[322] USGS, “Lime 2023,” *Mineral Commodity Summaries*. US Geological Survey, Reston, VA, 2024.
[323] USGS and C. C. Tuck, “Iron and steel slag 2017-2021,” 2022. [Online]. Available: https://www.usgs.gov/centers/national-minerals-information-center/iron-and-steel-statistics-and-information
[324] American Coal Ash Association, “ACAA 2010-2022 Coal Combustion Product Production & Use Survey Report,” *Coal Combustion Products Production & Use Reports*. American Coal Ash Association, 2022. [Online]. Available: https://acaa-usa.org/publications/production-use-reports/
[325] USGS, “Clays Mineral Commodity Summaries 2017-2021 Tables,” US Geological Survey, 2022.
[326] EIA, “Table 15. Coal Supply, Disposition, and Prices,” *Annual Energy Outlook 2023*. US Energy

Information Administration, Washington, D.C.
[327] EIA, “The National Energy Modeling System,” US Energy Information Administration, 2023. doi: 10.17226/1997.
[328] EIA, “Annual Energy Outlook 2023,” US Energy Information Administration, Washington, D.C., 2023.
[329] EIA, “Total Coal Consumption,” *Coal Data Browser*. US Energy Information Administration, Washington, D.C., 2022. [Online]. Available: https://www.eia.gov/coal/data/browser/#/topic/20?agg=0,1&geo=g&sec=vs&linechart=COAL.CONS_TOT.US-8.A~COAL.CONS_TOT.US-9.A~COAL.CONS_TOT.US-10.A&columnchart=COAL.CONS_TOT.US-98.A&map=COAL.CONS_TOT.US-3.A&freq=A&start=2001&end=2022&ctype=map&ltype=pin&rtype
[330] A. Pascale and E. D. Larson, “Princeton’s net zero America study. Annex J: Iron and steel industry transition,” 2021.
[331] S. Nimbalkar, “Potential Decarbonization Strategies and Challenges for the U.S. Iron & Steel Industry.” US Department of Energy, 2022.
[332] World Steel Association, “Steel Facts,” Brussels, Belgium, 2018.
[333] USGS, “Iron and Steel 2012-2023,” 2024.
[334] USGS, “2021 clay statistics -tables only release,” *Mineral Yearbook*. 2021.
[335] USGS, “2021 Iron and steel slag Annual Tables,” *Mineral Yearbook*. US Geological Survey, Reston, VA, 2023.
[336] “What is LC3 ?” Accessed: Mar. 28, 2024. [Online]. Available: https://lc3.ch/
[337] Y. Wang, L. E. Burris, C. R. Shearer, R. D. Hooton, and P. Suraneni, “Characterization and reactivity of size-fractionated unconventional fly ashes,” *Mater. Struct.*, vol. 56, no. 3, p. 49, Apr. 2023, doi: 10.1617/s11527-023-02140-w.
[338] Y. Wang, L. Burris, R. D. Hooton, C. R. Shearer, and P. Suraneni, “Effects of unconventional fly ashes on cementitious paste properties,” *Cem. Concr. Compos.*, vol. 125, p. 104291, Jan. 2022, doi: 10.1016/j.cemconcomp.2021.104291.
[339] G. Innocenti, D. J. Benkeser, J. E. Dase, X. Wirth, C. Sievers, and K. E. Kurtis, “Beneficiation of ponded coal ash through chemi-mechanical grinding,” *Fuel*, vol. 299, p. 120892, Sep. 2021, doi: 10.1016/j.fuel.2021.120892.
[340] A. C. P. Martins *et al.*, “Steel slags in cement-based composites: An ultimate review on characterization, applications and performance,” *Constr. Build. Mater.*, vol. 291, p. 123265, Jul. 2021, doi: 10.1016/j.conbuildmat.2021.123265.
[341] USGS, “Iron and Steel 2021 Annual Tables,” *Mineral Yearbook*. US Geological Survey, Reston, VA, 2023.
[342] S.-T. Yi, E. Yang, and J.-C. Choi, “Effect of specimen sizes, specimen shapes, and placement directions on compressive strength of concrete,” *Nucl. Eng. Des.*, vol. 236, no. 2, pp. 115–127, Jan. 2006, doi: 10.1016/j.nucengdes.2005.08.004.
[343] C. Meyer, “The greening of the concrete industry,” *Cem. Concr. Compos.*, vol. 31, no. 8, pp. 601–605, 2009, doi: 10.1016/j.cemconcomp.2008.12.010.
[344] R. Snellings, P. Suraneni, and J. Skibsted, “Future and emerging supplementary cementitious materials,” *Cem. Concr. Res.*, vol. 171, p. 107199, Sep. 2023, doi: 10.1016/j.cemconres.2023.107199.
[345] J. Bolomey, “Détermination de la résistance à la compression des mortiers et bétons,” *Bull. Tech. Suisse Romande*, vol. 51, no. 11, p. 126, 1925, doi: https://doi.org/10.5169/seals-395100.
[346] R. Feret, “Sur la compacité des mortiers hydrauliques,” *Ann Pntas Chaussees*, vol. 4, pp. 5–164, 1892.
[347] D. A. Abrams, “Design of Concrete Mixtures,” *Bull. Struct. Mater. Res. Lab. Lewis Inst. Chic.*, 1919, doi: 10.14359/17636.
[348] A. Oner, S. Akyuz, and R. Yildiz, “An experimental study on strength development of concrete containing fly ash and optimum usage of fly ash in concrete,” *Cem. Concr. Res.*, vol. 35, no. 6, pp.

1165–1171, 2005, doi: http://dx.doi.org/10.1016/j.cemconres.2004.09.031.
[349] A. Oner and S. Akyuz, “An experimental study on optimum usage of GGBS for the compressive strength of concrete,” *Cem. Concr. Compos.*, vol. 29, no. 6, pp. 505–514, 2007, doi: http://dx.doi.org/10.1016/j.cemconcomp.2007.01.001.
[350] C. Chen, G. Habert, Y. Bouzidi, A. Jullien, and A. Ventura, “LCA allocation procedure used as an incitative method for waste recycling: An application to mineral additions in concrete,” *Resour. Conserv. Recycl.*, vol. 54, no. 12, pp. 1231–1240, Oct. 2010, doi: 10.1016/j.resconrec.2010.04.001.
[351] CEN European Committee for Standardization, “NF EN 206-1, Concrete - Part 1 : specification, performance, production and conformity,” 2024.
[352] CEN European Committee for Standardization, “BS EN 206:2013, Concrete - Specification, performance, production and conformity,” 2013.
[353] B. Abdelkader, K. El-Hadj, and E. Karim, “Efficiency of granulated blast furnace slag replacement of cement according to the equivalent binder concept,” *Cem. Concr. Compos.*, vol. 32, no. 3, pp. 226–231, Mar. 2010, doi: 10.1016/j.cemconcomp.2009.11.004.
[354] S. Joseph *et al.*, “Mechanical properties of concrete made with calcined clay: a review by RILEM TC-282 CCL,” *Mater. Struct.*, vol. 56, no. 4, p. 84, May 2023, doi: 10.1617/s11527-023-02118-8.
[355] F. Zunino *et al.*, “Hydration and mixture design of calcined clay blended cements: review by the RILEM TC 282-CCL,” *Mater. Struct.*, vol. 55, no. 9, p. 234, Nov. 2022, doi: 10.1617/s11527-022-02060-1.
[356] M. Thomas, “Optimizing the Use of Fly Ash in Concrete,” Portland cement association, Skokie, Illinois, 2007.
[357] P. R. Cunningham, P. G. Green, S. J. Parikh, J. T. Harvey, and S. A. Miller, “Engineering the performance of post-consumer calcium carbonate from carpet in cement-based materials through pre-treatment methods,” *Constr. Build. Mater.*, vol. 368, p. 130451, Mar. 2023, doi: 10.1016/j.conbuildmat.2023.130451.
[358] ACAA, “2019 Coal Combustion Product (CCP) Production & Use Survey Report,” American Coal Ash Association, Farmington Hills, MI, 2019.
[359] D. Harris and L. Fitzgerald, “Life-cycle cost analysis (LCCA): a comparison of commercial flooring,” *Facilities*, vol. 35, no. 5–6, pp. 303–318, 2017, doi: 10.1108/F-10-2015-0071.
[360] Cascadia Consulting Group and Carpet America Recovery Effort, “Interim Report to CalRecycle Analysis of Carpet Discards Formula,” 2021.
[361] The Mathworks Inc., “MATLAB,” *23.2.0.2428915 (R2023b) Update 4*. The MathWorks Inc., Natick, Massachusetts, 2023.
[362] H. Wickham *et al.*, “Welcome to the Tidyverse,” *J. Open Source Softw.*, vol. 4, no. 43, p. 1686, Nov. 2019, doi: 10.21105/joss.01686.
[363] T. L. Pedersen, “ggforce: Accelerating ‘ggplot2.’” 2024. [Online]. Available: https://ggforce.data-imaginist.com

Appendix A. **Supplemental information for a material flow analysis of US carpets**

Part 1: Import, export, and production data for tufted carpet

Table A.1. Carpet production data by year based on data from Industrial Research Report (IRR) from the Wharton School of Business, [1] The United States Census Bureau (US Census) reports, [2]–[21] and Carpet America Recovery Effort (CARE) [22]–[37]

Year	Production (m^2)	Source	Year	Production (m^2)	Source
2018	721316038	CARE	1983	848147998	US Census
2017	745134489	CARE	1982	713780717	US Census
2016	761127114	CARE	1981	791997053	US Census
2015	773280658	CARE	1980	846824409	US Census
2014	745140121	CARE	1979	967220008	US Census
2013	767898271	CARE	1978	928122709	US Census
2012	742760463	CARE	1977	857721652	US Census
2011	800670600	CARE	1976	744382129	US Census
2010	834890368	US Census	1975	655243465	US Census
2009	846214872	US Census	1974	724085982	US Census
2008	1026853422	US Census	1973	789549709	US Census
2007	1165995824	US Census	1972	716514016	US Census
2006	1376999162	US Census	1971	569376567	US Census
2005	1571621099	US Census	1970	505029069	US Census
2004	1521393278	US Census	1969	470459398	US Census
2003	1460658685	US Census	1968	427264242	US Census
2002	1449436188	US Census	1967	361340644	US Census
2001	1401240155	US Census	1966	340899848	US Census
2000	1464942999	US Census	1965	314173048	US Census
1999	1436798965	US Census	1964	266654278	US Census
1998	1403776129	US Census	1963	146817547	IRR
1997	1281993395	US Census	1962	121007644	IRR
1996	1259237363	US Census	1961	97670838	IRR
1995	1222165164	US Census	1960	83022394	IRR
1994	1209064726	US Census	1959	71888109	IRR
1993	1141173722	US Census	1958	59557828	IRR
1992	1093973517	US Census	1957	47188165	IRR
1991	987079696	US Census	1956	38826644	IRR
1990	1059617894	US Census	1955	29588862	IRR
1989	1030695425	US Census	1954	22596667	IRR
1988	1034320872	US Census	1953	13594422	IRR
1987	1016542303	US Census	1952	8740286	IRR
1986	993286267	US Census	1951	5085157	IRR
1985	919264780	US Census	1950	3224524	IRR
1984	885158323	US Census			

Table A.2. Imports and exports of carpet compared to production (in m^2) based on data from the U.S. Census Bureau [2], [3] and the U.S.A. Trade Online Database [38] (UTO). Exported carpet is shown as negative and imported carpet is shown as positive.

Year	Imported (m^2)	Exported (m^2)	Source	Year	Imported (m^2)	Exported (m^2)	Source
2018	60337169	99525113	[38]	**1997**	83479666	26884465	[38]
2017	63921536	89891714	[38]	**1996**	79628181	24539317	[38]
2016	62997582	81748705	[38]	**1995**	73059480	23675940	[38]
2015	63624795	84484448	[38]	**1994**	78707224	20475133	[38]
2014	73554296	86555820	[38]	**1993**	101012920	13323495	[38]
2013	71265619	77730017	[38]	**1992**	86653391	12583883	[38]
2012	69091243	75630073	[38]	**1991**	89500000	10900000	[2], [3]
2011	67577382	68930603	[38]	**1990**	58500000	10900000	[2], [3]
2010	66558920	69655915	[38]	**1989**	43000000	20000000	[2], [3]
2009	57458454	60201105	[38]	**1988**	39500000	13800000	[2], [3]
2008	77831458	62665982	[38]	**1987**	28800000	14400000	[2], [3]
2007	71598682	66172721	[38]	**1986**	20900000	15400000	[2], [3]
2006	75757403	69851017	[38]	**1985**	17800000	19800000	[2], [3]
2005	74416417	56394224	[38]	**1984**	26700000	18200000	[2], [3]
2004	70311852	58213472	[38]	**1983**	36400000	4800000	[2], [3]
2003	64588589	54685788	[38]	**1982**	52600000	4300000	[2], [3]
2002	66291163	48055492	[38]	**1981**	57513000	1511000	[2], [3]
2001	66386686	43130442	[38]	**1980**	61028000	1735000	[2], [3]
2000	76639364	37356406	[38]	**1979**	32889000	2846000	[2], [3]
1999	77123042	33875433	[38]	**1978**	4492900	1779000	[2], [3]
1998	75852183	27842114	[38]				

Table A.3. Assumption or method for estimating values when requisite data were not reported

Parameter	Range Filled	Method or Assumption	Purpose
% Tufted carpet	2011-2018	Assumed as average of years 1990-2010	Used to calculate sq. meter of tufted in the US
% Import & % Export	1950-1977	Assumed that percentages from 1978 were constant during 1950-1977	
% Nylon, PET, and PP Front-fiber	2011-2016	Interpolation, linear, using data from 2010 and 2017	Used to estimate fiber disposals
% Nylon and PET Front-fiber	1980-1986	Interpolation, linear, using data from 1979 and 1987	
% PP Front-fiber	1980-1991	Interpolation, linear, using data from 1979 and 1992	
% Manmade backing	1984-2010	Modeled as 100% after 1983, and 100% PP	Used to calculate backing
% Manmade backing	1964-1967	Modeled as 0% before 1968	
% Cotton, Jute, or Paper backing	1966 & 1967	Interpolation, linear, using data from 1965 and 1968	

Note: PP = Polypropylene, PET = polyethylene terephthalate

Table A.4. Average carpet composition used to calculate mass of carpet constituents

Input	Value	Source
Face weight per yard	0.792 (kg/m^2 carpet)[a]	Average from Census Data [2]–[21]
Carpet weight per yard	2.316 (kg/m^2 carpet)[b]	Average from CARE [22]–[37]
Percentage of tufted carpet as a fraction of all carpet produced	90.75%	Census Data (average 1990 - 2011) [2]–[21]
Face-fiber mass %	47.5 %	Reported average (range: 45-50%), [39]
PC4 mass %	44%	Sum (1) + (2)
(1) Styrene-butadiene latex mass %	9%	Reported average (range:8-10%), [39]
(2) CaCO3 by mass %	35%	Reported average (range:30-40%), [39]
Polypropylene from backing	10%	Sum (3) + (4)
(3) Primary backing mass %	5%	Reported average (range:4-6%) [39]
(4) Secondary backing mass %	5%	Reported average (range:4-6%) [39]
[a] 1.46 lb/yd^2; [b] 4.27 lb/yd^2		

Table A.5. Review of carpet lifespans in literature

Author(s)	Publication year	System	Application	Lifespan (y)	Source
Keoleian, et al.	2001	Broadloom	residential	8	[40]
Bowyer, et al.	2019	Broadloom / modular	commercial	11 / 25	[41]
Harris and Fitzgerald	2017	Broadloom / modular	commercial	10 / 15	[42]
Robinson	1996	Broadloom	commercial	10	[43]
Moussatche and Languell	2001	Modular	commercial	10-12	[44]
Outhred	1995	Broadloom	residential	5	[45]
Petersen and Solberg	2004	Broadloom	residential	9-10	[46]
Realff, et al.	2009	Broadloom		5-10	[47]
Scheuer, et al.	2003	Broadloom / modular	commercial	12 / 12	[48]
Junnila, et al.	2006	Broadloom	commercial	4-25	[49]
Wang	2006			5-10	[50]
Stephan, et al.	2018	Nylon / wool	commercial	10 / 10	[51]
Seiders, et al.	2007		residential	8-10	[52]
Rauf and Crawford	2015		residential	10	[53]

Part 2: Calculating sales from Carpet America Recovery Effort reported disposals

Carpet America Recovery Effort (CARE) has collected yearly carpet sales data since 2007. They use survey data to estimate yearly discards as a function of sales, replacement rates, and carpet deselection, and carpet mass. Depending on year, either Equation A.1 or Equation A.2 has been used (where S = Carpet sales; R = percent of carpet to replace existing carpet; P = Average weight of carpet; D = pounds of carpet from demolition projects not replaced; and DS = Deselection pound resulting from a decision to remove but not replace carpet)

$$Discards = \big((S * R) * P\big) + D \quad [1]$$ Equation A.1

$$Discards = \big((S * R) * P\big) + D + DS \quad [2]$$ Equation A.2

CARE annual reports typically do not report the measured sales volumes, but they do report other values used to estimated discards and the calculated discard estimate. Thus, initially measured carpet sales data can be found using the reported values with the rearranged versions of Equation A.1 or Equation A.2 shown as Equation A.3 and Equation A.4, respectively. See **Table A.6.** Sales calculations for tufted carpet from 2009-2018 and the supporting data for calculations collected from annual CARE reports [22]–[37].values from CARE reports.

$$S = \frac{Discards - D}{P * R}$$ Equation A.3

$$S = \frac{Discards - D - DS}{P * R}$$ Equation A.4

Table A.6. Sales calculations for tufted carpet from 2009-2018 and the supporting data for calculations collected from annual CARE reports [22]–[37].

Year	D% [3]	P (kg/m^2)	R	DS%[4]	Estimated Discards (kg)	Estimated Discards (m^2)	Recalculated sales (m^2)
2018	0.56%	2.441	74%	0.75%	1.45E+09	6.28E+08	7.95E+08
2017	0.55%	2.387	78%	0.75%	1.54E+09	6.60E+08	8.11E+08
2016	0.57%	2.387	78%	0.75%	1.59E+09	6.83E+08	8.36E+08
2015	0.60%	2.278	79%	0.75%	1.54E+09	6.71E+08	8.53E+08
2014	0.55%	2.278	82%	0.75%	1.54E+09	6.71E+08	8.21E+08
2013	0.55%	2.278	87%	-	1.68E+09	7.25E+08	8.44E+08
2012	1.30%	2.278	85%	-	1.59E+09	6.93E+08	8.19E+08
2011	1.30%	2.278	85%	-	1.72E+09	7.47E+08	8.86E+08
2010	1.30%	2.278	85%	-	1.54E+09	6.60E+08	7.80E+08
2009	1.30%	2.278	85%	-	1.68E+09	7.28E+08	8.61E+08

[1] From CARE report, 2012 [37]
[2] From CARE report, 2014 [25]
[3] This value is calculated in reports using a percentage (reported by CARE) of total sales (*i.e., D = S*R*P*D%)*
[4] This value is calculated in reports using a percentage (reported by CARE) of sales *(i.e., DS = S*R*P*DS%)*

Part 3: Virgin material flows

To draw comparisons of polymers from carpet disposed to the markets for virgin plastics, annual polymer production data from 1995 to 2014 in the US as show in **Table A.7**.

Table A.7. *Annual polypropylene, nylon, and polyethylene production (metric ton) in the United States. Data collected from the Commodity Research Bureau reports* [54]–[56]

Year	Polypropylene (metric ton)	Nylon (metric ton)	Polyethylene (metric ton)
1995	4.94E+06	4.63E+05	1.09E+07
1996	5.44E+06	5.00E+05	1.20E+07
1997	6.04E+06	5.54E+05	1.23E+07
1998	6.27E+06	5.83E+05	1.26E+07
1999	7.03E+06	6.12E+05	1.35E+07
2000	7.07E+06	6.33E+05	1.63E+07
2001	7.32E+06	5.26E+05	1.52E+07
2002	7.75E+06	5.82E+05	1.62E+07
2003	7.94E+06	5.92E+05	1.58E+07
2004	8.40E+06	6.16E+05	1.72E+07
2005	8.15E+06	5.68E+05	1.63E+07
2006	8.52E+06	5.76E+05	1.75E+07
2007	8.82E+06	5.87E+05	1.80E+07
2008	7.61E+06	5.21E+05	1.60E+07
2009	7.54E+06	4.28E+05	1.67E+07
2010	7.83E+06	4.66E+05	1.70E+07
2011	7.45E+06	5.02E+05	1.69E+07
2012	7.41E+06	5.41E+05	1.73E+07
2013	7.45E+06	5.62E+05	1.75E+07
2014	7.46E+06	5.89E+05	1.79E+07

To compare PC4 removal to the yearly consumption of cements and limestone, we used data from US Geological Survey mineral yearbooks as show in **Table A.8**.

Table A.8. *Annual cement production and interground limestone data from 1993-2019. Data collected from USGS mineral yearbook reports:* [57]–[82]

Year	Cement (metric ton)	Interground limestone (metric ton)
1993	7.90E+04	0
1994	7.84E+04	0
1995	8.01E+04	0
1996	8.00E+04	0
1997	8.44E+04	0
1998	8.71E+04	0
1999	9.10E+04	1.14E+03
2000	9.39E+04	1.26E+03
2001	9.56E+04	1.60E+03
2002	1.07E+05	1.33E+03
2003	1.09E+05	1.53E+03
2004	1.25E+05	1.81E+03
2005	1.14E+05	2.23E+03
2006	1.14E+05	2.38E+03
2007	1.12E+05	2.15E+03
2008	1.01E+05	1.92E+03
2009	7.36E+04	1.51E+03
2010	7.85E+04	1.55E+03
2011	8.00E+04	1.50E+03
2012	8.68E+04	1.72E+03
2013	9.05E+04	1.93E+03
2014	9.73E+04	2.35E+03
2015	9.77E+04	2.47E+03
2016	9.95E+04	2.67E+03
2017	1.01E+05	3.07E+03
2018	1.01E+05	2.86E+03
2019	1.03E+05	2.75E+03

Part 4: Expanded annual environmental impacts that could be mitigated from material substitution

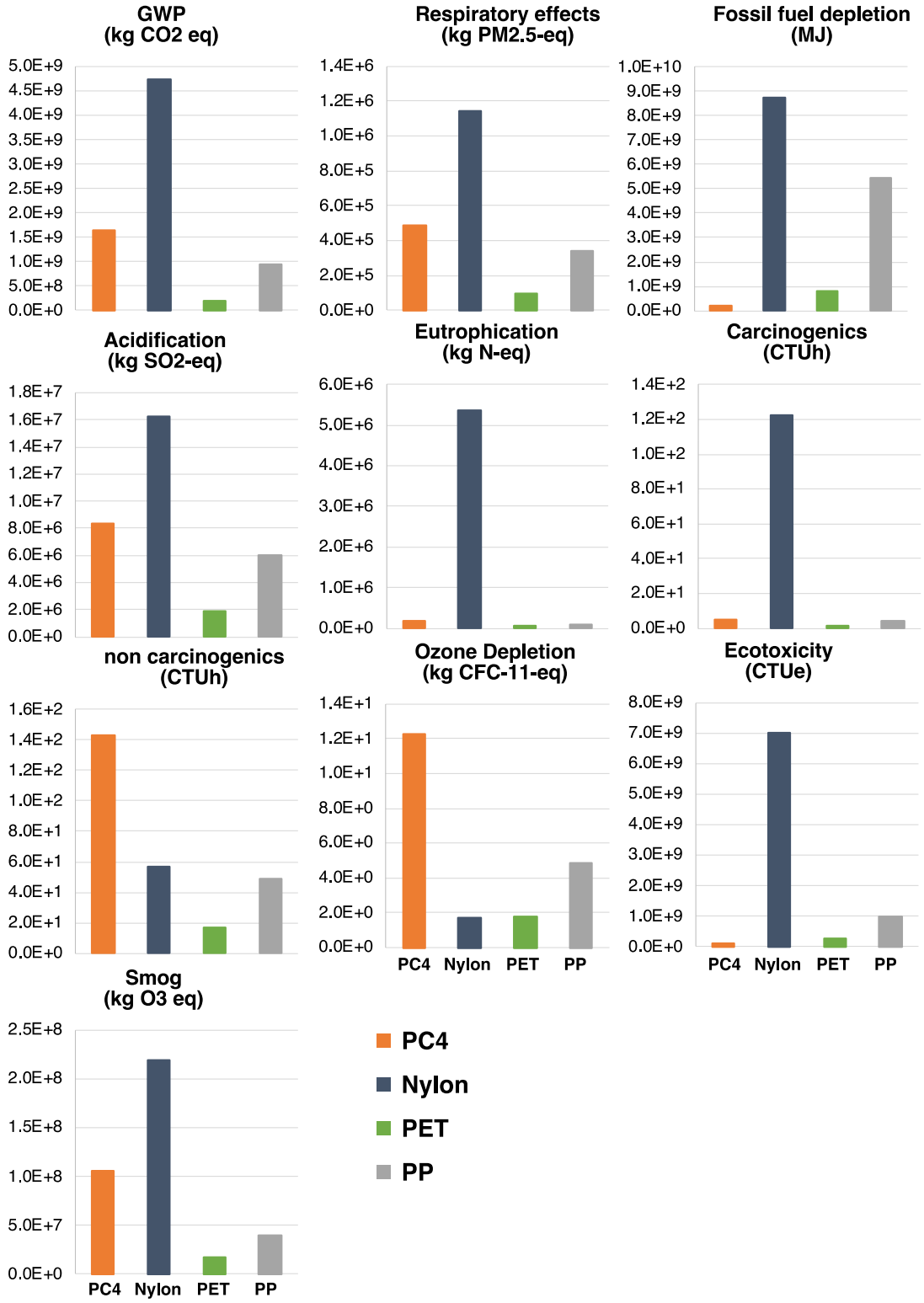

Figure A.1. Average annual impacts from virgin material production that could be avoided through use of recycled carpet products: PC4 (substituted for cement production) between 1999-2019 as well as nylon, PET, and PP substituted for virgin polymer production from 1995-2014.

Data sources for Appendix A:

[1] R. W. Kirk, *The carpet industry; present status and future prospects*, 1000th ed. Philadelphia, Pennsylvania: Industrial Research Unit, Wharton School of Finance and Commerce; distributed by University of Pennsylvania Press, 1970.

[2] U.S. Census Bureau, "Current Industrial Reports: Carpet and Rugs 1985-1992, MA-22Q(85-92)," Washington D.C., 1993. Accessed: Mar. 05, 2021. [Online]. Available: https://hdl.handle.net/2027/pst.000031277693.

[3] U.S. Census Bureau, "Current Industrial Reports Series: Rugs, Carpet, and Carpeting 1968-1985, MQ-22Q(68-85)," Washington D.C., 1986. Accessed: Mar. 05, 2021. [Online]. Available: https://hdl.handle.net/2027/pst.000031323284.

[4] U.S. Census Bureau, "Current Industrial Reports: Carpet and Rugs 2000, MA314Q(00)-1," Washington D.C., 2001.

[5] U.S. Census Bureau, "Current Industrial Reports: Carpet and Rugs 1998, MA314Q(98)-1," Washington D.C., 1999. [Online]. Available: www.stat-usa.gov/.

[6] U.S. Census Bureau, "Current Industrial Reports: Carpet and Rugs 1997, MA22Q(97)-1," Washington D.C., 1998.

[7] U.S. Census Bureau, "Current Industrial Reports: Carpet and Rugs - 1995, MA22Q(95)-1," Washington D.C., 1996.

[8] U.S. Census Bureau, "Carpet and Rugs Summary 1993, MA22Q(93)-1," Washington D.C., 1994.

[9] U.S. Census Bureau, "Carpet and Rugs - 2010, MA314Q(10)-1," Washington D.C., 2011.

[10] U.S. Census Bureau, "Carpet and Rugs - 2009, MA314Q(09) - 1," Washington D.C., 2010.

[11] U.S. Census Bureau, "Current Industrial Reports: Rugs, Carpets, and Carpeting 1964-1967, MA-22Q(64-67)," Washington D.C., 1968. Accessed: Mar. 05, 2021. [Online]. Available: https://hdl.handle.net/2027/pst.000031277693.

[12] U.S. Census Bureau, "Current Industrial Reports: Carpet and Rugs 1996, MA22Q(96)," Washington D.C., 1997.

[13] U.S. Census Bureau, "Current Industrial Reports: Carpet and rugs 2001, MA314Q(01)-1," Washington D.C., 2002.

[14] U.S. Census Bureau, "Carpet and rugs - 2008, MA314Q(08)," Washington D.C., 2009.

[15] U.S. Census Bureau, "Carpet and Rugs - 2007, MA314Q(07)," Washington D.C., 2008.

[16] U.S. Census Bureau, "Current Industrial Reports: Carpet and Rugs 2006, MA314Q(06)-1," Washington D.C., 2007.

[17] U.S. Census Bureau, "Current Industrial Reports: Carpet and rugs 2004, MA314Q(04)-1," Washington D.C., 2005.

[18] U.S. Census Bureau, "Current Industrial Reports: Carpet and rugs 2005, MA314Q(05)-1," Washington D.C., 2006.

[19] U.S. Census Bureau, "Current Industrial Reports: Carpet and Rugs 2003, MA314Q(03)-1," Washington D.C., 2004.

[20] U.S. Census Bureau, "Current Industrial Reports: Carpet and Rugs 2002, MA314Q(02)-1," Washington D.C., 2003. [Online]. Available: www.stat-usa.gov/.

[21] U.S. Census Bureau, "Current Industrial Reports: Carpet and Rugs 1999, MA314Q(99)-1," Washington D.C., 2000.

[22] Carpet America Recovery Effort, "CARE 2002 Annual Report," Dalton, Georgia, 2003. Accessed: Apr. 22, 2020. [Online]. Available: https://carpetrecovery.org/resources/annual-reports/.

[23] Carpet America Recovery Effort, "CARE 2003 Annual Report," Dalton, Georgia, 2004. Accessed: Apr. 22, 2020. [Online]. Available: https://carpetrecovery.org/resources/annual-reports/.

[24] Carpet America Recovery Effort, "CARE 2013 Annual Report," Dalton, Georgia, 2014. Accessed: Apr. 22, 2020. [Online]. Available: https://carpetrecovery.org/resources/annual-reports/.

[25] Carpet America Recovery Effort, "CARE 2014 Annual Report," Dalton, Georgia, 2015. Accessed: Apr. 22, 2020. [Online]. Available: https://carpetrecovery.org/resources/annual-reports/.

[26] Carpet America Recovery Effort, "CARE 2015 Annual Report," Dalton, Georgia, 2016. Accessed: Apr. 22, 2020. [Online]. Available: https://carpetrecovery.org/resources/annual-reports/.

[27] Carpet America Recovery Effort, "CARE 2016 Annual Report," Dalton, Georgia, 2017. Accessed: Apr. 22, 2020. [Online]. Available: https://carpetrecovery.org/resources/annual-reports/.

[28] Carpet America Recovery Effort, "CARE 2018 Annual Report," Dalton, Georgia, 2019. Accessed: Apr. 22, 2020. [Online]. Available: https://carpetrecovery.org/wp-content/uploads/2019/11/CARE-2018-Annual-Report-Final.pdf.

[29] Carpet America Recovery Effort, “CARE 2017 Annual Report,” Dalton, Georgia, 2018. Accessed: Apr. 22, 2020. [Online]. Available: https://carpetrecovery.org/resources/annual-reports/.
[30] Carpet America Recovery Effort, “CARE 2004 Annual Report,” Dalton, Georgia, 2005. Accessed: Apr. 22, 2020. [Online]. Available: https://carpetrecovery.org/resources/annual-reports/.
[31] Carpet America Recovery Effort, “CARE 2005 Annual Report,” Dalton, Georgia, 2006. Accessed: Apr. 22, 2020. [Online]. Available: https://carpetrecovery.org/resources/annual-reports/.
[32] Carpet America Recovery Effort, “CARE 2006 Annual Report,” Dalton, Georgia, 2007. Accessed: Apr. 22, 2020. [Online]. Available: https://carpetrecovery.org/resources/annual-reports/.
[33] Carpet America Recovery Effort, “CARE 2008 Annual Report,” Dalton, Georgia, 2009. Accessed: Apr. 22, 2020. [Online]. Available: https://carpetrecovery.org/resources/annual-reports/.
[34] Carpet America Recovery Effort, “CARE 2009 Annual Report,” Dalton, Georgia, 2010. Accessed: Apr. 22, 2020. [Online]. Available: https://carpetrecovery.org/resources/annual-reports/.
[35] Carpet America Recovery Effort, “CARE 2010 Annual Report,” Dalton, Georgia, 2011. Accessed: Apr. 22, 2020. [Online]. Available: https://carpetrecovery.org/resources/annual-reports/.
[36] Carpet America Recovery Effort, “CARE 2011 Annual Report,” Dalton, Georgia, 2012. Accessed: Apr. 22, 2020. [Online]. Available: https://carpetrecovery.org/resources/annual-reports/.
[37] Carpet America Recovery Effort, “CARE 2012 Annual Report,” Dalton, Georgia, 2013. Accessed: Apr. 22, 2020. [Online]. Available: https://carpetrecovery.org/resources/annual-reports/.
[38] U.S. Census Bureau, “USA Trade Online (UTO) Database Import and Export Data for HS-Codes: 5703100000, 5703200000, 5703300000, & 5703900000,” *USA Trade Online Database* . .
[39] M. Realff, “The role of using carpet as a fuel in carpet recovery system development,” 2014. Accessed: Mar. 05, 2021. [Online]. Available: https://carpetrecovery.org/wp-content/uploads/2014/04/Carpet_Alternative_Fuel_Realff.pdf.
[40] G. A. Keoleian, S. Blanchard, and P. Reppe, “Life-Cycle Energy Costs, and Strategies for Improving a Single-Family House,” *J. Ind. Ecol.*, vol. 4, no. 2, pp. 135–156, 2001, doi: 10.1162/108819800569726.
[41] J. L. Bowyer, E. Pepke, K. Fernholz, C. Henderson, H. Groot, and G. Erickson, “Comparison of Environmental Impacts of Flooring Alternatives,” 2019. [Online]. Available: http://www.dovetailinc.org/report_pdfs/2009/dovetailfloors0809.pdf.
[42] D. Harris and L. Fitzgerald, “Life-cycle cost analysis (LCCA): a comparison of commercial flooring,” *Facilities*, vol. 35, no. 5–6, pp. 303–318, 2017, doi: 10.1108/F-10-2015-0071.
[43] J. Robinson, “Plant and equipment acquisition: a life cycle costing case study,” *Facilities*, vol. 14, no. 5/6, pp. 21–25, May 1996, doi: 10.1108/02632779610117099.
[44] H. Moussatche and J. Languell, “Flooring materials-life-cycle costing for educational facilities,” *Facilities*, vol. 19, no. 10, pp. 333–343, 2001, doi: 10.1108/02632770110399370.
[45] D. R. Outhred, “Reserves for Replacement in Apartment Properties,” *Appraisal J.*, vol. 63, no. 1, pp. 69–80, Jan. 1995, Accessed: Mar. 05, 2021. [Online]. Available: https://search.proquest.com/openview/c57b03565423094b99c26ab20f5e8ce3/1?pq-origsite=gscholar&cbl=35147.
[46] A. K. Petersen and B. Solberg, “Greenhouse Gas Emissions and Costs Over the Life Cycle of Wood and Alternative Flooring Materials,” *Clim. Chang.*, vol. 64, no. 1, pp. 143–167, 2004, doi: 10.1023/B:CLIM.0000024689.70143.79.
[47] M. J. Realff, D. Newtonf, and J. C. Ammons, “Modeling and Decision-making for Reverse Production System Design for Carpet Recycling Modeling and Decision-making for Reverse Production System Design for Carpet Recycling,” vol. 5000, 2009, doi: 10.1080/00405000008659550.
[48] C. Scheuer, G. A. Keoleian, and P. Reppe, “Life cycle energy and environmental performance of a new university building : modeling challenges and design implications,” *Energy Build.*, vol. 35, no. 10, pp. 1049–1064, Nov. 2003, doi: 10.1016/S0378-7788(03)00066-5.
[49] S. Junnila, A. Horvath, and A. A. Guggemos, “Life-cycle assessment of office buildings in Europe and the United States,” *J. Infrastruct. Syst.*, vol. 12, no. 1, pp. 10–17, Mar. 2006, doi: 10.1061/(ASCE)1076-0342(2006)12:1(10).
[50] Y. Wang, “Carpet Recycling Technologies,” in *Recycling in textiles*, 2006, pp. 58–70.
[51] S. J. Davis *et al.*, “Net-zero emissions energy systems,” *Science (80-.).*, vol. 360, no. 6396, p. eaas9793, 2018, doi: 10.1126/science.aas9793.
[52] D. Seiders *et al.*, *NAHB / Bank of America Home Equity Study of Life Expectancy of Home Components*. Washington D.C. : National Association of Home Builders (NAHB), 2007.
[53] A. Rauf and R. H. Crawford, “Building service life and its effect on the life cycle embodied energy of

buildings," *Energy*, vol. 79, no. C, pp. 140–148, 2015, doi: 10.1016/j.energy.2014.10.093.
[54] Commodity Research Bureau, "Plastics," in *The CRB Commodity Yearbook 2006*, C. J. Lown, A. L. Kelly, and R. W. Asplund, Eds. Hoboken, New Jersey: John Wiley & Sons, Inc., 2006, pp. 203–204.
[55] Commodity Research Bureau, "Plastics," in *The CRB Commodity Yearbook 2015*, C. J. Lown, E. A. Pikat, and R. W. Asplund, Eds. Chicago, Illinois: Commodity Research Bureau, 2015, pp. 211–212.
[56] Commodity Research Bureau, "Plastics," in *The CRB Commodity Yearbook 2017*, E. A. Pikat, C. J. Lown., and R. W. Asplund, Eds. Chicago, Illinois: Commodity Research Bureau, 2017, pp. 211 & 212.
[57] C. Solomon, "Cement," *US Geological Survey Minerals Information*. 1994, [Online]. Available: https://minerals.usgs.gov/minerals/pubs/commodity/cement/170494.pdf.
[58] H. G. van Oss, "Cement," Reston, VA, 1995.
[59] H. G. van Oss, "Cement Tables," Reston, VA, 2004.
[60] H. G. van Oss, "Cement Tables," Reston, VA, 2005.
[61] H. G. van Oss, "Cement Tables," Reston, VA, 2006.
[62] H. G. van Oss, *Cement Tables*. Reston, VA, 2007.
[63] H. G. van Oss, "Cement Tables," Reston, VA, 2008.
[64] H. G. van Oss, "Cement Tables," Reston, VA, 2009.
[65] H. G. van Oss, "Cement Tables," Reston, VA, 2010.
[66] H. G. van Oss, "Cement Tables," Reston, VA, 2011.
[67] H. G. van Oss, "Cement Tables," Reston, VA, 2012.
[68] H. G. van Oss, "Cement Tables," Reston, VA, 2013.
[69] H. G. van Oss, "Cement," Reston, VA, 1996.
[70] H. G. van Oss, "Cement Tables," Reston, VA, 2014.
[71] US Geological Survey, "Cement Tables," Reston, VA, 2015.
[72] H. G. van Oss, "Cement Tables," Reston, VA, 2016.
[73] K. C. Curry and H. G. van Oss, "Cement Tables," Reston, VA, 2017.
[74] US Geological Survey, "Cement, advance data release of the 2018 annual tables," Reston, VA, 2018.
[75] US Geological Survey, "Cement, advance data release of the 2019 annual tables," Reston, VA, 2019.
[76] H. G. van Oss, "Cement," Reston, VA, 1997.
[77] H. G. van Oss, "Cement," Reston, VA, 1998.
[78] H. G. van Oss, "Cement," Reston, VA, 1999.
[79] H. G. van Oss, "Cement," Reston, VA, 2000.
[80] H. G. van Oss, "Cement," 2001.
[81] H. G. van Oss, "Cement Tables," Reston, VA, 2002.
[82] H. G. van Oss, "Cement Tables," Reston, VA, 2003.

Appendix B. . **Supplemental Information for characterization of as-received PC4 in cement-based materials**

Table B.1. Sieve passing rate for PC4, quarried ground limestone, fine aggregate, and coarse aggregate

Sieve Specification	PC4, % Passing	Ground Limestone, % Passing	5 mm Aggregate, % Passing	10 mm Aggregate, % Passing	25 mm Aggregate, % Passing
37.5 (1-1/2 in)	-	-	-	100.00%	100.00%
25 (1 in)	-	-	-	100.00%	100.00%
19 mm (3/4 in)	-	-	-	100.00%	94.1%
12.5 mm (1/2 in)	-	-	-	100.00%	47.8%
9.5 mm (3/8 in)	-	-	-	99.2%	15.7%
4.75 mm (No. 4)	100%	-	99.95%	17.7%	0.6%
2.36 mm (No. 8)	100%	-	89.1%	2.1%	0.2%
2.00 mm (No. 10)	100%	-	80.5%	-	-
1.18 mm (No. 16)	99.7%	-	56.3%	-	-
600 µm (No. 30)	99.9%	-	29.9%	-	-
420 µm (No. 40)	99.39%	100%	18.9%	-	-
300 µm (No. 50)	98.88%	100%	10.4%	-	-
150 µm (No. 100)	64.47%	100%	2.1%	-	-
125 µm (No. 120)	-	99.8%	-	-	-
75 µm (No. 200)	23.65%	95.8%	0.2%	-	-
45 µm (No. 325)	-	82.0%	-	-	-

"-" indicates sieve sizes not tested

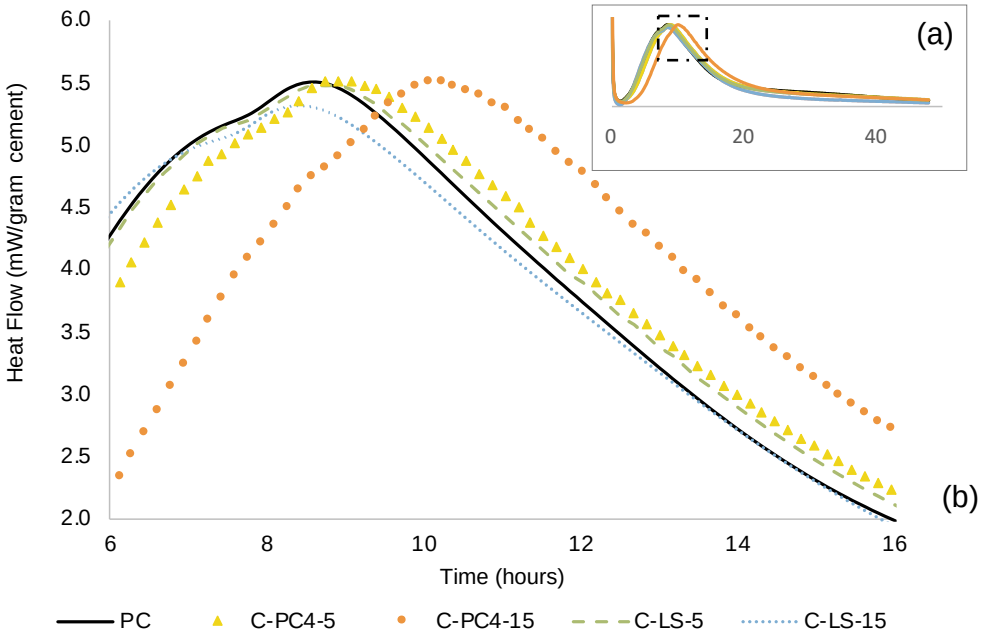

Figure B.1. Heat flow normalized to mass of cement of different binder mixtures with 5% or 15% replacement of cement with either PC4 or Limestone showing (a) Heat flow over the 48-hour testing period and (b) heat flow for the region indicated by the rectangle in (a).

Appendix C. . **Supplemental Information for a material flow analysis of rice hull and rice straw ash**

Part 1: Data to model annual rice production in the US and GHG impacts from Portland cement

2.1. Annual Rice production statistics

Annual rice production statistics, as collected and reported by the United States (US) Department of Agriculture (USDA) were used model the maximum yearly flow of rice hull and rice straw from rice grain production. The USDA reported the total for the entire US (US Total) and totals for states which are a significant producer of rice products (i.e., Arkansas, California, Louisiana, Mississippi, Missouri, Texas). The annual planted area data used is provided in US Imperial and Metric units in **Table C.1** and the annual rice yield per acre is provided in **Table C.2**, with data also in US Imperial and Metric units. Both tables show annual data from 2017 to 2022 as reported in USDA Rice Yearbook [1].

Table C.1. Annual area planted with rice paddy (state and US total) as reported by the US Department of Agriculture [1]

Planted Area	**… in units of acres**					
Year	*2017*	*2018*	*2019*	*2020*	*2021*	*2022*
Arkansas	1161000	1441000	1161000	1461000	1211000	1106000
California	445000	506000	503000	517000	407000	256000
Louisiana	400000	440000	425000	480000	420000	425000
Mississippi	115000	140000	117000	166000	105000	85000
Missouri	169000	224000	187000	228000	199000	155000
Texas	173000	195000	157000	184000	190000	195000
US Total	2463000	2946000	2550000	3036000	2532000	2222000
Planted Area	**… in units of hectares**					
Year	*2017*	*2018*	*2019*	*2020*	*2021*	*2022*
Arkansas	469840	583153	469840	591246	490075	447583
California	180085	204771	203557	209223	164707	103600
Louisiana	161874	178062	171992	194249	169968	171992
Mississippi	46539	56656	47348	67178	42492	34398
Missouri	68392	90650	75676	92268	80533	62726
Texas	70011	78914	63536	74462	76890	78914
US Total	996742	1192205	1031949	1228627	1024665	899212

Table C.2. Average annual rice yield (State-level and US total) as reported by the US department of Agriculture [1]

Yield / Area	**… in units of lbs / acre**					
Year	*2017*	*2018*	*2019*	*2020*	*2021*	*2022*
Arkansas	7490	7520	7480	7500	7630	7410
California	8410	8620	8460	8720	9050	8760
Louisiana	6710	7130	6380	6820	6870	6660
Mississippi	7400	7350	7350	7420	7540	7370
Mississippi	7440	7770	7370	7250	8040	7940
Texas	7260	7970	7350	8150	6860	6510
United States	7507	7692	7473	7619	7709	7383
Yield / Area	**… in units of kg / hectare**					
Year	*2017*	*2018*	*2019*	*2020*	*2021*	*2022*
Arkansas	8395	8429	8384	8406	8552	8305
California	9426	9662	9482	9774	10144	9819
Louisiana	7521	7992	7151	7644	7700	7465
Mississippi	8294	8238	8238	8317	8451	8261
Mississippi	8339	8709	8261	8126	9012	8900
Texas	8137	8933	8238	9135	7689	7297
United States	8414	8622	8376	8540	8641	8275

2.2. Modeling inputs for quantifying greenhouse gas impacts of Portland cement production

The OpenConcrete Tool [2] and life cycle inventories (LCI) included in the tool were used to quantify the US average and state-level averages for GHG impacts (CO_2-eq) associated with Portland cement production. State-level averages for GHG impacts were modeled using the state-level average cement kiln type mix (**Table C.3**) [3], state-level average electricity grid mix (**TableC.4**) [4], state-level average kiln fuel mix (**Table C.5**) [5]. US average GHG impacts were modeled using the US average cement kiln type mix (**Table C.3**) [3], and US average electricity grid mix (**TableC.4**) [4], and US averages for kiln fuel mix (**Table C.5**) [5].

Table C.3. Input values for United States (US) and State-level average kiln type mix (%) [2,3]

	Wet	*Dry*	*Preheater*	*Precalciner*
Arkansas	100.0%	0.0%	0.0%	0.0%
California	0.0%	15.0%	0.0%	85.0%
Louisiana	28.0%	13.0%	20.0%	39.0%
Mississippi	100.0%	0.0%	0.0%	0.0%
Missouri	40.0%	15.0%	0.0%	45.0%
Texas	20.0%	0.0%	20.0%	60.0%
US Average	27.9%	12.9%	20.0%	39.2%

TableC.4. Input values for United States (US) and State-level average electricity mix (%) [2,4]

	Coal	*Oil*	*Natural Gas*	*Biomass*	*Nuclear*	*Hydro-electric*	*Geo-thermal*	*Solar*	*Wind*
Arkansas	44.1%	0.1%	30.3%	2.0%	18.7%	4.5%	0.0%	0.3%	0.0%
California	0.1%	0.0%	45.9%	3.1%	9.3%	13.4%	6.0%	13.8%	7.2%
Louisiana	11.6%	4.3%	60.3%	2.6%	16.8%	1.2%	0.0%	0.0%	0.0%
Mississippi	8.3%	0.0%	78.0%	2.3%	10.9%	0.0%	0.0%	0.5%	0.0%
Mississippi	73.4%	0.1%	8.5%	0.2%	13.1%	1.1%	0.0%	0.1%	3.5%
Texas	23.4%	0.0%	50.2%	0.3%	8.6%	0.2%	0.0%	0.7%	15.9%
US Average	27.5%	0.6%	35.1%	1.6%	19.4%	6.9%	0.4%	1.5%	6.5%

Table C.5. Input values for United State average kiln fuel mix (%) [2,5]

Coal	*Oil*	*Biomass*	*Fossil Waste*	*Petroleum Coke*	*Natural Gas*	*Solid Waste*	*Liquid Waste*
57.5%	0.6%	0.0%	0.0%	15.4%	11.1%	10.1%	5.4%

Data sources:

[1] U.S. Department of Agriculture, U.S. Rice Acreage, production, and yield, Rice Yearb. (2023). https://www.ers.usda.gov/data-products/rice-yearbook/rice-yearbook/#U.S. Acreage, Production, Yield, and Farm Price (accessed December 1, 2023).

[2] A. Kim, P.R. Cunningham, K. Kamau-Devers, S.A. Miller, OpenConcrete: a tool for estimating the environmental impacts from concrete production, Environ. Res. Infrastruct. Sustain. 2 (2022) 041001. https://doi.org/10.1088/2634-4505/ac8a6d.

[3] M.L. Marceau, M.A. Nisbet, M.G. VanGeem, Portland Cement Association, Life cycle inventory of Portland cement manufacture, Portland Cement Association, Skokie, Illinois, 2006.

[4] US Enviroment Protection Agency (EPA), Power Profiler, EGrid Summ. Tables. (2018). https://www.epa.gov/egrid/power-profiler#/.

[5] H.G. van Oss, Minerals yearbook: cement 2012, United States Geological Survey, Reston, VA, 2015.

Appendix D. **Supplemental Information for pre-combustion leaching treatments of rice hull and rice straw**

Table D.1. Gradation of rice hulls and rice straw, after it was milled

Mesh Size	Particle Size (mm)	% Retained at each stage (sums to100%)	
		Straw	Hull
1"	25.40	4.7%	0.0%
3/4"	19.00	17.7%	0.0%
1/2"	12.70	17.0%	0.0%
3/8"	9.51	1.2%	0.0%
#4	4.76	24.9%	0.2%
#8	2.38	16.7%	66.9%
#10	2.00	3.1%	9.1%
#16	1.19	5.7%	10.3%
#30	0.595	4.2%	9.7%
#40	0.420	1.1%	1.3%
Pan	<0.420	3.8%	2.5%

Table D.2. Soluble salt, micronutrient removal, and change in pH of leachate solutions (n=1)

	K (mg/L)	Ca (mg/L)	Mg (mg/L)	Na (mg/L)	Zn (mg/L)	Cu (mg/L)	Mn (mg/L)	Fe (mg/L)
Measurement Precision	0.05	2	1.215	2.3	0.005	0.01	0.005	0.01
H_3PO_4 Straw Leachate	437.26	53	34.628	15.6	1.284	0.13	41.299	1.52
H_3PO_4 Hull Leachate	339.30	42	22.356	3.0	0.664	0.08	11.594	2.23
Water Straw Leachate	805.54	-10	30.861	39.6	0.460	0.17	18.750	0.94
Water Hull Leachate	226.55	-10	-0.729	-1.2	0.160	0.05	1.560	0.20
H_3PO_4 Solution (Prior to Leaching)	1.11	12	5.710	18.6	0.033	0.038	<0.005	0.13
Water Solution (Prior to Leaching)	1.08	13	6.439	20.0	0.006	<0.01	<0.005	<0.01

Table D.3. Post-treatment biomass feedstock properties (n=3)

	Moisture content, %ab	Ash content, %db	Volatile matter, %db	Fixed carbon, %db
Hull, unleached	5.74 (0.21)	22.10 (0.58)	59.72 (0.30)	18.18 (0.36)
Hull, water leached	5.31 (0.18)	21.03 (0.37)	62.30 (0.41)	16.67 (0.11)
Hull, acid leached	9.72 (0.19)	25.40 (0.66)	51.68 (0.68)	22.92 (0.07)
Straw, unleached	6.90 (0.79)	18.52 (0.56)	65.08 (0.57)	16.39 (0.32)
Straw, water leached	7.11 (0.11)	17.72 (0.15)	66.71 (0.35)	15.57 (0.34)
Straw, acid leached	0.82 (0.10) [b]	28.98 (0.20)	46.46 (0.26)	24.56 (0.21)

Values in "( )" are standard deviation, db is dry basis, [a] ab is "air-dry basis" moisture content for leached biomass after dewatering and oven drying. [b] for this sample, the straw was dried first and then milled; moisture contents for all other samples occurred prior to milling.

Table D.4. Trace elements, LOI, and specific gravity of rice-based ashes and Type II/V PC (n=1)

ID	Ba (ppm)	Sr (ppm)	Zr (ppm)	V (ppm)[a]	Cl (%)[a]	LOI (%)	Density (g/cm^3)
Detection Limit	*2*	*2*	*1*	*5*	*0.01*	*0.01*	*0.01*
S-U-600	116	80	4	6	1.52	4.95	2.53
S-U-850	106	67	3	10	0.14	0.93	2.30
S-U-1100	106	70	7	8	0.01	0.99	2.21
S-W-600	19	20	3	7	<0.01	0.54	2.28
S-W-850	115	86	3	10	0.02	1.00	2.32
S-W-1100	112	82	3	<5	0.02	0.39	2.31
S-A-600	23	17	3	<5	<0.01	4.41	2.60
S-A-850	22	16	3	20	<0.01	1.96	2.24
H-U-600	19	18	4	<5	0.14	2.90	2.33
H-U-850	18	21	3	<5	<0.01	0.50	2.20
H-U-1100	21	20	3	<5	0.01	0.27	2.14
H-W-600	18	23	3	<5	<0.01	2.09	2.38
H-W-850	19	25	3	<5	<0.01	0.51	2.29
H-W-1100	21	19	4	<5	<0.01	0.11	2.34
H-A-600	5	4	3	<5	<0.01	4.17	2.31
H-A-850	4	4	3	<5	<0.01	0.35	2.35
Type II/V PC[b]	171	1107	63	84	0.01	2.43	-

[a] '<' indicates value is below detection limit, [b]"-" indicates value not determined for PC

Appendix E. **Supplemental Information for post-combustion treatment of rice hull and rice straw ash**

Table E.1. Tukey test results comparing Rice Straw mixtures with w/b = 0.59

Rice Straw Ashes Mixtures	7 Day, w/b = 0.59				28 Day, w/b = 0.59			
	diff	**lwr**	**upr**	**p adj**	**diff**	**lwr**	**upr**	**p adj**
CTRL & 30%GBFS	7.2395	2.5347	11.9442	0.0014	-0.5171	-7.3443	6.3101	0.9994
M-RSA & 30%GBFS	-0.8618	-5.5666	3.8429	0.9809	-2.2408	-9.0680	4.5864	0.8601
10%RSA-30%GBFS & 30%GBFS	-4.4816	-9.1863	0.2232	0.0666	-6.0329	-12.8601	0.7943	0.0996
U-RSA & 30%GBFS	0.0000	-4.7047	4.7047	1.0000	-5.3434	-12.1706	1.4838	0.1729
M-RSA & CTRL	-8.1013	-12.8061	-3.3966	0.0004	-1.7237	-8.5509	5.1035	0.9403
10%RSA-30%GBFS & CTRL	-11.7211	-16.4258	-7.0163	0.0000	-5.5158	-12.3430	1.3114	0.1513
U-RSA & CTRL	-7.2395	-11.9442	-2.5347	0.0014	-4.8263	-11.6535	2.0009	0.2523
10%RSA-30%GBFS & M-RSA	-3.6197	-8.3245	1.0850	0.1852	-3.7921	-10.6193	3.0351	0.4779
U-RSA & M-RSA	0.8618	-3.8429	5.5666	0.9809	-3.1026	-9.9298	3.7245	0.6587
U-RSA & 10%RSA-30%GBFS	4.4816	-0.2232	9.1863	0.0666	0.6895	-6.1377	7.5167	0.9980

TableE.2. Tukey test results comparing Rice Hull Ash mixtures with w/b = 0.47

Rice Hull Ash, w/b = 0.47 Mixtures	7 Day, w/b = 0.47				28 Day, w/b = 0.47			
	diff	**lwr**	**upr**	**p adj**	**diff**	**lwr**	**upr**	**p adj**
M-F14b & 30%GBFS	9.4803	2.5966	16.3640	1.50E-03	7.9290	-2.5792	18.4371	2.86E-01
10%F14b-30%GBFS & 30%GBFS		-11.3653	2.4021	4.86E-01	-3.6197	-14.1279	6.8884	9.75E-01
M-F20 & 30%GBFS	0.8618	-6.0219	7.7455	1.00E+00	-10.1698	-20.6779	0.3384	6.49E-02
10%F20-30%GBFS & 30%GBFS	-12.4106	-19.2943	-5.5269	1.74E-05	-14.1342	-24.6424	-3.6261	2.07E-03
M-B20 & 30%GBFS	-3.9645	-10.8482	2.9192	6.51E-01	-9.3079	-19.8161	1.2002	1.21E-01
10%B20-30%GBFS & 30%GBFS	-15.3408	-22.2245	-8.4571	1.85E-07	-20.8566	-31.3648	-10.3485	2.48E-06
CTRL & 30%GBFS	7.2395	0.3558	14.1232	3.24E-02	-1.3790	-11.8871	9.1292	1.00E+00
M-F14a & 30%GBFS	3.7921	-3.0916	10.6758	7.04E-01	1.3790	-9.1292	11.8871	1.00E+00
10%F14a-30%GBFS & 30%GBFS	-6.7224	-13.6061	0.1613	6.05E-02	-13.2724	-23.7806	-2.7642	4.65E-03
10%F14b-30%GBFS & M-F14b	-13.9619	-20.8456	-7.0782	1.56E-06	-11.5487	-22.0569	-1.0406	2.14E-02
M-F20 & M-F14b	-8.6184	-15.5021	-1.7347	5.17E-03	-18.0987	-28.6069	-7.5906	4.11E-05
10%F20-30%GBFS & M-F14b	-21.8908	-28.7745	-15.0072	1.41E-11	-22.0632	-32.5714	-11.5551	7.28E-07
M-B20 & M-F14b	-13.4448	-20.3285	-6.5611	3.48E-06	-17.2369	-27.7450	-6.7287	9.81E-05
10%B20-30%GBFS & M-F14b	-24.8211	-31.7048	-17.9374	7.77E-13	-28.7856	-39.2938	-18.2774	9.66E-10

Rice Hull Ash, w/b = 0.47 Mixtures	7 Day, w/b = 0.47				28 Day, w/b = 0.47			
	diff	**lwr**	**upr**	**p adj**	**diff**	**lwr**	**upr**	**p adj**
CTRL & M-F14b	-2.2408	-9.1245	4.6429	9.83E-01	-9.3079	-19.8161	1.2002	1.21E-01
M-F14a & M-F14b	-5.6882	-12.5719	1.1955	1.83E-01	-6.5500	-17.0582	3.9581	5.47E-01
10%F14a-30%GBFS & M-F14b	-16.2027	-23.0864	-9.3190	4.98E-08	-21.2014	-31.7095	-10.6932	1.75E-06
M-F20 & 10%F14b-30%GBFS	5.3434	-1.5403	12.2271	2.52E-01	-6.5500	-17.0582	3.9581	5.47E-01
10%F20-30%GBFS & 10%F14b-30%GBFS	-7.9290	-14.8127	-1.0453	1.33E-02	-10.5145	-21.0227	-0.0063	4.98E-02
M-B20 & 10%F14b-30%GBFS	0.5171	-6.3666	7.4008	1.00E+00	-5.6882	-16.1963	4.8200	7.24E-01
10%B20-30%GBFS & 10%F14b-30%GBFS	-10.8592	-17.7429	-3.9755	1.90E-04	-17.2369	-27.7450	-6.7287	9.81E-05
CTRL & 10%F14b-30%GBFS	11.7211	4.8374	18.6048	5.06E-05	2.2408	-8.2674	12.7489	9.99E-01
M-F14a & 10%F14b-30%GBFS	8.2737	1.3900	15.1574	8.34E-03	4.9987	-5.5095	15.5069	8.44E-01
10%F14a-30%GBFS & 10%F14b-30%GBFS	-2.2408	-9.1245	4.6429	9.83E-01	-9.6527	-20.1608	0.8555	9.50E-02
10%F20-30%GBFS & M-F20	-13.2724	-20.1561	-6.3887	4.55E-06	-3.9645	-14.4726	6.5437	9.56E-01
M-B20 & M-F20	-4.8263	-11.7100	2.0574	3.83E-01	0.8618	-9.6463	11.3700	1.00E+00
10%B20-30%GBFS & M-F20	-16.2027	-23.0864	-9.3190	4.98E-08	-10.6869	-21.1950	-0.1787	4.34E-02
CTRL & M-F20	6.3776	-0.5060	13.2613	8.95E-02	8.7908	-1.7173	19.2990	1.71E-01
M-F14a & M-F20	2.9303	-3.9534	9.8140	9.12E-01	11.5487	1.0406	22.0569	2.14E-02
10%F14a-30%GBFS & M-F20	-7.5842	-14.4679	-0.7005	2.09E-02	-3.1026	-13.6108	7.4055	9.91E-01
M-B20 & 10%F20-30%GBFS	8.4461	1.5624	15.3298	6.58E-03	4.8263	-5.6818	15.3345	8.69E-01
10%B20-30%GBFS & 10%F20-30%GBFS	-2.9303	-9.8140	3.9534	9.12E-01	-6.7224	-17.2305	3.7858	5.11E-01
CTRL & 10%F20-30%GBFS	19.6501	12.7664	26.5337	3.09E-10	12.7553	2.2471	23.2634	7.45E-03
M-F14a & 10%F20-30%GBFS	16.2027	9.3190	23.0864	4.98E-08	15.5132	5.0050	26.0214	5.46E-04
10%F14a-30%GBFS & 10%F20-30%GBFS	5.6882	-1.1955	12.5719	1.83E-01	0.8618	-9.6463	11.3700	1.00E+00
10%B20-30%GBFS & M-B20	-11.3763	-18.2600	-4.4927	8.61E-05	-11.5487	-22.0569	-1.0406	2.14E-02
CTRL & M-B20	11.2040	4.3203	18.0877	1.12E-04	7.9290	-2.5792	18.4371	2.86E-01
M-F14a & M-B20	7.7566	0.8729	14.6403	1.67E-02	10.6869	0.1787	21.1950	4.34E-02
10%F14a-30%GBFS & M-B20	-2.7579	-9.6416	4.1258	9.37E-01	-3.9645	-14.4726	6.5437	9.56E-01
CTRL & 10%B20-30%GBFS	22.5803	15.6966	29.4640	5.87E-12	19.4777	8.9695	29.9858	1.01E-05
M-F14a & 10%B20-30%GBFS	19.1329	12.2493	26.0166	6.48E-10	22.2356	11.7274	32.7437	6.11E-07
10%F14a-30%GBFS & 10%B20-30%GBFS	8.6184	1.7347	15.5021	5.17E-03	7.5842	-2.9239	18.0924	3.44E-01
M-F14a & CTRL	-3.4474	-10.3311	3.4363	8.02E-01	2.7579	-7.7503	13.2661	9.96E-01
10%F14a-30%GBFS & CTRL	-13.9619	-20.8456	-7.0782	1.56E-06	-11.8935	-22.4016	-1.3853	1.60E-02
10%F14a-30%GBFS & M-F14a	-10.5145	-17.3982	-3.6308	3.21E-04	-14.6514	-25.1595	-4.1432	1.26E-03

TableE.3. Tukey test results comparing Rice Hull Ash mixtures with w/b = 0.59

Rice Hull Ash, w/b = 0.59; mixtures	7 Day, w/b = 0.59				28 Day, w/b = 0.59			
	diff	**lwr**	**upr**	**p adj**	**[illegible]**		**[illegible]**	**dj**
M-F14b & 30%GBFS	1.8961	-2.9597	6.7518	9.82E-01	6.0329	-1.0179	13.0837	1.70E-01
10%F14b-30%GBFS & 30%GBFS	-7.7566	-12.6123	-2.9009	5.76E-05	-4.4816	-11.5324	2.5692	6.12E-01
U-F14b & 30%GBFS	0.6895	-4.1663	5.5452	1.00E+00	-3.1026	-10.1535	3.9482	9.53E-01
M-F20 & 30%GBFS	-3.1026	-7.9584	1.7531	6.03E-01	-4.1369	-11.1877	2.9140	7.26E-01
10%F20-30%GBFS & 30%GBFS	-9.1356	-13.9913	-4.2798	1.48E-06	-3.1026	-10.1535	3.9482	9.53E-01
U-F20 & 30%GBFS	-4.4816	-9.3373	0.3741	9.88E-02	-5.6882	-12.7390	1.3627	2.41E-01
M-B20 & 30%GBFS	-7.0671	-11.9229	-2.2114	3.37E-04	-8.1013	-15.1522	-1.0505	1.13E-02
10%B20-30%GBFS & 30%GBFS	-11.8935	-16.7492	-7.0377	8.60E-10	11.2040	-18.2548	-4.1531	6.23E-05
U-B20 & 30%GBFS	-11.8935	-16.7492	-7.0377	8.60E-10	14.4790	-21.5298	-7.4281	1.44E-07
CTRL & 30%GBFS	7.2395	2.3838	12.0952	2.18E-04	-0.5171	-7.5679	6.5337	1.00E+00
M-F14a & 30%GBFS	1.6806	-3.4697	6.8309	9.96E-01	1.3790	-5.6719	8.4298	1.00E+00
10%F14a-30%GBFS & 30%GBFS	-6.2053	-11.0610	-1.3495	2.75E-03	0.3447	-6.7061	7.3956	1.00E+00
U-F14a & 30%GBFS	1.5513	-3.3044	6.4071	9.97E-01	0.0000	-7.0508	7.0508	1.00E+00
10%F14b-30%GBFS & M-F14b	-9.6527	-14.5084	-4.7969	3.65E-07	10.5145	-17.5653	-3.4637	2.12E-04
U-F14b & M-F14b	-1.2066	-6.0623	3.6491	1.00E+00	-9.1356	-16.1864	-2.0847	2.22E-03
M-F20 & M-F14b	-4.9987	-9.8544	-0.1430	3.79E-02	10.1698	-17.2206	-3.1189	3.88E-04
10%F20-30%GBFS & M-F14b	-11.0316	-15.8873	-6.1759	8.71E-09	-9.1356	-16.1864	-2.0847	2.22E-03
U-F20 & M-F14b	-6.3776	-11.2334	-1.5219	1.83E-03	11.7211	-18.7719	-4.6702	2.44E-05
M-B20 & M-F14b	-8.9632	-13.8189	-4.1075	2.35E-06	14.1342	-21.1851	-7.0834	2.75E-07
10%B20-30%GBFS & M-F14b	-13.7895	-18.6452	-8.9338	9.50E-12	17.2369	-24.2877	-10.1861	8.18E-10
U-B20 & M-F14b	-13.7895	-18.6452	-8.9338	9.50E-12	20.5119	-27.5627	-13.4611	9.45E-12
CTRL & M-F14b	5.3434	0.4877	10.1992	1.88E-02	-6.5500	-13.6009	0.5008	9.41E-02
M-F14a & M-F14b	-0.2155	-5.3657	4.9348	1.00E+00	-4.6540	-11.7048	2.3969	5.53E-01
10%F14a-30%GBFS & M-F14b	-8.1013	-12.9571	-3.2456	2.33E-05	-5.6882	-12.7390	1.3627	2.41E-01
U-F14a & M-F14b	-0.3447	-5.2005	4.5110	1.00E+00	-6.0329	-13.0837	1.0179	1.70E-01
U-F14b & 10%F14b-30%GBFS	8.4461	3.5903	13.3018	9.37E-06	1.3790	-5.6719	8.4298	1.00E+00
M-F20 & 10%F14b-30%GBFS	4.6540	-0.2018	9.5097	7.28E-02	0.3447	-6.7061	7.3956	1.00E+00
10%F20-30%GBFS & 10%F14b-30%GBFS	-1.3790	-6.2347	3.4768	9.99E-01	1.3790	-5.6719	8.4298	1.00E+00
U-F20 & 10%F14b-30%GBFS	3.2750	-1.5807	8.1307	5.17E-01	-1.2066	-8.2574	5.8443	1.00E+00
M-B20 & 10%F14b-30%GBFS	0.6895	-4.1663	5.5452	1.00E+00	-3.6197	-10.6706	3.4311	8.67E-01
10%B20-30%GBFS & 10%F14b-30%GBFS	-4.1369	-8.9926	0.7189	1.74E-01	-6.7224	-13.7732	0.3285	7.62E-02

Rice Hull Ash, w/b = 0.59; mixtures	7 Day, w/b = 0.59				28 Day, w/b = 0.59			
	diff	**lwr**	**upr**	**p adj**				**dj**
U-B20 & 10%F14b-30%GBFS	-4.1369	-8.9926	0.7189	1.74E-01	-9.9974	-17.0482	-2.9466	5.22E-04
CTRL & 10%F14b-30%GBFS	14.9961	10.1404	19.8518	3.96E-12	3.9645	-3.0864	11.0153	7.78E-01
M-F14a & 10%F14b-30%GBFS	9.4372	4.2869	14.5875	2.80E-06	5.8605	-1.1903	12.9114	2.03E-01
10%F14a-30%GBFS & 10%F14b-30%GBFS	1.5513	-3.3044	6.4071	9.97E-01	4.8263	-2.2245	11.8772	4.94E-01
U-F14a & 10%F14b-30%GBFS	9.3079	4.4522	14.1636	9.28E-07	4.4816	-2.5692	11.5324	6.12E-01
M-F20 & U-F14b	-3.7921	-8.6478	1.0636	2.85E-01	-1.0342	-8.0850	6.0166	1.00E+00
10%F20-30%GBFS & U-F14b	-9.8250	-14.6808	-4.9693	2.29E-07	0.0000	-7.0508	7.0508	1.00E+00
U-F20 & U-F14b	-5.1711	-10.0268	-0.3153	2.68E-02	-2.5855	-9.6364	4.4653	9.89E-01
M-B20 & U-F14b	-7.7566	-12.6123	-2.9009	5.76E-05	-4.9987	-12.0495	2.0521	4.36E-01
10%B20-30%GBFS & U-F14b	-12.5829	-17.4387	-7.7272	1.40E-10	-8.1013	-15.1522	-1.0505	1.13E-02
U-B20 & U-F14b	-12.5829	-17.4387	-7.7272	1.40E-10	11.3763	-18.4272	-4.3255	4.56E-05
CTRL & U-F14b	6.5500	1.6943	11.4057	1.21E-03	2.5855	-4.4653	9.6364	9.89E-01
M-F14a & U-F14b	0.9911	-4.1592	6.1414	1.00E+00	4.4816	-2.5692	11.5324	6.12E-01
10%F14a-30%GBFS & U-F14b	-6.8948	-11.7505	-2.0390	5.18E-04	3.4474	-3.6035	10.4982	9.02E-01
U-F14a & U-F14b	0.8618	-3.9939	5.7176	1.00E+00	3.1026	-3.9482	10.1535	9.53E-01
10%F20-30%GBFS & M-F20	-6.0329	-10.8886	-1.1772	4.10E-03	1.0342	-6.0166	8.0850	1.00E+00
U-F20 & M-F20	-1.3790	-6.2347	3.4768	9.99E-01	-1.5513	-8.6022	5.4995	1.00E+00
M-B20 & M-F20	-3.9645	-8.8202	0.8912	2.25E-01	-3.9645	-11.0153	3.0864	7.78E-01
10%B20-30%GBFS & M-F20	-8.7908	-13.6465	-3.9351	3.73E-06	-7.0671	-14.1180	-0.0163	4.89E-02
U-B20 & M-F20	-8.7908	-13.6465	-3.9351	3.73E-06	10.3421	-17.3930	-3.2913	2.87E-04
CTRL & M-F20	10.3421	5.4864	15.1979	5.63E-08	3.6197	-3.4311	10.6706	8.67E-01
M-F14a & M-F20	4.7832	-0.3670	9.9335	9.41E-02	5.5158	-1.5350	12.5666	2.84E-01
10%F14a-30%GBFS & M-F20	-3.1026	-7.9584	1.7531	6.03E-01	4.4816	-2.5692	11.5324	6.12E-01
U-F14a & M-F20	4.6540	-0.2018	9.5097	7.28E-02	4.1369	-2.9140	11.1877	7.26E-01
U-F20 & 10%F20-30%GBFS	4.6540	-0.2018	9.5097	7.28E-02	-2.5855	-9.6364	4.4653	9.89E-01
M-B20 & 10%F20-30%GBFS	2.0684	-2.7873	6.9242	9.63E-01	-4.9987	-12.0495	2.0521	4.36E-01
10%B20-30%GBFS & 10%F20-30%GBFS	-2.7579	-7.6136	2.0978	7.65E-01	-8.1013	-15.1522	-1.0505	1.13E-02
U-B20 & 10%F20-30%GBFS	-2.7579	-7.6136	2.0978	7.65E-01	11.3763	-18.4272	-4.3255	4.56E-05
CTRL & 10%F20-30%GBFS	16.3750	11.5193	21.2308	3.66E-12	2.5855	-4.4653	9.6364	9.89E-01
M-F14a & 10%F20-30%GBFS	10.8161	5.6659	15.9664	8.34E-08	4.4816	-2.5692	11.5324	6.12E-01

Rice Hull Ash, w/b = 0.59; mixtures	7 Day, w/b = 0.59				28 Day, w/b = 0.59			
	diff	**lwr**	**upr**	**p adj**	**[illegible]**		**[illegible]**	**dj**
10%F14a-30%GBFS & 10%F20-30%GBFS	2.9303	-1.9255	7.7860	6.87E-01	3.4474	-3.6035	10.4982	9.02E-01
U-F14a & 10%F20-30%GBFS	10.6869	5.8311	15.5426	2.21E-08	3.1026	-3.9482	10.1535	9.53E-01
M-B20 & U-F20	-2.5855	-7.4413	2.2702	8.34E-01	-2.4132	-9.4640	4.6377	9.94E-01
10%B20-30%GBFS & U-F20	-7.4119	-12.2676	-2.5561	1.40E-04	-5.5158	-12.5666	1.5350	2.84E-01
U-B20 & U-F20	-7.4119	-12.2676	-2.5561	1.40E-04	-8.7908	-15.8416	-1.7400	3.88E-03
CTRL & U-F20	11.7211	6.8654	16.5768	1.36E-09	5.1711	-1.8798	12.2219	3.82E-01
M-F14a & U-F20	6.1622	1.0119	11.3125	6.82E-03	7.0671	0.0163	14.1180	4.89E-02
10%F14a-30%GBFS & U-F20	-1.7237	-6.5794	3.1320	9.92E-01	6.0329	-1.0179	13.0837	1.70E-01
U-F14a & U-F20	6.0329	1.1772	10.8886	4.10E-03	5.6882	-1.3627	12.7390	2.41E-01
10%B20-30%GBFS & M-B20	-4.8263	-9.6821	0.0294	5.29E-02	-3.1026	-10.1535	3.9482	9.53E-01
U-B20 & M-B20	-4.8263	-9.6821	0.0294	5.29E-02	-6.3776	-13.4285	0.6732	1.15E-01
CTRL & M-B20	14.3066	9.4509	19.1623	5.25E-12	7.5842	0.5334	14.6351	2.41E-02
M-F14a & M-B20	8.7477	3.5974	13.8980	1.59E-05	9.4803	2.4295	16.5311	1.26E-03
10%F14a-30%GBFS & M-B20	0.8618	-3.9939	5.7176	1.00E+00	8.4461	1.3952	15.4969	6.68E-03
U-F14a & M-B20	8.6184	3.7627	13.4742	5.92E-06	8.1013	1.0505	15.1522	1.13E-02
U-B20 & 10%B20-30%GBFS	0.0000	-4.8557	4.8557	1.00E+00	-3.2750	-10.3258	3.7758	9.31E-01
CTRL & 10%B20-30%GBFS	19.1329	14.2772	23.9887	3.61E-12	10.6869	3.6360	17.7377	1.57E-04
M-F14a & 10%B20-30%GBFS	13.5740	8.4238	18.7243	8.10E-11	12.5829	5.5321	19.6338	5.00E-06
10%F14a-30%GBFS & 10%B20-30%GBFS	5.6882	0.8324	10.5439	8.94E-03	11.5487	4.4979	18.5996	3.34E-05
U-F14a & 10%B20-30%GBFS	13.4448	8.5890	18.3005	1.79E-11	11.2040	4.1531	18.2548	6.23E-05
CTRL & U-B20	19.1329	14.2772	23.9887	3.61E-12	13.9619	6.9110	21.0127	3.80E-07
M-F14a & U-B20	13.5740	8.4238	18.7243	8.10E-11	15.8579	8.8071	22.9088	1.07E-08
10%F14a-30%GBFS & U-B20	5.6882	0.8324	10.5439	8.94E-03	14.8237	7.7729	21.8746	7.51E-08
U-F14a & U-B20	13.4448	8.5890	18.3005	1.79E-11	14.4790	7.4281	21.5298	1.44E-07
M-F14a & CTRL	-5.5589	-10.7092	-0.4086	2.33E-02	1.8961	-5.1548	8.9469	9.99E-01
10%F14a-30%GBFS & CTRL	-13.4448	-18.3005	-8.5890	1.79E-11	0.8618	-6.1890	7.9127	1.00E+00
U-F14a & CTRL	-5.6882	-10.5439	-0.8324	8.94E-03	0.5171	-6.5337	7.5679	1.00E+00
10%F14a-30%GBFS & M-F14a	-7.8859	-13.0362	-2.7356	1.32E-04	-1.0342	-8.0850	6.0166	1.00E+00
U-F14a & M-F14a	-0.1293	-5.2796	5.0210	1.00E+00	-1.3790	-8.4298	5.6719	1.00E+00
U-F14a & 10%F14a-30%GBFS	7.7566	2.9009	12.6123	5.76E-05	-0.3447	-7.3956	6.7061	1.00E+00

Appendix F. **Projected paste masses and GHG emissions (expanded)**

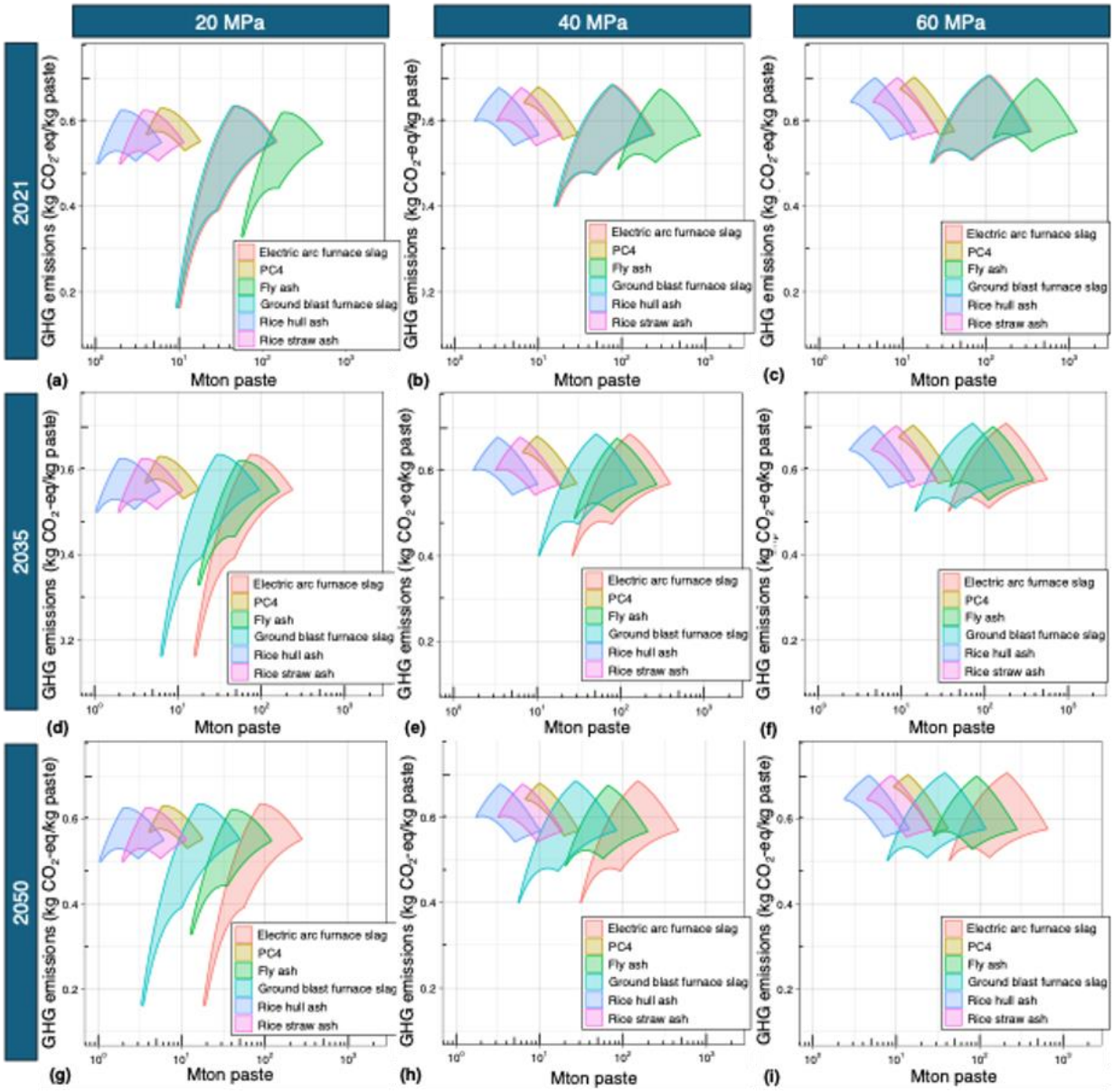

Figure F.1. Figure showing potential maximum paste generation and associated GHG emissions in 2021, 2035, and 2050 for paste compressive strengths of 20 MPa, 40MPa, and 60 MPa.